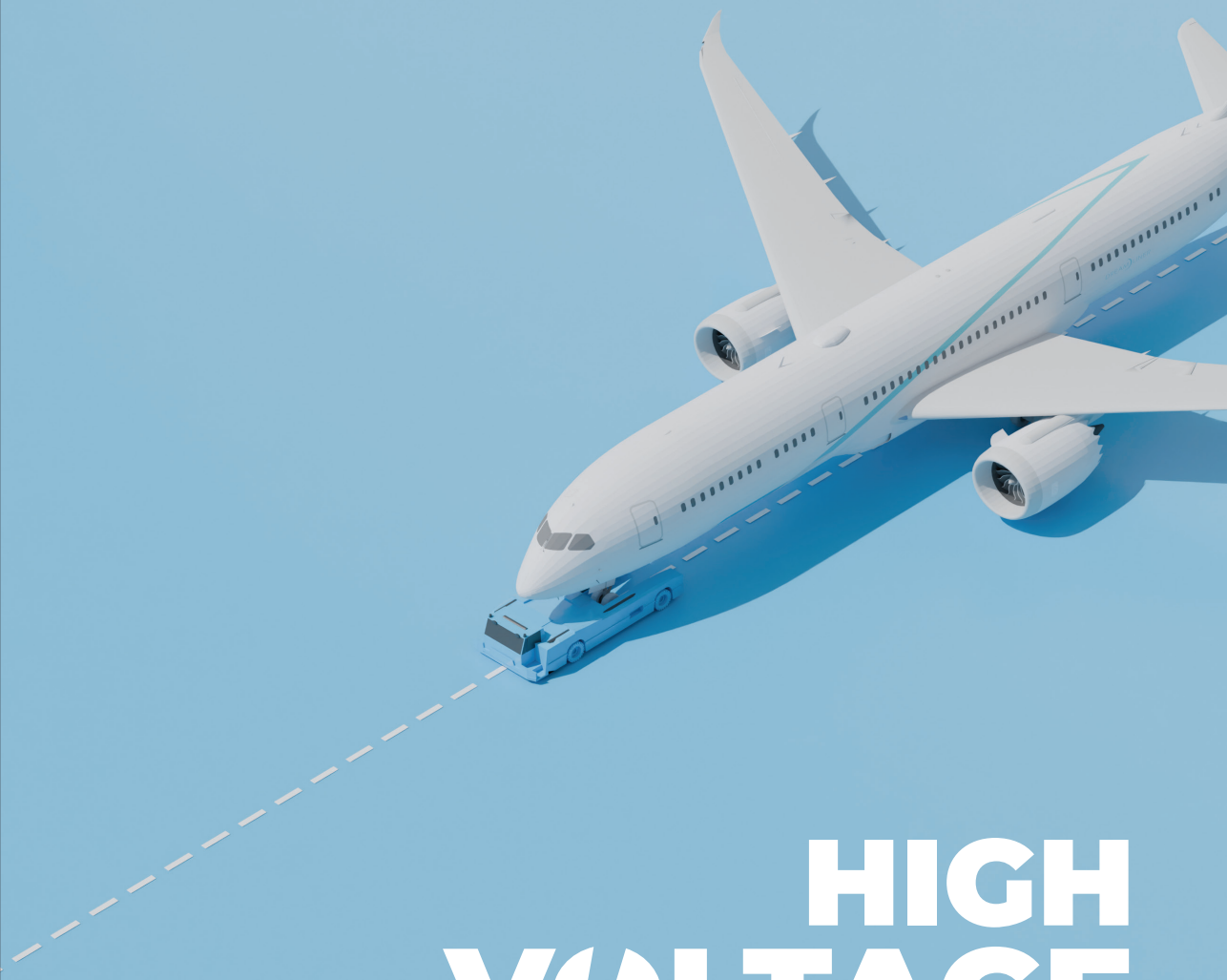

HIGH VOLTAGE HORIZONS

Infrastructure and operations planning for electric aviation

Simon van Oosterom

High Voltage Horizons

Infrastructure and operations planning for electric aviation

High Voltage Horizons

Infrastructure and operations planning for electric aviation

Dissertation

for the purpose of obtaining the degree of doctor
at Delft University of Technology,
by the authority of the Rector Magnificus, prof. dr. ir. T.H.J.J. van der Hagen,
chair of the Board of Doctorates
to be defended publicly on
Tuesday 24 June 2025 at 12:30 o'clock

by

Simon Johannes Maria VAN OOSTEROM

Master of Science in Applied Mathematics,
Delft University of Technology, The Netherlands,
geboren in Amersfoort, The Netherlands.

This dissertation has been approved by the promotors.

Composition of the doctoral committee:

Rector Magnificus,	chairperson
Prof. dr. ir. J.M. Hoekstra,	Delft University of Technology, *promotor*
Dr. M.A. Mitici,	Universiteit Utrecht, *copromotor*
Independent members:	
Prof. dr. ir. S.P. Hoogendoorn,	Delft University of Technology
Prof. dr. D. Delahaye,	Ecole Nationale de l'Aviation Civile, France
Prof. Dr. -Ing. M. Schultz,	Universität der Bundeswehr München, Germany
Prof. dr. J.A.S. Gromicho,	Universiteit van Amsterdam
Em. prof. dr. D.G. Simons,	Delft University of Technology

This research was funded by the European Union's SESAR Joint Undertaking (JU) under grant agreement No. 892869 (Advanced Engine-Off Navigation project).

Keywords: Sustainable Aviation, Electric Aircraft, Airport Operations, Electric Taxiing, Electric Vertical Take-Off and Landing Aircraft, Fleet Scheduling, Infrastructure Sizing, Predictive Maintenance Planning

Printed by: Ridderprint

Cover by: Simon van Oosterom

ISBN 978-94-6518-076-2

An electronic copy of this dissertation is available at
https://repository.tudelft.nl/.

Voyager rend modeste.
Vous voyez quelle petite place vous occupez dans le monde.

Travel makes one modest.
You see what a tiny place you occupy in the world.

Gustav Flaubert

Contents

Acknowledgements

There is only one name on the cover of this dissertation. This is of course a false representation of how it came to be. Nobody generates ideas or writes them down just by himself. We owe so much more to our environment then can ever be done justice in two pages of acknowledgements. But I'll give it a shot anyway, here we go!

First and foremost, thank you Mihaela. Thank you for your guidance, for your support, and for your patience. What started out as a 6 months co-supervision has turned into an awesome four-and-a-half year project together. You were always invested in our work, always curious, and always persistent during research. But more important than being competent, you were always kind, understanding, and fun. I so much enjoyed our conversations, first in Delft, later in Utrecht, both one-on-one and as a group with Juseong, Inge and Mike. It has been a blast!

Thank you Jacco. Thank you for helping me finding the right focus during research and for your critical eye. You have an invaluable body of knowledge, not only about aviation but about science, research, and society in general. Even though your schedule is insane, I appreciate that there was always time somewhere during the day if I needed your guidance.

Thank you, to all the PhDs and postdocs. Over four years, I have had the pleasure of being part of not one, but three sections. Moving has been stressful at times, but has also been an enriching experience, and because of it I have gotten to know many more of you much better then otherwise. Ingeborg, for being a mentor to me during the process, Mike, for your groundedness, underappreciated but invaluable in this hectic world, and Juseong, for your wisdom and for introducing me to Korean food. To the Amorgossians, I say Yamas! To Marie Bieber and Iordanis Tseremoglou (aka Chicago-crew, also a shout-out to PJ Proesmans), to Malte von der Burg (rib-breaker in both possible ways), Thomas Piogier (BFC enthousiast), Haonan Li (owner of moderate BFC Humphry), Matthieu Vert (Myko-), and Hao Ma (-nos). To Marta Ribeiro, Andrei Badea, Andres Morfin Veytia, Jan Groot, and Esther Roosenbrand, thank you for making me feel welcome in the ATM/CNS section (and for the endless Catan nights, discussions on chess and Rubik's Cubes and Pizzabakkers excursions). Thanks to the other PhDs and PostDocs, Qichen Deng, Gülçin Ermiş, Chengpeng Jiang, Mahdi Noorafza, Wenhua Qu, Rowenna Wijlens, Gijs de Rooij, Ilias Parmaksizoglou, Sasha Vlaskin, Fazlur Rahman, Prashant, Aidana Tassanbi, Maria Luís Patrício, Nils Ahrenhold, Lisanne Heuseveldt, Philip de Bruin, João Borrego, Guilia Leto, Karim Aly, Timo Stienstra, Sam Randeraad, Phillipe Lothaller, Daniel Acevedo, Fynn

Oppermann, Sara Habib, Bob van Dillen and Mihai Constantinov[1].

Of course, thanks to the professors and staff in Operations & Environment! To Alessandro, an OR-hero, to AEON-partner Alexei, to group leader Bruno Santos, to Elise for all the interesting RHIA events, to Henk for your insights on being a good academic, to Joost for all the programming tips, to Junzi for being a bridge between the PhDs and the staff, to Marloes and Nathalie for organizing all the group events, and to Paul for the nice discussions on the aviation industry).

Thank you to my friends, for your kindness and companionship. I will not attempt to name everyone, to avoid the risk of missing someone. Thank you Sjoerd, my oldest friend and a hallmark of authenticity and persistence, and Dennis, my partner in crime for great discussions on the intricateness of fictional worlds and the craziness of the real one. To Arthur, an erudite and ambitious source of inspiration, Jochem, the best thinker on the place of science and academics in society, I always look forward to our next trip together. To my housemates at GamaLama, Dolf, Max and Ben, for all advice, activities and PtdB campaigns. To the critical thinkers and reading club organizers Atay, Femmie, Jacob and Job. And to everyone from PK who shares the healthy passion for the sea and an unhealthy compulsion to wake up at 3 AM for some good wind and swell, Astrid, Bart, Bèr, Britt, Christie, Daniel, Emiel, Feike, Femke, Gwen, Jelle, Job, Jop, Jurgen, Lucas, Marit, Max, Meike, Mo, Nienke, Noa, Ruben, Sarah, Shawn, Steven, Tammo, Wieke, Wouter and Wouter. Watching everyone grow together and support each other, its just the best.

Last, thank you to my family. To José, Wim, Els, Herman, Tom, Linda, Maarten, Pieter, Plonie, Mien and Piet. Thank you Patrick, for being an amazing brother and co-media producer when we grew up, for sharing your passion for books, and for your support now. Thanks to my parents, for always being there to listen with patience. Thanks for believing in me to finish the dissertation when I had doubts myself. Thanks for a childhood free of worries and full of freedom to explore and experience. I could not have asked for more.

[1] and of course to their beloved ones, especially Jenny, Joost, Caro, Matthäus, Roy, Helena and Teona

Summary

Over the last half-century, the aviation industry has enabled worldwide connectivity at short travel times and at a relatively affordable price point. Over the course of these years, the fuel-efficiency of aircraft has significantly improved, reducing the environmental impact per passenger. However, the current growth of the industry outpaces the fuel-efficiency, nullifying the environmental gains. In the future, radically different aircraft concepts will be required. In this light, electric aviation technologies pose an interesting group of opportunities which can be deployed in different operating conditions. Three specific developments in electric aviation are (i) external electric taxiing, a new paradigm for aircraft to traverse the airport using Electric Towing Vehicles (ETVs), (ii) electric commuter aircraft, the first generation of electric aircraft for commercial purposes, and (iii) electric Vertical Take-Off and Landing (eVTOL) aircraft, used for urban air mobility.

These technologies will impact aviation operations, as well as the way these operations are planned. Battery performance plays a key part in this, as we are faced with the shorter vehicle range, long charging times, underdeveloped charging infrastructure at airports, and new maintenance requirements due to battery degradation. New operations planning models are required to address these challenges and accommodate these constraints. This dissertation aims to contribute to the incorporation of electric aviation technologies by developing these models and optimization algorithms. Special attention is paid to modelling and addressing stochastic elements of operations, and to the interactions between different planning stages, from infrastructure development to rescheduling. The developed algorithms enable solution generation within an appropriate optimization time, and are applied at several case studies at airports and airlines.

The first subject of this dissertation is the creation of a comprehensive model for the implementation of ETVs at large airports, with a focus on ETV scheduling. This ETV schedule comprises an assignment of ETVs to to-be-towed aircraft, together with information when each ETV is to recharge its battery. An efficient ETV schedule, with a tight assignment and well spread charging moments, increases the number of aircraft which can be towed by an ETV, thereby increasing the environmental benefits as well as reducing the required number of ETVs to provide a given service level. We build on existing studies in three ways. These are (i) the development of realistic charging assumptions, (ii) the integration of taxiway traffic coordination, and (iii) the incorporation of disruption management.

The first goal is to benchmark the existing ETV scheduling models with one that has

realistic charging assumptions. Specifically, we consider that the charging power decreases when approaching a full charge, and allow for preemptive charging. From a review of the existing models, our first ETV scheduling model is developed. This model is formulated as a mixed-integer linear programming model (MILP), and optimization of this model is performed using a branch-and-bound (B&B) algorithm. The different models are compared in a case study.

Building on this, we develop an optimization model for ETV scheduling that integrates the taxiway traffic coordination with ETV scheduling. This concerns the routing of aircraft and ETVs across the airport taxiways and service roads, while avoiding (near) collisions. An efficient routing reduces the taxiing time of aircraft and driving time of ETVs, while also preventing inefficient stop-and-go situations. A framework is proposed in which a full-day ETV schedule is created by sequentially optimizing surface movements and optimizing the ETV-to-aircraft assignment. For this purpose, two algorithms are developed: two sequential MILPs solved with the branch-and-bound algorithm, and a dynamic model solved by two greedy algorithms. For the surface movement optimization problem, the greedy algorithm is able to achieve a near-optimal routing with significantly reduced computational requirements. Contrasting, the greedy algorithm exhibits a significant gap with respect to the MILP when considering the ETV-to-aircraft assignment and charging schedule creation. This shows the necessity of a non-greedy algorithm for this problem.

This model is completed by the creation of an ETV scheduling algorithm that is able to retain performance under flight schedule disruptions. Disruptions such as early arrivals and late departures are commonplace at large airports, and ETV scheduling algorithms are required to account for this. A dynamic data-driven scheduling model is developed, which both anticipates and reacts to disruptions. It is used to simulate ETV operations at several days at a large airport, with real-time updates of the flight arrival/departure times. Thirty days of historical flight data are used to predict flight delays. The results show that the ability to anticipate disruptions enables more-robust schedules, with a higher environmental benefit per ETV.

The second subject of this dissertation is the implementation of small electric aircraft. The first generation of these aircraft can be deployed in remote areas, such as archipelagoes or fjords. For the charging operations, a battery swapping system is considered. This system has the advantage of significantly reducing the turnaround time, as well as the ability to spread the charging power across the day more evenly. We consider a charging infrastructure sizing and charging operations scheduling model for a network of electric aircraft. An efficient charging schedule reduces the required charging infrastructure, and conversely, an appropriate charging infrastructure reduces operational disruptions.

The scheduling model considers when the battery of each aircraft is recharged, given a specified charging infrastructure. The schedule is made to minimize operational disruptions while spreading electricity demand as best as possible. This model is integrated into the recharge infrastructure sizing model as a subroutine. By considering different levels of traffic around the year, a balanced charging infrastructure is obtained. The model is optimized with a simulated annealing algorithm, where the scheduling model is formulated as a MILP and is addressed with a branch-and-bound algorithm. The

method is applied in a case study to a domestic network considering one year of operations. The results show that this approach allows for significant cost reductions.

The third subject of this dissertation are the eVTOL aircraft. We aim to create a predictive maintenance framework for the eVTOL batteries which is integrated into operations. This maintenance schedule comprises the times which each eVTOL in a fleet is maintained, while ensuring that capacity is not exceeded. Using battery sensor measurements, health prognostics can be made. The ability to create these and implement them adequately into maintenance operations minimizes the number of breakdowns while maximizing the used battery life. Two models are presented for predictive battery maintenance planning: (i) a two-stage probabilistic remaining useful life (RUL) prognostics and (ii) an end-to-end maintenance cost prognostics framework. When applied to a case study, the results show the merit of the end-to-end planning framework, with fewer breakdowns and lower maintenance costs.

The objective of this dissertation has been the creation of operations optimization algorithms for electrified aviation. Special attention has been paid to the interaction between the planning phases involved: from infrastructure development to asset scheduling to disruption management. Data-driven algorithms have been developed to address the uncertainties which occur within the different phases. The models can provide support for the implementation of these technologies into aviation operations. Future work could address the integration of the different algorithms into an overall planning framework. Additionally, it could address the creation of fairness constraints. Also, when the technology readiness of the ETVs and aircraft is at a higher level, more accurate performance models can be leveraged to improve the quality of the results of the developed algorithms. Overall, this dissertation provides a starting point for airport and airline planners when considering electric aviation technologies.

Samenvatting

De afgelopen vijftig jaar heeft de luchtvaart gezorgd voor wereldwijde verbondenheid door korte reistijden en een relatief goede betaalbaarheid. Het brandstofverbruik van vliegtuigen is in die tijd veel beter geworden, wat ervoor heeft gezorgd dat de klimaatimpact per passagier steeds lager is. Echter, de groei van de luchtvaartsector zorgt voor een netto toename van uitstoot. In de toekomst zullen dus radicale verbeteringen nodig zijn. Elektrificatie van de luchtvaart biedt in deze context mogelijkheden op verschillende terreinen. Drie concrete ontwikkelingen voor elektrificatie zijn (i) extern elektrisch taxiën, een nieuwe procedure voor vliegtuigen om zich over vliegvelden te verplaatsen met behulp van Elektrische Taxi Voertuigen (*Electric Towing Vehicles*, ETVs), (ii) kleine elektrische vliegtuigen, geschikt voor forensen en als zakenvliegtuigen, en (iii) elektrisch verticaal opstijgende en landende vliegtuigen (*electric Vertical Take-Off and Landing aircraft*, eVTOL), geschikt voor stedelijke mobiliteit.

Deze technologieën hebben impact op de processen op luchthavens en van luchtvaartmaatschappijen, en op de manier waarop deze gepland worden. De prestaties van batterijen zijn hier essentieel, gegeven de kortere rij/vliegbereik, lange laadtijden, onontwikkelde oplaadinfrastructuur en nieuwe onderhoudseisen. Nieuwe besliskundige modellen en algoritmes zijn nodig om deze uitdagingen te beantwoorden en rekening te houden met deze beperkingen. Het doel van dit proefschrift is om bij te dragen aan de implementatie van de elektrificatie van de luchtvaart door deze modellen en algoritmes te ontwikkelen. We besteden speciale aandacht aan het modelleren van de stochastische elementen van de luchtvaartprocessen en aan de interactie tussen de verschillende planningsfases, van het aanleggen van infrastructuur tot het omgaan met verstoringen. De algoritmes genereren oplossingen binnen gepaste tijden en worden getest op verschillende casussen op luchthavens en luchtvaartmaatschappijen.

Het eerste onderwerp van deze scriptie is het modelleren van ETV processen op grote luchthavens, met de focus op het inroosteren van ETVs. Dit rooster omschrijft welk vliegtuig door welke ETV versleept wordt, en wanneer de ETVs opgeladen worden. Met een efficiënt rooster kan een ETV meer vliegtuigen slepen, waardoor de klimaatwinst groter is of het aantal benodigde ETVs lager is. Wij bouwen op eerder onderzoek op drie manieren. Dit zijn (i) realistische aannames voor het opladen van ETVs, (ii) de integratie met de coördinatie van verkeer op de taxibanen en (iii) het omgaan met verstoringen.

Als eerste zijn bestaande ETV rooster modellen vergeleken met een realistisch oplaadmodel. Het door ons ontwikkelde model houdt er rekening mee dat de oplaadsnelheid afneemt als batterijen voller raken, en staat toe dat het opladen onderbroken mag

worden. Dit model is geformuleerd als een *Mixed-Integer Linear Programming* (MILP) model, wat geoptimaliseerd wordt met een *Branch-and-Bound* (B&B) algoritme. De modellen worden vergeleken in een casus.

Hierop voortbouwend is een optimalisatiemodel ontwikkeld, waarin het coördineren van het verkeer op de taxibaan wordt geïntegreerd in het inroosteren van ETVs. Dit gaat over het uitkiezen van routes die de (gesleepte) vliegtuigen gebruiken, en het voorkomen dat deze te dicht bij elkaar komen. Een goede coördinatie verminderd de taxi-tijd en rijtijd van ETVs, en voorkomt inefficiënte stop-en-start situaties. Een raamwerk wordt voorgesteld dat opeenvolgend het verkeer coördineert, en de toewijzing van ETVs aan vliegtuigen optimaliseert. Hiertoe worden twee algoritmes voorgesteld: een MILP dat met een *Branch-and-Bound* wordt geoptimaliseerd, en een dynamisch model dat door een *greedy* algoritme wordt opgelost. De coördinatie van het verkeer wordt nagenoeg optimaal gedaan door het *greedy* algoritme, dat tegelijkertijd ook minder rekenkracht nodig heeft. Aan de andere hand is er een groot gat van het *greedy* model tot de MILP voor de ETV-vliegtuig toewijzing. Dit laat zien niet-*greedy* model nodig is voor dit probleem.

Het model is voltooid door een ETV-inroosteralgoritme dat om weet te gaan met verstoringen in het vliegschema. Verstoringen van het vliegschema zijn in hoge mate aanwezig, en inspelen hierop is daarom essentieel. Een datagedreven ETV inroosteralgoritme is ontwikkeld dat niet alleen reageert op verstoringen, maar deze ook anticipeert. Het is gebruikt om ETV processen te simuleren in een casus op een groot vliegveld, waar live updates van de aankomst- en vertrektijden binnenkomen. Historische data van dertig dagen wordt gebruikt om deze verstoringen te voorspellen. Met deze casus wordt het belang van het anticiperen van verstoringen aangetoond door het maken van meer robuuste roosters met lagere klimaatimpact door taxiën.

Het tweede onderwerp van dit proefschrift is de implementatie van de eerste generatie kleine elektrische vliegtuigen. Deze zijn geschikt voor afgelegen gebieden, zoals in fjorden of in een archipel. We nemen aan dat de batterijen van vliegtuigen tussen vluchten door verwisseld worden. Dit heeft als voordeel dat het de doorlooptijd beperkt en de vraag naar elektriciteit beter over de dag verdeeld. We beschouwen het optimaliseren van de oplaadinfrastructuur en de oplaadroosters voor een netwerk van deze vliegtuigen. Een efficiënt oplaadrooster zorgt ervoor dat minder infrastructuur nodig is, en omgekeerd zorgt een geschikte infrastructuur ervoor dat verstoringen door het opladen minimaal blijven.

Het oplaadrooster optimialisatiemodel bepaald voor elk vliegveld wanneer elke batterij wordt opgeladen, gebruikmakend van een bepaalde oplaadinfrastructuur. Dit wordt gedaan zodat de verstoringen minimaal blijven en de vraag naar elektriciteit over de dag wordt verdeeld. Dit model is geïntegreerd als subroutine in een optimalisatiemodel voor de oplaadinfrastructuur. Door verschillen in het vliegschema door het jaar heen te beschouwen wordt een gebalanceerde infrastructuur voorgesteld. Het model wordt geoptimaliseerd met een *simulated annealing* algoritme, het oplaadrooster wordt geoptimaliseerd met een *branch-and-bound* algoritme. Het model is toegepast in een casus van een Noorse luchtvaartmaatschappij. Hier wordt aangetoond dat het meenemen van de variaties in verkeer door het jaar heen leidt tot een significante kostenreductie.

Het derde onderwerp van dit proefschrift zijn de nieuwe eVTOL vliegtuigen. Deze kunnen worden gebruikt voor bijvoorbeeld stedelijk persoonsvervoer of voor medische

ondersteuning. Een raamwerk voor voorspellend onderhoud van batterijen van eVTOLs wordt ontwikkeld. Dit omvat het maken van een onderhoudsrooster voor de eVTOLs, waarbij de capaciteit niet wordt overschreden. Beslissingen over het onderhoud worden ondersteund door gebruik te maken van sensoren in de batterijen. Een goede implementatie hiervan minimaliseert het aantal defecten terwijl de batterijen zo lang mogelijk gebruikt worden. Twee modellen zijn ontwikkeld: een twee-fasen model dat gebruik maakt van probabilistische voorspellingen van de resterende levensduur (*Remaining Useful Life*, RUL), en een geïntegreerd model dat gebruik maakt van voorspellingen van de onderhoudskosten. In een casus voor een vloot van eVTOLs wordt de kracht van het geïntegreerde model aangetoond, die resulteert in minder defecten en lagere onderhoudskosten.

Door dit proefschrift heen zijn verschillende optimalisatiemodellen ontwikkeld voor het plannen en roosteren van processen voor elektrische luchtvaart. De interactie tussen de verschillende planningsfases heeft hierin een belangrijke rol gespeeld: van de ontwikkeling van infrastructuur tot het inroosteren van voertuigen en het omgaan met verstoringen. Datagedreven algoritmes zijn ontwikkeld om te kunnen omgaan met de onzekerheden in de verschillende planningsfases. Deze modellen kunnen samen worden gebruikt om de implementatie van elektrische technologieën in de luchtvaart te ondersteunen. Vervolgstudies kunnen geweid worden aan de integratie van de verschillende modellen van dit proefschrift in een holistisch raamwerk. Daarnaast kan aandacht besteed worden aan het eerlijk verdelen van lasten en lusten in het inroosteringsproces. Door deze modellen te ontwikkelen, biedt dit proefschrift een vertrekpunt voor luchthavens en vliegtuigmaatschappijen die overwegen om over te gaan op elektrische voertuigen.

CHAPTER 1

Introduction

1

1.1 The period

> It was the best of times, it was the worst of times...
>
> *Charles Dickens*

The current state of the aviation industry reminds us of Charles Dickens' opening of *A Tale of Two Cities* [1].

It is the *best of times*. After suffering a devastating blow at the hand of the Covid-19 pandemic, business is booming [2]. Year-on-year, aviation connects more people, increasing understanding of other cultures and enabling a globalized economy [3]. One could say that this has enabled an unprecedented peace. By increasing efficiency, flying has shifted from a luxury for a few, and is one of the only goods which is more-or-less insensitive to inflation [4, 5]. But it is also safer then ever before. Due to better regulations and aircraft constructions, there is only one accident in 1,26 million flights [6]. Looking at these figures, it seems like aviation has a bright future ahead.

But it is also *the worst of times*, for aviation is also changing the world for the worse. The effects of anthropogenic-induced climate change are being reported, and the contribution of aviation here is well established [7, 8]. Aviation operations contributes to about 3.5% of this impact in several ways by emitting carbon oxides (CO2 and CO) [9], nitrogen oxides (NO and NO2) [10] and sulfur oxides (SOx) [11], as well as the formation of contrails (line-shaped clouds of water vapour) [12]. We observe an increase in severe storms in one place, an increase in drought in others, a loss of species, a decrease in food production, and an increase in pressure on physical and mental health [13]. Furthermore, these effects are most notable in the 'global south' [14–16]. The industry may connect a part of the world population, but the negative externalities are placed on others.

It seems like *the winter of despair*. Though 3.5% appears small in the larger picture, stabilizing or even reducing emissions is challenging for the aviation sector [17]. It is true that aircraft become more efficient with every generation [18, 19]; it is also true that airports and airlines pay increasing attention to the sustainability of their operations [20]. One can see these trends in Figure 1.1, which shows the fuel burn per traveled passenger per kilometer (RPK) [21]. However, this increase in efficiency is followed by reduced costs, which is followed by more flown kilometers: the sector is expected to grow 4-5% annually in the near future. This effect, the Jevons-paradox, has annihilated the gains achieved in efficiency, as also shown in Figure 1.1. Compared to 1990, the RPK volume has quadrupled, and the total aviation emissions have doubled. A further increase of efficiency of aircraft is not expected to reduce emissions in the future [22].

But it is also *the spring of hope*. For the aviation sector to become sustainable, something more then incremental efficiency gains, which are traditionally

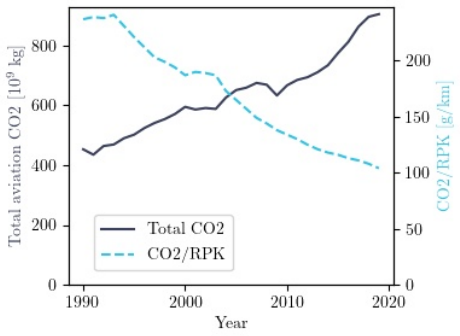

Figure 1.1.: Total CO2 and CO2/RPK emissions from the aviation sector from 1990 to 2020 [21].

economically motivated, are put forward. The organizations within the industry have pledged themselves to drastically reduce their climate impact, by 2050 [23–26]. The European Union and the United States aim for a 90% and 100% reduction in CO2 emissions, respectively [27, 28]. The aim of this thesis is to contribute to the spring of hope, but to also be mindful of the limitations, as shown at the end of the beginning of *A Tale*:

> ... in short, the period was so far like the present period, that some of its noisiest authorities insisted on its being received, for good or for evil, in the superlative degree of comparison only.
>
> *Charles Dickens*

1.2 Sustainable aviation: a flight to the future

The year 2050 appears to be a long time from the present, but meeting these environmental goals requires a large package of measures. A combination of reducing the required energy for flights, changing which energy source is used, and capturing whatever CO2 is still emitted is required. A lot of the technologies and legislation needed for this transition will not be available by the end of the decade, but are promising avenues to large gains. Others can be deployed to reduce emissions in the short to medium term. These measures can bridge the gap until new technologies become widely available. Within the aviation transition, four different streams are present: improvements in aircraft and engine technologies, sustainable aviation fuels (SAFs), operations improvements, and economic measures.

How aircraft are designed and which fuels are used are the two most important factors for the aviation environmental impact. As can be seen in Figure 1.1, past innovations have already significantly improved the aircraft: these are more fuel

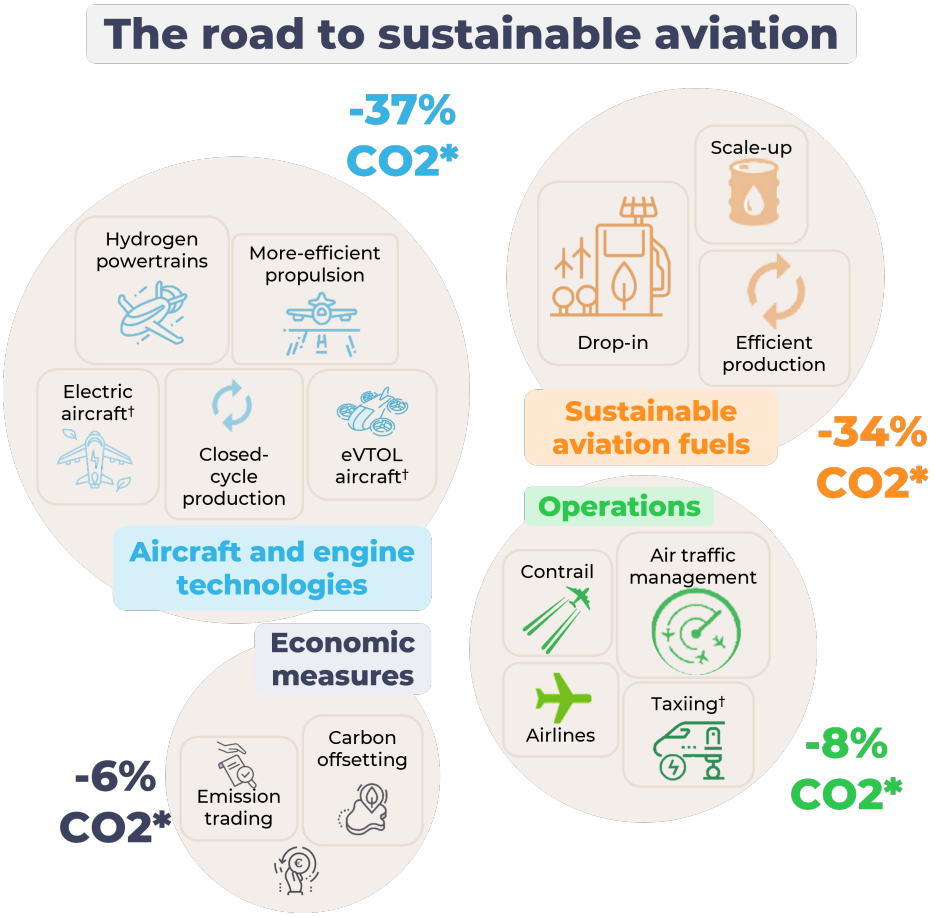

Figure 1.2.: Pathways to reducing aviation climate impact. *: CO_2 reduction share by 2050, based on Destination 2050 [29]. †: addressed in this thesis.

efficient and quieter then ever-before. Incremental innovations in engine and wing design [30], the introduction of new composite materials [31], radical new aircraft designs [32], and sustainable fabrication methods can further reduce emissions without a different powertrain. Combined, these improvements are estimated to reduce fuel burn by 30% compared to the existing generation [29].

Though these aircraft would be more efficient, they still contribute to climate change by using fossil fuels. Using alternative fuels removes most of the other emissions. These are: sustainable aviation fuels (SAFs), hydrogen, and electricity. SAFs are a synthesized [33–36] are almost net-zero. These fuels can be used in existing aircraft on their own, or mixed with kerosene. This enables intercontinental aviation with large passenger volumes. Due to range limitations, hydrogen-powered aircraft form an opportunity for short-haul flights [29]. The hydrogen is either

burned in a jet-engine [37], or used by a fuel cell to generate electricity for a propeller [38, 39]. Last, (hybrid-)electric aircraft form an opportunity for small regional lines, business jets, or personal transportation. These carry a battery which supplies electricity to a propeller [40, 41]. An interesting application of electricity is the electric vertical take-off and landing aircraft, which substitutes helicopters and drones [42]. Together with a reduction in demand by introducing these technologies, these new aircraft with different energy sources contribute to 84% of the projected CO2 reduction by 2050 [29]. But unfortunately, these will only be widely available on a longer term.

While waiting for improved aircraft designs and alternative energy sources, improved operations and economic measures can reduce aviation's climate impact on the short term. Improved operations entail more efficient use of assets by airlines, zero-emission taxiing, improved air traffic management (ATM), and reducing the influence of contrails. Within Europe, the implementation of the Single European Sky (SES) and the SES ATM Research program (SESAR) enable technologies that reduce CO2 emissions both during taxiing and in flight [43]. Economic measures put a price on emissions, ensuring that airlines/manufacturers take the climate-impact of their operations into account. For this, the ICAO carbon offsetting scheme for international aviation (CORSIA) covers international flights since 2021. Additionally, the emissions trading system (ETS) caps and reduces emissions for all flights within the European Economic Area [44]. Together, these measures constitute the remaining 14% of CO2 reductions by 2050.

1.3 Electrifying aviation: short-term gains and long-term revolutions

This thesis aims to contribute towards climate-neutrality of aviation by evaluating three concepts with which the industry can electrify. These technologies range from being close to implementation and providing relatively quick and straightforward pathways to mitigate the effects, to radically reforming the market.

Concept 1: electric taxiing, reducing ground emissions in current operations

At the moment, aircraft use one or both their engines to navigate around the airport, taxiing As the engines are optimized for the flight-phase, taxiing with them yields a very low efficiency [45, 46]. As such, studies found that 7% of the total flight fuel use can be attributed to taxiing [47, 48], a percentage which is way larger then the distance traversed. It is in this phase that a relatively quick way to reduce emissions can be found.

Electric taxiing systems are a promising way to reduce these emissions [48, 49]. By using these technologies, the jet engines are not used to propel the aircraft. Of electric taxiing systems, two variants exist: internal (on-board) and external systems.

First, Internal systems employ a motor within the aircraft's landing gear, which is powered by an on-board power supply. They require a change to the aircraft, but a minimal change to airport operations. An example can be seen in Figure 1.3a. Second, external systems, called Electric Taxiing Vehicles (ETVs) tow the aircraft along the taxiway. They require a minimal change to the aircraft, but a large change in air-side operations. An example can be seen in Figure 1.3b. These technologies already exist and are implemented at airports [50, 51]. Directives for operational implementation of these vehicles have been studied as well [52].

Concept 2: electric aircraft, towards zero airborne pollution

If electric taxiing and other operational improvements with *existing* aircraft are successfully implemented, the climate-impact of aviation with decrease by roughly a third [29]. As such, two third of the climate impact is still unaccounted for. On the long term, the path to a sustainable aviation sector will have to include radical new aircraft designs. A large number of intracontinental flights can be replaced by creating and improving high-speed rail connectivity [55–58]. Of the remaining flights, hydrogen aircraft seem feasible for long distances. For short distance flights with lower passenger volumes, however, electric aircraft (eAC) are an attractive technology [40, 59, 60].

The advantages inherit to electric aircraft stem from the simplicity of the design. Analogous to electric cars, the powertrain of an eAC has a reduced number of moving components. It lacks, e.g., a gearbox, fuel pump and cylinders [61, 62]. This enables eAC to have a high energy efficiency, as there is less energy wasted in moving components [63, 64]. As a consequence, fuel costs are lower then for conventional vehicles. Additionally, the reduction of the number of components also reduces the maintenance required for the vehicles. This reduces the down-time of the eAC, as well as the associated maintenance costs [65, 66]. Concluding, after a higher initial investment, eAC can be operated at a lower cost when compared to their conventional counterparts.

Considering these advantages, eAC present an opportunity for regional aviation [67, 68]. Regional, or commuter, airlines operate smaller aircraft over shorter distances. A number of these airlines have shown interest in acquiring an eAC and assisting in its development [69]. An example of an electric aircraft is shown in Figure 1.4.

Concept 3: electric urban air mobility, a whole new mode of transport

The first two techniques we discussed are ways in which current aviation operations can become more sustainable. This is not the case for the last one: eVTOLs. Across the world, urbanization is taking place. Now, more people live in cities then outside of them [70–72]. Against this background, urban congestion is becoming a serious problem. Urban Air Mobility (UAM) is an envisioned air transportation concept,

(a) The WheelTug, an example of an internal towing system [53].

(b) The TaxiBot, an example of an external towing system (an ETV)[54].

Figure 1.3.: Examples of aircraft towing systems.

Figure 1.4.: The Eviation Alice, the first 10 passenger pure-electric aircraft (image: Eviation).

where innovative aircraft could safely and efficiently transport passengers and cargo within urban areas by rising above traffic congestion on the ground [73]. This can be done sustainably by using electric Vertical Take-Off and Landing (eVTOL) vehicles.

More than 150 companies are in the process of developing prototypes in a fierce competition between startups, including Kitty Hawk (US), Lilium (Germany), Joby Aviation (US), E-Hang (China), Volocopter (Germany), as well as large firms like Airbus (with a special A3 by Airbus located in Silicon Valley), Boeing (US), Bell (US) and Embraer (Brazil) [74]. An example of an eVTOL can be seen in Figure 1.5.

Technology markers: Each of the technologies is given it's own marker. Chapters concerning electric towing vehicles (ETVs) are given maker . Chapters concerning electric aircraft are labeled . Chapters discussing eVTOLs are labeled .

Figure 1.5.: eVTOL concept by Beta Technologies [75].

1.4 The challenges of electric aviation operations planning

Many types of airline and airport operations have been standard practices for decades. However, the technologies introduced in Section 1.3 bring new operations and with them, new challenges. Two of these are discussed in this thesis.

Challenge 1: Battery performance limitations

Today, commercial aviation exists by the grace of its operational efficiency: the ability to take its assets, and use them as often and as useful as possible [76]. An indication of how important this is, is given by budget airlines. Before the Covid-19 pandemic, these airlines were the most profitable airlines in the United States and the European continent, with a margin of around €0.13 per available seat per traveled kilometer (ASK). This was possible because these aircraft were used with little down time: around 12 daily flying hours per aircraft. After the pandemic, this only dropped to 10.5 hours, but this drop of around 10 percent caused all its profit margins to vanish [77].

In this light, the introduction of electric vehicles into aviation presents a challenge. The reason for this is twofold. The first is the fallout of the low energy density (both volumetric and gravimetric) of batteries, compared to petrol and kerosene. Currently, the most considered option for aviation application, Li-ion batteries, carry 0.2-0.3 kWh/kg and 0.6 kWh/L [78], compared to 12 kWh/kg and 9.7 kWh/L for kerosene [79]. As such, the amount of energy on a vehicle is limited, resulting in a limited range and a requirement to increase the number of stops. Second, recharging electric vehicles takes significantly longer then refuelling their combustion-engine equivalents. Because of this, they are unavailable for a significant portion of the day. A comparison of the performances of electric towing vehicles, aircraft, and eVTOLS, and their combustion-engine counterparts is given in Table 1.1.

Given the performance limitations, it is of paramount importance to use these electric technologies as efficient as possible. Regardless of the application, this requires a fluid schedule which is, given the available assets, robust for

Application	Powertrain*	Vehicle	Energy [kWh]	Charging/fueling time [min]
Aircraft (10 pax)	E	Eviation Alice	800	60 [80]
	ICE	Csessna 402	7600	15 [81]
Aircraft towing vehicle	E	TaxiBot NB	400	120 [82]
	ICE	TMX-550 tractor	3000	5 [83]
Urban air mobility	E	Honda eVTOL	200	60 [84]
	ICE	Airbus H120	4000	15 [85]

*) E: electric, ICE: internal combustion engine

Table 1.1.: Range and charging/fueling time for electric and internal combustion engine vehicles.

operational disruptions. Algorithms to plan operations which both account for the limitations imposed by batteries and real-world uncertainties are currently missing or underdeveloped.

These scheduling challenges are multi-stage problems, as shall further discussed in Section 1.6. As such, solving these problems requires an interconnected approach: a multi-stage predict-then-optimize formulation. In this approach, the decisions in each stage are made in anticipation of the impact these have during the next stage. Given that this impact cannot always determined deterministically, estimates for this will have to be made. This can be done separately from the optimization problem, or in an integrated, end-to-end framework [86]. Once these estimates are determined, they are used to plan operations. Different frameworks have been developed to perform this. Of these frameworks, (two- or multi-stage) Stochastic Programming and (Adaptive) Robust Optimization are the most generally applicable, but problem-dependent frameworks have also been developed [87, 88]. The models and algorithms which we develop to the presented challenges all fit within this framework of multi-stage predict-then-optimize.

Creating a schedule for a fleet of assets to perform a set of tasks which need to be performed at a given time can be formulated as a *Vehicle Routing Problem with Time Windows* (VRP-TW) [89, 90]. Typical objectives for this problem are the minimization of the number of required vehicles [91] or the transportation costs [92]. In parallel, two branches of the VRP problem have been researched: the *Electric* VRP-TW (or E-VRP-TW) and the *stochastic* VRP-TW. In an E-VRP-TW, vehicles are equipped with a battery which needs to be recharged, taking a significant amount of time [93]. Algorithms considered for this problem are the branch price-and-cut [94] and adaptive large neighbourhood search [95]. Stochastic VRP-TWs consider situations in which some parameters are given as random variables whose distributions are known [96]. Some studies consider a *dynamic* setting, in which case these parameter distributions change over time. These are addressed using local descent algorithm [97] or robust optimization [92]. Only a few studies consider a stochastic or dynamic E-VRP-TW. Uncertainties in transfer and recharging time are addressed in these studies [98, 99]. None of these studies, however, has discussed how uncertainties

in time windows can be addressed. Bridging this research gap and expanding the models to accommodate electric assets is a key challenge.

For charging infrastructure sizing, existing studies focus on a single-stage approach [100–104]. In these approaches, the infrastructure is optimized for a single mode of operations, i.e. a single flight schedule. A baseline for the total electricity demand has been determined by Lindberg et al. [102, 103]. To mitigate the infrastructure requirements, the infrastructure for a battery swapping system has been studied [100, 101]. However, by using a single stage approach, these studies ignore the fact that charging infrastructure has to be developed prior to the flight schedule. As such a multi-stage optimization approach, which takes the flight schedule variability into account is required. The two-stage concept has been developed for on-demand charging operations (e.g. for electric consumer vehicles) [105–107], based on stochastic inter-arrival times. This is performed using queuing and scheduling theory. However, the mode of operations for airlines has not been studied in this context. Bridging this gap is the main challenge for the sizing of charging infrastructure at airports.

Challenge 2: Battery maintenance concerns

The most important obstacles to the introduction of new technologies in aviation are safety concerns [108]. This holds especially for concepts which are not an incremental upgrade of existing operations, but comprise a different technology all-together, like the ones discussed in Section 1.3. The introduction of batteries to aviation operations introduces new risks, which need to be managed: batteries need to be able to achieve a given performance level, and cannot fault while airborne. In order to avoid this, maintenance procedures are required. As such, the second main challenge which is addressed in this thesis concerns the prognostics and health management (PHM) of using battery-powered vehicles in aviation. By using data-driven approaches for fault detection and forecasting, PHM has been shown to reduce the risk of breakdowns while minimizing maintenance costs [109, 110].

In recent years, studies have started to focus on the estimation of the state-of-health (SOH) of batteries from sensor data [111–113]. These estimates are extrapolated to determine the remaining number of cycles during which the battery can be safely operated. These estimates can be used as input data for maintenance planning in a predictive maintenance framework [114]. However, most of these studies are limited to batteries subject to a constant load. This is opposed to airborne operations, where batteries are put under large loads in the landing and take-off phases. A few recent studies have developed SOH estimations for airborne operations [**mitici??**, 115, 116]. These studies have however not addressed how the SOH prognostics can be implemented in operations scheduling, a research gap identified by Patrizi et al. [117]. The absence of frameworks and algorithms for predictive battery maintenance in aviation is a key research gap which is addressed in this thesis.

1.5 Designing operations planning algorithms: Research objective

The previous section highlighted the interest in operations optimization algorithms for electric vehicles in the aviation domain. Considering the need to decarbonize the industry, these algorithms would provide insight into the effects of integrating electric vehicles into current operations. Hence, the research design objective of this dissertation is:

Main Research Objective

The design of data-driven models to perform operations planning of the above-mentioned technologies, integrated into current operations, for optimal efficiency.

In this objective, the term efficiency refers to the utilization of the technologies, but is context-dependent. In general, the term implies the highest possible use of the assets while causing minimum disturbances for the users (the passengers).

The research objective is divided into three sub-objectives, each corresponding to an aspect of aviation operations: asset routing and assignment, infrastructure sizing, and maintenance operations planning. Figure 1.6 provides an overview of the research objectives, combined with the chapters in which they are addressed.

1.5.1 Objective 1: Electric asset routing and assignment

The introduction of electric vehicles into operations requires knowledge on what to do when the batteries run empty. As such, we formulate the first sub-objective:

Research Objective 1.1

To design a charging policy for electric towing vehicles, in order to tow as many aircraft as possible.

Secondly, the introduction of all these vehicles increases the amount of traffic on the taxiways, which need to be processed with as little delays as possible. Addressing this issue is the second objective:

Research Objective 1.2

To design a centralized on-line routing algorithm for electric towing vehicles, which minimizes the total towing time, for a given airport and flight schedule.

The results of these two objectives are integrated into an application that maximizes the use of the ETVs:

Research Objective 1.3

To design an online aircraft-to-ETV assignment model that minimizes the taxiing emissions using an ETV fleet of a given size, while also minimizing taxiing disruptions, flight schedule.

All these three objectives are related to the final question of determining the required and optimal size of an ETV fleet for an airport. These objectives are addressed in Chapters 2, 3 and 4.

Objective 2: Charging infrastructure scheduling and planning

In order to determine the required charging infrastructure for an airport, we need to know how to best make use of an infrastructure of a certain size on a certain day. This is performed in the first objective:

Research Objective 2.1

To design a model to optimize the battery charging operations for a given charging infrastructure and day of operations, assuming a battery swapping system, for minimal operational costs.

Using this information, we can determine the optimal charging infrastructure over all days of operations:

Research Objective 2.2

To design a model to determine the optimal charging infrastructure size for a given airport, assuming a battery swapping system, for minimal investment and operational costs.

These objectives are addressed in Chapter 5.

Objective 3: Battery maintenance planning

In order to know when to replace the batteries, we need to know when they are unsafe for use. This is done based on sensor measurements. At any moment, we can determine if a battery should be used or not. However, maintenance cannot be planned on the spot, but needs to be planned days/weeks in advance (based on the application). As such, we aim to develop an algorithm which predicts when a battery will become inoperable.

Research Objective 3.1

To develop a prognostics and health management model for batteries.

Using this information, we aim to develop an algorithm which plans the maintenance for the batteries. This planning algorithm should use batteries as long as possible, but should also avoid battery failures:

Research Objective 3.2

To develop a planning model which uses these prognostics to perform maintenance planning for a fleet of vehicles operating from a central hub airport, for minimal operational costs.

These objectives are addressed in Chapters 6 and 7.

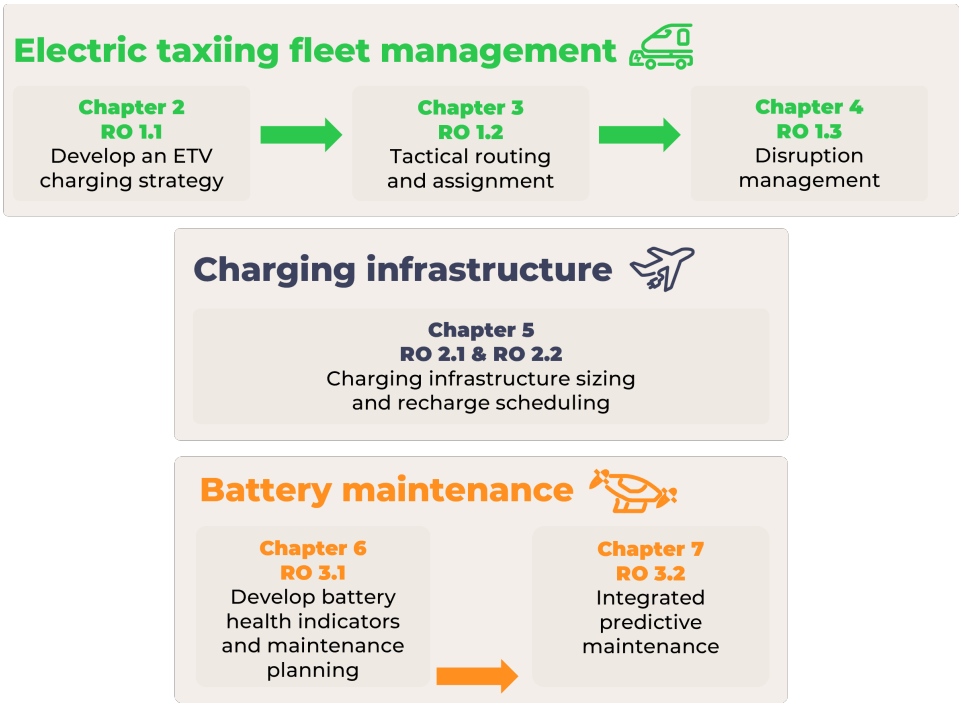

Figure 1.6.: Overview of the challenges addressed in this dissertation, together with the chapters in which these are discussed.

1.6 Research approach and scope

In this thesis, we consider three problems related to technologies introduced in Section 1.3: managing a fleet of electric towing vehicles (ETV), managing charging operations for electric aircraft (eAC), and maintenance planning for batteries for a fleet of electric vertical take-off and landing aircraft (eVTOL).

1

Each problem is considered from three planning phases: the strategical-, tactical-, and operational planning phase. During the strategical phase, long-term decisions are made. Infrastructure development and fleet acquisition is done in this phase. During the tactical phase, medium-long term decisions are made. The assets (infrastructure and vehicle fleets) are fixed, as is the demand, and this planning phase deals with assigning the assets to fulfill the demand as best as possible. During the operational phase, real-time decisions are made. It addresses the problem of responding when delays, or other disruptions, occur. As before, the assets and demand are fixed, but changes do occur that obstruct an optimal use. During the strategical and tactical planning phase, the events that can arise during the operational phase should be taken into account.

Planning phase indicators for chapters: We have introduced three planning phases: strategic (master-planning , sizing, and infrastructure acquisition), tactical (timetabling, assignment), and operational (disruption management). Chapters are labeled if they consider strategic, if they consider tactic, and if they consider operational planning.

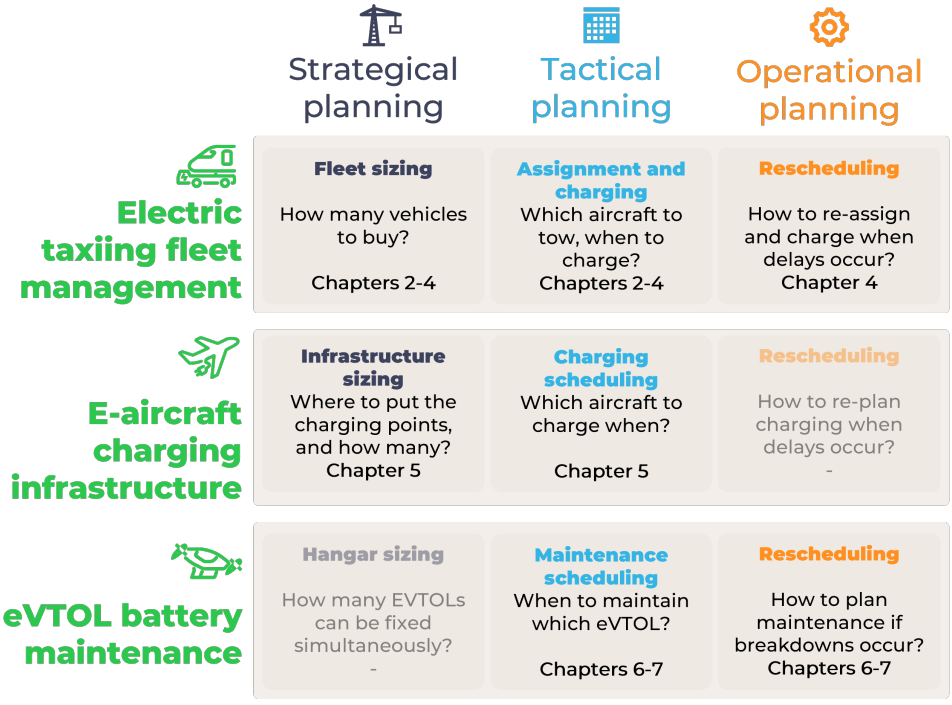

Figure 1.7.: Overview of the planning problems addressed in this dissertation.

This thesis addresses the three infrastructure/asset sizing and scheduling problems mentioned above, with a focus on the inter-connectivity of the three planning phases.

For the ETV scheduling problem, the strategical phase considers the question of how many ETVs are required at an airport. Next, the tactical phase considers the assignment of ETVs to aircraft as well as determining when to recharge the ETVs. This is done to reduce taxiing emissions as much as possible, while minimizing the extra taxiing time. These two phases are addressed in Chapter 2-4 of this thesis. Last, during the operational phase, this schedule is performed, and adapted whenever disruptions occur. How this can be done, how disruptions can be anticipated in the schedule, and how this influences ETV fleet sizing is addressed in Chapter 4. The problem is approached as a nested rolling horizon mixed-integer linear program.

For the eAC battery swapping and charging problem, a fleet of electric aircraft with swappable batteries need to be recharged as efficiently as possible. During the strategical phase, one considers the sizing of the charging capacity and the number of spare batteries at each airport. During the tactical phase, the flight schedule is known, and one needs to decide how to use this infrastructure in such a way that electricity costs and delays are minimized. These two phases addressed in Chapter 5. It is addressed as a two-stage stochastic programming problem. This schedule is performed, and when disruptions occur, the operational problem considers the schedule recovery. This is not addressed in this thesis.

Last, for the battery maintenance problem, predictive maintenance is modeled for a fleet of eVTOLs. During operations, eVTOL batteries degrade and need to be replaced before breakdown. The batteries are monitored, and the sensors provide information on the state-of-health of the battery. Using this information, the battery breakdown time can be predicted, and based on this and the hangar capacity, maintenance can be planned. During the strategical phase, the hangar capacity and number of required eVTOLs for operations are determined. This is not addressed in this thesis. During the tactical phase, a maintenance schedule is created based on the last known battery data. During the operational phase, this schedule is adapted once breakdowns occur. These stages are addressed in Chapters 6 and 7 of this Thesis.

1.7 Outline of the thesis

This dissertation aims at providing methods to model operations of the electric aviation technologies introduced in section 1.3, and to design algorithms that address the challenges posed in Section 1.4. These contribute towards the objectives mentioned in Section 1.5. An overview of this thesis is shown in Figure 1.6. To assist in navigating through the chapters, chapter markers are used:

Chapters 2 through 4 consider the routing and assignment problem for electric vehicles, and are applied to ETVs (1.3). The final result of this chapters is a framework which models ETV operations at a large airport, within the scope mentioned in Section 1.6. A fleet of ETVs is operated in such a way that the taxiing emissions are minimized. The planning framework considers all three planning

phases. The result is applied in a case study at Amsterdam Airport Schiphol.

Chapter 2 starts with formulating a tactical ETV operations model and an ETV to aircraft assignment algorithm. The objective of the assignment algorithm is to minimize the number of vehicles which need to be deployed to tow all aircraft. As such, it also considers the strategic planning problem of fleet sizing. This model and algorithm serve as the starting point from which frameworks of the subsequent chapters are created. Basic assumptions are made regarding the vehicle dynamics. Three charging policies are developed and tested using this framework, and the optimal charging policy is used in further chapters (objective 1.1).

Based on the optimal charging policy determined in chapter 2, a comprehensive tactical ETV operations model is created in Chapter 3. A day at an airport is considered, with a fixed flight schedule. These flights need to be towed by ETVs. ETV operations is modeled as a series of two Mixed-Integer Linear Programs. The first of these routes the ETVs and aircraft across the airport such that collisions are avoided (objective 1.2). This is done with the objective of minimizing the total driving and towing time. The second uses the model from Chapter 2 to assign ETVs to aircraft. Again, the objective is to minimize the required number of ETVs. A rolling horizon schedule recovery is made. This model is the first step towards objective 1.3.

The framework from Chapter 3 is able to plan ETV operations, but has access to an unlimited amount of ETVs. However, in reality, ETVs are acquired years before the actual day of operations, and their number cannot be easily varied from day to day. Furthermore, the algorithm used is able to deal with disruptions, but is not able to anticipate them. To overcome these limitations, this model and solution algorithm were expanded upon in Chapter 4. The model assumes a flight schedule, where arrival and departure times can be updated during the day, and the ETV schedule can be modified to react to it. A fixed-sized ETV fleet is assumed. The assignment algorithm anticipates disruptions while creating the ETV schedule. Using this model, a cost-benefit analysis for the number of ETVs at the airport is performed, combining all three planning phases.

Chapter 5 discusses the charging infrastructure required to facilitate the transition to electric aviation. The framework encompasses both the tactic and strategic planning phases. During the tactic planning phase, a scheduling algorithm determines how to use existing charging infrastructure efficiently: causing as little delay as possible and using electricity during off-peak hours. This contributes towards objective 2.1 This model is embedded in a strategic framework which performs a cost-benefit analysis on the size of the infrastructure, thereby contributing towards objective 2.2. The model is applied to an airline operating electric aircraft.

Last, in Chapters 6 and 7, a predictive maintenance scheduling framework for batteries is developed. This framework encompasses the tactical and operational planning phases. It studies how sensor measurements from batteries used in aviation

can be used to predict the breakdown time. This information is then integrated into the maintenance schedule for optimal utilization of the batteries. Chapter 6 discusses a conventional framework in which these two problems are solved sequentially. Chapter 7 introduces an integrated method for this predictive maintenance problem. These frameworks are applied to eVTOL batteries, and contribute towards objectives objective 3.1 and objective 3.2.

Chapter 8 brings the findings from the three research lines together, and discusses these in the context of the sustainability of the aviation sector. Other aspects, such as the ones outside the scope from Section 1.6 are discussed. Furthermore, it summarizes the most important conclusions of the thesis, with respect to the research objectives (Section 1.5) and provides recommendations for future studies.

references

[1] C. Dickens. *A Tale of Two Cities*. James Nisbet & Company, Limited, 1902. URL: https://books.google.nl/books?id=5EIPAAAAQAAJ.

[2] International Air Transport Association. *Global Outlook for Air Transport*. Tech. rep. Montreal: IATA, 2024. URL: https://www.iata.org/en/iata-repository/publications/economic-reports/global-outlook-for-air-transport-june-2024-report/.

[3] R. V. Petrescu, R. Aversa, B. Akash, R. Bucinell, A. Apicella, and F. I. Petrescu. *History of Aviation - A Short Review*. en. SSRN Scholarly Paper. Rochester, NY, Nov. 2017. URL: https://papers.ssrn.com/abstract=3073974 (visited on 12/02/2024).

[4] J.-P. Rodrigue. *The Geography of Transport Systems*. en. 6th ed. Routhledge, 2024. ISBN: 978-1-03-238040-7. URL: https://www.routledge.com/The-Geography-of-Transport-Systems/Rodrigue/p/book/9781032380407 (visited on 12/04/2024).

[5] R. A. Zachariah, S. Sharma, and V. Kumar. "Systematic review of passenger demand forecasting in aviation industry". en. In: *Multimedia Tools and Applications* 82.30 (Dec. 2023), pp. 46483–46519. ISSN: 1573-7721. DOI: 10.1007/s11042-023-15552-1. URL: https://doi.org/10.1007/s11042-023-15552-1 (visited on 12/02/2024).

[6] N. Careen, M. Searle, and A. Poehlitz. *IATA Annual Safety Report*. Tech. rep. 60. Montreal: IATA, 2023. URL: https://www.iata.org/contentassets/a8e49941e8824a058fee3f5ae0c005d9/safety-report-executive-and-safety-overview-2023.pdf.

[7] J. Penner, D. Lister, D. Griggs, D. Dokken, and M. McFarland. *Aviation and the Global Atmosphere*. Tech. rep. Intergovernmental Panel on Climate Change, 1999. URL: https://www.ipcc.ch/site/assets/uploads/2018/03/av-en-1.pdf.

[8] D. S. Lee, D. W. Fahey, P. M. Forster, P. J. Newton, R. C. N. Wit, L. L. Lim, B. Owen, and R. Sausen. "Aviation and global climate change in the 21st century". In: *Atmospheric Environment* 43.22 (2009). Number: 22, pp. 3520–3537. ISSN: 1352-2310. DOI: https://doi.org/10.1016/j.atmosenv.2009.04.024. URL: http://www.sciencedirect.com/science/article/pii/S1352231009003574.

[9] H. Ritchie and M. Roser. "What share of global CO2 emissions come from aviation?" In: *Our World in Data* (Apr. 2024). URL: https://ourworldindata.org/global-aviation-emissions (visited on 12/02/2024).

[10] F. D. A. Quadros, M. van Loo, M. Snellen, and I. C. Dedoussi. “Nitrogen deposition from aviation emissions”. In: *Science of The Total Environment* 858 (Feb. 2023), p. 159855. ISSN: 0048-9697. DOI: 10.1016/j.scitotenv.2022.159855. URL: https://www.sciencedirect.com/science/article/pii/S0048969722069558 (visited on 12/02/2024).

[11] C. Witham, N. Kristiansen, F. Beckett, and F. Marenco. *Towards a global sulphur dioxide forecast capability for aviaiton*. Tech. rep. 648. Exeter, United Kingdom: Met Office, Oct. 2021.

[12] D. K. Singh, S. Sanyal, and D. J. Wuebbles. “Understanding the role of contrails and contrail cirrus in climate change: a global perspective”. English. In: *Atmospheric Chemistry and Physics* 24.16 (Aug. 2024). Publisher: Copernicus GmbH, pp. 9219–9262. ISSN: 1680-7316. DOI: 10.5194/acp-24-9219-2024. URL: https://acp.copernicus.org/articles/24/9219/2024/ (visited on 12/02/2024).

[13] UNCA. “Causes and Effects of Climate Change”. In: *United Nation Climate Action* (2024). URL: https://www.un.org/en/climatechange/science/causes-effects-climate-change.

[14] I. Anguelovski, E. Chu, and J. Carmin. “Variations in approaches to urban climate adaptation: Experiences and experimentation from the global South”. In: *Global Environmental Change* 27 (July 2014), pp. 156–167. ISSN: 0959-3780. DOI: 10.1016/j.gloenvcha.2014.05.010. URL: https://www.sciencedirect.com/science/article/pii/S095937801400106X (visited on 12/04/2024).

[15] T. Malmqvist. *People in Global South are most worried about climate change, survey finds*. en-US. Sept. 2024. URL: https://globescan.com/2024/09/11/insight-of-the-week-public-concern-for-climate-change-by-region/ (visited on 12/04/2024).

[16] K. Richardson. *Global South Countries are more Vulnerable to Climate Change than we are in the North – DDRN*. en-GB. Aug. 2024. URL: https://ddrn.dk/16310/ (visited on 12/04/2024).

[17] J. I. Hileman, E. De la Rosa Blanco, P. A. Bonnefoy, and N. A. Carter. “The carbon dioxide challenge facing aviation”. In: *Progress in Aerospace Sciences* 63 (Nov. 2013), pp. 84–95. ISSN: 0376-0421. DOI: 10.1016/j.paerosci.2013.07.003. URL: https://www.sciencedirect.com/science/article/pii/S0376042113000663 (visited on 12/02/2024).

[18] J. Singh, S. K. Sharma, and R. Srivastava. “Managing Fuel Efficiency in the Aviation Sector: Challenges, Accomplishments and Opportunities”. en. In: *FIIB Business Review* 7.4 (Dec. 2018). Publisher: SAGE Publications India, pp. 244–251. ISSN: 2319-7145. DOI: 10.1177/2319714518814073. URL: https://doi.org/10.1177/2319714518814073 (visited on 12/02/2024).

[19] F. Afonso, M. Sohst, C. M. A. Diogo, S. S. Rodrigues, A. Ferreira, I. Ribeiro, R. Marques, F. F. C. Rego, A. Sohouli, J. Portugal-Pereira, H. Policarpo, B. Soares, B. Ferreira, E. C. Fernandes, F. Lau, and A. Suleman. “Strategies towards a more sustainable aviation: A systematic review”. In: *Progress in Aerospace Sciences* 137 (Feb. 2023), p. 100878. ISSN: 0376-0421. DOI: 10.1016/j.paerosci.2022.100878. URL: https://www.sciencedirect.com/science/article/pii/S0376042122000707 (visited on 12/02/2024).

[20] C. S. Webster, R. Henderson, and A. F. Merry. “Sustainable quality and safety improvement in healthcare: further lessons from the aviation industry”. English. In: *British Journal of Anaesthesia* 125.4 (Oct. 2020). Publisher: Elsevier, pp. 425–429. ISSN: 0007-0912, 1471-6771. DOI: 10.1016/j.bja.2020.06.045. URL: https://www.bjanaesthesia.org/article/S0007-0912(20)30505-5/fulltext (visited on 12/02/2024).

[21] ATAG. *Fact sheet #3: Tracking aviation efficiency*. Tech. rep. Aivation Benefits, Feb. 2021. URL: https://aviationbenefits.org/media/167475/fact-sheet_3_tracking-aviation-efficiency-v2.pdf.

[22] IATA. *Global Outlook for Air Transport*. Tech. rep. Montreal: IATA, 2022. URL: https://www.iata.org/en/iata-repository/publications/economic-reports/global-outlook-for-air-transport---december-2022/ (visited on 05/01/2023).

[23] UNFCCC. *Paris Agreement*. Tech. rep. Paris: United Nations, 2015. URL: https://unfccc.int/sites/default/files/english_paris_agreement.pdf (visited on 06/23/2021).

[24] UNFCCC. *International Aviation Climate Ambition Coalition - COP26 Declaration*. https://ukcop26.org/cop-26-declaration-international-aviation-climate-ambition-coalition/. Nov. 2021. (Visited on 01/12/2022).

[25] IATA. *Resolution on the Implementation of the Aviation “CNG2020” Strategy*. 2013. URL: https://www.iata.org/contentassets/e8a7f8d96c554acd8e5fbbc09eb56559/agm69-resolution-cng2020.pdf.

[26] ICAO. *Consolidated statement of continuing ICAO policies and practices related to environmental protection – Climate change*. 2010. URL: https://www.icao.int/environmental-protection/37thAssembly/A37_Res19_en.pdf.

[27] European Union. *Long-term low greenhouse gas emission development strategy or the European Union and its Member States*. Tech. rep. Zagreb: European Union, Mar. 2020.

[28] Gina McCarthy. *The long-term strategy of the United States: Pathways to Net-Zero Greenhouse Gas Emissions by 2050*. Tech. rep. Washington D.C.: United States Department of State and the United States Executive Office of the President, Nov. 2021.

[29] NLR and SEO. *Destination 2050 - a route to net zero european aviation*. Tech. rep. Brussels, Belgium: European Commisision, 2021.

[30] K. Abu Salem, G. Palaia, and A. A. Quarta. “Review of hybrid-electric aircraft technologies and designs: Critical analysis and novel solutions”. In: *Progress in Aerospace Sciences*. Special Issue on Green Aviation 141 (Aug. 2023), p. 100924. ISSN: 0376-0421. DOI: 10.1016/j.paerosci.2023.100924. (Visited on 12/19/2024).

[31] B. Parveez, M. I. Kittur, I. A. Badruddin, S. Kamangar, M. Hussien, and M. A. Umarfarooq. “Scientific Advancements in Composite Materials for Aircraft Applications: A Review”. en. In: *Polymers* 14.22 (Jan. 2022). Number: 22 Publisher: Multidisciplinary Digital Publishing Institute, p. 5007. ISSN: 2073-4360. DOI: 10.3390/polym14225007. (Visited on 12/19/2024).

[32] W. Oosterom and R. Vos. “Conceptual Design of a Flying-V Aircraft Family”. In: *AIAA AVIATION 2022 Forum*. _eprint: https://arc.aiaa.org/doi/pdf/10.2514/6.2022-3200. American Institute of Aeronautics and Astronautics, 2022. DOI: 10.2514/6.2022-3200. URL: https://arc.aiaa.org/doi/abs/10.2514/6.2022-3200 (visited on 12/19/2024).

[33] S. Hamdan, O. Jouini, A. Cheaitou, Z. Jemai, T. A. Granberg, and B. Josefsson. “Air traffic flow management under emission policies: Analyzing the impact of sustainable aviation fuel and different carbon prices”. en. In: *Transportation Research Part A: Policy and Practice* 166 (Dec. 2022), pp. 14–40. ISSN: 0965-8564. DOI: 10.1016/j.tra.2022.09.013. URL: https://www.sciencedirect.com/science/article/pii/S0965856422002476 (visited on 12/13/2022).

[34] K. S. Ng, D. Farooq, and A. Yang. “Global biorenewable development strategies for sustainable aviation fuel production”. In: *Renewable and Sustainable Energy Reviews* 150 (Oct. 2021), p. 111502. ISSN: 1364-0321. DOI: 10.1016/j.rser.2021.111502. URL: https://www.sciencedirect.com/science/article/pii/S1364032121007814 (visited on 12/04/2024).

[35] L. Zhang, T. L. Butler, and B. Yang*. “Recent Trends, Opportunities and Challenges of Sustainable Aviation Fuel”. en. In: *Green Energy to Sustainability*. Section: 5 _eprint: https://onlinelibrary.wiley.com/doi/pdf/10.1002/9781119152057.ch5. John Wiley & Sons, Ltd, 2020, pp. 85–110. ISBN: 978-1-119-15205-7. DOI: 10.1002/9781119152057.ch5. URL: https://onlinelibrary.wiley.com/doi/abs/10.1002/9781119152057.ch5 (visited on 12/04/2024).

[36] V. Undavalli, O. B. Gbadamosi Olatunde, R. Boylu, C. Wei, J. Haeker, J. Hamilton, and B. Khandelwal. “Recent advancements in sustainable aviation fuels”. In: *Progress in Aerospace Sciences* 136 (Jan. 2023), p. 100876. ISSN: 0376-0421. DOI: 10.1016/j.paerosci.2022.100876. URL: https://www.sciencedirect.com/science/article/pii/S0376042122000689 (visited on 12/04/2024).

[37] G. Choubey, Y. D, W. Huang, L. Yan, H. Babazadeh, and K. M. Pandey. “Hydrogen fuel in scramjet engines - A brief review”. In: *International Journal of Hydrogen Energy* 45.33 (June 2020), pp. 16799–16815. ISSN: 0360-3199. DOI: 10.1016/j.ijhydene.2020.04.086. (Visited on 12/19/2024).

[38] G. D. Brewer. *Hydrogen Aircraft Technology*. New York: Routledge, Nov. 2017. ISBN: 978-0-203-75148-0. DOI: 10.1201/9780203751480.

[39] B. Khandelwal, A. Karakurt, P. R. Sekaran, V. Sethi, and R. Singh. “Hydrogen powered aircraft : The future of air transport”. In: *Progress in Aerospace Sciences* 60 (July 2013), pp. 45–59. ISSN: 0376-0421. DOI: 10.1016/j.paerosci.2012.12.002. URL: https://www.sciencedirect.com/science/article/pii/S0376042112000887 (visited on 12/02/2024).

[40] B. Sarlioglu and C. T. Morris. “More Electric Aircraft: Review, Challenges, and Opportunities for Commercial Transport Aircraft”. In: *IEEE Transactions on Transportation Electrification* 1.1 (June 2015). Conference Name: IEEE Transactions on Transportation Electrification, pp. 54–64. ISSN: 2332-7782. DOI: 10.1109/TTE.2015.2426499. URL: https://ieeexplore.ieee.org/abstract/document/7098414 (visited on 12/02/2024).

[41] A. W. Schäfer, S. R. H. Barrett, K. Doyme, L. M. Dray, A. R. Gnadt, R. Self, A. O'Sullivan, A. P. Synodinos, and A. J. Torija. "Technological, economic and environmental prospects of all-electric aircraft". en. In: *Nature Energy* 4.2 (Feb. 2019), pp. 160–166. ISSN: 2058-7546. DOI: 10.1038/s41560-018-0294-x. URL: http://www.nature.com/articles/s41560-018-0294-x (visited on 05/03/2022).

[42] B. G. Franciscone and E. Fernandes. "Challenges to the Operational Safety and Security of eVTOL Aircraft in Metropolitan Regions: A Literature Review". en. In: *Journal of Airline Operations and Aviation Management* 2.1 (Aug. 2023). Number: 1, pp. 45–56. ISSN: 2949-7698. DOI: 10.56801/jaoam.v2i1.2. (Visited on 12/19/2024).

[43] T. Bolić and P. Ravenhill. "SESAR: The Past, Present, and Future of European Air Traffic Management Research". In: *Engineering* 7.4 (Apr. 2021), pp. 448–451. ISSN: 2095-8099. DOI: 10.1016/j.eng.2020.08.023. (Visited on 12/19/2024).

[44] X. Fageda and J. J. Teixidó. "Pricing carbon in the aviation sector: Evidence from the European emissions trading system". In: *Journal of Environmental Economics and Management* 111 (Jan. 2022), p. 102591. ISSN: 0095-0696. DOI: 10.1016/j.jeem.2021.102591. (Visited on 12/19/2024).

[45] M. E. J. Stettler, G. S. Koudis, S. J. Hu, A. Majumdar, and W. Y. Ochieng. "The impact of single engine taxiing on aircraft fuel consumption and pollutant emissions". en. In: *The Aeronautical Journal* 122.1258 (Dec. 2018). Publisher: Cambridge University Press, pp. 1967–1984. ISSN: 0001-9240, 2059-6464. DOI: 10.1017/aer.2018.117. URL: https://www.cambridge.org/core/journals/aeronautical-journal/article/impact-of-single-engine-taxiing-on-aircraft-fuel-consumption-and-pollutant-emissions/495FF8A62B2949D921456BC07BA68A64 (visited on 05/08/2023).

[46] M. E. J. Stettler, S. Eastham, and S. R. H. Barrett. "Air quality and public health impacts of UK airports. Part I: Emissions". In: *Atmospheric Environment* 45.31 (Oct. 2011), pp. 5415–5424. ISSN: 1352-2310. DOI: 10.1016/j.atmosenv.2011.07.012. URL: https://www.sciencedirect.com/science/article/pii/S135223101100728X (visited on 12/04/2024).

[47] H. Khadilkar and H. Balakrishnan. "Estimation of aircraft taxi fuel burn using flight data recorder archives". en. In: *Transportation Research Part D: Transport and Environment* 17.7 (Oct. 2012), pp. 532–537. ISSN: 13619209. DOI: 10.1016/j.trd.2012.06.005. (Visited on 11/15/2021).

[48] M. Lukic, P. Giangrande, A. Hebala, S. Nuzzo, and M. Galea. "Review, Challenges, and Future Developments of Electric Taxiing Systems". In: *IEEE Transactions on Transportation Electrification* 5.4 (Dec. 2019). Conference Name: IEEE Transactions on Transportation Electrification, pp. 1441–1457. ISSN: 2332-7782. DOI: 10.1109/TTE.2019.2956862.

[49] N. M. Dzikus, R. Wollenheit, M. Schaefer, and V. Gollnick. "The Benefit of Innovative Taxi Concepts: The Impact of Airport Size, Fleet Mix and Traffic Growth". en. In: *2013 Aviation Technology, Integration, and Operations Conference*. Los Angeles, CA: American Institute of Aeronautics and Astronautics, Aug. 2013. ISBN: 978-1-62410-225-7. DOI: 10.2514/6.2013-4212. (Visited on 11/01/2021).

[50] B. von den Hoff, M. Snellen, and D. G. Simons. "Noise assessment of taxibotted versus conventional taxiing operations using a phased microphone array". In: *INTER-NOISE and NOISE-CON Congress and Conference Proceedings* 263.5 (Aug. 2021), pp. 1152–1163. DOI: 10.3397/IN-2021-1765.

[51] K. Hein and S. Baumann. “ACOUSTICAL COMPARISON OF CONVENTIONAL TAXIING AND DISPATCH TOWING – TAXIBOT´S CONTRIBUTION TO GROUND NOISE ABATEMENT”. en. In: Daejaon, Sept. 2016.

[52] M. Cousy, V. Peyruqueou, C. Pierre, P. Cyrille, D.-B. Vo, J. Garcia, M. Mihaela, S. van Oosterom, A. Sharpanskykh, M. v. D. Burg, P. Roling, E. Spiller, S. Gottofredi, and P. Lanzi. “AEON: Toward a concept of operation and tools for supporting engine-off navigation for ground operations”. en. In: Oct. 2022. URL: https://enac.hal.science/hal-03859908 (visited on 02/20/2024).

[53] Spyros Georgilidakis. *WheelTug – Planes Pushing Themselves Out Of The Gate?* https://mentourpilot.com/wheeltug-planes-pushing-themselves-out-of-the-gate/. Mar. 2021. (Visited on 03/04/2021).

[54] KLM. *Eerste KLM-passagiersvlucht met Taxibot*. https://nieuws.klm.com/eerste-klm-passagiersvlucht-met-taxibot/. Dec. 2024. (Visited on 12/10/2024).

[55] M. Givoni and D. Banister. “Role of the Railways in the Future of Air Transport”. In: *Transportation Planning and Technology* 30.1 (Feb. 2007). Publisher: Routledge _eprint: https://doi.org/10.1080/03081060701208100, pp. 95–112. ISSN: 0308-1060. DOI: 10.1080/03081060701208100. URL: https://doi.org/10.1080/03081060701208100 (visited on 12/04/2024).

[56] S. Singh. “From Planes to Trains — The Era of High-Speed Rail”. en. In: *New Mega Trends: Implications for our Future Lives*. Ed. by S. Singh. London: Palgrave Macmillan UK, 2012, pp. 181–200. ISBN: 978-1-137-00809-1. DOI: 10.1057/9781137008091_10. URL: https://doi.org/10.1057/9781137008091_10 (visited on 12/04/2024).

[57] P. Pellegrini and J. Rodriguez. “Single European Sky and Single European Railway Area: A system level analysis of air and rail transportation”. In: *Transportation Research Part A: Policy and Practice* 57 (Nov. 2013), pp. 64–86. ISSN: 0965-8564. DOI: 10.1016/j.tra.2013.09.004. URL: https://www.sciencedirect.com/science/article/pii/S0965856413001687 (visited on 12/04/2024).

[58] L. Donat. “Connecting Europe with a Rail Renaissance - Eight measures to revive the European rail system”. en. In: (Nov. 2020). Publisher: <bound method Organization.get_name_with_acronym of <Organization: Germanwatch>>. URL: https://policycommons.net/artifacts/1555025/connecting-europe-with-a-rail-renaissance/2244834/ (visited on 12/04/2024).

[59] M. Bazargan. *Airline Operations and Scheduling*. 2nd ed. Surrey: Ashgate Publishing Company, 2010.

[60] N. Thapa, S. Ram, S. Kumar, and J. Mehta. “All electric aircraft: A reality on its way”. en. In: *Materials Today: Proceedings* 43 (2021), pp. 175–182. ISSN: 22147853. DOI: 10.1016/j.matpr.2020.11.611. URL: https://linkinghub.elsevier.com/retrieve/pii/S2214785320392853 (visited on 05/03/2022).

[61] J. G. Hayes and G. A. Goodarzi. *Electric Powertrain: Energy Systems, Power Electronics and Drives for Hybrid, Electric and Fuel Cell Vehicles*. en. Google-Books-ID: tshQDwAAQBAJ. John Wiley & Sons, Feb. 2018. ISBN: 978-1-119-06364-3.

[62] D. Crolla and B. Mashadi. *Vehicle Powertrain Systems*. en. Google-Books-ID: N8rrnOv_kBoC. John Wiley & Sons, Dec. 2011. ISBN: 978-1-119-96102-4.

[63] T. Hofman and C. Dai. “Energy efficiency analysis and comparison of transmission technologies for an electric vehicle”. In: *2010 IEEE Vehicle Power and Propulsion Conference*. ISSN: 1938-8756. Sept. 2010, pp. 1–6. DOI: 10.1109/VPPC.2010.5729082. URL: https://ieeexplore.ieee.org/abstract/document/5729082 (visited on 12/04/2024).

[64] A. Albatayneh, M. N. Assaf, D. Alterman, and M. Jaradat. “Comparison of the Overall Energy Efficiency for Internal Combustion Engine Vehicles and Electric Vehicles”. en. In: *Environmental and Climate Technologies* 24.1 (Jan. 2020), pp. 669–680. ISSN: 2255-8837. DOI: 10.2478/rtuect-2020-0041. URL: https://www.sciendo.com/article/10.2478/rtuect-2020-0041 (visited on 12/04/2024).

[65] Z. Liu, J. Song, J. Kubal, N. Susarla, K. W. Knehr, E. Islam, P. Nelson, and S. Ahmed. “Comparing total cost of ownership of battery electric vehicles and internal combustion engine vehicles”. In: *Energy Policy* 158 (Nov. 2021), p. 112564. ISSN: 0301-4215. DOI: 10.1016/j.enpol.2021.112564. URL: https://www.sciencedirect.com/science/article/pii/S0301421521004341 (visited on 12/04/2024).

[66] M. M. Maciel Monjon and C. Monzu Freire. “Conceptual Design and Operating Costs Evaluation of a 19-seat All-Electric Aircraft for Regional Aviation”. In: *2020 AIAA/IEEE Electric Aircraft Technologies Symposium (EATS)*. Aug. 2020, pp. 1–16. URL: https://ieeexplore.ieee.org/abstract/document/9235144 (visited on 12/04/2024).

[67] J. Eaton, M. Naraghi, and J. G. Boyd. “Market capabilities and environmental impact of all-electric aircraft”. In: *Transportation Research Part D: Transport and Environment* 124 (Nov. 2023), p. 103944. ISSN: 1361-9209. DOI: 10.1016/j.trd.2023.103944. URL: https://www.sciencedirect.com/science/article/pii/S1361920923003413 (visited on 12/04/2024).

[68] S. Baumeister, T. Krstić Simić, and E. Ganić. “Emissions reduction potentials in business aviation with electric aircraft”. In: *Transportation Research Part D: Transport and Environment* 136 (Nov. 2024), p. 104415. ISSN: 1361-9209. DOI: 10.1016/j.trd.2024.104415. URL: https://www.sciencedirect.com/science/article/pii/S1361920924003729 (visited on 12/04/2024).

[69] Woodrow Bellamy III. *Airlines Show Growing Interest in Electric and Hydrogen-Powered Aircraft*. en. July 2021. URL: https://www.aviationtoday.com/2021/07/19/airlines-show-growing-interest-electric-hydrogen-powered-aircraft/ (visited on 12/04/2024).

[70] D. Gu, K. Andreev, and M. E. Dupre. “Major Trends in Population Growth Around the World”. In: *China CDC Weekly* 3.28 (July 2021), pp. 604–613. ISSN: 2096-7071. DOI: 10.46234/ccdcw2021.160. URL: https://www.ncbi.nlm.nih.gov/pmc/articles/PMC8393076/ (visited on 12/04/2024).

[71] E. L. Glaeser. *Urbanization and its Discontents*. Working Paper. Mar. 2020. DOI: 10.3386/w26839. URL: https://www.nber.org/papers/w26839 (visited on 12/04/2024).

[72] M. Wang and N. Debbage. “Urban morphology and traffic congestion: Longitudinal evidence from US cities”. In: *Computers, Environment and Urban Systems* 89 (Sept. 2021), p. 101676. ISSN: 0198-9715. DOI: 10.1016/j.compenvurbsys.2021.101676. URL: https://www.sciencedirect.com/science/article/pii/S0198971521000831 (visited on 12/04/2024).

[73] L. A. Garrow, B. J. German, and C. E. Leonard. “Urban air mobility: A comprehensive review and comparative analysis with autonomous and electric ground transportation for informing future research”. en. In: *Transportation Research Part C: Emerging Technologies* 132 (Nov. 2021), p. 103377. ISSN: 0968-090X. DOI: 10.1016/j.trc.2021.103377. (Visited on 12/13/2022).

[74] L. Granado, M. Ben-Marzouk, E. S. Saenz, Y. Boukal, and S. Jugé. “Machine learning predictions of lithium-ion battery state-of-health for eVTOL applications”. In: *Journal of Power Sources* 548 (2022), p. 232051.

[75] Brian Jenkins. *BETA Technologies A250 eVTOL Prototype Aircraft*. https://upload.wikimedia.org/wikipedia/commons/1/1c/BETA_Technologies_A250_eVTOL_Prototype_Aircraft.jpg. Oct. 2024. (Visited on 10/24/2024).

[76] G. Kaya, U. Aydın, B. Ülengin, M. A. Karadayı, and F. Ülengin. “How do airlines survive? An integrated efficiency analysis on the survival of airlines”. In: *Journal of Air Transport Management* 107 (Mar. 2023), p. 102348. ISSN: 0969-6997. DOI: 10.1016/j.jairtraman.2022.102348. (Visited on 12/19/2024).

[77] X. Gao, X. Zhao, Q. Yu, and W. Ge. “Assessing Airline Operational Efficiency during the COVID-19 Pandemic: A Comparative Study of Pre- and Post-Pandemic Performance”. EN. In: (Dec. 2024). Publisher: American Society of Civil Engineers, pp. 3573–3584. DOI: 10.1061/9780784485484.340. (Visited on 12/19/2024).

[78] P. Stenzel, M. Baumann, J. Fleer, B. Zimmermann, and M. Weil. *Database development and evaluation for techno-economic assessments of electrochemical energy storage systems*. Pages: 1342. May 2014. ISBN: 978-1-4799-2449-3. DOI: 10.1109/ENERGYCON.2014.6850596.

[79] Olje- og energidepartementet. *Renewable energy production in Norway*. en-GB. Redaksjonellartikkel. Publisher: regjeringen.no. May 2016. URL: https://www.regjeringen.no/en/topics/energy/renewable-energy/renewable-energy-production-in-norway/id2343462/ (visited on 12/22/2022).

[80] Eviation. *Alice*. en-US. July 2022. URL: https://www.eviation.com/aircraft/ (visited on 11/22/2022).

[81] J. W. R. Taylor and K. Munson. *Jane’s all the world’s aircraft 1982-83*. eng. 73th ed. OCLC: 819022685. Taipei: Rainbom - Bridge Book, 1983.

[82] E. v. Baaren and P. Roling. “Design of a zero emission aircraft towing system”. English. In: *AIAA AVIATION Forum, 17-21 June 2019, Dallas, Texas*. American Institute of Aeronautics and Astronautics Inc. (AIAA), 2019, AIAA. DOI: 10.2514/6.2019-2932. URL: https://research.tudelft.nl/en/publications/design-of-a-zero-emission-aircraft-towing-system (visited on 06/15/2021).

[83] AERO. *TLD TMX-550 Aircraft Towing Tractor*. URL: https://www.aerospecialties.com/aviation-ground-support-equipment-gse-products/tow-tugs-pushback-tractors/large-20000-dbp/tld-tmx-550/ (visited on 12/19/2024).

[84] Grepow. *What Is An eVTOL And How To Choose Batteries For It? | Grepow*. URL: https://www.grepow.com/blog/what-is-an-evtol-and-how-to-choose-batteries-for-it.html (visited on 12/19/2024).

[85] P. Jackson. *Jane's All the World's Aircraft 2007/2008*. en. Google-Books-ID: pVgbAAAACAAJ. Jane's Information Group, 2007. ISBN: 978-0-7106-2792-6.

[86] B. Tang and E. B. Khalil. "PyEPO: a PyTorch-based end-to-end predict-then-optimize library for linear and integer programming". en. In: *Mathematical Programming Computation* (July 2024). ISSN: 1867-2957. DOI: 10.1007/s12532-024-00255-x. (Visited on 08/29/2024).

[87] W. K. K. Haneveld, M. H. v. d. Vlerk, and W. Romeijnders. *Stochastic Programming: Modeling Decision Problems Under Uncertainty*. en. Google-Books-ID: wQO5DwAAQBAJ. Springer Nature, Oct. 2019. ISBN: 978-3-030-29219-5.

[88] D. Bertsimas and M. Sim. "The Price of Robustness". en. In: *Operations Research* (Feb. 2004). Publisher: INFORMS. DOI: 10.1287/opre.1030.0065. URL: https://pubsonline.informs.org/doi/abs/10.1287/opre.1030.0065 (visited on 09/28/2023).

[89] O. Bräysy and M. Gendreau. "Vehicle Routing Problem with Time Windows, Part I: Route Construction and Local Search Algorithms". en. In: *Transportation Science* 39.1 (Feb. 2005), pp. 104–118. ISSN: 0041-1655, 1526-5447. DOI: 10.1287/trsc.1030.0056. (Visited on 01/27/2022).

[90] O. Bräysy and M. Gendreau. "Vehicle Routing Problem with Time Windows, Part II: Metaheuristics". en. In: *Transportation Science* 39.1 (Feb. 2005), pp. 119–139. ISSN: 0041-1655, 1526-5447. DOI: 10.1287/trsc.1030.0057. (Visited on 01/27/2022).

[91] M. A. Figliozzi. "An iterative route construction and improvement algorithm for the vehicle routing problem with soft time windows". en. In: *Transportation Research Part C: Emerging Technologies* 18.5 (Oct. 2010), pp. 668–679. ISSN: 0968090X. DOI: 10.1016/j.trc.2009.08.005. (Visited on 01/31/2022).

[92] D. Taş. "Electric vehicle routing with flexible time windows: a column generation solution approach". In: *Transportation Letters* 13.2 (Feb. 2021). Publisher: Taylor & Francis _eprint: https://doi.org/10.1080/19427867.2020.1711581, pp. 97–103. ISSN: 1942-7867. DOI: 10.1080/19427867.2020.1711581. URL: https://doi.org/10.1080/19427867.2020.1711581 (visited on 02/27/2023).

[93] R. Conrad and M. A. Figliozzi. "The Recharging Vehicle Routing Problem". In: Institute of Industrial & System Engineers, 2011. URL: https://web.cecs.pdx.edu/~maf/Conference_Proceedings/2011_The_Recharging_Vehicle_Routing_Problem.pdf.

[94] G. Desaulniers, F. Errico, S. Irnich, and M. Schneider. "Exact Algorithms for Electric Vehicle-Routing Problems with Time Windows". en. In: *Operations Research* 64.6 (Dec. 2016), pp. 1388–1405. ISSN: 0030-364X, 1526-5463. DOI: 10.1287/opre.2016.1535. (Visited on 01/27/2022).

[95] M. Keskin and B. Çatay. "Partial recharge strategies for the electric vehicle routing problem with time windows". en. In: *Transportation Research Part C: Emerging Technologies* 65 (Apr. 2016), pp. 111–127. ISSN: 0968-090X. DOI: 10.1016/j.trc.2016.01.013. URL: https://www.sciencedirect.com/science/article/pii/S0968090X16000322 (visited on 02/03/2023).

[96] V. Pillac, M. Gendreau, C. Guéret, and A. L. Medaglia. “A review of dynamic vehicle routing problems”. In: *European Journal of Operational Research* 225.1 (Feb. 2013), pp. 1–11. ISSN: 0377-2217. DOI: 10.1016/j.ejor.2012.08.015. URL: https://www.sciencedirect.com/science/article/pii/S0377221712006388 (visited on 09/21/2023).

[97] S. Lorini, J.-Y. Potvin, and N. Zufferey. “Online vehicle routing and scheduling with dynamic travel times”. In: *Computers & Operations Research* 38.7 (July 2011), pp. 1086–1090. ISSN: 0305-0548. DOI: 10.1016/j.cor.2010.10.019. URL: https://www.sciencedirect.com/science/article/pii/S0305054810002480 (visited on 09/21/2023).

[98] L. Zhang, Z. Liu, L. Yu, K. Fang, B. Yao, and B. Yu. “Routing optimization of shared autonomous electric vehicles under uncertain travel time and uncertain service time”. In: *Transportation Research Part E: Logistics and Transportation Review* 157 (Jan. 2022), p. 102548. ISSN: 1366-5545. DOI: 10.1016/j.tre.2021.102548. URL: https://www.sciencedirect.com/science/article/pii/S1366554521003069 (visited on 09/27/2023).

[99] E. Messaoud. “A chance constrained programming model and an improved large neighborhood search algorithm for the electric vehicle routing problem with stochastic travel times”. en. In: *Evolutionary Intelligence* 16.1 (Feb. 2023), pp. 153–168. ISSN: 1864-5917. DOI: 10.1007/s12065-021-00648-0. URL: https://doi.org/10.1007/s12065-021-00648-0 (visited on 09/27/2023).

[100] M. Mitici, M. Pereira, and F. Oliviero. “Electric flight scheduling with battery-charging and battery-swapping opportunities”. en. In: *EURO Journal on Transportation and Logistics* 11 (Jan. 2022), p. 100074. ISSN: 2192-4376. DOI: 10.1016/j.ejtl.2022.100074. (Visited on 10/25/2022).

[101] C. Y. Justin, A. P. Payan, S. I. Briceno, B. J. German, and D. N. Mavris. “Power optimized battery swap and recharge strategies for electric aircraft operations”. en. In: *Transportation Research Part C: Emerging Technologies* 115 (June 2020), p. 102605. ISSN: 0968-090X. DOI: 10.1016/j.trc.2020.02.027. (Visited on 06/16/2021).

[102] F. Doctor, T. Budd, P. D. Williams, M. Prescott, and R. Iqbal. “Modelling the effect of electric aircraft on airport operations and infrastructure”. en. In: *Technological Forecasting and Social Change* 177 (Apr. 2022), p. 121553. ISSN: 00401625. DOI: 10.1016/j.techfore.2022.121553. (Visited on 05/03/2022).

[103] M. Lindberg and J. Leijon. “Effects on Airport Operations from a New Regional Electric Flight Network in Northern Scandinavia”. In: *2024 IEEE International Conference on Electrical Systems for Aircraft, Railway, Ship Propulsion and Road Vehicles & International Transportation Electrification Conference (ESARS-ITEC)*. Nov. 2024, pp. 1–6. DOI: 10.1109/ESARS-ITEC60450.2024.10819765. (Visited on 01/20/2025).

[104] A. Kinene, S. Birolini, M. Cattaneo, and T. A. Granberg. “Electric aircraft charging network design for regional routes: A novel mathematical formulation and kernel search heuristic”. In: *European Journal of Operational Research* 309.3 (Sept. 2023), pp. 1300–1315. ISSN: 0377-2217. DOI: 10.1016/j.ejor.2023.02.006. URL: https://www.sciencedirect.com/science/article/pii/S037722172300125X (visited on 10/04/2023).

[105] F. Schneider, U. W. Thonemann, and D. Klabjan. “Optimization of Battery Charging and Purchasing at Electric Vehicle Battery Swap Stations”. In: *Transportation Science* 52.5 (Oct. 2018). Publisher: INFORMS, pp. 1211–1234. ISSN: 0041-1655. DOI: 10.1287/trsc.2017.0781. (Visited on 10/25/2022).

[106] B. Sun, X. Tan, and D. H. K. Tsang. “Optimal Charging Operation of Battery Swapping and Charging Stations With QoS Guarantee”. In: *IEEE Transactions on Smart Grid* 9.5 (Sept. 2018). Conference Name: IEEE Transactions on Smart Grid, pp. 4689–4701. ISSN: 1949-3061. DOI: 10.1109/TSG.2017.2666815.

[107] B. Sun, X. Sun, D. H. K. Tsang, and W. Whitt. “Optimal battery purchasing and charging strategy at electric vehicle battery swap stations”. en. In: *European Journal of Operational Research* 279.2 (Dec. 2019), pp. 524–539. ISSN: 0377-2217. DOI: 10.1016/j.ejor.2019.06.019. (Visited on 10/21/2022).

[108] A. J. Stolzer, R. L. Sumwalt, and J. J. Goglia. *Safety Management Systems in Aviation*. 3rd ed. Boca Raton: CRC Press, Apr. 2023. ISBN: 978-1-00-328612-7. DOI: 10.1201/9781003286127.

[109] K. Ranasinghe, K. Guan, A. Gardi, and R. Sabatini. “Review of advanced low-emission technologies for sustainable aviation”. en. In: *Energy* 188 (Dec. 2019), p. 115945. ISSN: 0360-5442. DOI: 10.1016/j.energy.2019.115945. URL: https://www.sciencedirect.com/science/article/pii/S0360544219316299 (visited on 05/01/2023).

[110] G. dos Reis, C. Strange, M. Yadav, and S. Li. “Lithium-ion battery data and where to find it”. In: *Energy and AI* 5 (Sept. 2021), p. 100081. ISSN: 2666-5468. DOI: 10.1016/j.egyai.2021.100081. (Visited on 01/20/2025).

[111] X. Shu, S. Shen, J. Shen, Y. Zhang, G. Li, Z. Chen, and Y. Liu. “State of health prediction of lithium-ion batteries based on machine learning: Advances and perspectives”. In: *iScience* 24.11 (Nov. 2021), p. 103265. ISSN: 2589-0042. DOI: 10.1016/j.isci.2021.103265. (Visited on 01/20/2025).

[112] J. C. Chen, T.-L. Chen, W.-J. Liu, C. C. Cheng, and M.-G. Li. “Combining empirical mode decomposition and deep recurrent neural networks for predictive maintenance of lithium-ion battery”. In: *Advanced Engineering Informatics* 50 (Oct. 2021), p. 101405. ISSN: 1474-0346. DOI: 10.1016/j.aei.2021.101405. (Visited on 01/20/2025).

[113] C. Chen, G. Tao, J. Shi, M. Shen, and Z. H. Zhu. “A Lithium-Ion Battery Degradation Prediction Model With Uncertainty Quantification for Its Predictive Maintenance”. In: *IEEE Transactions on Industrial Electronics* 71.4 (Apr. 2024). Conference Name: IEEE Transactions on Industrial Electronics, pp. 3650–3659. ISSN: 1557-9948. DOI: 10.1109/TIE.2023.3274874. (Visited on 01/20/2025).

[114] J. Lee and M. Mitici. “An integrated assessment of safety and efficiency of aircraft maintenance strategies using agent-based modelling and stochastic Petri nets”. In: *Reliability Engineering & System Safety* 202 (Oct. 2020), p. 107052. ISSN: 0951-8320. DOI: 10.1016/j.ress.2020.107052. (Visited on 12/08/2024).

[115] M. Mitici, B. Hennink, M. Pavel, and J. Dong. “Prognostics for Lithium-ion batteries for electric Vertical Take-off and Landing aircraft using data-driven machine learning”. In: *Energy and AI* 12 (Apr. 2023), p. 100233. ISSN: 2666-5468. DOI: 10.1016/j.egyai.2023.100233. (Visited on 02/28/2024).

[116] L. Granado, M. Ben-Marzouk, E. Solano Saenz, Y. Boukal, and S. Jugé. “Machine learning predictions of lithium-ion battery state-of-health for eVTOL applications”. In: *Journal of Power Sources* 548 (Nov. 2022), p. 232051. ISSN: 0378-7753. DOI: 10.1016/j.jpowsour.2022.232051. (Visited on 04/03/2024).

[117] G. Patrizi, Luca Martiri, A. Pievatolo, A. Magrini, G. Meccariello, L. Cristaldi, and N. D. Nikiforova. “A Review of Degradation Models and Remaining Useful Life Prediction for Testing Design and Predictive Maintenance of Lithium-Ion Batteries”. en. In: *Sensors* 24.11 (Jan. 2024). Number: 11 Publisher: Multidisciplinary Digital Publishing Institute, p. 3382. ISSN: 1424-8220. DOI: 10.3390/s24113382. (Visited on 01/20/2025).

CHAPTER 2

Scheduling electric towing for aircraft: developing charging policies

Electric towing vehicles (ETVs) present a short-term avenue to reduce aviation emissions without requiring changes to the aircraft. In the following three chapters, an ETV fleet operations model and algorithm with disruption management are developed. This model needs to account for the time that ETVs need to recharge their batteries. For aviation applications, this can amount to a significant fraction of the day. These recharging moments need to be spread out during the day to prevent unavailability and to spread out electricity demand.

Previously developed models have either neglected or assumed simplistic recharging models. In this chapter, we introduce a realistic charging model, and benchmark its performance against the existing ones. To do this, simplified ETV fleet management model is introduced. This is a mixed-integer linear program, which determines the ETV-to-aircraft assignment for an entire day of operations, which minimizes the number of required ETVs.

We illustrate our approach for one day of operations at a large European airport. In this case study, we show that the developed charging policy reduces the required fleet size to tow all aircraft reduces by 27% for the best-practice existing policies.

Parts of this chapter have been published :

S. van Oosterom, M. Mitici, and J. Hoekstra. "Analyzing the impact of battery capacity and charging protocols on the dispatchment of electric towing vehicles at a large airport". In: *AIAA AVIATION 2022 Forum*. AIAA AVIATION Forum. American Institute of Aeronautics and Astronautics, June 2022. DOI: 10.2514/6.2022-3920

2.1 Introduction

Striving to meet climate-neutral targets set by the Paris Accords [2] and the Glasgow Climate Pact [3], the aviation industry aims for net-zero emissions by 2050 [4, 5]. For some actors, like the Schiphol Group airport operator [6], the first step to achieve this is by creating climate neutral ground operations by 2030.

Aircraft taxiing has been shown to be a large contributor to airport ground emissions, and will have to be addressed in order to achieve zero ground emissions. In fact, it has been shown that around 56% of the NO_x emissions at London Heathrow result from taxiing aircraft [7]. Additionally, taxiing from and to the runway has been estimated to produce between 4% and 9% of the total flight emissions [8].

One of the promising means to reduce emissions in the near future is to tow aircraft using Electric Towing Vehicles (ETVs). The management of a fleet of ETVs is, however, a complex scheduling problem. It concerns the assignment of to-be-towed aircraft to ETVs, while ensuring that enough time remains for the vehicles to recharge their batteries, which can take up to several hours. An efficient management of the ETV fleet is key for a successful implementation.

ETV fleet management optimization has been addressed scarcely, and only with simple battery recharging policies. For instance, in Soltani et al. [9] the authors consider an ETV fleet where each vehicle has to be assigned to a subset of flights from a given flight schedule such that the environmental impact of the ETV fleet is maximized. The authors consider a charging policy where ETVs can only recharge during the night. As such, the energy available for each ETV is limited, and hence it can tow only a limited number of aircraft. The same problem has been addressed by Van Baaren and Roling [10], while allowing for multiple battery charges during the day. This study assumes a charging policy where ETVs can recharge their battery throughout the day, and where their batteries are charged up to full capacity at each visit. The authors also assume that ETVs charge for a fixed amount of time, irrespective of the remaining state of charge of the batteries. This, however, results in an overestimation of the charging time. As a consequence, the required vehicle fleet size is overestimated and the ETV available for towing are used inefficiently.

To address these limitations, we consider the management of a fleet of ETVs with a preemptive charging policy. Here, the charging time of ETVs depends on the residual battery charge, and allows for multiple partial recharging opportunities during the day of the operations. Also, the ETVs do not necessarily recharge to their maximum capacity at each visit to a charging station. All flights that are eligible to be towed are towed by ETVs. As such, the objective of our optimization problem is to minimize the required number of ETVs to tow all aircraft. The output of the model is an assignment of ETVs to aircraft throughout the day, as well as a battery recharging schedule for each ETV. We formulate our model as a Mixed Integer Linear Programming problem.

We illustrate our approach for a day of operations at Amsterdam Airport Schiphol, where we analyze the impact of the ETV battery size and used charging policy. We compare our preemptive charging policy with the ones used in Soltani et al. [9] and in Van Baaren and Roling [10]. The flight schedule from the 14th of December of 2019 is used, where 750 flights are considered eligible to be towed. We consider a range of ETV battery

capacities between 100 kWh and 500 kWh, where 500 kWh is sufficiently large to tow aircraft continuously. Special attention is given to the nominal case where the battery capacity is 320 kWh. In this case, ETVs are able to tow about 10 aircraft on a single charge.

The results show that the partial charging policy provides a significant reduction in ETV fleet size over the formulations used in Van Baaren and Roling and in Soltiani et al.. In the nominal case (320 kWh batteries), the ETV scheduling model with a preemptive charging policy requires a fleet of 29 ETVs, whereas the methods from Van Baaren and Roling and from Soltani et al. require 40 ETVs and 66 ETVs, respectively. Second, we observe a significant trade-off between the ETV battery size and the required fleet size. Decreasing the battery size from 320 kWh to 100 kWh results in requiring 12 additional ETVs, whereas an increase to 500 kWh or more is required in order to remove battery life as a constraining factor.

The remainder of this chapter is organized as follows. In Section 2.2 the ETV scheduling problem is introduced, and in Section 2.3 we describe the energy consumption model of the ETVs. A Mixed Integer Linear Programming formulation of the ETV scheduling problem is presented in Section 2.4, and this model is applied in a case study in Section 2.5. Finally, the conclusions of this study are presented in Section 2.6.

2.2 Problem description - Electric Towing Vehicles scheduling

We consider the dispatchment of a fleet of ETVs for towing aircraft to and from gates and runways. During the day, the ETVs may need to recharge their batteries. While recharging, the ETVs are not available for towing. We study the impact of the maximum battery capacity of the and the policies for battery charging on the size of the fleet of ETVs.

2.2.1 Airport taxiway and service road network

We consider an airport with two road networks: the taxiway network, used by aircraft towed by ETVs, and the service road network, used for ETVs not attached by an aircraft. The taxiway network is given by a graph $G_X = (N_X, E_X)$ consisting of nodes N_X and directed edges E_X. Distances on the taxiway network are given by $d_X : E_X \rightarrow \mathbb{R}$. The service road network, used by ETVs to traverse the airport when not towing aircraft, is given by the graph $G_S = (N_S, E_S)$ with nodes N_S and edges E_S. Distances on the service road network are given by $d_S : E_S \rightarrow \mathbb{R}$.

Let N_R and N_G denote the set of runway entrance and exit nodes and gate nodes, respectively. These are the locations where an aircraft can be picked-up or dropped-off by an ETV. These nodes are in both the taxiway and service road network ($N_R \cup N_G \subset N_X \cap N_S$). Finally, there are a number of ETV recharging stations within the service road network: $N_{CS} \subset N_S$. Figure 2.1 gives an example of the airport road networks.

We are interested in determining the minimum size of a fleet of ETVs such that all aircraft operating a set of flights A are towed. For this fleet of ETVs we will propose an assignment of ETVs to tow specific flights from A, and a battery recharging schedule

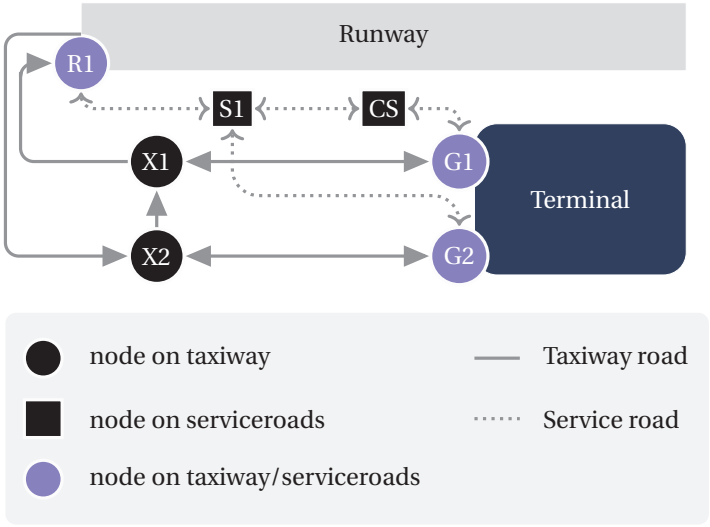

Figure 2.1.: Example of an airport taxiway network and a service road network. Here $N_X = \{R1, X1, X2, G1, G2\}$, $E_X = \{(R1, X2), (X2, X1), (X1, R1), (X1, G1), (G1, X1), (G2, X2), (X2, G2)\}$, $N_S = \{R1, S1, CS, G1, G2\}$ and $E_S = \{\{R1, S1\}, \{S1, G2\}, \{S1, CS\}, \{CS, G1\}\}$. The runway entrance and exit is located at node $R1$, and the gates are located at nodes $G1$ and $G2$. The charging station is located at node CS.

conform a charging policy.

2.2.2 ETV specifications

We consider a single type of ETV to tow all eligible flights. These ETVs are equipped with a battery of capacity Q, which has a gravimetric energy density of m_q. The basic mass of an ETV, excluding the battery, is given by m_0. The total mass of an ETV is given by $m = m_0 + m_q Q$. The power required by ETVs to traverse the airport is given by P, which is a function of the velocity and towed mass. Finally, ETVs recharge their batteries with power P^c.

We assume that ETVs traverse the road networks with constant velocity and using the shortest path. A velocity of v_x and v_s is maintained on the taxiway and service roads respectively. For any two nodes $m, n \in N_X$, denote the shortest distance from m to n on G_X (using d_X as a distance metric) as $d_X^{SP}(m, n)$. Similarly, for two nodes $m, n \in N_S$, denote the shortest distance from m to n in G_S (using d_S as a distance metric) as $d_S^{SP}(m, n)$. Both d_X^{SP} and d_S^{SP} can be computed with, e.g., Dijkstra's shortest path algorithm.

2.2.3 Aircraft arrival/departure flight schedule

Let the interval T denote a day of operations at the airport, with a length of 24 hours. Let A denote the set of flights which arrives at or departs from the airport during T and are eligible/certified to be towed by an ETV. Each arriving aircraft is to be towed from its pick-up runway node in N_R to its drop-off gate node in N_G; the reverse holds for departing aircraft. For an aircraft $a \in A$, let $n_a^p \in N_G \cup N_R$ denote its pick-up location and let $n_a^d \in N_G \cup N_R$ denote its drop-off location. The time at which a is to be picked-up at n_a^p is given by $t_a^p \in T$. As such, the drop-off time of a at n_a^d is given by $t_a^d = t_a^p + d_X^{SP}(n_a^p, n_a^d)/v_X$.

2.2.4 ETV battery charging policy

By towing aircraft and driving across the service roads, ETVs deplete their battery. ETVs recharge their batteries at one of the charging station in N_{CS}. Charging is done with power P^c. At the end of the day of operations, all vehicles return to a depot $n^{dep} \in N_{CS}$ to fully recharge their battery before the start of the next day of operations.

In this chapter we consider three different charging policies:

1. **ETV battery night-charging (NC)**: This battery charging policy assumes that the ETVs are recharged only after performing their last tow of the day. In other words, we assume that the battery of the ETVs is large enough to support several towing tasks during a day of operations. Recharging is required only during the night, when no more towing tasks need to be performed. This policy has been used in Soltani et al. [9].

2. **The constant-time ETV battery charging (CTC)**: This battery charging policy allows for ETVs to charge throughout the day of operations. Under this policy, every time ETVs re-charge their batteries they are charged to full capacity. Battery recharging takes a constant time Q/P^c, irrespective of the residual charge of the battery. This policy has been used in Van Baaren and Roling [10].

3. **The partial ETV battery charging (PC)**: This battery charging policy allows for ETV battery charging throughout the day, but permits preemptive charging. As such, ETVs may leave the charging station without a full battery. The charge loaded in the battery depends on the time spent at the charging station.

Fig. 2.2 shows a simple example of charging policies NC, CTC and PC. For simplicity, in this example we assume that towing an aircraft always requires 30% of the battery capacity of an ETV. The NC policy postpones charging for the night period, while CTC and PC policies allow for battery charging during the day.

2.3 ETV energy consumption

The energy consumed by an ETV per unit of time, P, depends on the velocity v and mass that it is towing m_{tow}:

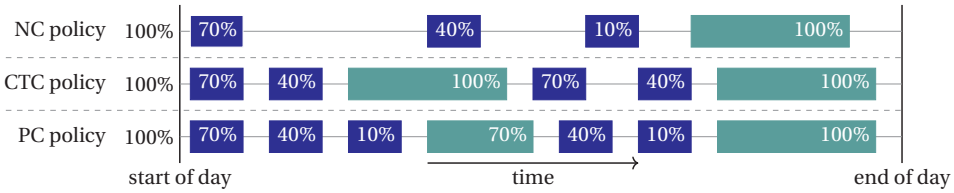

Figure 2.2.: Example of ETV battery re-charging schedules under charging policies NC, CTC, and PC. In this example, towing an aircraft always requires 30% of the ETV battery capacity (blue blocks). ETV battery recharging is indicated by green boxes.

$$P(v, m_{tow}) = \mu^g(v)(m + m_{tow})gv, \tag{2.1}$$

$$\mu^g(v) = \mu^0\left(1 + v/v^0\right), \tag{2.2}$$

where μ^g is the coefficient of rolling resistance, which depends on the velocity and on the constants μ^0 and v^0. The gravitational acceleration is denoted by g. As such, the energy consumed by an ETV while towing aircraft $a \in A$ is denoted by $q^X(a)$ and is given by:

$$q^X(a) = d_X^{SP}(n_a^p, n_a^d)P(v_x, m_a)/v_x \tag{2.3}$$

The energy required by an ETV to traverse the service roads (where $m_{tow} = 0$) from n to $m \in N_S$ is given by:

$$q^S(n, m) = d_S^{SP}(n, m)P(v_s, 0)/v_s \tag{2.4}$$

For simplicity, we use the following notation for aircraft $a, b \in A$:

$$q_f^S(a) := q^S(n^{dep}, n^p(a)), \qquad q_l^S(a) := q^S(n^d(a), n^{dep}), \qquad q_d^S(a, b) := q^S(n^d(a), n^p(b)), \tag{2.5}$$

where $q_f^S(a)$ denotes the energy to drive from the depot to the pick-up point of a, $q_l^S(a)$ the energy to drive from the drop-off point of a back to the depot. Finally, $q_d^S(a, b)$ denotes the required energy to drive directly from the drop-off point of a to the pick-up point of b.

2.4 Scheduling Model formulation with different charging policies

In this section, we propose a Mixed Integer Linear Programming (MILP) to optimally schedule a fleet of ETVs for aircraft towing and battery re-charging. We consider multiple battery charging policies (see Section 2.2.4).

2.4.1 Notation

Depending on the assumed charging policy, ETVs may have the opportunity to recharge their battery between aircraft towing tasks. ETVs always use the charging station closest to the pick-up point of their next task b, which is denoted by $n^C(b) \in N^{CS}$. We use the following abbreviations for energy consumption:

$$q^S_{C1}(a) := q^S(n^C(a), n^p(a)), \tag{2.6}$$

$$q^S_{C2}(a,b) := q^S(n^d(a), n^C(b)) + q^S(n^C(b), n^p(b)), \tag{2.7}$$

where $q^S_{C1}(a)$ denotes the required energy to drive to the pick-up point of aircraft $a \in A$ from $n^C(a)$, and $q^S_{C2}(a,b)$ denotes the required energy to drive from the drop-off point of b to the pick-up point of a via $n^C(b)$.

Next, we define the sets of aircraft which can be towed by the same ETV consecutively. Let A^{in}_a and A^{out}_a denote the sets of aircraft which can be towed before and after towing a, respectively. For $a \in A$, let $b \in A^{out}_a$ if $t^d(a) + d^{SP}_S(n^d(a), n^p(b))/v_s \leq t^p(b)$. For two tasks $a \in A, b \in A^{out}_a$, let $t^C(a,b)$ denote the available charging time between towing a and b. Let $t^C_l(a)$ denote the available charging time after towing a until the end of the day.

Under the CTC policy, it is possible to charge between towing a and b if $t^C(a,b)$ is longer then Q/P^c, the time required to fully recharge a depleted battery. We denote this set by $A^{CTC}_a \subset A^{out}_a$. Under the PC policy, it is possible to charge between towing a and b if $t^C(a,b)$ is positive and if, after charging, the state of charge of the ETV at the start of towing b can be larger than it would have been if it did not charge. We denote this set by $A^{PC}_a \subset A^{out}_a$.

2.4.2 Decision variables

We consider the following decision variables in order to determine the order in which the aircraft are towed:

$$x_{ab} = \begin{cases} 1 & \text{if } a,b \in A \text{ are} \\ & \text{towed consecutively} \\ 0 & \text{else} \end{cases} \quad x^f_a = \begin{cases} 1 & \text{if } a \in A \text{ is the} \\ & \text{first an ETV tows} \\ 0 & \text{else} \end{cases} \quad x^l_a = \begin{cases} 1 & \text{if } a \in A \text{ is the} \\ & \text{last an ETV tows} \\ 0 & \text{else} \end{cases} \tag{2.8}$$

Additionally, the q variables follow the battery state throughout the day of operations:

$$q_a \in [q^X(a), Q] \qquad \text{ETV battery state-of-charge at the start of towing } a \in A \tag{2.9}$$

2.4.3 Objective function

We aim to minimize the required size of the ETV fleet such that all flights from A can be towed; denote this number by n_{ETV}. We claim that $n_{ETV} = \min_{x,q}\{\sum_{a\in A} x^f_a\}$. In order

to see this, note that all flights can only be towed by one ETV and hence that for $a \in A$, $x_a^f = 1$ implies that a unique ETV has to leave the depot and start its day by towing a. Conversely, if for a specific ETV there is no flight that it serves first on the day, it is not towing any flights at all that day and hence is not required.

2.4.4 Constraints

We consider the following constraints. These hold for all three charging policies:

$$x_a^f + \sum_{b \in A_a^{in}} x_{ba} = 1 \qquad \forall a \in A, \tag{2.10}$$

$$x_a^l + \sum_{b \in A_a^{out}} x_{ab} = 1 \qquad \forall a \in A, \tag{2.11}$$

$$q_a \leq Q - x_a^f q_f^S(a) \qquad \forall a \in A, \tag{2.12}$$

$$0 \leq q_a - x_a^l (q^X(a) + q_l^S(a)) \qquad \forall a \in A, \tag{2.13}$$

$$Q \leq q_a - \left[q^X(a) - q_l^S(a)\right] + P^c t_l^C(a) + Q(1 - x_b^l) \qquad \forall a \in A. \tag{2.14}$$

Constraint (2.10) ensures that each aircraft a is either the first towed aircraft of the day by an ETV or is preceded by another aircraft that is towed. Constraint (2.11) ensures that each aircraft is either the last towed aircraft of the day by an ETV or an ETV subsequently tows another aircraft. Constraint (2.12) limits the battery charge at the start of the day, and Constraint (2.13) ensures that at the end of the day the ETV has sufficient energy to reach the depot. Last, Constraint (2.14) ensures that there is enough time to recharge the battery of an ETV at the end of the day.

NC policy specific constraints

Under the NC policy, charging is only performed after the last towing task (at the end of the day of operations). Constraints (2.14) ensure that there is enough time for recharging before the start of a new day of operations. Throughout the day, the battery charge depends only on what task has been executed previously:

$$q_b \leq q_a - x_{ab}(q^X(a) + q^S(a,b)) + (1 - x_{ab})Q \qquad \forall a \in A, b \in A_a^{out} \tag{2.15}$$

This constraint limits the battery state-of-charge between two consecutively aircraft towing tasks.

CTC policy specific constraints

Under the CTC policy, charging is performed between two towing tasks if and only if the available charging time in-between is large enough to fully recharge the battery. As such, the following two constraints determine the state of charge of the ETV throughout the day:

$$q_b \leq q_a - x_{ab}(q^X(a) + q^S(a,b)) + (1 - x_{ab})Q \qquad \forall a \in A, b \in A_a^{out} \setminus A_a^{CTC}, \tag{2.16}$$

$$q_b \leq Q - x_{ab} q_C^S(b) \qquad \forall a \in A, b \in A_a^{CTC}. \tag{2.17}$$

Constraint (2.16) is identical to constraint (2.15) of the NC-policy, but only applies to the couples of aircraft between towing which the ETVs battery cannot be fully charged. When this can be done, it is replaced with Constraint (2.17), which resets the ETV battery to full capacity.

PC policy specific constraints

Under the PC policy, batteries may be partially charged throughout the day of operations. In order to accommodate this, an additional constraint is added:

$$q_b \leq q_a - x_{ab}(q^X(a) + q^S(a,b)) + Q(1 - x_{ab}) \qquad \forall a \in A, b \in A_a^{out} \setminus A_a^{PC}, \tag{2.18}$$

$$q_b \leq Q - x_{ab} q_C^S(b) \qquad \forall a \in A, b \in A_a^{PC}, \tag{2.19}$$

$$q_b \leq q_a - x_{ab}(q^X(a) + q_C(a,b) - P^c t^C(a,b)) + Q(1 - x_{ab}) \qquad \forall a \in A, b \in A_a^{PC}. \tag{2.20}$$

Constraints (2.18) and (2.19) are the same as Constraints (2.16) and (2.17) before. Constraint (2.20) limits the ETV battery charge if a charging station is visited between towing two aircraft. This is done by adding the charged energy $P^C t^C(a,b)$ to the ETV battery.

2.5 Comparing the charging policies: case study at Amsterdam Airport

In this section, we apply the ETV scheduling models in a case study at Amsterdam Airport Schiphol (AAS), using the flight schedule of December 14, 2019. First, we shall study the ETV schedules for the different charging policies assuming a single battery size in Subsection 2.5.1. After this, we shall compare the optimal fleet size for different combinations of ETV battery sizes and charging policies in Subsection 2.5.2.

Figure 2.3 shows the map of AAS which we use for our case study, based one the Schiphol aerodrome charts [11]. The runway and gate nodes are indicated by vertically hatched circles and the charging stations (C1 up to C5) are indicated by horizontally hatched circles. The ETV depot is assumed to be located at charging station C5. The service roads and taxiway network are indicated by dashed and solid lines, respectively.

We consider the flight schedule of an entire day of operations at AAS, using flight data from December 14, 2019. We assume that the narrow-body aircraft, 750 in total, are eligible to be towed by an ETV. Figure 2.4 shows the distribution of arriving and departing narrow-body aircraft throughout the day. Flights arrive/depart between 6 AM (on December 14) and 3 AM (on December 15). The masses of the towed aircraft are given by either the MTOW, for departing flights, or the EOW, for arriving flights.

Finally, the ETV specifications can be found in Table 2.1. The ETVs use Li-Ion batteries with a specific energy density of 6.25 kg/kWh [12].

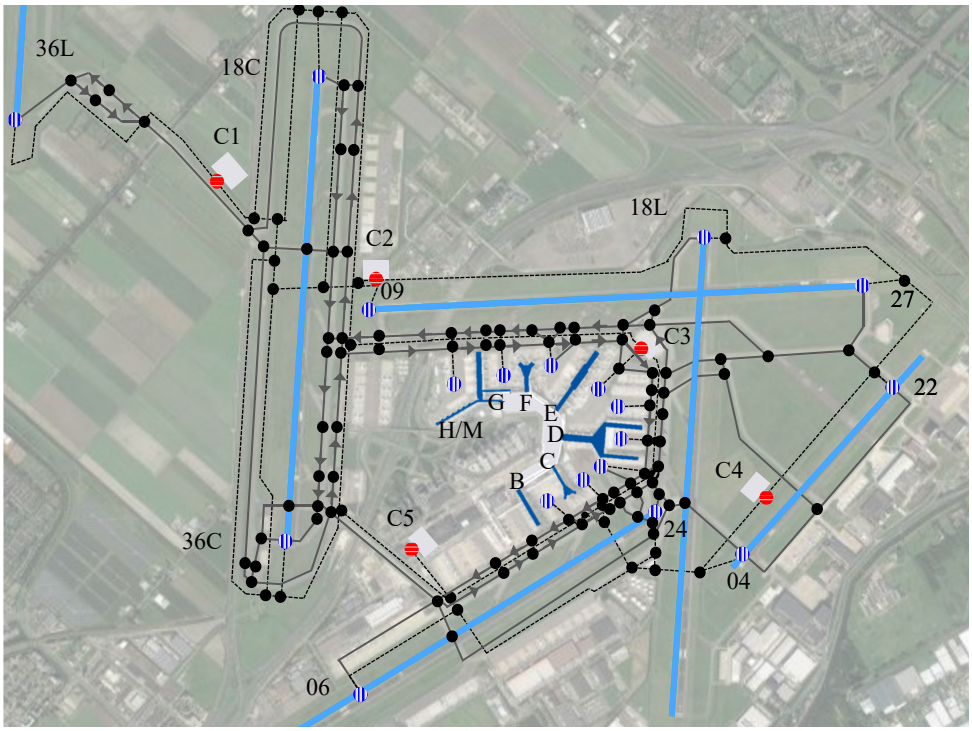

Figure 2.3.: Runways N^R and gate nodes N^G, together with taxiways (solid lines), service roads (dashed lines) and charging stations (C1, ..., C5) at AAS. The map is based on the Schiphol aerodrome charts [11].

Parameter	Explanation	Value
Q [kWh]	Battery capacity	100 - 500
m_0 [kg]	ETV base mass	12000 [10]
m_q [kg/kWh]	ETV battery energy density	6.25 [12]
P^c [kW]	Charging power	100 [10]
μ_0[-]	Rolling resistance coefficient	0.1 [13]
v_0 [km/h]	Rolling resistance base velocity	41.16 [13]
v_s [km/h]	Service road velocity	30 [14]
v_x [km/h]	Towing velocity	42.5 [15]

Table 2.1.: Electric towing vehicle specifications.

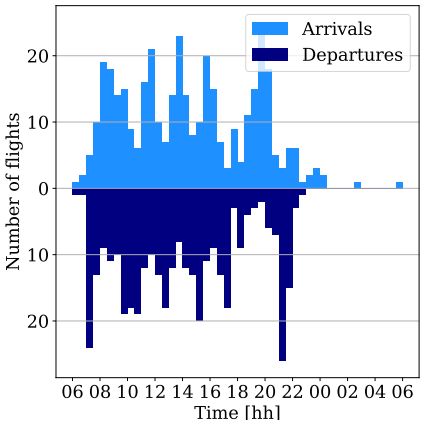

Figure 2.4.: Distribution of $t^p(a)$ for all narrow-body aircraft arriving and departing from AAS on December 14, 2019.

2.5.1 Results: Nominal battery size

First, we consider a base case in which we assume that the ETVs will be equipped with batteries with a capacity $Q = 320$ kWh. In this case, the NC, CTC, and PC policies require a fleet size of 66, 40 and 29, respectively. Figures 2.5a, 2.5b and 2.5c show Gannt-charts for the ETV schedules for the NC, CTC and PC policy, respectively. When an ETV is towing an aircraft, a solid blue bar is displayed, and when it is recharging its battery, a hatched green bar is displayed. Specifications of the schedules are detailed in Table 2.2, which gives the average number of towed aircraft, charging cycles and utilization time per ETV. A charging cycle is given as a switch from discharging a battery to charging. The utilization time is defined as the total time during which an ETV is either towing an aircraft, driving across the service roads or charging, i.e. the total time it is not idle. Last, the corresponding state-of-charge of the ETV of these schedules can be found in Figure 2.6.

As can be seen in the schedule, and in the schedule specifications in Table 2.2, using the NC policy has a drastic impact on the ETV utilization. Because of the choice to only recharge the battery once every day of operations, the number of aircraft which an ETV can tow is relatively limited to just over 11 on average. Towing these aircraft and recharging the battery takes an ETV roughly no more then half of the day of operations (e.g. from 7AM to 1PM for ETV 2), and thus leaves the ETV out of service for the other half of the day. Hence, for this combination of Q and P, night charging does not seem to provide an efficient solution.

When using the CTC policy, the ETVs tow 18.75 aircraft on average (+65% compared to the NC policy) at the cost of requiring 1.85 charging cycles on average. In Figure 2.5b one can see that the tows are distributed much more evenly throughout the day per ETV and that the utilization is larger than when using the NC policy. On the other hand, there are still relatively large gaps in the schedule (e.g. between 4PM and 8PM for ETV 1) as a result of charging only if the time gap is large enough.

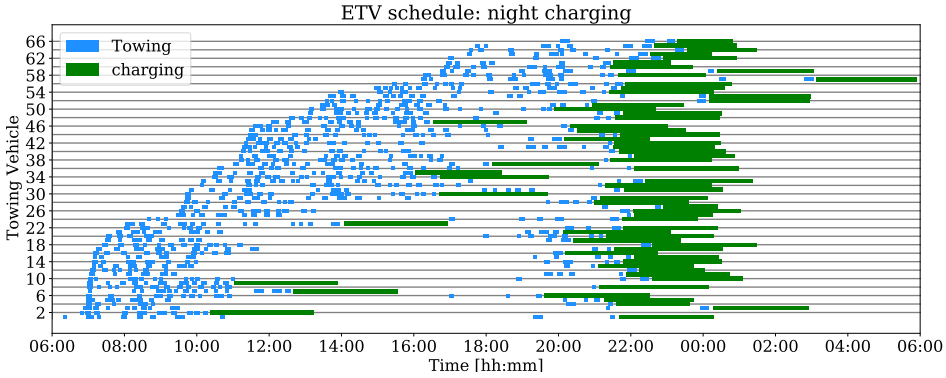

(a) ETV schedule for the night-charging (NC) policy.

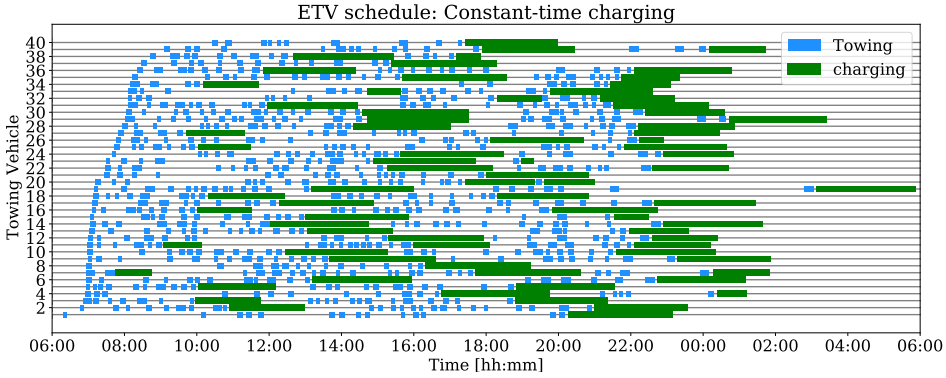

(b) ETV schedule for the constant-time-charging (CTC) policy.

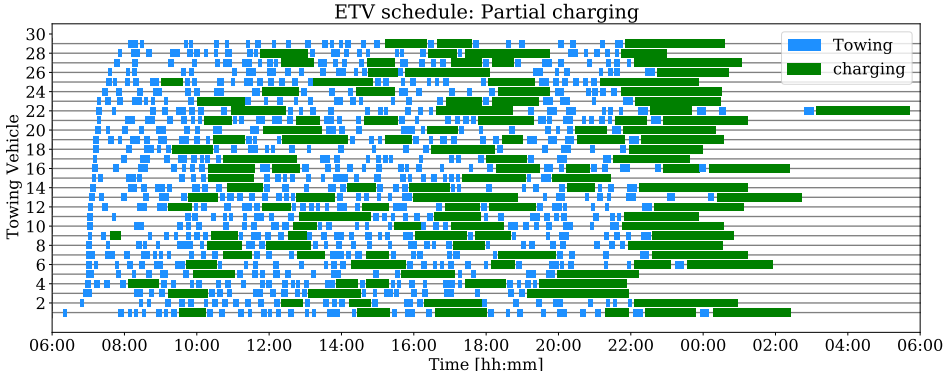

(c) ETV schedule for the preemptive charging (PC) policy

Figure 2.5.: ETV schedules for the nominal use case with a battery capacity of 320 kWh for charging policies NC, CTC and PC. Blue bars indicate an ETV is towing an aircraft. Green hatched bars indicate that an ETV is recharging its battery.

Finally, when using the PC policy the highest ETV fleet utilization is used, the ETVs tow 25.86 aircraft on average (+ 128% compared to the NC policy) at the cost or requiring 4.17 charging cycles. In Figure 2.5c, one can see that similar to the CTC policy the ETVs tow aircraft evenly distributed throughout the day, but that there are much less long gaps in which they are idle. This is also reflected by the average utilization time of 12:26 hours.

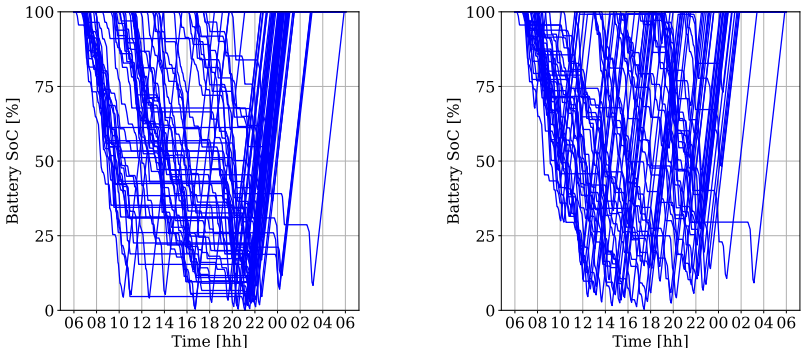

(a) SoC of the ETVs for the night-charging (NC) policy.

(b) SoC of the ETVs for the constant-time-charging (CTC) policy.

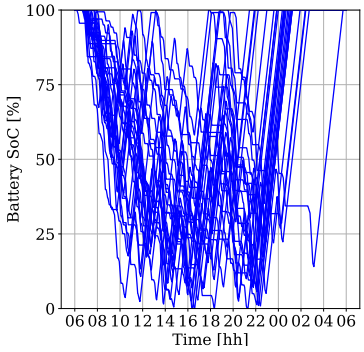

(c) SoC of the ETVs for the preemptive charging (PC) policy

Figure 2.6.: State-of-Charge of the ETV batteries for the nominal use case with a battery capacity of 320 kWh for charging policies NC, CTC and PC. These graphs correspond to the schedules from Figure 2.5

2.5.2 Results: ETV fleet size vs ETV battery capacity

Last, Figure 2.7 shows the impact of the ETV battery capacity on the required towing vehicle fleet size. We have varied the battery capacity between $Q = 100$ and $Q = 500$ kWh in steps of $\Delta Q = 20$ kWh. For each value of Q, we have applied the models from Section

Charging policy	Towed aircraft	Average Charging cycles	Utilization [hh:mm]
NC	11.36	1.00	05:29
CTC	18.75	1.85	08:55
PC	25.86	4.17	12:26

Table 2.2.: Specifications of the ETV schedules from Figure 2.5 for the three corresponding charging policies. *Towed aircraft, Charging cycles, and Utilization* give the average number of towed aircraft, charging cycles, and non-idle time per ETV.

2.4 for each of the three charging policies, in order to obtain the minimum possible fleet size. The fleet sizes for each charging policy are graphed in Figure 2.7. It highlights the nominal case of Subsection 2.5.1, where $Q = 320$ kWh, with a larger gray marker. Finally, without battery life constraints, the minimum required fleet size is 24 ETVs, and this line is also displayed in Figure 2.7.

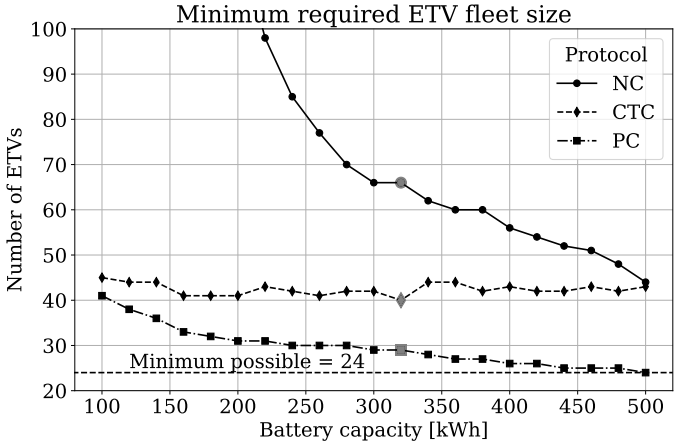

Figure 2.7.: Pareto front of the required number of ETVs to tow all eligible flights against the battery capacity of an ETV, for each charging policy (night charging (NC), constant time charging (CTC), and partial charging (PC)). The nominal case where $Q = 320$ kWh is highlighted with a larger, gray, marker. The smallest possible fleet size (when battery constraints are ignored) is 24 ETVs.

There are a number of notable features in Figure 2.7. First, for any value of Q the ETV fleet size is always smallest for the PC policy, followed by the CTC policy and by the NC policy. For the PC policy, the fleet size varies between 41 and 24 ETVs, such that for $Q = 500$ kWh, the battery capacity is no longer a limiting factor in the ETV schedule. For the CTC policy, the fleet size varies between 45 and 40 ETVs. Finally, the vehicle fleet for the NC policy varies between 210 ETVs, outside the bounds of this graph, and 45 ETVs. In the best case scenario, the CTC and the NC policy require a 67% and 87% larger fleet

then the PC policy, respectively, but in all cases it provides the smallest fleet size.

The second notable feature of Figure 2.7 is that the vehicle fleet size for the CTC policy is almost not sensitive to the battery capacity. Instead of decreasing with increasing battery size, the ETV fleet size remains more-or-less constant, and even attains its smallest value at $Q = 320$ kWh, almost in the middle of the domain of Q. This could be explained by the fact that when the battery size increases, and thus the number of aircraft which can be towed on a single charge with it, the time that an ETV has to retire to charge its battery also increases with it. Hence on average, the number of aircraft which can be towed within a given time remains constant. This continues up until the moment when the battery size is sufficiently large to not form a constraining factor in the schedule anymore.

This is opposed by the NC policy, which is very sensitive to the ETV battery size. This can be explained by the fact that the number of aircraft which can be towed by an ETV on a single charge is approximately linear in Q. As each ETV in the NC policy only uses one battery charge, the number of required ETVs should be proportional with $1/Q$, which corresponds to the results.

2.6 Conclusion

This chapter compares the effect of battery size and recharging policy on the impact which electric towing vehicles (ETVs) are able to make at large airports. This is done by using a Mixed-Integer-Linear-Optimization program to determine the smallest possible ETV fleet required to tow all considered aircraft. We consider three versions of this model, corresponding to the three charging policies: night, constant time, and partial charging. The first two of these are taken from the state-of-the-art literature on ETV scheduling problems. The battery size considered ranges from 100 kWh to 500 kWh.

We have applied the model in a case study at Amsterdam Airport Schiphol and found that the partial charging policy yields a significant improvement over the other policies. The considered flight schedule consists of 750 narrow-body aircraft, arriving throughout the day of operations. In the nominal case, when we consider an ETV battery of 320 kWh, the required fleet size is 66, 40 (-39%) and 29 (-56%) for the night charging, constant time charging, and partial charging policy, respectively. Additionally, it was found that the constant time charging policy is almost insensitive to the battery size.

In the next chapters, this charging policy is used as a basis on which the full ETV scheduling models are built. With these models, a cost-benefit analysis of the environmental impact as a function of the ETV fleet size is performed. Future research could consider Additionally, future research could study the economic trade-off between the number of required ETVs and the charging cycles which an ETV needs per day.

references

[1] S. van Oosterom, M. Mitici, and J. Hoekstra. "Analyzing the impact of battery capacity and charging protocols on the dispatchment of electric towing vehicles at a large airport". In: *AIAA AVIATION 2022 Forum*. AIAA AVIATION Forum. American Institute of Aeronautics and Astronautics, June 2022. DOI: 10.2514/6.2022-3920.

[2] European Commission. *Paris Agreement*. 2015. URL: https://ec.europa.eu/clima/eu-action/international-action-climate-change/climate-negotiations/paris-agreement_en.

[3] UNFCCC. *International Aviation Climate Ambition Coalition - COP26 Declaration*. https://ukcop26.org/cop-26-declaration-international-aviation-climate-ambition-coalition/. Nov. 2021. (Visited on 01/12/2022).

[4] IATA. *Resolution on the Implementation of the Aviation "CNG2020" Strategy*. 2013. URL: https://www.iata.org/contentassets/e8a7f8d96c554acd8e5fbbc09eb56559/agm69-resolution-cng2020.pdf.

[5] ICAO. *Consolidated statement of continuing ICAO policies and practices related to environmental protection – Climate change*. 2010. URL: https://www.icao.int/environmental-protection/37thAssembly/A37_Res19_en.pdf.

[6] Schiphol. *Emission free by 2030*. https://www.schiphol.nl/en/schiphol-as-a-neighbour/page/emission-free-by-2030/. Dec. 2019. (Visited on 11/11/2021).

[7] N. Dzikus, J. Fuchte, A. Lau, and V. Gollnick. "Potential for Fuel Reduction through Electric Taxiing". en. In: *11th AIAA Aviation Technology, Integration, and Operations (ATIO) Conference*. Virginia Beach, VA: American Institute of Aeronautics and Astronautics, Sept. 2011. ISBN: 978-1-60086-941-9. DOI: 10.2514/6.2011-6931. (Visited on 11/15/2021).

[8] H. Khadilkar and H. Balakrishnan. "Estimation of aircraft taxi fuel burn using flight data recorder archives". en. In: *Transportation Research Part D: Transport and Environment* 17.7 (Oct. 2012), pp. 532–537. ISSN: 13619209. DOI: 10.1016/j.trd.2012.06.005. (Visited on 11/15/2021).

[9] M. Soltani, S. Ahmadi, A. Akgunduz, and N. Bhuiyan. "An eco-friendly aircraft taxiing approach with collision and conflict avoidance". en. In: *Transportation Research Part C: Emerging Technologies* 121 (Dec. 2020), p. 102872. ISSN: 0968-090X. DOI: 10.1016/j.trc.2020.102872. (Visited on 12/13/2022).

[10] E. v. Baaren and P. Roling. "Design of a zero emission aircraft towing system". English. In: *AIAA AVIATION Forum, 17-21 June 2019, Dallas, Texas*. American Institute of Aeronautics and Astronautics Inc. (AIAA), 2019, AIAA. DOI: 10.2514/6.2019-2932. URL: https://research.tudelft.nl/en/publications/design-of-a-zero-emission-aircraft-towing-system (visited on 06/15/2021).

[11] LVNL - Air Traffic Control the Netherlands. *EHAM airport profile*. English. https://www.lvnl.nl/eaip/2021-12-16-AIRAC/html/eAIP/EH-AD-2.EHAM-en-GB.html. Aug. 2019. (Visited on 12/14/2021).

[12] M. S. Ziegler and J. E. Trancik. "Re-examining rates of lithium-ion battery technology improvement and cost decline". In: *Energy & Environmental Science* 14.4 (2021), pp. 1635–1651. DOI: 10.1039/d0ee02681f. URL: https://doi.org/10.1039%2Fd0ee02681f.

[13] N. E. Daidzic. "Determination of taxiing resistances for transport category airplane tractive propulsion". eng. In: *Advances in aircraft and spacecraft science* 4.6 (2017). Publisher: Techno-Press, pp. 651–677. ISSN: 2287-528X. DOI: 10.12989/aas.2017.4.6.651. URL: http://koreascience.or.kr/article/JAKO201732060819214.page (visited on 05/02/2023).

[14] Health, Safety and Environment office Schiphol. *Schiphol Regulations*. Tech. rep. Hoofddorp, Jan. 2020. URL: https://www.schiphol.nl/en/download/1640595066/43q9kGoE92CccmEeC6pdf.

[15] M. Lukic, P. Giangrande, A. Hebala, S. Nuzzo, and M. Galea. "Review, Challenges, and Future Developments of Electric Taxiing Systems". In: *IEEE Transactions on Transportation Electrification* 5.4 (Dec. 2019). Conference Name: IEEE Transactions on Transportation Electrification, pp. 1441–1457. ISSN: 2332-7782. DOI: 10.1109/TTE.2019.2956862.

CHAPTER 3

Scheduling electric towing for aircraft: routing and tactical assignment


In order to benchmark an ETV management model with disruption management, an algorithm that creates an optimal ETV schedule is required. In this chapter, such a model is developed. It assumes that the flight delays information is known in advance. The preemptive charging policy presented in the previous chapter is used.

The model addresses the ETV routing and ETV-to-aircraft assignment problems sequentially, using two mixed-integer linear programming models. These ensures that tows are performed as quick as possible, while a minimal number of ETVs is used. Additionally, we provide a first step for the operational ETV planning, by showing how these models can be embedded in a rolling horizon framework that accounts for flight delays.

We apply our proposed frameworks to several days of operations at Amsterdam Airport Schiphol. When comparing the routing algorithm with a greedy model, we observe a slight increase in the average towing time, most notable during the peak hours. The greedy algorithm does, on the other hand, required more vehicles to perform all flights. When flight delays are introduced, we show that this rolling horizon framework model results in 95% of the flights being towed. This provides a baseline for the full ETV fleet management algorithm developed in the next chapter.

Parts of this chapter have been published as:

S. van Oosterom, M. Mitici, and J. Hoekstra. "Dispatching a fleet of electric towing vehicles for aircraft taxiing with conflict avoidance and efficient battery charging". en. In: *Transportation Research Part C: Emerging Technologies* 147 (Feb. 2023), p. 103995. ISSN: 0968-090X. DOI: 10.1016/j.trc.2022.103995

3.1 Introduction

Aircraft taxiing is one of the main contributors to ground-based aviation emissions [2, 3]. In fact, aircraft taxiing accounts for 54% of the total emissions associated with the landing/take-off cycle [4]. As an example, studies at Heathrow airport have shown that 56% of the total nitrogen-oxides emissions are due to taxiing aircraft [5]. Also, on-ground fuel consumption has been estimated to be as high as 7% of the average of the total flight fuel consumption [2, 6]. To meet climate-neutrality targets for aviation, there is an urgent need for new technologies and procedures to reduce emissions during aircraft taxiing.

Electric vehicles that tow aircraft between runways and gates are seen as a key enabling technology for emissions reduction. Preliminary studies have shown that employing hybrid-electric vehicles for aircraft towing already reduces the CO_2 emissions during taxiing by 82% [4]. A full Electric Towing Vehicles (ETV) is expected to further reduce emissions during taxiing. Dispatching ETVs to tow aircraft is, however, a challenging scheduling problem for which two main aspects need to be addressed: (1) algorithms are needed to efficiently allocate ETVs to tow aircraft and to recharge ETVs' batteries, and (2) algorithms are needed to route the aircraft towed by ETVs such that a minimum separation distance between any two towed aircraft is maintained at all times, such that collisions are avoided. To the best of our knowledge, a framework for ETV dispatching that fully addresses these aspects in an integrated way is lacking. Routing algorithms for ETVs enable a safe and efficient management of the airport ground movements, yet the availability and capabilities of ETVs for routing is inherently dependent on the ETVs' charging schedules and on the actual allocation of ETVs to aircraft. Reversely, an efficient allocation of ETVs for charging and aircraft towing tasks is dependent on the routing of the ETV-towed aircraft in the taxiway system. In this chapter, we propose to address the two scheduling aspects in one integrated framework.

The dispatching of a generic vehicle fleet has frequently been posed in existing literature as a vehicle routing problem with time windows (VRP-TW). The VRP-TW problem requires that a fleet of vehicles is scheduled to visit a set of customers within a given time window (see Braysy et al. [7, 8]). Often considered objectives for the VRP-TW problem are the minimization of transport costs [9], travelled distance [10], or the size of the fleet of vehicles [11].

For generic electric vehicles which have battery charging requirements, solutions to the Electric-VRP-TW (E-VRP-TW) problem have been proposed. Initial studies assume a recharging policy where each visit of an electric vehicle to a recharging station takes a fixed amount of time, and the battery is charged to full capacity. During this re-charging time, the vehicles cannot visit customers. Conrad and Figliozzi [12] propose an iterative construction algorithm to minimize the required number of vehicles. Erdoğan and Miller-Hooks [13] propose a density-based clustering algorithm (DBCA) heuristic which minimizes the travelled distance. Omidvar and Tavakkoli-Moghaddam [14] propose a genetic algorithm (GA) which minimizes the transportation cost of the fleet of electric vehicles.

Further studies [15, 16] extend the E-VRP-TW problem by considering a battery recharge time which depends on the residual state-of-charge of the battery. Here also, the batter-

ies are charged to full capacity every time. In Schneider et al. [15] a tabu search (TS) algorithm is developed to minimize the travelled distance. Hiermann et al. [16] propose an adaptive large neighbourhood search (ALNS) heuristic which minimizes the required fleet size. Compared to the E-VRP-TW problems with fixed charging times, as in earlier studies [12–14], tests on the VRP-TW Solomon instances [17] by Schneider et al. [15] have shown that this charging assumption leads to a decrease in transportation costs of up to 10%. Building on this, an extension of the E-VRP-TW problem is proposed, where the recharging time not only depends on the residual state-of-charge of batteries, but partial charging of these batteries is also allowed [18–20]. Desaulniers et al. [18] consider the minimization of the travelled distance and develop a branch price & cut (BPC) algorithm to solve the problem to optimality. Keskin and Çatay [19] and Lin et al. [20] respectively develop an ALNS and a variable neighbourhood search (VNS) heuristic to minimize the transport costs. Keskin and Çatay [19], demonstrate that their model is able to further decrease transport costs with up to 5%, when applied on the Solomon instances.

When applied to the dispatching of ETVs for aircraft towing, the E-VRP-TW problem is only considered with simple battery charging policies such as fixed charging times, as discussed in Chapter 2. In Soltani et al. [21], ETVs are assumed to have an infinite battery life, i.e., no charging is required for these ETVs throughout the day of operations. Thus, this problem reduces to a general vehicle VRP-TW. Specific to ETVs, the authors ensure that the routing of the towing ETVs is done such that the towed aircraft do not collide with each other, by ensuring a minimum separation distance between any two ETVs. The proposed model is applied at Montreal International Airport on a schedule with 215 flights. Realistic ETV specifications [3], however, show that the capacity of the ETV batteries are limited and that multiple battery recharging moments are expected throughout a day of operations. These are unaccounted for by Soltani et al. but will impact the availability of the ETVs, and hence their schedule.

Van Baaren and Roling [22] consider the E-VRP-TW problem where ETVs take a fixed amount of time to recharge their batteries to full capacity, irrespective of the remaining state-of-charge of the battery. In contrast to Soltani et al., van Baaren and Roling do not ensure a minimum separation distance between towing ETVs as a part of the ETV dispatchment problem. The model is applied at Amsterdam Airport Schiphol for 1230 arriving and departing aircraft that are towed with ETVs. However, as presented in Chapter 2, the constant-time battery recharging assumption has been shown to result in a lower vehicle fleet utilization when compared to the models with state-of-charge dependent recharge times [19].

In this chapter we propose a two-phase mixed integer linear program to dispatch a fleet of ETVs at a large airport during a full day of operations. We propose an *integrated* approach by considering both the routing of towing ETVs across the taxiways, as well as the scheduling of ETVs for aircraft towing and battery recharge. We expand the charging model of Chapter 2, by including a non-linear power charging. Our model ensures that, while towing, the ETVs (and aircraft) maintain a minimum separation distance. Sequentially, our model assigns ETVs to towing tasks while taking into account the need of ETVs to recharge their batteries. The charging schedule is based on a preemptive charging policy and considers the residual state-of-charge of the batteries.

We illustrate our method for one day of operations at Amsterdam Airport Schiphol

(AAS). A total of 913 arriving and departing flights are considered for towing throughout the day. These flights are operated by a mix of narrow-body, wide-body and heavy-wide-body aircraft, each with its own designated ETV type. The results show that a fleet of 38 ETVs is required to tow these aircraft for a total average of 4 hours. Also, the battery recharge moments for these ETVs are distributed throughout the day, with a maximum demand for charging in the period 17:00-19:00, i.e. just before the peak evening hours at the airport. To further support the management of ETV in practice, we also propose a simple, Greedy ETV Fleet Dispatchment (GEFD) algorithm. GEFD reduces the computational time 50-fold in our case study at AAS, compared with our proposed mixed integer linear program, with an optimality gap of 5%.

The main contributions of the chapter are:

1. We propose an end-to-end management framework for ETVs that integrates the routing of the ETVs in the taxiway system with the scheduling of these ETVs for aircraft towing and battery re-charging;
2. We include a partial battery recharging policy for ETVs, which is identified as a research gap [22];
3. We propose a Greedy heuristic for ETV management, which is shown to achieve an optimality gap of 5% relative to our optimal solutions.

The remainder of this chapter is organized as follows. In Section 3.2 we introduce the ETV dispatching problem taking. We then propose a model for the energy consumption and recharging rates of the ETVs in Section 3.3. In Section 3.4 we develop our ETV dispatchment optimization models. In Section 3.5 we illustrate our problem for one day of operations at Amsterdam Airport Schiphol. We compare the performance of our models with the performance of our proposed GEFD heuristic in Section 3.6. Finally, concluding remarks and future research directions are given in Section 3.7.

3.2 Tactical scheduling for electric towing vehicles

We consider an airport where each day, the dispatching of an ETV fleet has to be optimized. While using ETVs to tow aircraft across the taxiways, collisions have to be avoided. During the day, these ETVs may also need to re-charge their batteries. An overview of all the used notation can be found in Table A.2.

3.2.1 Airport taxiways and service road networks

Let N_R be the set of runway entrance and exit nodes, and let N_G be the set of gates. These sets are connected by two networks. First we consider the directed graph $G_X = (N_X, E_X)$, the taxiway network which consists of junctions N_X and taxiway roads E_X. The taxiway is connected to the runways and gates via edges $E_X^G \subseteq N_X \times N_G$ and $E_X^R \subseteq N_X \times N_G$. Let $d_X : E_X \cup E_X^G \cup E_X^R \to \mathbb{R}^+$ and $v_X : E_X \cup E_X^G \cup E_X^R \to \mathbb{R}^+$ denote the length of- and maximum

speed on- an edge of network G_X. The aircraft are assumed to be attached to an ETV while on G_X. When ETVs are not towing an aircraft, then these use a service road network to traverse the airport. This is represented by the undirected graph $G_S = (N_S, E_S)$, with E_S the set of service roads and N_S the set of junctions of the service roads. The service roads are connected to the runways and gates via edges $E_S^G \subseteq N_S \times N_G$ and $E_S^R \subseteq N_S \times N_G$. Let $d_S : E_S \cup E_S^G \cup E_S^R \to \mathbb{R}^+$ denote the length of an edge d_S of network G_S. On all edges of G_S, a maximum speed of v_S is in place. Figure 3.1 shows an example of G_X and G_S at an airport.

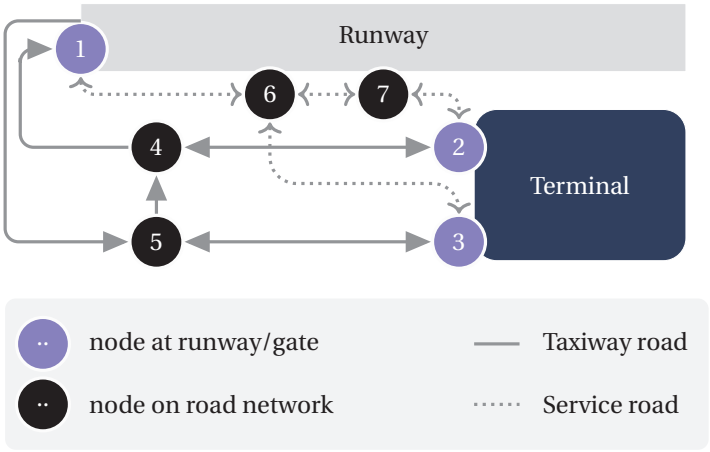

Figure 3.1.: Example of an airport taxiway and serviceroad network. The runway entrance and exit is located at node 1, and the gates are located at nodes 2 and 3. The taxiway is shown with *solid* lines, while the service roads are shown in *dashed* lines, while traffic directions are indicated with arrowheads. In this example: $N^R = \{1\}$, $N^G = \{2,3\}$, $N_X = \{4,5\}$, and $N_S = \{6,7\}$, such that: $E_X = \{(5,4)\}$, $E_X^G = \{(2,4),(4,2),(3,5),(5,3)\}$, $E_X^R = \{(1,5),(4,1)\}$, $E_S = \{\{6,7\}\}$, $E_S^G = \{\{2,7\},\{3,6\}\}$, and $E_S^R = \{\{6,1\}\}$.

3.2.2 Towing tasks

Let T denote a day of operations at the airport, such that $|T| = 24$ hours. Let A be the set of aircraft which arrive or depart at the airport during T. Each aircraft from A represents a towing task: it needs to taxi from a node in N^R to one in N^G or vice versa. A towing task is defined as a tuple (n^s, t^s, n^e, m), where n^s is the node from where the task is started, $n^s : A \to N^R \cup N^G$, t^s is the first moment when this towing task can start, $t^s : A \to T$, and n^e the destination node for the aircraft, $n^e : A \to N^R \cup N^G$. Finally, $m : A \to \mathbb{R}^+$ is the mass of the aircraft.

The aircraft are categorized into three weight classes $W = \{\text{NB, WB, H-WB}\}$, denoting narrow-body, wide-body and heavy-wide-body aircraft, and into arriving and departing flights. Let $A^{arr,w}$ and $A^{dep,w}$ denote the arriving and departing aircraft of weight class $w \in W$, respectively. Finally, let $A^w := A^{arr,w} \cup A^{dep,w}$.

3.2.3 ETV towing process

We assume the following ETV towing process (see Figure 3.2). A departing aircraft $a \in A^{dep,w}$ is first connected to an ETV at a gate node $n^s(a)$, which takes t^{Con} time units. The aircraft is then pushed back onto the taxiway system G_X. Let t^{PB} denote the duration of this push-back. The aircraft is towed across G_X up to the runway entrance node $n^e(a)$. Finally, the aircraft and the ETV are disconnected, which takes t^{DCon} time. After this, the aircraft engine is warmed-up for t^{EWU} time and it proceeds to take-off.

In the case of an aircraft arrival at the airport, following landing, the aircraft's engine is first cooled down before it is attached to an ETV. Cooling down the engines takes t^{ECD} time.

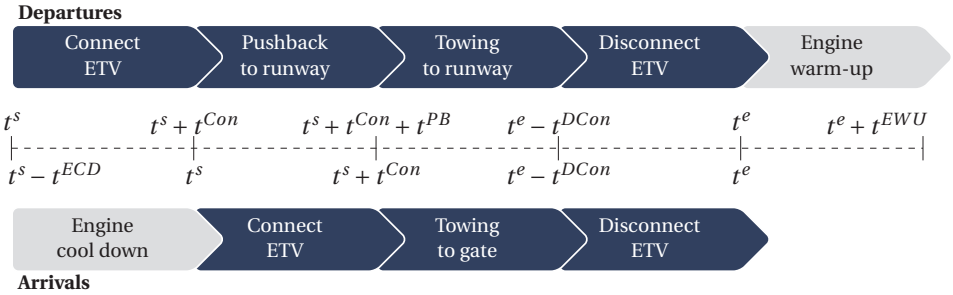

Figure 3.2.: Towing process for a departing/arriving aircraft. The ETV is connected to the aircraft in the time period $[t^s, t^e]$, marked by the green, darker, fields.

3.2.4 ETV specifications

We assume a dedicated type of ETV to service each aircraft weight class $w \in W$. Whether in reality ETVs will be able to tow aircraft from smaller weight classes is not known at this moment, it may e.g. be hindered by incompatible mechanical couplings. Each type of ETV is equipped with a battery of capacity Q_w, has a mass of m_w, and a top-speed of v_w. We assume that on the service roads, ETVs drive at velocity v_S. When towing an aircraft across the taxi system G_X, the ETV's velocity is limited by v_w, and ETVs traverse an edge $e \in E_X$ at a constant velocity between a maximum $v^w_{max}(e) = \min\{v_X(e), v_w\}$ and a minimum $v^w_{min} : (E_X \cup E^G_X \cup E^R_X) \to \mathbb{R}^+$. In short, the minimum and maximum velocity for towing is defined for each edge in G_X and for a given type of aircraft. Besides, an aircraft is allowed to accelerate and decelerate at a maximum rate of a^{max}. Finally, let P_w denote the energy required to drive an ETV per unit time, where P_w is a function of the weight of the aircraft being towed and the ETV's velocity.

3.2.5 Routing and separation distance policy

We assume the following routing policy for aircraft and ETVs traversing G_X and G_S. First, when ETVs are using the service roads G_S, they travel the shortest path on G_S, using d_S as a distance metric. We assume that they do not have to maintain distance from each other

in this phase. For the aircraft, which are towed by an ETV when traversing G_X, conflicts between aircraft are avoided by imposing a minimum separation distance d^w_{sep} between any pair of aircraft (see Figure 3.3). Aircraft are always towed to their destination using the shortest path in G_X, using d_X as a distance metric. Doing so minimizes the energy required to tow the aircraft, while separation distance infringements can be resolved by adjusting the towing speed between v^w_{min} and v^w_{max}.

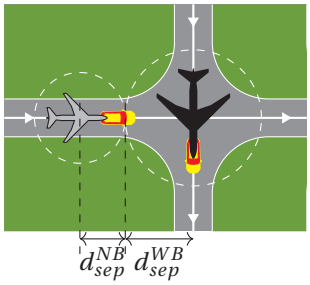

Figure 3.3.: Minimum distance separation between a narrow-body and a wide-body aircraft.

3.2.6 ETV charging policy

Between consecutive towing tasks, ETVs may have the opportunity to recharge their batteries. This is done at one of the charging stations located along the service road, which are located at nodes $N^{CS} \subset N_S$. We use the following battery charging policy for an ETV. Firstly, partial recharging is allowed. This means that an ETV does not need to fully charge its battery during a visit to a charging station. Secondly, ETVs end their day of operations with charge Q_w (a full battery). Thirdly, the last full battery recharge is done during the night at depot $n^{dep} \in N^{CS}$. Finally, every visit to a charging station should allow at least t^c_{min} time for charging.

3.2.7 ETV dispatching objective

Taking into account the i) airport layout, ii) flight schedule for an entire day of operations, iii) the ETV specifications, iv) routing and charging policies, we are interesting in optimizing the ETV dispatchment such that we avoid conflicts between towed aircraft and the dispatched fleet of ETVs is optimally sized to tow all considered aircraft.

3.3 Energy consumption and charging model for towing vehicles

We consider the following power $P_w(v,m)$ consumed by an ETV of weight class w traveling at velocity v, with a towed mass m. If the ETV is not towing an aircraft, $m=0$.

$$P_w(v,m) = \mu_w^g(v)(m_w+m)gv, \tag{3.1}$$

$$\mu_w^g(v) = \mu_w^0\left(1+\frac{v}{v_w^0}\right), \tag{3.2}$$

Here, μ^g denotes the Coefficient of Rolling Resistance, which depends on v and constants v_w^0 and μ_w^0 [22].

Let q denote the total energy consumption of a towing task (aircraft towed by ETV from node n^s to n^e) or drive (ETV driving in G_S),

$$q = \int_{T'} P_w(v(t),m)\mathrm{d}t \tag{3.3}$$

Given that we assume a constant velocity V^s to traverse an edge in G_S and a constant velocity V^X to traverse an edge in G_X, (3.3) becomes:

$$q = \int_{T'} P_w(v(t),m)\mathrm{d}t = \sum_{i=1}^{k-1}\frac{d(n_i,n_{i+1})}{v_i}P_w(v_i,m), \tag{3.4}$$

where n_i and n_{i+1} are consecutively visited junctions in G_X or G_S, and v_i is the velocity at which the ETV travels between these nodes.

When ETVs traverse G_S, they travel the shortest path at constant velocity v_s. In this case, (3.4) is simplified as:

$$q_w^S(n_1,n_k) := \sum_{i=1}^{k-1}\frac{d(n_i,n_{i+1})}{v_s}P_w(v_s,m) = \frac{\sum_i d(n_i,n_{i+1})}{v_s}P_w(v_s,m) = t^S(n_1,n_k)P_w(v_s,m), \tag{3.5}$$

where q_w^S and t^S denote the required charge and traveling time between nodes n_1 and n_k, respectively.

ETVs can recharge their batteries at one of the charging stations. We assume that the charging time follows a bi-linear profile, used previously in Mitici et al. [23]. Up to $\alpha Q^w (< Q^w)$, the battery is charged at a rate of P_w^c (fast-charging), and from αQ^w it becomes βP_w^c (slow-charging). Figure 3.4 shows the bi-linear and actual charging profiles.

3.4 Tactical scheduling LP formulation

The schedule management of a fleet of ETVs, i.e., deciding which aircraft is towed by which ETV and when ETVs recharge their batteries, directly depends on the way the towed aircraft are routed across the taxiway system. Firstly, the availability of an ETV for a new towing task depends on the taxi time of the previously towed aircraft. Secondly, the

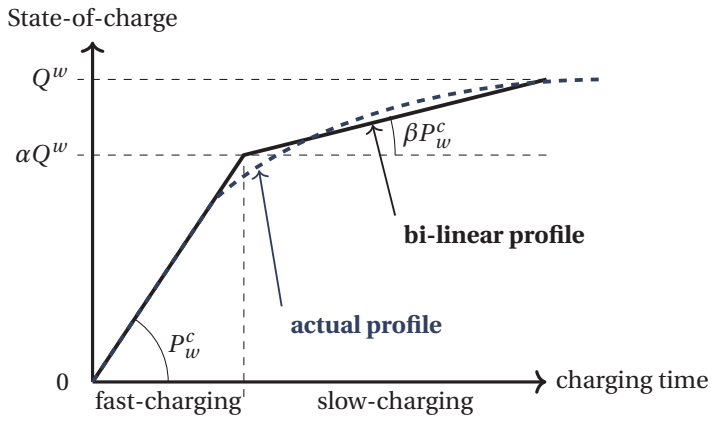

Figure 3.4.: The actual and bi-linear charging profile.

state-of-charge of an ETV battery depends on the energy used to tow aircraft in previous taxiing operations. The taxi time and the ETV battery state-of-charge, in turn, depend on the distance covered, and speed maintained, during taxiing.

As such, we first propose a MILP which manages the traffic of the towed aircraft on the taxiway (Subsection 3.4.1). The aircraft are routed to their destination along the shortest paths in the airport taxiway system. In order to ensure that aircraft maintain a minimum separation distance, the velocities with which they are towed are adjusted. The velocities are optimized to minimize the caused delay. The choice of routing the ETVs across the shortest path is motivated by the fact that this requires the least energy per towing, which maximizes the environmental impact of using ETVs.

Next, the obtained velocities of the towed aircraft are used to optimally schedule a fleet of ETVs (Subsection 3.4.2). We propose a second MILP to schedule ETVs either to tow aircraft or to recharge their batteries. The fleet of ETVs is sized such that all considered aircraft are towed.

3.4.1 Phase 1 - Towing aircraft while maintaining minimum separation distance

Let us first introduce the following notation. We define a path traversed by $a \in A$ as:

Definition 3.4.1 *The path of a towing task $a \in A$, denoted by $N_a = (n^a_0, n^a_1, n^a_2, ..., n^a_{k_a})$ is the shortest path in G_X between $n^s(a) = n^a_0$ and $n^e(a) = n^a_{k_a}$, using $d_X(\cdot)$ as a distance metric. The set of all edges on the path of this aircraft is denoted as $E_a := \{(n^a_i, n^a_{i+1})\}_{i \in \{1,...,k_a-1\}}$.*

For each $n \in N_X \cup N_R \cup N_G$, let $A_n \subseteq A$ be the aircraft for which $n \in N_a$. We are interested in determining the velocity at which to tow each aircraft at each road segment, i.e., the velocity profile:

Definition 3.4.2 *A velocity profile of a towing task $a \in A^w$ is a mapping $v^a : E_a \rightarrow \mathbb{R}^+$, such that $v^w_{min}(e) \leq v^a(e) \leq v^w_{max}(e)$ for all $e \in E_a$.*

For each edge $e \in E_X \cup E_X^G \cup E_X^R$ and aircraft weight class $w \in W$, the shortest and longest times in which a weight class w aircraft can traverse e are denoted as $t^w_{min}(e) = d_X(e)/v^w_{max}(e)$ and $t^w_{max}(e) = d_X(e)/v^w_{min}(e)$, respectively. The latter is always finite, and as such the aircraft never stands still during towing and the static resistance never needs to be overcome. Let $t^{end}_{min}(a) = \sum_{e \in N_a} t^w_{min}(e) + t^{Con} + \mathbb{1}_{a \in \cup_{w \in W} A^{arr,w}}(t^{PB})$ denote the earliest time at which aircraft $a \in A$ can reach its destination.

Finally, we determine the sets that describe which pairs of aircraft can cause separation distance infringements. There are three separate cases in which these infringements can occur: when two aircraft cross each other at a node, when one tries to overtake another on an edge, and when two towed aircraft encounter each other head-on on an edge. For this, let $t^{min}_{n,d}(a)$ and $t^{max}_{n,d}(a)$ denote the first and last time aircraft a can be within distance d of node n. These are determined using t^w_{min}, t^w_{max}, and $t^s(a)$.

First, let A^{con}_n denote the set of pairs of aircraft which can cause separation distance infringements at a node $n \in N_X \cup N_R \cup N_G$. Let $a, b \in A_n$ with a and b of weight classes w_a and w_b. These are included in A^{con}_n if there exists velocity profiles for a and b such that when a is at node n, b can be within the separation distance of node n or vice versa (see Figure 3.3):

$$\{a, b\} \in A^{con}_n \Leftrightarrow t^{min}_{n,d}(a) \leq t^{max}_{n,0}(b) \wedge t^{min}_{n,0}(b) \leq t^{max}_{n,d}(a) \text{ with } d = d^{w_a}_{sep} + d^{w_b}_{sep}$$

Second, let A^{ot}_{nm} denote the set of pairs of aircraft which can cause separation distance infringements when towed aircraft trail each other on the same edge. Specifically, a pair of towed aircraft $a, b \in A$ with $(n, m) \in E_a \cup E_b$ is included in A^{ot}_{nm} if there exist velocity profiles for a and b such that a overtakes b on (n, m) or vice versa (see Figure 3.5a):

$$\{a, b\} \in A^{\text{ot}}_{nm} \Leftrightarrow t^{min}_{n,0}(a) \leq t^{max}_{n,0}(b) \wedge t^{min}_{m,0}(b) \leq t^{max}_{m,0}(a)$$

Third, let A^{ho}_{nm} denote the set of pairs of aircraft which can cause separation distance infringements on a pair of edges (n, m), with $(m, n) \in E_X \cup E_X^R \cup E_X^G$, when the towed aircraft taxi in opposite directions. A pair of towed aircraft a, b such that $(n, m) \in E_a$ and $(m, n) \in E_b$ is included in A^{ho}_{nm} if there exist velocity profiles for a and b such that a is on (n, m) and b is on (m, n) simultaneously and the towed aircraft encounter each other head-on (see Figure 3.5b):

$$\{a, b\} \in A^{\text{ho}}_{mn} \Leftrightarrow t^{min}_{n,0}(a) \leq t^{max}_{n,0}(b) \wedge t^{min}_{m,0}(b) \leq t^{max}_{m,0}(a)$$

Decision variables

We consider the following set of decision variables:

$$t^a_n \in \mathbb{R}, \qquad \text{arrival time of } a \in A \text{ at } n \in N_a.$$

Using these, the velocity profile of aircraft a is given by $v^a((n, m)) = \left(t^a_m - t^a_n\right)/d_X((n, m))$.

We also consider the following two auxiliary decision variables to ensure a minimum separation between any two towed aircraft:

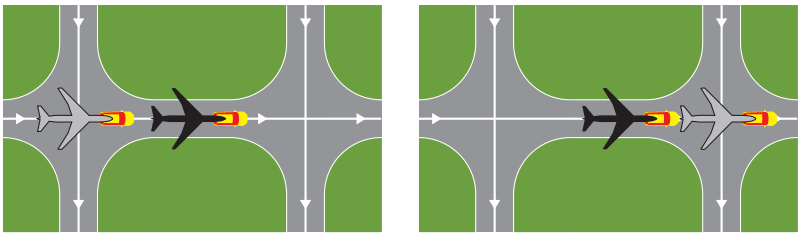

(a) Towed aircraft overtaking each other on the same taxiway.

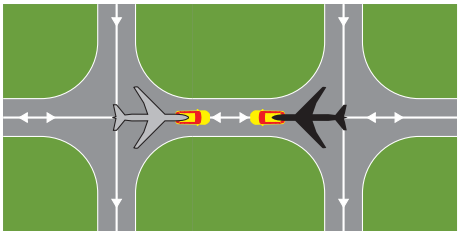

(b) Towed aircraft encountering head-on on the same taxiway.

Figure 3.5.: Causes for a separation distance infringement besides the situation shown in Figure 3.3.

$\Delta t_n^a \in \mathbb{R}^+$, time that $a \in A$ takes to taxi for a distance d_{sep} after arriving at $n \in N_a$,

$z_n^{ab} = \begin{cases} 1, & \text{if } a \in A \text{ passes node } n \in N_a \cap N_b \text{ before } b \in A \text{ passes node } n, \\ 0, & \text{otherwise,} \end{cases}$

such that a node $n \in N_a$ cannot be visited by other towed aircraft between t_n^a and $t_n^a + \Delta t_n^a$ without generating separation distance infringements. The values of these variables can be deduced from the t variables. If $(n,m) \in E_a$, then Δt_n^a is given by $\Delta t_n^a = \left(t_m^a - t_n^a\right) \dfrac{d_{sep}}{d_X((n,m))}$. The z variables determine the order in which the aircraft visit the nodes.

Objective function

We consider the following objective function that minimizes the maximum delay of towed aircraft as a result of keeping a minimum separation distance between any two towed aircraft:

$$\min_{t,\Delta t,z} \max_{a \in A} \left\{ t_{n^e(a)}^a - t_{min}^{end}(a) \right\}, \tag{3.6}$$

where $t_{n^e(a)}^a$ and $t_{min}^{end}(a)$ denote the arrival time of aircraft $a \in A$ at its destination node after ensuring a minimum separation d_{sep} with all other towed aircraft, and the earliest time at which aircraft $a \in A$ can reach its destination node, respectively.

Constraints

We consider the following constraints:

$$t^a_{n^s(a)} = t^s(a) + t^{Con} \qquad \forall w \in W, a \in A^{arr,w} \tag{3.7}$$

$$t^a_{n^s(a)} \geq t^s(a) + t^{Con} + t^{PB} \qquad \forall w \in W, a \in A^{dep,w} \tag{3.8}$$

$$t^a_m + t^w_{min}((m,n)) \leq t^a_n \qquad \forall w \in W, a \in A^w, (m,n) \in E_a \tag{3.9}$$

$$t^a_m + t^w_{max}((m,n)) \geq t^a_n \qquad \forall w \in W, a \in A^w, (m,n) \in E_a \tag{3.10}$$

$$\frac{t^a_n - t^a_m}{d_X((m,n))} - \frac{t^a_m - t^a_l}{d_X((l,m))} \leq \frac{a^{max} t^w_{min}((m,n))}{(v^w_{max}((l,m)))^2} \qquad \forall w \in W, a \in A^w, (l,m),(m,n) \in E_a \tag{3.11}$$

$$\frac{t^a_m - t^a_l}{d_X((l,m))} - \frac{t^a_n - t^a_m}{d_X((m,n))} \leq \frac{a^{max} t^w_{min}((m,n))}{(v^w_{max}((l,m)))^2} \qquad \forall w \in W, a \in A^w, (l,m),(m,n) \in E_a \tag{3.12}$$

$$\Delta t^a_n = (t^a_m - t^a_n)\frac{d_{sep}}{d_X((n,m))} \qquad \forall a \in A, (n,m) \in E_a \tag{3.13}$$

$$t^b_n \geq t^a_n + \Delta t^a_n - z^{ba}_n |T| \qquad \forall n \in N_X \cup N_R \cup N_G, \{a,b\} \in A^{\text{con}}_n \tag{3.14}$$

$$z^{ab}_n - z^{ab}_m = 0 \qquad \forall (n,m) \in E_X \cup E^R_X \cup E^G_X, \{a,b\} \in A^{\text{ho}}_{nm} \tag{3.15}$$

$$z^{ab}_n - z^{ab}_m = 0 \qquad \forall (n,m) \in E_X \cup E^R_X \cup E^G_X, \{a,b\} \in A^{\text{ot}}_{nm} \tag{3.16}$$

$$z^{ab}_n + z^{ba}_n = 1 \qquad \forall (n,m) \in E_X \cup E^R_X \cup E^G_X, \{a,b\} \in A^{\text{con}}_n \cup A^{\text{ho}}_{nm} \cup A^{\text{ot}}_{nm} \tag{3.17}$$

Constraint (3.7) ensures that all arriving aircraft start taxiing at the earliest possible moment in order to clear the runway exits as soon as possible. Constraint (3.8) is the equivalent of Constraint (3.7) for departing aircraft. In comparison to arrival aircraft, however, departing aircraft may depart later from their gate than $t^s(a)$. Constraints (3.9) and (3.10) ensure that aircraft do not taxi faster or slower then their maximum and minimum speed, respectively. Constraints (3.11) and (3.12) limit the maximum acceleration and deceleration of the aircraft. Constraint (3.13) defines the time it takes an aircraft to distance itself d_{sep} from node n. Constraint (3.14) ensures that separation distance is maintained by any pair of towed aircraft a, b at node n, as shown in Figure 3.3. Constraints (3.15) and (3.16) ensures that there are no separation distance infringements by two aircraft which use the edge in the opposite-, and the same-, direction, respectively. These correspond to Figures 3.5b and 3.5a. Finally, constraint (3.17) defines the order in which two aircraft a and b pass a node n.

The domain of each variable is specified in Eq. (3.18), (3.19) and (3.20):

$$t^a_n \in \mathbb{R} \qquad \forall a \in A, n \in N_a \tag{3.18}$$

$$\Delta t^a_n \in \mathbb{R}^+ \qquad \forall a \in A, n \in N_a \tag{3.19}$$

$$z^{ab}_n \in \{0,1\} \qquad \forall n \in N_X \cup N_R \cup N_G, \{a,b\} \in A^{\text{con}}_n \tag{3.20}$$

3.4.2 Phase 2 - Scheduling towing tasks and battery recharging moments for ETVs

Having obtained the routing of the ETVs in the taxi system, we now propose a MILP to assign ETVs to towing tasks and battery recharging moments. Since each aircraft weight

class $w \in W$ has its own designated ETV type, we pose the MILP for a specific aircraft weight class.

Let $t^{end}(a) := t^a_{n^e(a)} + t^{DCon}$ denote the time an ETV finishes towing aircraft a. Let $t^a_{nm} := t^a_m - t^a_n$ denote the time a takes to traverse edge (n,m). Then, the energy needed to tow task a is given by:

$$q^X(a) := \sum_{nm \in E_a} t^a_{nm} P_w \left(v^a((n,m)), m(a)\right),$$

where v^a is the velocity profile of a and $m(a)$ its mass (see Section 3.3).

Let A^{in}_a and A^{out}_a be the set of towing tasks which can be performed before and after towing task a by the same ETV, respectively, with:

$$A^{in}_a := \{b \in A^w : t^e(b) + t^S(n^e(b), n^s(a)) \leq t^s(a)\},$$
$$A^{out}_a := \{b \in A^w : a \in A^{in}_b\}.$$

In between two towing tasks a and b, ETVs may have the opportunity to recharge their battery at a charging station in N^C. ETVs always use the charging station closest to their next towing task. We denote this station by $n^C(b)$. For simplicity, we introduce the following abbreviations for the required energy of several types of movements of ETVs on the service road system (see Section 3.3):

$$q^S_f(a) := q^S_w(n^{dep}, n^s(a)),$$
$$q^S_l(a) := q^S_w(n^e(a), n^{dep}),$$
$$q^S(a,b) := q^S_w(n^e(a), n^s(b)),$$
$$q^S_C(a,b) := q^S_w(n^e(a), n^{CS}(b)) + q^S_w(n^{CS}(b), n^s(b)),$$
$$q^S_C(a) := q^S_w(n^{CS}(a), n^{st}(a)).$$

Here, q^S_f denotes the energy required to drive from the ETV depot to the start of a task, and q^S_l denotes the energy required to drive from the end of a task to the depot. These are the first and last movements made by an ETV on the day of operations. Also, $q^S(a,b)$ and $q^S_C(a,b)$ denote the energy to drive directly from the end of task a to the start of task b directly and via charging station $n^C(b)$, respectively. Finally, $q^S_C(a)$ denotes the energy required to drive from the charging station $n^C(a)$ to the start of task a.

For a pair of towing tasks a and b, let $t^c(a,b)$ denote the available time for charging between these tasks:

$$t^c(b,a) := \left[t^s(a) - t^S(n^{CS}(a), n^s(a))\right] - \left[t^e(b) + t^S\left(n^e(b), n^{CS}(a)\right)\right]$$

Finally, between performing two towing tasks a and b, an ETV is allowed to recharge if two conditions are met: i) the ETV should be able to arrive at b with a higher state of charge after recharging than if it drives directly from a to b, ii) the available charging time is at least t^c_{min}. For a towing task a, let $A_{C,a}$ denote the set of tasks which can be executed before task a for which these two conditions hold,

$$A_{C,a} := \{b \in A^{in}_a : t^c(b,a) > t^c_{min} \wedge q^{dr}(b,a) > q^{dr}_{CS}(b,a) - t^c(b,a) P^c_w\}.$$

Decision variables

We consider the following decision variables, which determine the order in which the towing tasks are performed by the ETVs:

$$x_{ab} = \begin{cases} 1 & \text{if aircraft } a \text{ is towed directly before } b, \\ 0 & \text{else,} \end{cases}$$

$$x_a^f = \begin{cases} 1 & \text{if aircraft } a \text{ is the first the ETV tows in a day,} \\ 0 & \text{else,} \end{cases}$$

$$x_a^l = \begin{cases} 1 & \text{if aircraft } a \text{ is the last the ETV tows in a day,} \\ 0 & \text{else.} \end{cases}$$

Additionally, the q variables keep track of the state-of-charge of the ETV batteries:

$$q_a \in \mathbb{R} \qquad \text{ETV battery charge at start of task } a.$$

Objective function

We consider the following objective function that minimizes the number of ETVs required to perform all towing tasks during a day:

$$\min_{x,q} \sum_{a \in A^w} x_a^f \tag{3.21}$$

Constraints

We consider the following constraints:

$$x_a^f + \sum_{b \in A_a^{in}} x_{ba} = 1 \qquad \forall a \in A^w \tag{3.22}$$

$$x_a^l + \sum_{b \in A_a^{out}} x_{ab} = 1 \qquad \forall a \in A^w \tag{3.23}$$

$$q_a \leq Q_w - x_a^f q_f^S(a) + Q_w(1 - x_a^f) \qquad \forall a \in A^w \tag{3.24}$$

$$0 \leq q_a - x_a^l(q^X(a) + q_l^S(a)) + Q_w(1 - x_a^l) \qquad \forall a \in A^w \tag{3.25}$$

$$q_b \leq q_a - x_{ab}(q^X(a) + q^S(a,b)) + Q_w(1 - x_{ab}) \qquad \forall b \in A^w, a \in A_b^{in} \setminus A_{C,b} \tag{3.26}$$

$$q_b \leq q_a - x_{ab}(q^X(a) + q_C^S(a,b) - P_w^c t^c(a,b)) + Q_w(1 - x_{ab}) \qquad \forall b \in A^w, a \in A_{C,b} \tag{3.27}$$

$$\begin{aligned} q_b \leq\ & q_a - x_{ab}(q^X(a) + q_C^S(a,b)) + Q_w(1 - x_{ab}) + \\ & (1-\beta)(\alpha Q - (q_a - x_{ab}(q^X(a) + q_C^S(a,b)))) + \beta P_w^c t^c(a,b) \end{aligned} \qquad \forall b \in A^w, a \in A_{C,b} \tag{3.28}$$

Eqs. (3.22) and (3.23) ensure that each towing task is executed by exactly one ETV. Eq. (3.24) limits the state-of-charge of the ETV whent a is the first task performed by that ETV

in a day. Eq. (3.25) ensures after an ETV performs its last task in a day, then that ETV still has enough energy to reach the depot. Eq. (3.26) limits the battery charge between tasks if the ETV does not visit a charging station in-between these tasks. Eqs. (3.27) and (3.28) calculate the new state of charge if a charging station is visited and fast or slow charging is used, respectively (see Figure 3.4). Finally, the domain of each decision variable is specified in Eqs. (3.29) and (3.30):

$$x_{ab}, x_a^f, x_a^l \in \{0,1\} \qquad \forall a \in A, b \in A_a^{out} \tag{3.29}$$

$$q^X(a) \leq q_a \leq Q_w - q_C^S(a) \qquad \forall a \in A. \tag{3.30}$$

3.5 Case study: Dispatching a fleet of ETVs at Amsterdam Airport Schiphol

Airport taxi system and service road system

Figure 3.6 shows the runway entrances and exists, N^R, and the gate nodes, N^G, together with the connecting road networks at AAS (based on the Schiphol aerodrome charts [24]). In total, there are 6 runways and 7 piers (B, C, D, E, F, G, H/M). These are converted to 10 runway nodes and 9 gate nodes, indicated by vertically hatched circles on the map. The edges of the taxiway and service road networks, which connects N^G and N^R, are indicated with solid and dashed lines, respectively. In the taxiway network, some of the edges can be traversed in one direction only, and this is indicated by arrows. We assume five charging stations N^{CS} = {C1,C2,C3,C4,C5} are available at AAS (indicated with horizontally hatched circles in Figure 3.6). We also assume that the ETV depot is centrally located at station n^{dep} = C5.

Aircraft to be towed at AAS during one day of operations

We consider the flight schedule of an entire day of operations at AAS, with data from the day of operations of December 14, 2019. Figure 3.7 shows the distribution of the earliest time to start towing, t^s, for all flights considered. This schedule consists of 913 flights (750 narrow-body, 147 wide-body, and 16 heavy-wide-body aircraft), arriving and departing on this day of operation. In 2019, the average number of arriving and departing flights at AAS was 1230 [25], making the 14th of December 2019 a relatively quiet but still representative day of traffic at AAS. Additionally, this selected day exhibits a varied mix of runway configurations since five out of the six runways at AAS (18R-36L, 18L-36R, 09-27, 04-22, and 06-24) are being used in eight different runway configurations throughout the day.

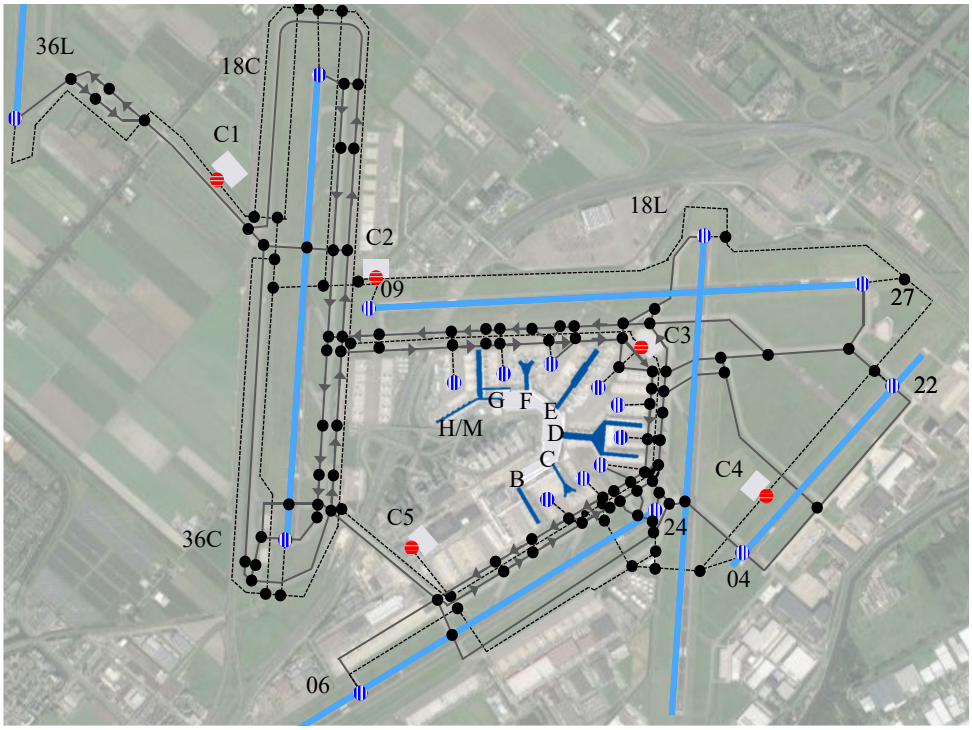

Figure 3.6.: Runways N^R and gate nodes N^G, together with taxiways (solid lines), service roads (dashed lines) and charging stations (C1, ..., C5) at AAS. The map is based on the Schiphol aerodrome charts [24].

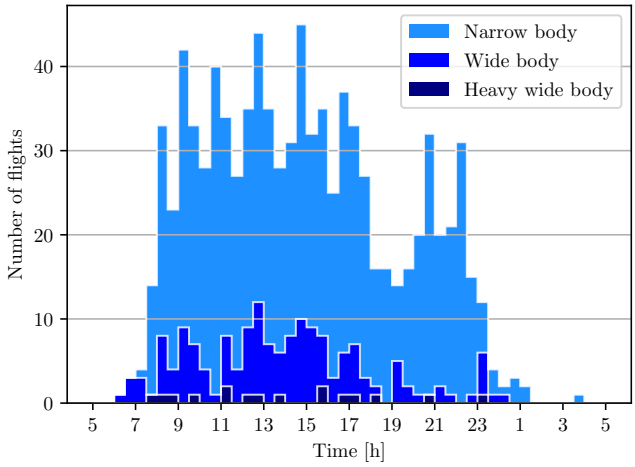

(a) By aircraft weight class, cumulative

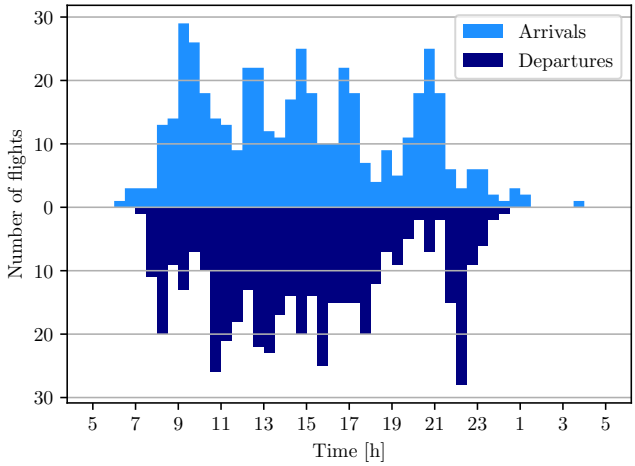

(b) By arrivals/departures

Figure 3.7.: Distribution of the earliest time to start towing, t^s, for all flights arriving/departing at AAS on December 14, 2019.

ETV specifications

Table 5.1 shows the ETV specifications assumed for our case study. These specifications are a function of the aircraft weight class (Table 3.1a) as well as additional non-weight-related parameters (Table 3.1b).

	Explanation	Value			Ref
w	weight class	NB	WB	H-WB	
v_w [km/h]	Maximum towing speed	42.5	37	37	[3]
P^c_w [kW]	charging power	100	350	500	[22]
m_w [10^3kg]	ETV mass	15	35	50	[22]
Q_w [kWh]	Battery capacity	400	1250	3200	[22]
$d^w_{sep}[m]$	separation distance	40	50	60	

(a) Parameters dependent on the aircraft weight class.

	Explanation	Value	Ref
$t^c_{min}[h]$	Minimum charging time	1	
$t^{ECD}[s]$	Engine-cool-down-time	180	[26]
$t^{Con}[s]$	Connect-time	60	
$t^{PB}[s]$	Push-back-time	120	[27]
$t^{DCon}[s]$	Disconnect-time	60	[27]
$t^{EWU}[s]$	Engine-warm-up-time	300	[26]
α	Charging curve coefficient	0.9	[23]
β	Charging curve coefficient	0.1	[23]
μ_0	Rolling resistance coefficient	0.1	[28]
v_0 [km/h]	Rolling resistance base velocity	41.16	[28]
v_s [km/h]	Service road velocity	30	[29]

(b) Additional parameters.

Table 3.1.: Electric towing specifications.

3.5.1 Results - Dispatching a fleet of ETVs at AAS

Results Phase 1 - Taxiing towed aircraft while avoiding separation distance infringements

Figure 3.8 shows the results obtained for the Phase 1 MILP. Figure 3.8a shows a histogram of the additional taxi time needed for ETVs to keep a minimum separation distance d_{sep}, i.e., $t^a_{n^e(a)} - t^{end}_{min}(a)$ for all $a \in A$. The maximum obtained additional taxi time is 90 seconds. Of the total 913 aircraft, only 26 aircraft require an additional taxi time of more than 60 seconds.

Figure 3.8b shows the average additional taxi time required by ETVs per 30 minute time windows. The highest additional taxi times are required during the peak hours of 11 AM, 1 PM and 3 PM. During these time periods, the number of arrivals at the airport is similar to the number of departures, as can be seen in Figure 3.7b. This causes large streams of in-and-outbound aircraft to be towed in opposite directions on some of the bidirectional roads in the taxiway network, which may lead to head-on encounters. Solving for these potential head-on separation distance infringements leads to longer taxiing times, compared to solving for infringements caused by trailing aircraft.

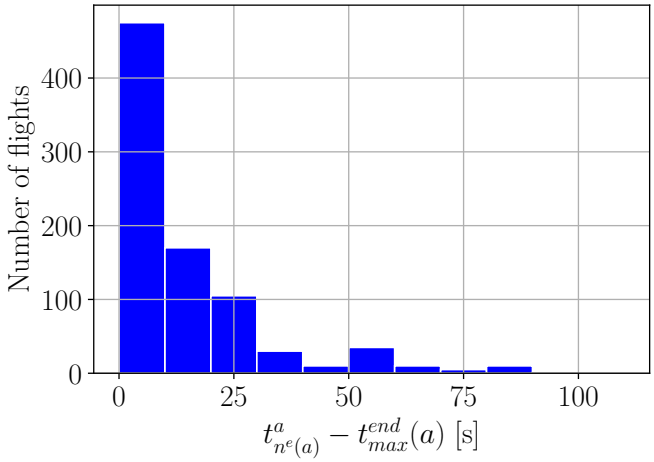

(a) Histogram of the additional taxi time.

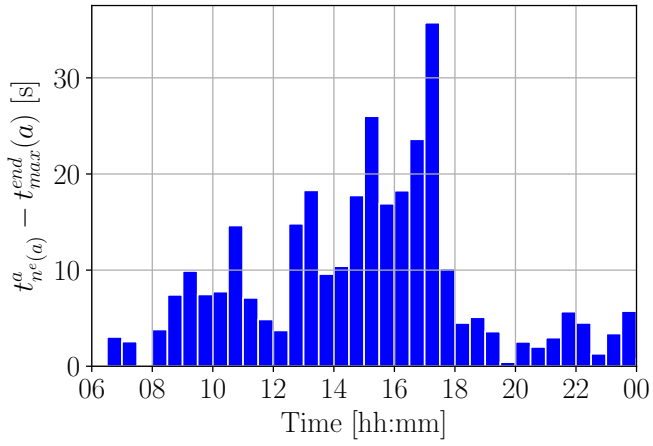

(b) Average additional taxi time every half-hour.

Figure 3.8.: Distribution of the additional required taxi time, $t^a_{n^e(a)} - t^{end}_{min}(a)$, in order to avoid separation distance infringements.

Figure 3.9 shows an example of a resolved minimum separation infringement between arriving and departing aircraft in the period 11:15-11:16 AM. The movements of aircraft 112, 114 and 115 are considered during these 60 seconds. Departing narrow-body aircraft 112 (Embraer 190) is towed by an ETV from pier E to runway entrance 24. It is trailed by narrow-body aircraft 114 (Embraer 175), which is also headed for runway entrance 24, but from pier D. These two aircraft meet arriving wide-body aircraft 115 (Boeing 787), which is towed from runway exit 04 to pier C. Should these aircraft use the fastest velocity profile on the shortest path from their origin node to destination node, then aircraft 112 and 115 intersect head-on in the taxi system between 11:15:20 and 11:15:40. Also, aircraft

114 will be within the minimum separation distance of aircraft 115 at 11:15:40. To avoid these two separation infringements, Model 1 specifies velocity profiles such that aircraft 112 and 114 are slowed down in order to let aircraft 115 pass before them.

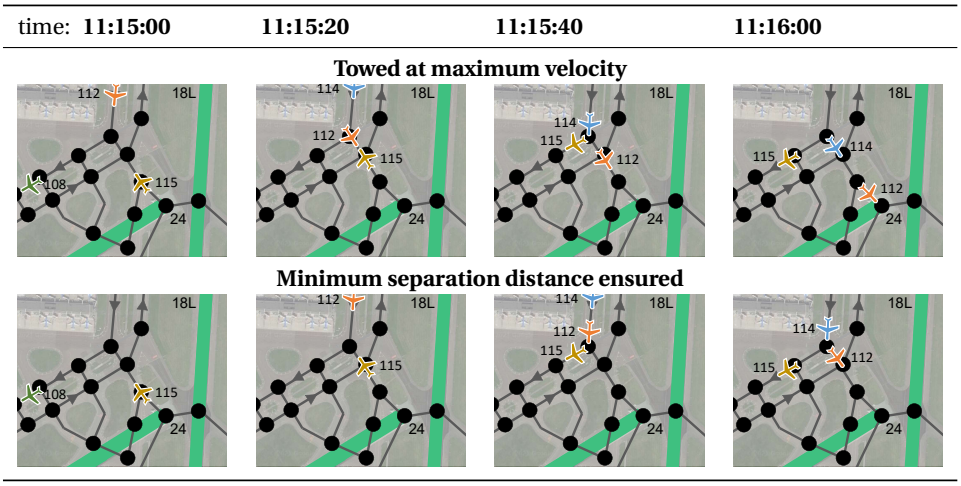

Figure 3.9.: Example - unrestricted aircraft velocity profile vs. the velocity profile proposed by Model 1, aircraft 112, 114, 115, between 11:15:00 and 11:60:00 in the morning.

Results Phase 2 - Scheduling towing tasks and battery recharging moments for ETVs

Figure 3.11 shows the ETVs' schedule for aircraft towing and recharging times when given the flight schedule of December 14, 2019 at AAS. A total of 38 ETVs are required to tow the aircraft. Out of these 38 ETVs, 26 ETVs are required for narrow-body aircraft, 10 ETVs are required for wide-body aircraft and 2 ETVs for heavy wide-body aircraft. At any moment in time, an ETV is either: i) towing an aircraft in the taxi system G_X (towing), ii) traversing the road system G_S (driving), iii) recharging its battery at a charging station (charging), or iv) waiting at a gate node, a runway exit or charging station (idle). When a ETV is in which state is indicated in Figure 3.11.

For heavy-wide body aircraft, two ETVs are needed since there are two simultaneous towing tasks around 4 PM. For wide-body aircraft, around 12 PM, there are 10 simultaneous towing tasks which leads to a need for 10 wide-body ETVs. These two moments are indicated by vertical lines in Figure 3.11. The number of narrow-body ETVs, however, is not limited by the number of simultaneous towing tasks. In fact, there are never 26 simultaneous towing tasks for narrow-body aircraft. The number of narrow-body ETVs is constrained by the battery specifications (limiting battery capacity and charging power).

The fact that the number of ETVs for narrow-body aircraft is limited by the battery specification is corroborated by Figure 3.10, which shows the state-of-charge for each of the ETVs throughout the day. The difference between fast- and slow-charging can be seen in this figure. The results show that the narrow-body ETV schedule is so tight that

it requires the full charge of the ETVs to be used. In constrast, the wide-body and heavy-wide-body ETVs require only 85% to 50% of their battery capacity, respectively, to carry out the schedule.

Table 3.2 shows the average time an ETV is either driving in the service road system G_S, towing an aircraft in the taxi system G_X, or charging its battery at a charging station. The ETVs spend similar fractions of their time towing, driving, or charging their batteries. As expected, ETVs for narrow body aircraft are utilized the highest fraction of the time, since the narrow body flight schedule is also comprised of the most flights and the most even distribution of flights throughout the day.

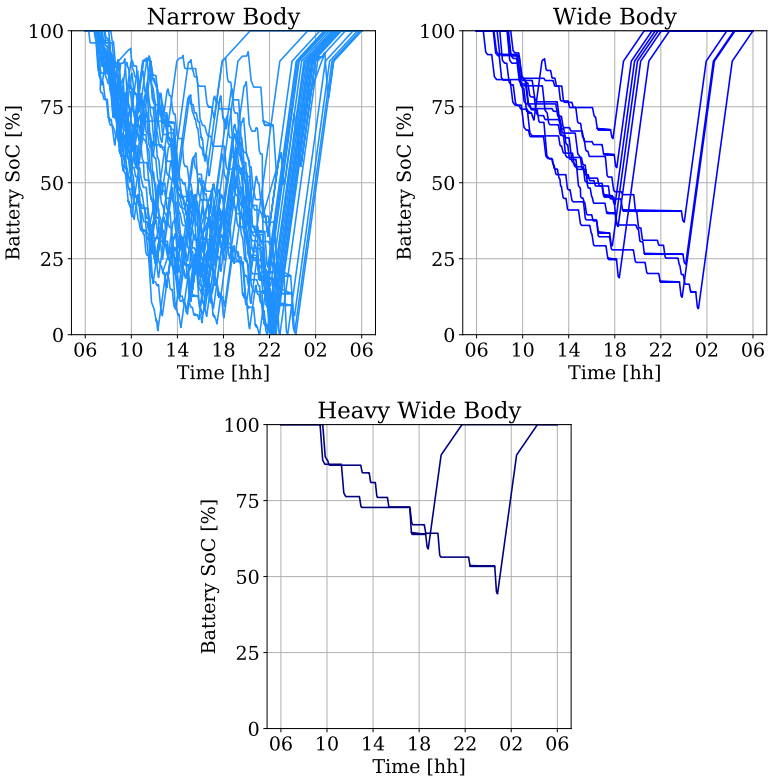

Figure 3.10.: State-of-charge of all dispatched ETVs, sorted by weight class, during the day of operations.

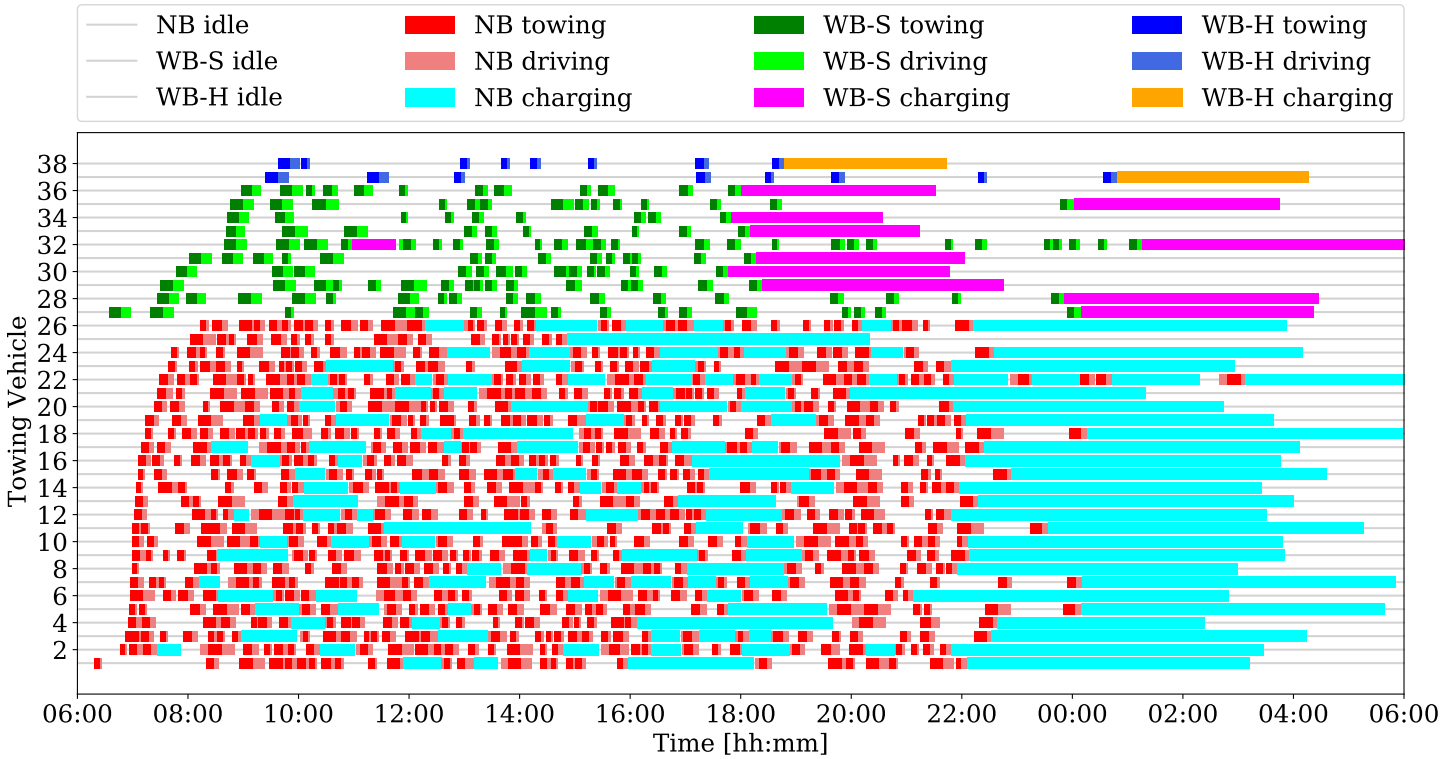

Figure 3.11.: ETV schedule for aircraft towing and battery recharging - December 14, 2019.

w	Driving [hh:mm]	Towing [hh:mm]	Charging [hh:mm]	Total [hh:mm]
NB	04:15	04:34	09:16	18:05
WB	02:21	02:21	03:54	8:47
H-WB	01:14	01:13	03:12	5:39

Table 3.2.: Average utilization time of the ETVs from each weight class, for the three activities: towing, driving, and charging.

3.5.2 Computation time vs. Number of towing tasks

Table 3.3 shows the total computational time required to obtain an optimized ETV fleet dispatchment for a day of operations for various flight schedule sizes. These results have been obtained with the Gurobi Optimizer 9.1, using an Intel Core i7-10610U. Here, the flight arrival and departure times are distributed throughout the day according to the distributions given in Figure 3.7. For a flight schedule with 2000 flights on a single day, corresponding to the number of flights at the worlds busiest airports [30], the ETV dispatchment is obtained in 7366 seconds, out of which 5745 seconds are needed to determine the ETV velocity profiles (Model 1), and 1621 seconds to create the ETV towing and battery charging schedule (Model 2).

Number of towing tasks	100	200	500	1000	1500	2000
Phase 1 [seconds]	9.42	22.3	118.1	498.3	1832	6442
Phase 2 [seconds]	0.19	0.91	9.54	79.2	580.3	1712
Total [seconds]	9.61	23.2	127.6	577.5	2412	8158

Table 3.3.: Running time of the Phase 1 and Phase 2 MILPs for different flight schedule sizes.

3.5.3 Electric aircraft towing during various levels of congestion at AAS

In order to evaluate our model for various levels of congestion at AAS, we apply our two-phase scheduling algorithm for additions days of operation. We consider four additional flight schedules from 2019 which range from ordinary to relatively busy days: March 9 (866 flights), April 13 (1080 flights), May 11 (1191 flights), and June 15 (1278 flights). Figure 3.12 shows the distribution of t_s of the arriving and departing flights on these days.

The minimum required number of ETVs to tow all flights on these days is given in Table 3.4. The ETV fleet size ranges from 39 (on March 9) to 50 (on June 15). It is interesting to note that while there are fewer flights on March 9 than there are on December 14, the required ETV fleet is larger. This can be explained by the relatively busy peak hours on

March 9 (see Figure 3.12).

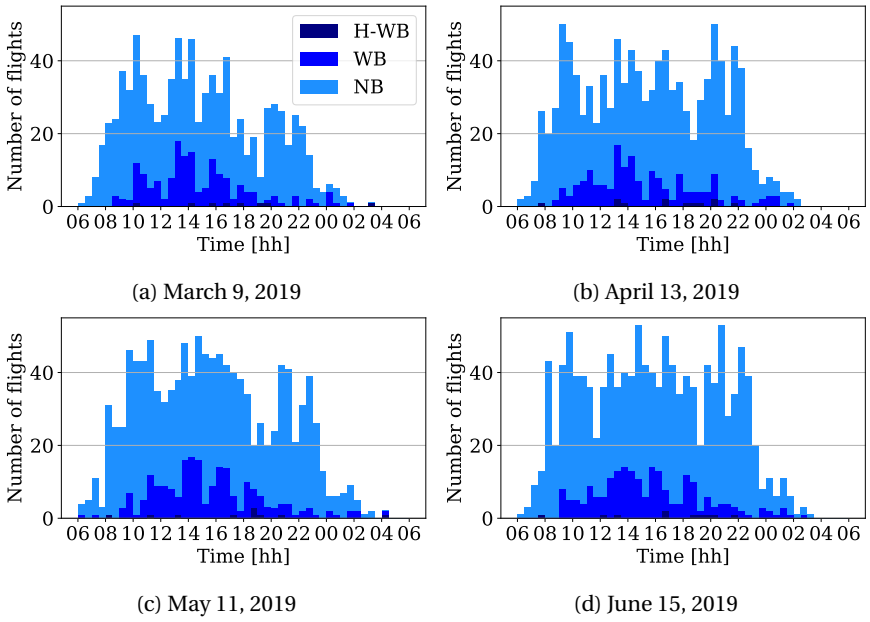

(a) March 9, 2019

(b) April 13, 2019

(c) May 11, 2019

(d) June 15, 2019

Figure 3.12.: Distribution of t^s for four different days during 2019 at Amsterdam Airport Schiphol, per weight class.

Day		NB	WB	H-WB	Total
December 14, 2019	FL	750	147	16	913
	ETV	26	10	2	38
March 9, 2019	FL	724	164	8	896
	ETV	27	11	1	39
April 13, 2019	FL	914	154	12	1080
	ETV	35	10	2	47
May 11, 2019	FL	969	190	10	1191
	ETV	36	11	2	49
June 15, 2019	FL	1040	195	10	1258
	ETV	37	12	2	50

Table 3.4.: Number of required ETVs for different flight days

Figure 3.13 shows the average number of flights towed by an ETV for each weight class per day. The high narrow-body ETV utilization, which increases for increasingly large

flight schedules, stands out. This is the results of the greater abundance of flights to which an ETV can be assigned; the same reason that narrow-body ETV utilization is relatively high compared to (heavy-)wide-body ETV utilization. Finally, for large flight schedules, it can be observed that the number of flights per ETV is approximately constant for each weight class , and hence that the number of ETVs grows approximately linearly with the number of flights.

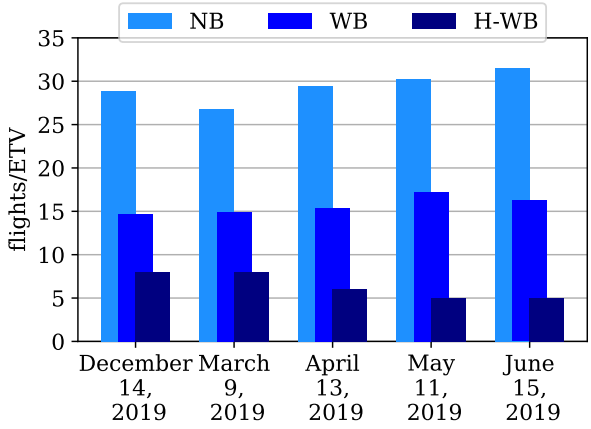

Figure 3.13.: Number of flights per ETV for the different days in 2019.

3.6 The Greedy towing vehicle fleet dispatching algorithm

In this section, we propose a Greedy ETV Fleet Dispatching algorithm (GEFD), which can easily be implemented in practice, and has a very competitive computational time. We are interested in assessing the performance of the GEFD algorithm against our proposed optimal ETV dispatching model (see Section 3.4).

3.6.1 The Greedy ETV Fleet Dispatching (GEFD) algorithm

Similar to Section 3.4, the GEFD performs three tasks: it routes the aircraft across the taxiway system G_X, assigns the aircraft to ETVs, and determines when the ETVs recharge their batteries. Compared with the optimization model in Section 3.4, the GEFD algorithm processes towing tasks sequentially rather than simultaneously.

Let E be a set of ETVs. We define the state of an ETV as follows:

Definition 3.6.1 *An ETV $e \in E$ is said to be in state $S_e \in \mathscr{S}$, $\mathscr{S} = (N^R \cup N^G \cup N_X \cup N_S) \times T \times \mathbb{R}^+$, where $S_e = (l_e, t_e, q_e)$ gives the position, time, and state-of-charge of the battery of ETV e at a specific moment, respectively.*

Whether an ETV is able to tow an aircraft depends on the last known state of this ETV since it needs to be able to reach the aircraft in time, and it has to have sufficient battery charge.

Definition 3.6.2 *Let the function $C : \mathscr{S} \times A \to \mathbb{R}$ denote the highest state of charge with which an ETV e can reach towing task $a \in A$, given its state S_e. It is the maximum of the two following states-of-charge:*

(i) The state-of-charge of e when it drives directly from S_e to $n^s(a)$,

(ii) The state-of-charge of e when it drives to $n^s(a)$ via a charging station and charges its battery for as long as possible, while still arriving before $t^s(a)$.

Finally we determine which ETVs are able to tow a towing task, given their last fixed states:

Definition 3.6.3 *Given its state S_e, an ETV e is able to perform towing task $a \in A$ if:*

(i) it is of the same weight class as the to-be-towed aircraft,

(ii) it is able to arrive at a before $t^s(a)$,

(iii) $C(S_e, a)$ is large enough for e to tow a, reach a charging station and fully recharge its battery before the end of the day.

The GEFD algorithm attempts to maximize the utilization of each ETV by sequentially assigning those ETVs to towing tasks that have the highest state-of-charge. This contributes to a fair workload distribution between the ETVs and a maximization of the number of aircraft an ETV tows per day. Battery charging is done opportunistically: if an ETV is idle for longer then t^c_{min} in-between two consecutive towing tasks, then this ETV will recharge its battery.

The algorithm is initialized for an ETV fleet size of 0 (line 1) and iterates over the fleet sizes using a bisection algorithm up to $|A^w|$. During every iteration, an ETV fleet is initialized where all vehicles are located at the depot at the start of the day with full batteries (line 5). To allocate all vehicles, the algorithm loops over the towing tasks (line 7) in ascending order of t_s. Each step it i) determines the set L of ETVs which are able to tow task a (line 11, using Definition 3.6.3), and ii) allocates the ETV $\hat{e}$ to a which can start towing it with the highest state of charge (line 18). The towing task is routed to its destination across the shortest path, while ensuring that the minimum separation distance is maintained from all previous towed aircraft using a time dependent shortest path algorithm (line 19, see e.g. [31]). The state of $\hat{e}$ is updated to its state at the moment when it has just detached from a (line 20). If there are no ETVs available to tow a, the fleet size is increased using the bisection algorithm (line 14), and the fleet is reassigned from the start of the day to ensure a fair workload distribution. If this does not occur, the fleet size is decreased using the bisection algorithm. Once the optimal fleet size is found, the GEFD algorithm terminates.

Algorithm 1: The GEFD (Greedy ETV Fleet Dispatching) algorithm

Data: Airport layout, Flight schedule A, ETV specifications
Result: ETV fleet size n_w for all weight classes, assignment of ETVs to aircraft, schedule of ETV recharge times

1 Initialize $n_w = 0$ for all $w \in W$;
2 Sort A by increasing t^s values;
3 **while** $n_w \leq |A^w|$ *for all* $w \in W$ **do**
4 **for** $w \in W$ **do**
5 Initialize fleet E of size n_w, all ETVs have state $S_e = (t_e = 0, l_e = n^{dep}, q_e = Q_w)$;
6 **end**
7 **for** $a \in A$ **do**
8 **for** $e \in E$ **do**
9 Determine $C(S_e, a)$;
10 **end**
11 Determine the ETVs which can tow a, denote this set as $L \subset E$;
12 **if** $L = \emptyset$ **then**
13 Let w be the weight class of a;
14 Increase n_w according to bisection algorithm ;
15 Go to line 3;
16 **else**
17 $\hat{e} = \arg\max_{e \in L} C(S_e, a)$;
18 Assign a to $\hat{e}$;
19 Route a across the taxiway system using $\hat{e}$;
20 $S_e \leftarrow (n^e(a), t^e(a), C(S_{\hat{e}}, a) - q^X(a))$;
21 **end**
22 **end**
23 Send all $e \in E$ to n^{dep} and charge;
24 Decrease n_w according to bisection algorithm;
25 **end**
26 **if** $\exists w \in W : n_w > |A^w|$ **then**
27 Instance is infeasible;
28 **else**
29 Solution found, terminate algorithm;
30 **end**

3.6.2 Results - The GEFD algorithm

We apply the GEFD algorithm at AAS using the same flight schedule as before of December 14, 2019. We have previously used this flight schedule to determine the performance of the models in Section 3.5.

First, we compare the results of the Phase 1 MILP from Section 3.4 and the aircraft routing of the GEFD algorithm. Figure 3.14 shows the additional required taxi time to

avoid separation distance infringements obtained with both the GEFD algorithm and the Phase 1 MILP. Figure 3.14a shows the distribution of the additional required taxiing time for both algorithms. The results show that using the GEFD algorithm gives higher additional taxi times for towed aircraft, up to a maximum of 110 seconds. The average additional taxi times of the Phase 1 MILP and the GEFD algorithm are 10.2 seconds and 13.4 seconds, respectively, resulting in an optimality gap of 22% when compared to the MILP model.

Figure 3.14b shows the distribution of the average additional taxi time throughout the day of operations. Specifically, the difference in the average additional taxi times between the Phase 1 MILP and the GEFD algorithm is shown. The results show that the largest differences can be found at the end of the peak hours: during 9:00 - 10:00 after the morning peak, during 14:00 - 15:00 after the first afternoon peak, and during 15:30 - 16:00 after the second afternoon peak. This reflects the characteristic of the GEFD algorithm which processes aircraft sequentially, instead of simultaneously, and thus postpones adding additional taxi times to AC it processes later.

Comparing the Phase 2 MILP and the GEFD algorithm, the results indicate that the GEFD algorithm requires an ETV fleet of 28 narrow-body, 10 wide-body, and 2 heavy-wide-body ETVs. This is only two more ETVs for the first weight class (see Figure 3.11).

Table 3.5 shows the utilization of the different ETVs for the solution obtained with the GEFD algorithm. The heavy-wide-body utilization is the same as when using our optimisation model (see Table 3.2). For the wide-body class, the average towing time is the same in the case of our optimisation model, while the driving and charging times are smaller. This is due to the fact that the GEFD scheduled for towing the ETV which can have the highest state of charge. When considering the difference in fleet size (26 against 28) the same can be found for the narrow-body weight class.

w	Driving [hh:mm]	Towing [hh:mm]	Charging [hh:mm]	Total [hh:mm]
NB	04:10	04:05	08:32	16:47
WB	02:08	02:19	04:02	8:29
H-WB	01:14	01:13	03:09	5:36

Table 3.5.: Average utilization time of the ETVs from each weight class, for the three activities: towing, driving, and charging.

3.6.3 Sensitivity to the number of towing tasks

In this section we compare the performances of the GEFD algorithm with the MILP ETV dispatchment optimization models on flight schedules of different sizes. These are the same ones as used in Subsection 3.5.2.

We first consider the computational efficiency of both methods. Figure 3.15 shows the running time of the GEFD algorithm against our optimisation models. For 100 towing tasks, the GEFD requires 1.04 seconds against 9.61 seconds for the optimal model. For

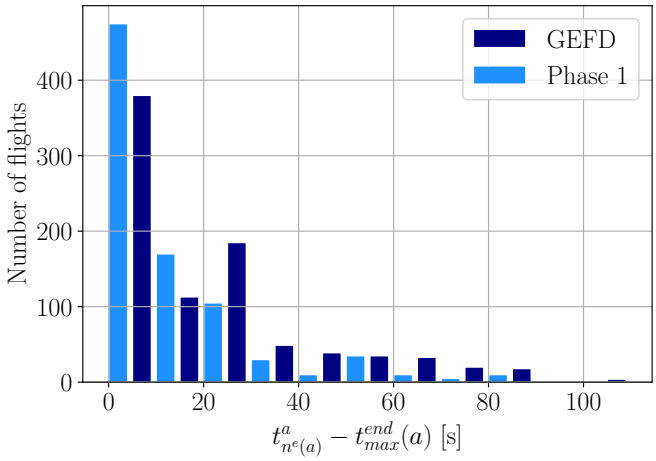

(a) Histogram of the additional taxi time for the optimization and the GEFD algorithm.

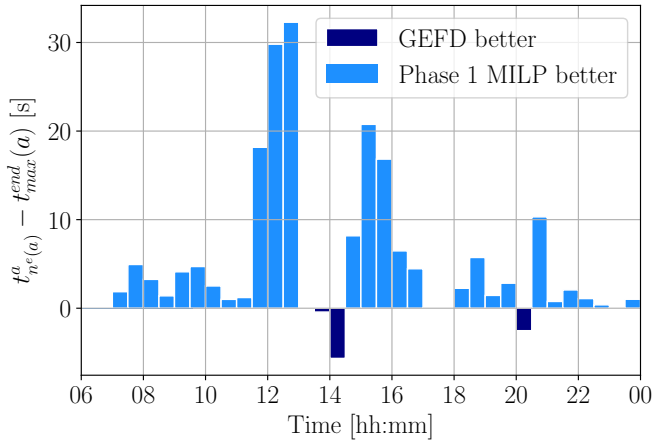

(b) Difference in the average additional taxi time every half-hour between the optimization and the GEFD algorithm.

Figure 3.14.: Distribution of the additional required taxi time, $t^a_{n^e(a)} - t^{end}_{min}(a)$, in order to avoid separation distance infringements.

2000 towing tasks, the running time of the GEFD algorithm is more then a hundred times faster then our optimisation model, requiring 19 seconds against 8158 seconds.

Next, we consider the objective value attained by both methods. Figure 3.16a shows the required number of ETVs for both the optimization and the GEFD algorithm for different sizes of the flight schedule. The results show that, to be able to tow all considered aircraft, the GEFD algorithm requires the same fleet size up to 200 towing tasks. However, for the instances with 500 or more towing tasks, the GEFD algorithm requires 2 through

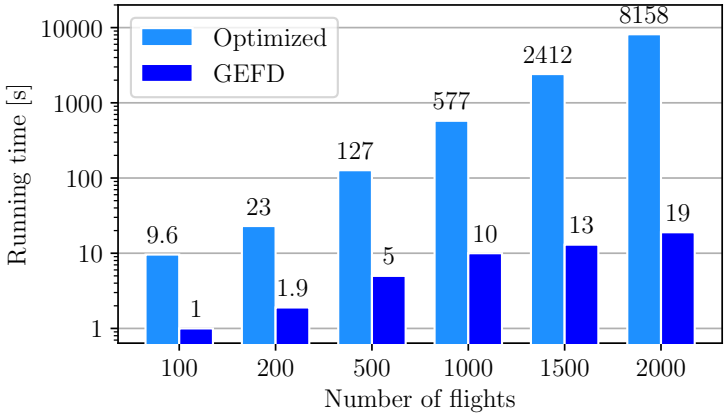

Figure 3.15.: Running time of optimization models and the GEFD algorithm - various flight schedule sizes.

4 additional ETVs to be able to tow all considered aircraft. However, the impact that this increase of the fleet of up to 6% has is relatively limited, as we shall show in the with the next result.

Finally, we study the impact of the difference between the fleet sizes of the GEFD algorithm and our optimization models. In Figure 3.16b, the GEFD algorithm is used but constrained to the fixed ETV fleet size determined using our Optimisation algorithm as graphed in Figure 3.16a. Specifically, the GEFD algorithm dispatches 11, 16, 31, 56, 74, and 92 ETVs to the flight schedules with 100, 200, 500, 1000, 1500, and 2000 towing tasks, respectively. When this fleet size is smaller then the one originally generated by the GEFD algorithm, also shown in Figure 3.16a, not all aircraft can be towed because of scheduling conflicts. These aircraft have to taxi on their own, and the number of times this occurs is graphed in Figure 3.16b.

Only in the case of a flight schedule with 100-200 arriving and departing aircraft, the ETV fleet size determined using our optimisation model is sufficiently large to tow all considered aircraft using the GEFD algorithm. For larger flight schedules, several aircraft cannot be towed by ETVs. For example, when considering 500 arriving and departing aircraft, there are not sufficiently many ETV to tow 2 of these. When considering 2000 arriving/departing aircraft 12 of these are not towed due to lack of available ETVs.

3.6.4 Rolling horizon scheduling when considering flight delays

As discussed in the previous subsection, the major advantage of the GEFD algorithm is that it has a relatively low running time. This presents the opportunity to reevaluate the ETV schedule in real-time when flight delays occur. In this section, the ability to dynamically schedule ETVs of the GEFD algorithm is compared with the MILP ETV

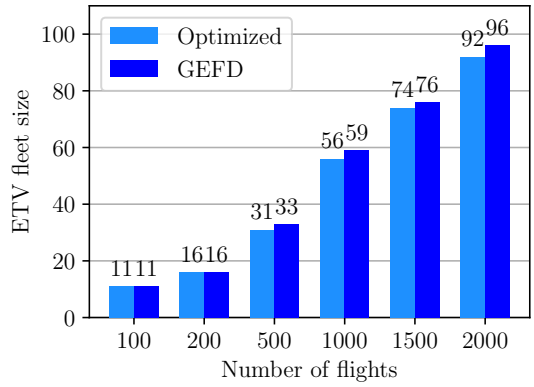

(a) Required ETV fleet size to be able to tow all flights when using the optimization and GEFD algorithms.

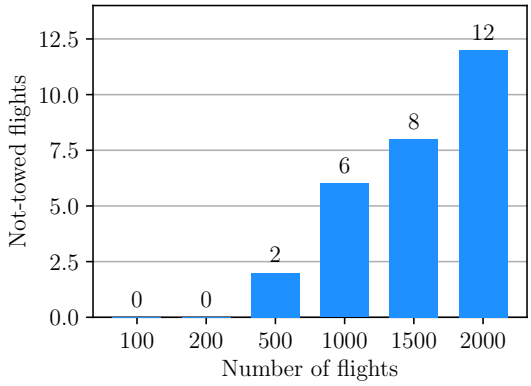

(b) Number of not towed flights when applying GEFD to to optimal fleet size. Non-zero when the GEFD required extra ETVs.

Figure 3.16.: Performance of the optimisation model (Section 3.4) vs. the GEFD algorithm.

dispatchment optimization algorithm.

The problem is now considered from a rolling horizon perspective: twice every hour the flight schedule is updated and the ETV schedule may be reevaluated. We assume that the flight delay is known thirty minutes before the actual arrival/departure time. Throughout the day no ETVs may be added to the schedule, and the new objective is to tow as many flights as possible. Both the GEFD and the MILP formulation are relaxed in order to allow flights to taxi without an ETV.

The rolling horizon approach is applied to the flight schedules from March 9, April 13,

May 11, June 15, and December 14 of 2019. Figure 3.17 shows the flight delays on these days; they have an average delay of 8 minutes with a standard deviation of 19 minutes. The minimum required fleet size for each day of operations, From Table 3.4, has been used.

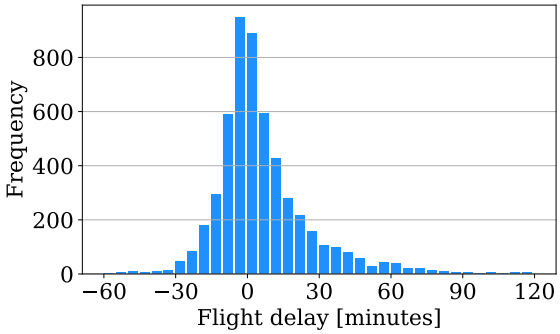

Figure 3.17.: Distribution of flight delays on March 9, April 13, May 11, June 15, and December 14, 2019 at AAS.

Figure 3.18 illustrates how the schedule of one narrow-body ETV evolves during the day of operation, in snapshots every three hours. The vertical red dashed lines show the current time. The distinction is made between already performed and planned events (tows, drives and charges).

Table 3.6 shows the number of flights which have not been towed after applying the rolling horizon approach for both methods. The not-towed flights are given both in absolute numbers and as a percentage of the total number of flights. The results show that there is a performance gap between the MILP and the GEFD, as they require 1.4% and 4.3% of the flights to taxi without ETV, respectively. Second, the algorithms assign a smaller fraction of flights to ETVs when the flight schedule becomes larger. This illustrates that increasing the utilization time of the ETVs (Figure 3.13) reduces the robustness of the schedule to delays.

Day of operation (2019)			Dec 14	Mar 9	Apr 6	May 7	Jun 15	Total
Number of flights			913	896	1080	1191	1258	5338
Not-towed flights	MILP	#	8	4	14	21	27	74
		%	0.9	0.6	1.3	1.6	2.1	**1.4**
	GEFD	#	26	29	42	57	75	229
		%	2.8	3.2	3.9	4.7	6.0	**4.3**

Table 3.6.: Flights not towed by ETVs when using the rolling horizon approach with the MILP ETV fleet dispatchment optimization and the GEFD heuristic algorithm. The not-towed flights are given in absolute numbers (#) and as a percentage of the total number of flights (%).

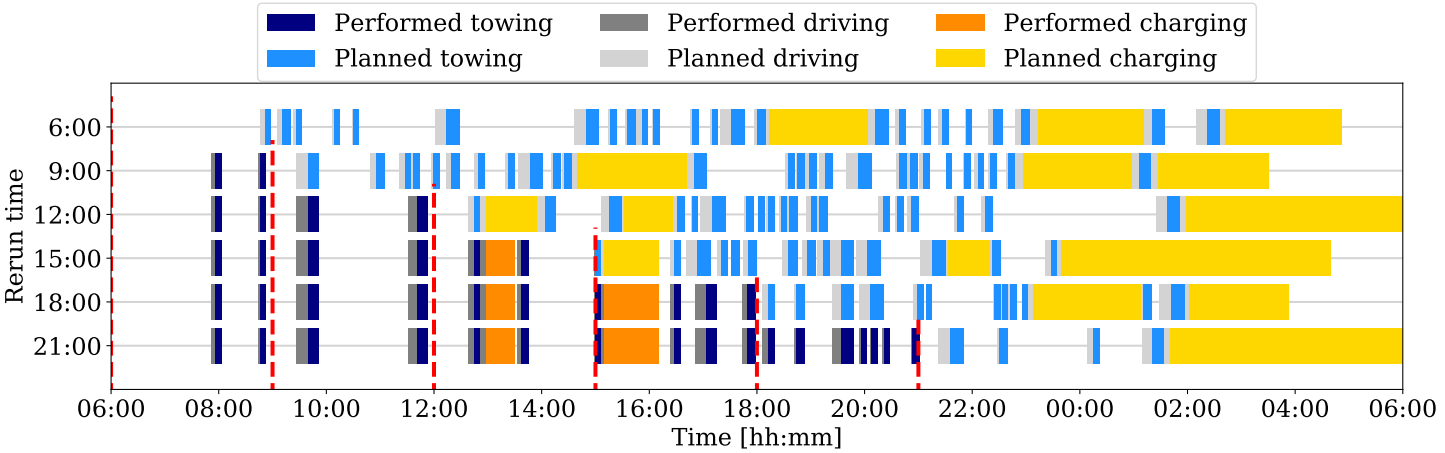

Figure 3.18.: Schedule evolution of one narrow-body ETV during the day, on December 14, 2019. The reevaluated schedules from 6:00 (start of the day), as well as 9:00, 12:00, 15:00, 18:00, and 21:00 are shown. For each time, the scheduled as well as actual flight arrival/departure times are used.

3.7 Conclusion

This chapter proposes an integrated framework to dispatch a fleet of electric towing vehicles (ETVs) at a large airport in the tactical planning phase. This framework integrates the routing of the ETVs in the taxiway system, where minimum separation distances are ensured at all times, with the scheduling of ETVs for towing aircraft and battery recharging. We consider realistic ETV specifications such as battery capabilities and kinematic properties. The charging of the batteries of the ETVs follows a partial recharging policy, i.e., the charging times depend on the residual state-of-charge of the batteries. The ETV routing and task scheduling problems as posed as mixed-integer linear programs.

Our framework is illustrated for five days of operations at Amsterdam Airport Schiphol. The results show that the size of the required ETV fleet increases approximately linear with the number of flights. This ranges from a fleet of 39 ETVs to tow 896 aircraft to a fleet of 50 to tow 1258 aircraft. Our model scales for up to 2000 arriving and departing flights per day, corresponding to the busiest airports in the world. We also propose a simple greedy heuristic for the management of the ETVs. Overall, this greedy heuristic achieves an optimality gap of 5%, while decreasing the computational time by up to 97%. Finally, the robustness of the dispatchment algorithms has been compared by introducing flight delays and solving the problem using a rolling horizon framework. It was shown that the optimization algorithm is able to reevaluate the schedule such that 98.6% of the flights can still be towed, whereas the greedy heuristic is able to reallocate 95.7% of the flights.

In the next chapter, we shall use the assignment model as a basis for the ETV dispatching framework. With this, a cost-benefit analysis of the environmental impact of the size of the fleet of ETVs is performed. At the same time, we expand the capabilities of the algorithm by not only reacting to flight delays, but by anticipating them in the schedule.

Future research could explore battery properties, such as degradation and the impact of weather conditions, in the model to better reflect realistic operations.

references

[1] S. van Oosterom, M. Mitici, and J. Hoekstra. "Dispatching a fleet of electric towing vehicles for aircraft taxiing with conflict avoidance and efficient battery charging". en. In: *Transportation Research Part C: Emerging Technologies* 147 (Feb. 2023), p. 103995. ISSN: 0968-090X. DOI: 10.1016/j.trc.2022.103995.

[2] H. Khadilkar and H. Balakrishnan. "Estimation of aircraft taxi fuel burn using flight data recorder archives". en. In: *Transportation Research Part D: Transport and Environment* 17.7 (Oct. 2012), pp. 532–537. ISSN: 13619209. DOI: 10.1016/j.trd.2012.06.005. (Visited on 11/15/2021).

[3] M. Lukic, P. Giangrande, A. Hebala, S. Nuzzo, and M. Galea. "Review, Challenges, and Future Developments of Electric Taxiing Systems". In: *IEEE Transactions on Transportation Electrification* 5.4 (Dec. 2019). Conference Name: IEEE Transactions on Transportation Electrification, pp. 1441–1457. ISSN: 2332-7782. DOI: 10.1109/TTE.2019.2956862.

[4] R. Camillere and A. Batra. "Assessing the environmental impact of aircraft taxiing technologies". In: *32nd Congress of the Int. Council of the Aeronautical Sciences*. Vol. 9. Shanghai, China, Sept. 2021.

[5] N. Dzikus, J. Fuchte, A. Lau, and V. Gollnick. "Potential for Fuel Reduction through Electric Taxiing". en. In: *11th AIAA Aviation Technology, Integration, and Operations (ATIO) Conference*. Virginia Beach, VA: American Institute of Aeronautics and Astronautics, Sept. 2011. ISBN: 978-1-60086-941-9. DOI: 10.2514/6.2011-6931. (Visited on 11/15/2021).

[6] T. Nikoleris, G. Gupta, and M. Kistler. "Detailed estimation of fuel consumption and emissions during aircraft taxi operations at Dallas/Fort Worth International Airport". en. In: *Transportation Research Part D: Transport and Environment* 16.4 (June 2011), pp. 302–308. ISSN: 13619209. DOI: 10.1016/j.trd.2011.01.007. (Visited on 11/15/2021).

[7] O. Bräysy and M. Gendreau. "Vehicle Routing Problem with Time Windows, Part I: Route Construction and Local Search Algorithms". en. In: *Transportation Science* 39.1 (Feb. 2005), pp. 104–118. ISSN: 0041-1655, 1526-5447. DOI: 10.1287/trsc.1030.0056. (Visited on 01/27/2022).

[8] O. Bräysy and M. Gendreau. "Vehicle Routing Problem with Time Windows, Part II: Metaheuristics". en. In: *Transportation Science* 39.1 (Feb. 2005), pp. 119–139. ISSN: 0041-1655, 1526-5447. DOI: 10.1287/trsc.1030.0057. (Visited on 01/27/2022).

[9] D. Taş, N. Dellaert, T. van Woensel, and T. de Kok. "The time-dependent vehicle routing problem with soft time windows and stochastic travel times". en. In: *Transportation Research Part C: Emerging Technologies* 48 (Nov. 2014), pp. 66–83. ISSN: 0968090X. DOI: 10.1016/j.trc.2014.08.007. (Visited on 01/31/2022).

[10] M. W. P. Savelsbergh. “The Vehicle Routing Problem with Time Windows: Minimizing Route Duration”. en. In: *ORSA Journal on Computing* 4.2 (May 1992), pp. 146–154. ISSN: 0899-1499, 2326-3245. DOI: 10.1287/ijoc.4.2.146. (Visited on 01/31/2022).

[11] M. A. Figliozzi. “An iterative route construction and improvement algorithm for the vehicle routing problem with soft time windows”. en. In: *Transportation Research Part C: Emerging Technologies* 18.5 (Oct. 2010), pp. 668–679. ISSN: 0968090X. DOI: 10.1016/j.trc.2009.08.005. (Visited on 01/31/2022).

[12] R.J. Conrad and Miguel Andres Figliozzi. “The Recharging Vehicle Routing Problem”. In: *2011 Industrial Engineering Research Conference (IERC)*. 2011. URL: https://web.cecs.pdx.edu/~maf/Conference_Proceedings/2011_The_Recharging_Vehicle_Routing_Problem.pdf.

[13] S. Erdoğan and E. Miller-Hooks. “A Green Vehicle Routing Problem”. en. In: *Transportation Research Part E: Logistics and Transportation Review*. Select Papers from the 19th International Symposium on Transportation and Traffic Theory 48.1 (Jan. 2012), pp. 100–114. ISSN: 1366-5545. DOI: 10.1016/j.tre.2011.08.001. (Visited on 06/15/2021).

[14] A. Omidvar and R. Tavakkoli-Moghaddam. “Sustainable vehicle routing: Strategies for congestion management and refueling scheduling”. In: *2012 IEEE International Energy Conference and Exhibition (ENERGYCON)*. Florence, Italy: IEEE, Sept. 2012, pp. 1089–1094. ISBN: 978-1-4673-1454-1 978-1-4673-1453-4 978-1-4673-1452-7. DOI: 10.1109/EnergyCon.2012.6347732. (Visited on 01/27/2022).

[15] M. Schneider, A. Stenger, and D. Goeke. “The Electric Vehicle-Routing Problem with Time Windows and Recharging Stations”. In: *Transportation Science* 48.4 (Mar. 2014). Publisher: INFORMS, pp. 500–520. ISSN: 0041-1655. DOI: 10.1287/trsc.2013.0490. (Visited on 06/11/2021).

[16] G. Hiermann, J. Puchinger, S. Ropke, and R. F. Hartl. “The Electric Fleet Size and Mix Vehicle Routing Problem with Time Windows and Recharging Stations”. en. In: *European Journal of Operational Research* 252.3 (Aug. 2016), pp. 995–1018. ISSN: 0377-2217. DOI: 10.1016/j.ejor.2016.01.038. (Visited on 06/15/2021).

[17] M. M. Solomon. “Algorithms for the Vehicle Routing and Scheduling Problems with Time Window Constraints”. en. In: *Operations Research* 35.2 (Apr. 1987), pp. 254–265. ISSN: 0030-364X, 1526-5463. DOI: 10.1287/opre.35.2.254. (Visited on 01/27/2022).

[18] G. Desaulniers, F. Errico, S. Irnich, and M. Schneider. “Exact Algorithms for Electric Vehicle-Routing Problems with Time Windows”. en. In: *Operations Research* 64.6 (Dec. 2016), pp. 1388–1405. ISSN: 0030-364X, 1526-5463. DOI: 10.1287/opre.2016.1535. (Visited on 01/27/2022).

[19] M. Keskin and B. Çatay. “Partial recharge strategies for the electric vehicle routing problem with time windows”. en. In: *Transportation Research Part C: Emerging Technologies* 65 (Apr. 2016), pp. 111–127. ISSN: 0968-090X. DOI: 10.1016/j.trc.2016.01.013. URL: https://www.sciencedirect.com/science/article/pii/S0968090X16000322 (visited on 02/03/2023).

[20] B. Lin, B. Ghaddar, and J. Nathwani. “Electric vehicle routing with charging/discharging under time-variant electricity prices”. en. In: *Transportation Research Part C: Emerging Technologies* 130 (Sept. 2021), p. 103285. ISSN: 0968090X. DOI: 10.1016/j.trc.2021.103285. (Visited on 01/18/2022).

[21] M. Soltani, S. Ahmadi, A. Akgunduz, and N. Bhuiyan. “An eco-friendly aircraft taxiing approach with collision and conflict avoidance”. en. In: *Transportation Research Part C: Emerging Technologies* 121 (Dec. 2020), p. 102872. ISSN: 0968-090X. DOI: 10.1016/j.trc.2020.102872. (Visited on 12/13/2022).

[22] E. v. Baaren and P. Roling. “Design of a zero emission aircraft towing system”. English. In: *AIAA AVIATION Forum, 17-21 June 2019, Dallas, Texas*. American Institute of Aeronautics and Astronautics Inc. (AIAA), 2019, AIAA. DOI: 10.2514/6.2019-2932. URL: https://research.tudelft.nl/en/publications/design-of-a-zero-emission-aircraft-towing-system (visited on 06/15/2021).

[23] M. Ramos Pereira. “Short-range route scheduling for electric aircraft with battery-charging and battery-swapping constraints”. en. MA thesis. Delft: Delft University of Technology, 2019. URL: https://repository.tudelft.nl/islandora/object/uuid%3A94a943e9-bb73-45dd-b395-d0df6d78a95a (visited on 06/16/2021).

[24] LVNL - Air Traffic Control the Netherlands. *EHAM airport profile*. English. https://www.lvnl.nl/eaip/2021-12-16-AIRAC/html/eAIP/EH-AD-2.EHAM-en-GB.html. Aug. 2019. (Visited on 12/14/2021).

[25] Schiphol. *Traffic review 2019*. English. https://www.schiphol.nl/en/download/b2b/1586959357/2a3AhGB6ciY86vBhVbFrPW.pdf. 2019. (Visited on 12/17/2019).

[26] N. M. Dzikus, R. Wollenheit, M. Schaefer, and V. Gollnick. “The Benefit of Innovative Taxi Concepts: The Impact of Airport Size, Fleet Mix and Traffic Growth”. en. In: *2013 Aviation Technology, Integration, and Operations Conference*. Los Angeles, CA: American Institute of Aeronautics and Astronautics, Aug. 2013. ISBN: 978-1-62410-225-7. DOI: 10.2514/6.2013-4212. (Visited on 11/01/2021).

[27] F. Dieke-Meier and Hartmut Fricke. “Expectations from a Steering Control Transfer to Cockpit Crews for Aircraft Pushback”. In: *2nd International Conference on Application and Theory of Automation in Command and Control Systems*. London, May 2012, pp. 62–70.

[28] N. E. Daidzic. “Determination of taxiing resistances for transport category airplane tractive propulsion”. eng. In: *Advances in aircraft and spacecraft science* 4.6 (2017). Publisher: Techno-Press, pp. 651–677. ISSN: 2287-528X. DOI: 10.12989/aas.2017.4.6.651. URL: http://koreascience.or.kr/article/JAKO201732060819214.page (visited on 05/02/2023).

[29] Health, Safety and Environment office Schiphol. *Schiphol Regulations*. Tech. rep. Hoofddorp, Jan. 2020. URL: https://www.schiphol.nl/en/download/1640595066/43q9kGoE92CccmEeC6awa4.pdf.

[30] A. Berthier. *ACI World data reveals COVID-19's impact on world's busiest airports*. https://aci.aero/2021/04/22/aci-world-data-reveals-covid-19s-impact-on-worlds-busiest-airports/. Apr. 2021. (Visited on 01/12/2022).

[31] H. D. Chon, D. Agrawal, and A. E. Abbadi. “FATES: Finding A Time dEpendent Shortest path”. en. In: *Mobile Data Management*. Ed. by G. Goos, J. Hartmanis, J. van Leeuwen, M.-S. Chen, P. K. Chrysanthis, M. Sloman, and A. Zaslavsky. Vol. 2574. Series Title: Lecture Notes in Computer Science. Berlin, Heidelberg: Springer Berlin Heidelberg, 2003, pp. 165–180. ISBN: 978-3-540-00393-9 978-3-540-36389-7. DOI: 10.1007/3-540-36389-0_12. (Visited on 01/17/2022).

CHAPTER 4

Scheduling electric towing for aircraft: assignment with flight time uncertainty

In this chapter, we present an ETV fleet scheduling framework that accounts for disruption management. In particular, we consider the uncertainty in the flight arrival and departure times. Addressing disruptions can be done by reacting to changes to the uncertain variables, or anticipating their stochastic nature. In the last chapter, we presented how a model can react to this uncertainty. In this chapter, we expand upon this model by creating one which both reacts to and anticipates uncertainty.

We pose this problem as a dynamic vehicle routing problem with uncertain time windows. The model of this problem is to minimize the sum of the costs of taxiing emissions and delays caused by towing. Using the latest (stochastic) flight schedule information, the ETV schedule is periodically updated. In between updates, a greedy algorithm ensures that the schedule is performed.

The framework is applied to a case study at Amsterdam Airport Schiphol. When comparing our algorithm with an oracle planner, which has full knowledge of the flight times in advance, our framework achieves 79.5% *of the highest possible cost reduction. Furthermore, we show that considering the uncertainty in the arrival/departure times, rather than using point estimates of these times, as done in the previous chapter, leads to a* 17.7% *additional cost reduction.*

Parts of this chapter have been published as:

S. van Oosterom and M. Mitici. "An environmentally-aware dynamic planning of electric vehicles for aircraft towing considering stochastic aircraft arrival and departure times". In: *Transportation Research Part C: Emerging Technologies* 169 (2024). DOI: 10.1016/j.trc.2024.104857

4.1 Introduction

The aviation industry is responsible for approximately 5% of the anthropomorphic climate impact [2]. Because it is a *hard-to-abate* sector with fast growth of 5% annually [3], this share is expected to increase in the coming years. Though the industry pledges to reduce its climate impact [4], climate neutrality will take many more years. The most effective ways to reduce emissions, such as the use of synthetic kerosene, electric aircraft and alternative aircraft configurations, will not be ready for a full scale roll-out before 2035 [5]. As such, in order to meet the challenge, improving operations using existing technology plays a vital part [6].

Introducing electric towing vehicles (ETVs) for aircraft to replace conventional aircraft taxing is a promising avenue to reduce aviation emissions [7, 8]. The deployment of these vehicles could reduce the CO2 emission during taxiing by 98% [8]. Even though the taxiing distance is relatively small compared with the entire flight, its climate impact is significant. In fact, by towing an aircraft to and from the runway with an electric towing vehicle, fuel savings of up to 6% on an average flight is achieved [7, 9].

The expected environmental benefits of ETVs have incentivized the study of ETV planning in the last few years, see for example Soltani et al. [10] and Van Oosterom et al. [11]. ETV planning considers the problem of assigning ETVs to aircraft for towing, while leaving time for ETV battery charging throughout the day. Existing studies, however, assume that the exact flight arrival and departure times are known at the start of the day [10, 11]. With this, the schedule for the entire day can be globally optimized during the *tactical* planning phase. This is an idealized perspective. In practice, flights are constantly arriving/departing earlier or later than scheduled (see Section 4.3) [12, 13]. To address this, we plan the operations of ETVs while accounting for the uncertainty in aircraft arrival/departure times. For this, we use estimates of the arrival/departure times. These times are continuously updated as the aircraft approaches its actual landing or take-off.

In this chapter, we propose a dynamic Electric Vehicle Routing Problem with Time Windows (E-VRP-TW) that plans the towing tasks and battery charging of a fleet of ETVs, taking into account the uncertainty in the aircraft arrival and departure times. These times and the associated uncertainties are updated over time as the aircraft come closer to the actual landing or take-off. Using a rolling horizon approach, the arrival/departure times are periodically updated and, in turn, the ETV planning is reevaluated. The objective of the ETV planning is to maximize the fuel savings due to the intelligent replacement of conventional taxiing with electric towing. At the same time, we ensure that flight delays induced by ETV operations are minimized. Together, these objectives define the cost reduction we aim to achieve by an intelligent planning of the ETVs. We illustrate our framework for electric towing of narrow-body aircraft at Amsterdam Airport Schiphol. Flight schedules during the summer and autumn of 2023 are considered, with an average of 998 flights per day. The distributions of the aircraft arrival and departure times are obtained based on historical flight schedules. The results show that an average cost reduction (fuel and ETV-induced delay costs) of €12104 per ETV per day is achieved, which is 79.5% of the cost reduction obtained when full knowledge of the aircraft arrival/departure times is available in advance. We also show that the consideration of

stochastic arrival/departure times leads to a higher cost reduction compared to the case when only average point estimates of these times are considered, which achieves an average cost reduction of €10276 per ETV per day (84.9% of the cost reduction achieved with our proposed approach).

The main contributions of this chapter are twofold:

(i) We pose the ETV planning problem as a dynamic Electric Vehicle Routing Problem with Time Windows (E-VRP-TW) that accounts for uncertain aircraft arrival and departure times. This addresses a current research gap in existing studies on ETV planning [14], where full knowledge of the aircraft arrival/departure times is assumed.

(ii) We show that considering arrival/departure times as stochastic variables, rather than using point estimates of these times, leads to significant cost reductions: an increase of 17.7%. This emphasizes the importance of planning based on distributions of the arrival/departure times, instead of averages.

The remainder of the chapter is organized as follows. Section 4.2 presents a literature review on which planning models have been developed for (stochastic) electric vehicle scheduling. Section 4.3 illustrates the uncertainty in flight arrival/departure times. We develop our ETV scheduling framework in Section 4.4 and 4.5, and present two benchmark ETV planning algorithms in Section 4.6. These are applied in a case study in Sections 4.7 and 4.8.

4.2 Prior work and contributions on stochastic vehicle routing

The planning of ETVs is related to the Vehicle Routing Problem with Time Windows (VRP-TW), where a set of vehicles has to visit a set of customers within their personal time window [15, 16]. The objective of this is the minimization of the fleet size to visit all customers [17], the travelled distance [18], or the total transportation costs [19]. Here, the main research directions are: VRP-TWs for electric vehicles, VRP-TWs with stochastic input data, and on VRP-TW applications to ETV management, see Table 4.1.

As electric vehicles become more popular, several VRP-TW variants which account for battery limitations have been developed. This E[lectric]-VRP-TW problem requires vehicles to stop at a charging station before their battery is depleted. First, recharging the battery was assumed to take a fixed amount of time, irrespective of the remaining battery charge. This additional constraint increases the required vehicle fleet size, as shown by Conrad and Figliozzi [20] and Erdogan and Miller-Hooks [21] and the service costs per customer, shown by Omidvar [22]. Subsequent research has been devoted to mitigating this effect. Firstly, a recharge time which is dependent on the state-of-charge was considered in Schneider et al.[23] and Hiermann et al. [24]. The latter has shown that this decreases transportation costs by 10% with respect to the fixed charging time. Secondly, some studies have proposed scheduling methods where vehicles are allowed partial recharging, such as Desaulniers et al. [25] and Keskin et al. [26]. These studies shows that partial recharging reduces the transportation costs by an additional

5%. Recent studies have improved the realism of the battery recharging process, by introducing batteries for which the recharge rate decreases when they approach full capacity [27–29].

Some elements of the (E-)VRP-TW problem have been carried over to the domain of ETVs. The topic was first introduced without considering battery limitations, similar to the VRP-TW problem, by Soltani et al. [10]. This study performs a cost-benefit analysis of the ETV fleet size. However, charging ETVs has been shown to take a significant amount of time during the day [8], and hence this study overestimates the ETV performance. Van Baaren and Roling [30] considered the E-VRP-TW problem for ETVs with constant charging times, as in Conrad and Figliozzi [20]. Lastly, the E-VRP-TW problem with partial charging, as in Keskin and Çatay [26] has been considered for ETVs by Van Oosterom et al. [31]. This model was used in a case study at Amsterdam Airport Schiphol to evaluate the minimum required ETV fleet size. It was shown that this approach significantly improves the ETV performance when compared with the the non-charging approach in Soltani et al. [10] and with the fixed charging time approach in Van Baaren and Roling [30]. Lastly, Zoutendijk and Mitici studied this problem with limits on the number of charging points [32].

To account for uncertainties in the charging and/or operations of electric vehicles, the E-VRP-TW has been expanded to include both *stochastic information* and *dynamic scheduling* [33]. *Stochastic information* considers instances where not all parameters of the problem are known with certainty (opposed to deterministic information), but their distributions are known and are taken into account in the models. *Dynamic scheduling* considers instances where parameters of the problem change during the execution of the schedule, and the schedule can be adapted (opposed to static scheduling). Problems can also be both stochastic and dynamic at the same time.

Research on optimizing VRPs under uncertainty started for conventional non-electric vehicles. Lorini et al. [34] and Taş et al. [35] studied a VRP where travelling times were uncertain and evolved (due to e.g. traffic jams). The former used the latest travel times to reroute vehicles and reduce travelling time (dynamic planning). Taş et al. [35] also considered this, but used robust optimization techniques [36] to account for this uncertainty beforehand (stochastic planning).

In recent years, dynamic and stochastic VRPs have also been studied for electric vehicles. Most studies address battery-related uncertainties, such as energy consumption by Pelletier et al. [37] and Zhang et al. [38] or charging time uncertainty by Keskin et al. [39]. Only Messaoud [40] studied the E-VRP-TW under travel time uncertainty, using chance-constrained programming [41]. However, this study only considers static planning, and thus ignores that more accurate information becomes available throughout the day.

Zoutendijk at al. [42] illustrated the possibility of deterministic but dynamic scheduling of ETVs with flight delay uncertainty. It was assumed that the actual arrival / departure time is known 30 minutes in advance and that the schedule may be updated accordingly. However, this method ignores the fact that flight times are not exactly known in advance, especially when considering departures (as it is shown in the next section). Hence, a realistic ETV scheduling implementation which accounts for flight delays is lacking.

Paper	Vehicles*	TW	Uncertainty	Dynamic	Algorithm
Savelsbergh [18]	ICE	yes	-	-	Local search
Conrad and Figliozzi [20]	EV	yes	-	-	Construction and improvement heuristic
Schneider et al. [23]	EV-soc	yes	-	-	variable neighbourhood and tabu search hybrid
Hiermann et al. [24]	EV-soc	yes	-	-	large neighbourhood search
Desaulniers et al. [25]	EV-preemp	yes	-	-	exact branch price-and-cut
Keskin and Çatay [26]	EV-preemp	yes	-	-	large neighbourhood search
Soltani et al. [10]	ICE	yes	-	-	branch and bound
Van Baaren and Roling [30]	EV-fc	yes	-	-	branch and bound
Van Oosterom et al. [31]	EV-preemp	yes	-	yes	branch and bound
Zoutendijk and Mitici [32]	EV-preemp	yes	-	-	adaptive large neighbourhood search
Lorini et al. [34]	ICE	no	travel times	yes	Local descent
Taş et al.[35]	ICE	yes	travel time	-	Tabu search
Pelletier et al. [37]	EV	no	energy consumption	no	adaptive large neighbourhood search
Keskin and Çatay [39]	EV-preemp	yes	charge station waiting time	no	adaptive large neighbourhood search
Zhang et al. [38]	EV	yes	energy consumption	no	robust branch-and-price
Messaoud[40]	EV-preemp	yes	travel time	no	large neighbourhood search
Zoutendijk et al. [42]	EV-preemp	yes	time windows	yes	branch and bound

*: "ICE"= Internal Combustion Engine; "EV" = Electric Vehicles, constant time charging;
"EV-soc"= Electric Vehicles, dynamic charge time; "EV-preemp"= Electric Vehicles, charging preemptively

Table 4.1.: Literature on dynamic and/or stochastic (E-)VRP(-TW) problems and applications to ETVs.

4.3 Stochastic aspect of aircraft arrival/departure times

In order to schedule ETVs efficiently, accurate information about the arrival and departure times of flights is required. Though the actual arrival and departure times are unknown, estimates for these are issued. Hours prior to landing, inbound flights are assigned an Estimated Landing Time (ELDT); hours prior to departure, outbound flights are assigned an Estimated Off-Block Time (EOBT, the moment an aircraft leaves the gate). These are updated at subsequent times $t_1, t_2, \ldots, t_n$, with $t_1 < t_2 < \ldots t_n$. Let $\text{ELDT}_f(t)$ or $\text{EOBT}_f(t)$ denote the ELDT or EOBT of a flight f at some time t, respectively. The actual landing/off-block time of a flight f is denoted as the ALDT or AOBT.

To assess the quality of the EOBT and ELDT, we are interested in the uncertainty of these estimates, i.e., ALDT - ELDT and AOBT - EOBT. Specifically, we consider the distribution of ALDT_f - $\text{ELDT}_f(t)$ or AOBT_f - $\text{EOBT}_f(t)$ when there is δ time remaining before the expected landing/off-block, i.e. when $ELDT_f(t) - t = \delta$ or $EOBT_f(t) - t = \delta$. For example, we consider the distribution of the ALDT - ELDT at the moment when it is expected that $\delta = 120$min are remaining until the landing of aircraft f. Let the random variables ΔOBT_δ and ΔLDT_δ denote the difference AOBT-EOBT and ALDT-ELDT when there is δ time remaining until the EOBT or ELDT.

Figure 4.1 shows the probability density of these variables at $\delta = 120$ min (4.1a, 4.1b), 30 min (4.1c, 4.1d), and 5 min (4.1e, 4.1f) remaining before the estimated landing/off-block, where ΔLDT_δ and ΔOBT_δ are empirically determined based on the flight schedules and actual landing/departure times at Amsterdam Airport Schiphol during July and August 2023. The results show that the uncertainty associated with the EOBT and ELDT, and especially in the case of the ELDT, reduces closer to the actual time of arrival or departure. For our ETV planning, we aim to integrate these random variables within the ETV planning. The ETV plan is reevaluated with every update of the EOBT and ELDT.

4.4 Electric towing scheduling with disruption management

We consider the following problem description of an environmentally-aware planning of ETVs taking into account stochastic arrival/departure times. An overview of the used notation can be found in A.2.

4.4.1 ETV model and towing process

Let V denote the set of ETVs. Each ETV is equipped with a battery with energy capacity E. Figure 4.2 illustrates the process of towing an aircraft using an ETV [31]. A departing aircraft is first connected to an ETV, which performs the push-back. The push-back starts at the AOBT (Actual Off-Block Time, Section 4.3). After that, the aircraft is towed to the runway and the ETV is disconnected at a holding point. Without the ETV, the aircraft warms up its engines, taxis onto the runway and takes off. An arriving aircraft follows the same steps in reverse order, and without a push-back phase. We aim to have an ETV

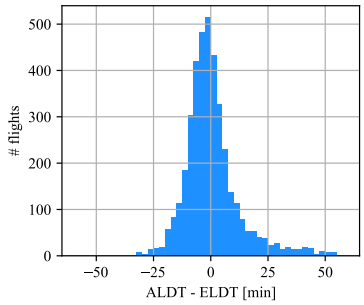

(a) ELDT error when δ = 120 min until expected landing.

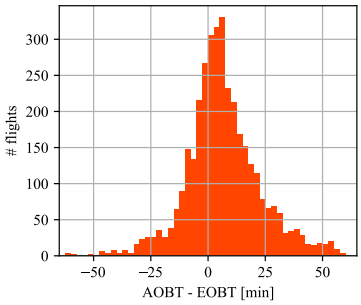

(b) EOBT error when δ = 120 min until expected off-block.

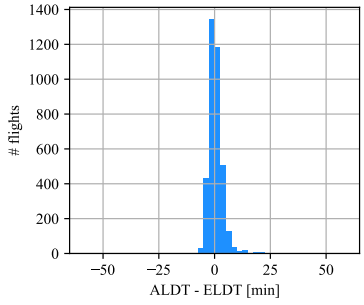

(c) ELDT error when δ = 30 min until expected landing.

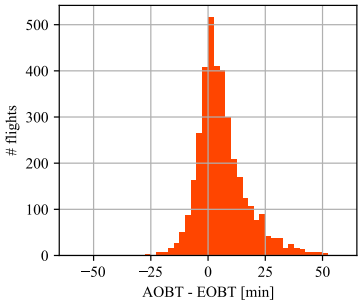

(d) EOBT error when δ =30 min until expected off-block.

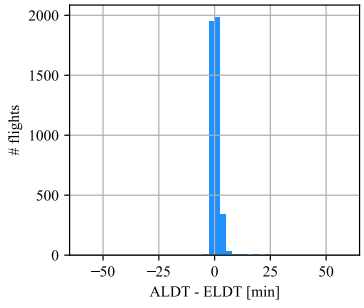

(e) ELDT error when δ = 5 min until expected landing.

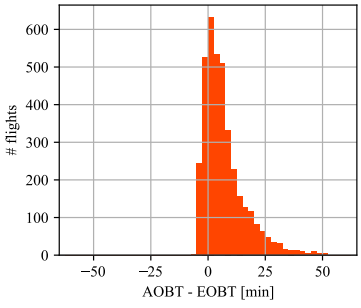

(f) EOBT error when δ = 5 min until expected off-block.

Figure 4.1.: Histogram of the uncertainty in the ELDT (Figs. 4.1a, 4.1c,4.1e) and the EOBT (Figs. 4.1b,4.1d, 4.1f) at Amsterdam Schiphol, with $\delta \in \{120, 30, 5\}$ min. Flights of narrow-body aircraft between July 1 - August 30 2023 (74458 flights) are considered.

at the aircraft as soon as the aircraft' engines have cooled down, at Δt^{ec} after the ALDT (Actual Landing Time).

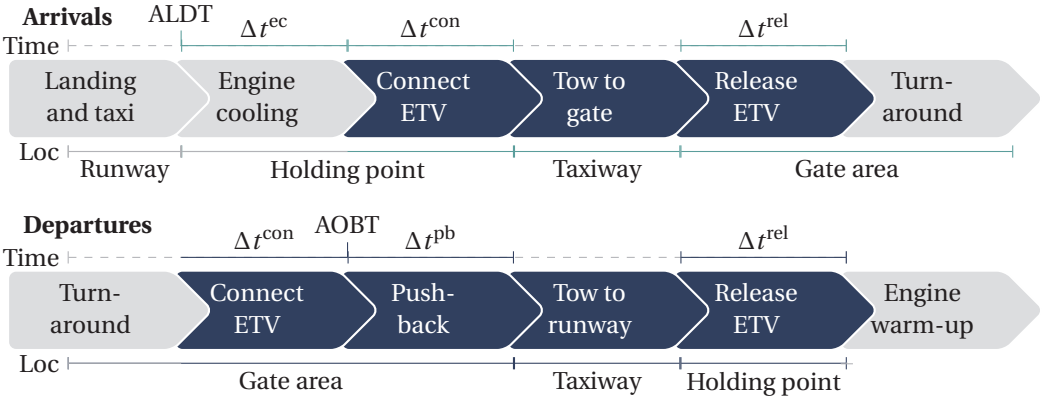

Figure 4.2.: Towing process for departing/arriving aircraft. An ETV is connected to an aircraft in the green time blocks [31].

The following is assumed:

(A1) ETVs tow aircraft at a constant velocity v^x and drive (while not towing) at a velocity v^s.

(A2) The energy used per unit distance, $\mathscr{E}(v,m)$, depends on the driving velocity v and towed mass m.

(A3) For the ETV battery charging process, we assume a bi-linear charging profile (see Figure 4.3) with parameters $\alpha,\beta \in (0,1)$ [43]. Up to αE, the battery is recharged with power P^c. From αE up to E, the battery recharges with power βP^c.

(A4) An ETV battery should be recharged for at least $\Delta t^c_{\min}$ time.

(A5) An ETV starts and ends the day of operations with a fully charged battery.

4.4.2 Airport taxiway and service roads

We consider an airport represented by a directed graph $G = (N, A)$. The set of nodes N contains the runway holding points and gates $N^{rg} \subset N$ and ETV charging stations $N^c \subset N$. One of the charging locations is also the depot of the ETVs, $n^{dep} \in N^c$. Let $l : A \to \mathbb{R}_+$ denote the lengths of the arcs of graph G. Arcs are either a taxiway $A^X \subset A$ or a service road $A^S \subset A$.

(A6) When towing an aircraft between gates and runways, ETVs use the shortest path using only arcs of the taxiway network A^X. The length of this shortest path is given by $d^X : N \times N \to \mathbb{R}_+$.

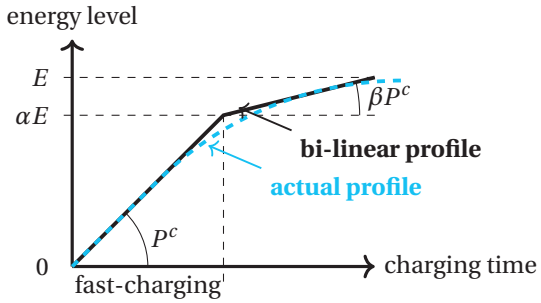

Figure 4.3.: Bilinear and actual charging profile. The battery energy level is given as a function of the charging time [31].

(A7) When not towing an aircraft, ETVs traverse the airport using the shortest path given the service road arcs A^S. The length of this path is given by $d^S : N \times N \to \mathbb{R}_+$.

(A8) ETVs always start and end their day at the depot $n^{dep} \in N^c$.

4.4.3 Arriving/Departing aircraft

We consider a period of time $T = [t_s, t_e]$, representing a day of operations starting at t_s and ending at t_e. During T, a set F of aircraft arrive to and depart from the airport which can be towed by ETVs. Let $F^{arr} \subset F$ and $F^{dep} \subset F$ denote the set of arriving and departing aircraft, respectively. Each $f \in F$ is defined by a tuple $(n^{\mathrm{p}}_f, n^{\mathrm{d}}_f, m_f, c^{\mathrm{taxi}}_f, c^{\mathrm{tow}}_f, \tau^{\mathrm{p}}_f)$,where $n^{\mathrm{p}}_f \in N^{rg}$ and $n^{\mathrm{d}}_f \in N^{rg}$ denote the locations where the aircraft should be picked up and dropped off by an ETV, and m_f denotes the mass of aircraft f. When no ETV is available to tow f, it must taxi by itself. A cost c^{taxi}_f is incurred when f taxis, due to fuel consumption and emissions. Towing f costs c^{tow}_f, related to the electricity consumed (where $c^{\mathrm{tow}}_f < c^{\mathrm{taxi}}_f$).

At a given time $t \in T$, with $\delta = EOBT_f(t) - t$ expected remaining time until off-block (or $\delta = ELDT_f(t) - t$ until landing), let $\tau^{\mathrm{p}}_f(t)$ denote the pick-up time of aircraft f, where:

$$\tau^{\mathrm{p}}_f(t) = \begin{cases} \Delta\mathrm{OBT}_\delta + EOBT_f(t) - \Delta t^{\mathrm{con}} & \text{if } f \in F^{dep}, \\ \Delta\mathrm{LDT}_\delta + ELDT_f(t) + \Delta t^{\mathrm{ec}} & \text{if } f \in F^{arr}, \end{cases} \tag{4.1}$$

where, $\tau^{\mathrm{p}}_f(t)$ is a stochastic variable since we don't know the AOBT/ALDT beforehand.

From $\tau^{\mathrm{p}}_f(t)$, the drop-off time of aircraft f is defined as:

$$\tau^{\mathrm{d}}_f(t) = \tau^{\mathrm{p}}_f(t) + \Delta t^{\mathrm{con}} + \mathbf{1}_{\{f \in F^{dep}\}} \Delta t^{\mathrm{pb}} + d^X(n^{\mathrm{p}}_f, n^{\mathrm{d}}_f)/v_x + \Delta t^{\mathrm{rel}}, \tag{4.2}$$

which is the first moment an ETV is disconnected after it has towed f and is available to proceed to its next task. Lastly, we define the overlap time τ^{o}_{fg} as the time by which an

ETV is early or too late to tow g, if g is towed subsequently after f. It is given by:

$$\tau^{o}_{fg}(t) = \tau^{p}_{g}(t) - \left(\tau^{d}_{f}(t) + d^{s}(n^{d}_{f}, n^{p}_{g})/v_{s}\right) \tag{4.3}$$

Figure 4.4 shows an example of the pick-up/drop-off random variables for two flights f and g: $\tau^{d}_{f}(t)$ and $\tau^{p}_{g}(t)$. Assume that $n^{d}_{f} = n^{p}_{g}$, such that an ETV can pick-up g immediately after dropping-off f. Note that the two random variables overlap, i.e. $\mathbb{P}[\tau^{o}_{fg}(t) > 0] > 0$, such that there is a non-zero probability that the tow of flight g starts before the end of the tow of flight f, thus one single ETV may not be able to tow both flights.

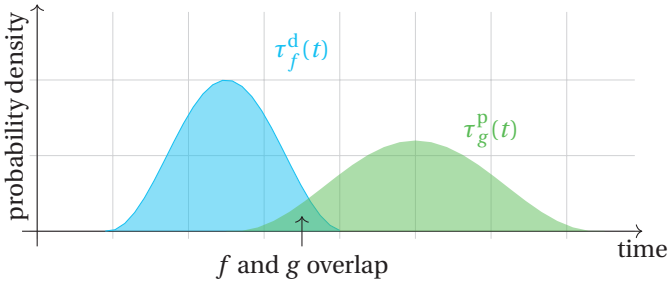

Figure 4.4.: Example of the pick-up time and drop-off time random variables of flights f and g, with $n^{p}_{g} = n^{d}_{f}$. With probability $\mathbb{P}[\tau^{o}_{fg}(t) > 0]$, the two aircraft cannot be towed with the same ETV.

We assume:

(A9) For $f \in F^{arr}$ to be towed, an ETV needs to be present at n^{p}_{f} by $ALDT_{f} + \Delta t^{ec}$ (see Figure 4.2).

(A10) If $f \in F^{dep}$ is towed, a monetary cost c^{d}_{f} is incurred for every unit of time an ETV is not present at n^{p}_{f} after the desired pick-up time $AOBT_{f} - \Delta t^{con}$ (see Figure 4.2).

4.4.4 Dynamically updating the ETV planning

As $\tau^{p}_{f}(t)$ is updated based on the updated ELDT or EOBT, the planning of the ETVs is reevaluated. Flights may be assigned to and unassigned from ETVs, and the ETV battery recharging times may change. This is allowed at any time $t \in T$. For this, we make the following assumptions:

(A11) An arriving aircraft may be assigned to or unassigned from an ETV at any moment before the pick-up time.

(A12) Up to a period Δt^{fix} from the current time t, the assignment of departing aircraft f to ETVs is fixed (while $\mathbb{E}[\tau^{p}_{f}(t)] < t + \Delta t^{fix}$). After that, the assignment of f can be changed.

Before the current time t, the ETV planning is fixed. Between t and $t + \Delta t^{fix}$, the ETV planning may be altered, but only arriving aircraft may be assigned or unassigned from an ETV. This is proposed in order to conform with assumption **(A9)**. In order to avoid a schedule which is too erratic in the near future, which would be difficult to be implemented by operators, the schedule for departing aircraft is fixed. After $t+\Delta t^{fix}$, the ETV schedule may be altered for both arriving and departing aircraft. Figure 4.5 shows how the ETV planning may be dynamically updated. Figure 4.5a shows the situation at t = 6 AM, and Figure 4.5b at t = 7 AM.

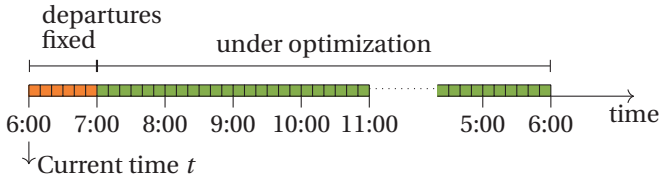

(a) at $t = 6:00$ AM.

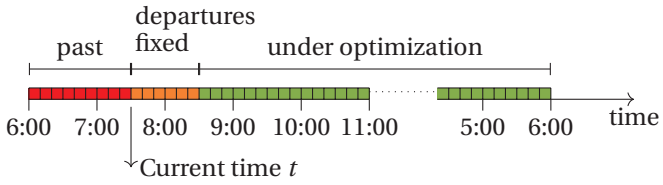

(b) at $t = 7:30$ AM.

Figure 4.5.: Illustration of two ETV planning reevaluation moments with T starting and ending at 6 AM and $\Delta t^{fix} = 1$ hour.

4.4.5 ETV scheduling objective

When no ETV tows an aircraft f, it taxis by itself. The resulting emissions lead to an (environmental) cost $c_f^{\text{taxi}} - c_f^{\text{tow}}$ per aircraft, which is a function of the aircraft type and taxi distance. Also, when departing aircraft are delayed because no ETV is available to tow them to the runway, a cost c_f^{d} per delayed aircraft is incurred per unit of time **(A10)**.

Given (i) a fleet of ETVs V, (ii) the airport layout (N, A), and (iii) the set of arriving and departing aircraft F, we aim to determine an environmentally-aware, dynamic ETV planning. This planning is conform all mentioned assumptions, and can be reevaluated at any time during the day. The objective is to minimize the total cost associated with a) the cost of taxiing emissions $c^{\text{taxi}} - c^{\text{tow}}$ due to ETVs not being available to tow aircraft, i.e. those aircraft that are taxiing by themselves, and b) the cost c^{d} associated with departure delays caused by towing.

4.5 Stochastic towing vehicle planning algorithm

In this section we propose a rolling horizon algorithm to plan operations for a fleet of ETVs that considers uncertain aircraft arrival and departure times. An overview of the used notation can be found in A.2.

At each moment, an ETV v is described by its state. This is given by a tuple $(n_v, t_v, E_v, F_v, S_v)$, which gives the current location, time, battery energy level, flights to tow, and the current activity, respectively. There are four possible ETV activities for S_v: tow, drive, charge, or idle. An ETV can be idle if it is waiting to tow an aircraft or when its battery is full and $F_v = \emptyset$.

Algorithm 2 shows the framework of our approach. The ETV state is initialized at the start of the day. The algorithm uses two subroutines which update the state of the ETVs. The first subroutine is a MILP that optimizes the ETV planning for the rest of the day (Section 4.5.1) while anticipating delays. The second is a greedy algorithm that performs the planning and resolves conflicts when delays occur (Section 4.5.2). Figure 4.5 shows two epochs of the rolling horizon algorithm, using $\Delta t^{fix} = 1$ hour.

Algorithm 2: Dynamic ETV planning framework.

Data: Airport layout, Day of operations $T = [t_s, t_e]$, fleet of ETVs V, set of flights F, Δt^{fix}, Δt^{reopt}, δt.
Result: Dynamic ETV schedule

```
Initialize current time t = t_s − Δt^fix;
Initialize ETV states: n_v = n^dep, t_v = t, E_v = E, F_v = {}, S_v = idle;
while t < t_e do
    Globally reevaluate the ETV schedule (Section 4.5.1) and update F_v for all ETVs;
    Set t' ← t + Δt^reopt ;
    while t ≤ t' do
        for v ∈ V if t_v ≤ t do
            Run ExecuteTows (Section 4.5.2) to obtain the new ETV state
              (n'_v, t'_v, E'_v, F'_v, S'_v);
            Set (n_v, t_v, E_v, F_v, S_v) ← (n'_v, t'_v, E'_v, F'_v, S'_v) ;
        end
        Set t ← t + δt;
        Update the flight EOBT and ELDT information;
    end
end
```

4.5.1 Global ETV planning

At any given time t during the day of operations T, we aim to optimize the planning of the ETVs for the remainder of the day of operations. We aim for a robust planning, anticipating the uncertainty in the pick-up times of the aircraft, the varying demand

for ETVs across the day, and the need to recharge the ETV batteries. This optimization generates a list of to-be-towed flights F_v for all ETVs.

We optimize the schedule for the period after t. Each ETV finishes the task it is performing at t, and is available for reassignment after this moment. Vehicle $v \in V$ is then located at node n_v^{a} at time τ_v^{a} with battery charge E_v. We define the following sets:

- Let F^{fix} be the set of departures f which were previously assigned to an ETV and have $EOBT_f(t) < t + \Delta t^{reopt}$.

- Let F' be the set of flights which can still be towed by the ETVs. These are the flights which can be reached on time by at least one of the ETVs in V, given their first availability $(n_v^{\mathrm{a}}, \tau_v^{\mathrm{a}}, E_v)$, with probability at least $\mathbb{P}_\phi$:

  $$F' := \left\{ f \in F : \exists v \in V : \mathbb{P}[\tau_f^{\mathrm{p}} \geq \tau_v^{\mathrm{a}} + d^s(n_v^{\mathrm{d}}, n_f^{\mathrm{p}})/v_s] \geq \mathbb{P}_\phi \right\} \setminus \left\{ f \in F^{dep} : \mathbb{E}[\tau_f^{\mathrm{p}}(t)] < t + \Delta t^{fix} \right\}.$$

  The set F' also includes an artificial flight f^{end} with $n_{f^{end}}^{\mathrm{p}} = n_{f^{end}}^{\mathrm{d}} = n^{dep}$, $\tau_{f^{end}}^{\mathrm{p}} = t_e$, and which requires charge E. This flight will be used in the MILP formulation (Section 4.5.1).

- Let $V_f \subset V$ be the ETVs which are able to tow flight $f \in F'$, given their first availability $(n_v^{\mathrm{a}}, \tau_v^{\mathrm{a}}, E_v)$.

- Let $F'_f \subset F'$ be the flights which can be towed before f by the same ETV.

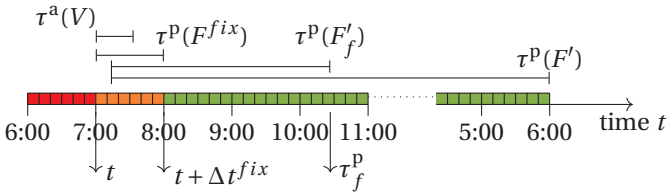

Figure 4.6.: Expected pick-up times of flights F' and F'_f for a flight $f \in F'$, denoted by $\tau^{\mathrm{p}}(F')$ and $\tau^{\mathrm{p}}(F'_f)$ respectively, together with the first availability times of the ETVs in V, denoted by $\tau^{\mathrm{a}}(V)$. The current time is t = 7 AM, and Δt^{fix} = 1 hour.

In between towing two aircraft f and g, an ETV may have the opportunity to recharge its battery at a charging station in N^c. ETVs use the station which requires the shortest detour between the drop-off point of f and the pick-up point of g, which is denoted by

n^c_{fg}. For simplicity, we introduce the following abbreviations:

$$E^X(f) := \mathscr{E}(m_f, v^x) d^X(n^{\mathrm{p}}_f, n^{\mathrm{d}}_f) \qquad f \in F', \tag{4.4a}$$

$$E^S(f,g) := \mathscr{E}(0, v^s) \begin{cases} d^S(n^{\mathrm{d}}_f, n^{\mathrm{p}}_g) & f \in F'_g \\ d^S(n^{\mathrm{a}}_f, n^{\mathrm{p}}_g) & f \in V_g \end{cases} \qquad g \in F', \tag{4.4b}$$

$$E^S_l(f) := \mathscr{E}(0, v^s) \begin{cases} d^S(n^{\mathrm{d}}_f, n^{dep}), \\ d^S(n^{\mathrm{a}}_f, n^{dep}), \end{cases} \qquad \begin{matrix} f \in F', \\ f \in V, \end{matrix} \tag{4.4c}$$

$$E^S_c(f,g) := \mathscr{E}(0, v^s) \begin{cases} \left(d^S(n^{\mathrm{d}}_f, n^c_{fg}) + d^S(n^c_{fg}, n^{\mathrm{p}}_g)\right) & f \in F'_g \\ \left(d^S(n^{\mathrm{a}}_f, n^c_{fg}) + d^S(n^c_{fg}, n^{\mathrm{p}}_g)\right) & f \in V_g \end{cases} \qquad g \in F', \tag{4.4d}$$

$$E^S_{c1}(f) := \mathscr{E}(0, v^s) \begin{cases} \max_{n^c \in N^c} d^S(n^{\mathrm{d}}_f, n^c) \\ \max_{n^c \in N^c} d^S(n^{\mathrm{a}}_f, n^c) \end{cases} \qquad \begin{matrix} f \in F', \\ f \in V. \end{matrix} \tag{4.4e}$$

Here, $E^X(f)$ denotes the energy required to tow aircraft f, $E^S(g,f)$ the energy required to drive directly from the drop-off of f to the pick-up of aircraft g, and $E^S_l(f)$ the energy required to drive from the drop-off of f to the depot. The energy required to drive from the drop-off of g to the pick-up of f via the charging station n^c_g is given by $E^S_c(g,f)$. It is assumed that ETVs use the shortest path in the network **(A2)**.

For an aircraft $f \in F'$ and an aircraft $g \in F'_f$ or ETV $v \in V_f$, we denote the available charging time before towing f as $\Delta t^c(g,f)$ and $\Delta t^c(v,f)$, which are both random variables, respectively. We allow an ETV to recharge if this time is longer than $\Delta t^c_{\min}$ with probability at least $\mathbb{P}_\theta$ **(A4)**. The sets of all aircraft and ETV departure points for which this holds are denoted by:

$$F'^c_f := \{g \in F'_f : \mathbb{P}[\Delta t^c(g,f) \geq \Delta t^c_{\min}] \geq \mathbb{P}_\theta\}, \qquad V^c_f := \{v \in V_f : \mathbb{P}[\Delta t^c(v,f) \geq \Delta t^c_{\min}] \geq \mathbb{P}_\theta\} \tag{4.5}$$

Decision variables

We consider the following indicator decision variables, which determine which aircraft are towed by each of the ETVs:

$$x_{fg} \in \{0,1\}, \qquad \text{with } g \in F', f \in F'_g \cup V_g, \tag{4.6a}$$

If $f \in V_g$ and $x_{fg} = 1$, aircraft g is the first towed aircraft by f after t. If $f \in F'_g$ and $x_{fg} = 1$, aircraft f and g are towed consecutively by the same ETV **(A11)** and **(A12)**. Different from previous ETV planning studies [10, 44], we do not require the decision variable x to keep track of the specific ETV, i.e. we do not define a decision variable x_{fgv} for each ETV $v \in V$. This significantly reduces the size of the MILP model.

We also define the variable E_f which tracks the battery energy level of the ETV batteries, i.e.,

$$E_f \in \mathbb{R}_+, \qquad \text{ETV battery energy level at the start of towing flight } f \tag{4.6b}$$

Objective function

We use the information about the uncertainty in the pick-up times to define the objective function. When no aircraft is towed, a total (environmental) cost $\sum_{f\in F'} c_f^{\text{taxi}}$ is incurred, which consists of the costs related to fuel consumption and emissions during taxiing. This cost is reduced by towing flights, and we aim to maximize this cost reduction. When ignoring delays, this reduction is given by:

$$\sum_{g\in F'}\left[\left(c_g^{\text{taxi}}-c_g^{\text{tow}}\right)\sum_{f\in F'_g\cup V_g} x_{fg}\right] = \sum_{g\in F'}\sum_{f\in F'_g\cup V_g}\tfrac{1}{2}\left(c_f^{\text{taxi}}-c_f^{\text{tow}}+c_g^{\text{taxi}}-c_g^{\text{tow}}\right)x_{fg}$$
$$:= \sum_{g\in F'}\sum_{f\in F'_g\cup V_g} c_{fg}(0)x_{fg},$$

where $c_{fg}(\cdot)$ denotes the cost reduction achieved when $x_{fg}=1$, i.e., when flight f is towed immediately after flight g by the same ETV. This coefficient is a function of the overlap time (defined in Section 4.4.3): $c_{fg}(\tau^{\text{o}})$. When $\tau^{\text{o}}>0$, g may have to be delayed, or one of the aircraft is not towed at all (thus it has to taxi on its own). We aim to maximize the expected cost reduction:

$$\max_{x,q}\sum_{g\in F'}\sum_{f\in F'_g\cup V_g}\mathbb{E}[c_{fg}(\tau^{\text{o}}_{fg}(t))]x_{fg}. \tag{4.7a}$$

As different assumptions are made for planning in- and outbound aircraft (Section 4.4.4), $\mathbb{E}[c_{fg}(\tau^{\text{o}}_{fg}(t))]$ has to be determined for all six possible cases when f is an ETV or in/outbound aircraft and g is an in/outbound aircraft as follows:

- Case 1: f **departure,** g **departure:** Both f and g have to be towed if they are assigned to ETVs **(A12)**. If the overlap time is positive, aircraft g needs to wait for the ETV to arrive. As such, we incur a delay cost $\tau^{\text{o}}c_g^{\text{d}}$. With this, we have:

  $$c_{fg}(\tau^{\text{o}}) = \tfrac{1}{2}\left(c_f^{\text{taxi}}-c_f^{\text{tow}}+c_g^{\text{taxi}}-c_g^{\text{tow}}\right)-c_g^{\text{d}}\max\{\tau^{\text{o}},0\},$$

  which has the expected value:

  $$\begin{aligned}\mathbb{E}[c_{fg}(\tau^{\text{o}}_{fg}(t))] &= \mathbb{E}\left[\tfrac{1}{2}\left(c_f^{\text{taxi}}-c_f^{\text{tow}}+c_g^{\text{taxi}}-c_g^{\text{tow}}\right)-c_g^{\text{d}}\max\{\tau^{\text{o}}_{fg}(t),0\}\right]\\ &= \tfrac{1}{2}\left(c_f^{\text{taxi}}-c_f^{\text{tow}}+c_g^{\text{taxi}}-c_g^{\text{tow}}\right)-\mathbb{E}\left[\max\{\tau^{\text{o}}_{fg}(t),0\}\right]c_g^{\text{d}}\\ &= \tfrac{1}{2}\left(c_f^{\text{taxi}}-c_f^{\text{tow}}+c_g^{\text{taxi}}-c_g^{\text{tow}}\right)-\mathbb{P}\left[\tau^{\text{o}}_{fg}(t)>0\right]\mathbb{E}\left[\tau^{\text{o}}_{fg}(t)|\tau^{\text{o}}_{fg}(t)>0\right]c_g^{\text{d}}\end{aligned} \tag{4.7b}$$

- Case 2: f **departure,** g **arrival:** Aircraft g can be either towed by an ETV or it can taxi by itself **(A11)**, whereas f needs to be towed **(A12)**. Aircraft g is not towed if there is overlap. In this case, we have:

  $$c_{fg}(\tau^{\text{o}}) = \tfrac{1}{2}(c_f^{\text{taxi}}-c_f^{\text{tow}})+\tfrac{1}{2}(c_g^{\text{tow}}-c_g^{\text{taxi}}) \qquad \text{if} \qquad \tau^{\text{o}}>0.$$

We obtain the expected value for the conditions $\tau^o_{fg} \leq 0$ and $\tau^o_{fg} > 0$:

$$\mathbb{E}\left[c_{fg}(\tau^o_{fg}) | \tau^o_{fg}(t) \leq 0\right] = \tfrac{1}{2}\left(c_f^{\text{taxi}} - c_f^{\text{tow}} + c_g^{\text{taxi}} - c_g^{\text{tow}}\right),$$
$$\mathbb{E}\left[c_{fg}(\tau^o_{fg}) | \tau^o_{fg}(t) > 0\right] = \tfrac{1}{2}\left(c_f^{\text{taxi}} - c_f^{\text{tow}} - c_g^{\text{taxi}} + c_g^{\text{tow}}\right),$$

which we substitute to compute the overall expected value:

$$\begin{aligned}
\mathbb{E}[c_{fg}(\tau^o_{fg}(t))] &= \mathbb{P}\left[\tau^o_{fg}(t) \leq 0\right] \tfrac{1}{2}\left(c_f^{\text{taxi}} - c_f^{\text{tow}} + c_g^{\text{taxi}} - c_g^{\text{tow}}\right) \\
&\quad + \mathbb{P}\left[\tau^o_{fg}(t) > 0\right] \tfrac{1}{2}\left(c_f^{\text{taxi}} - c_f^{\text{tow}} - c_g^{\text{taxi}} + c_g^{\text{tow}}\right) \\
&= \tfrac{1}{2}(c_f^{\text{taxi}} - c_f^{\text{tow}}) + \tfrac{1}{2}(c_g^{\text{taxi}} - c_g^{\text{tow}})\mathbb{P}[\tau^o_{fg}(t) \leq 0] \\
&\quad - \tfrac{1}{2}(c_g^{\text{taxi}} - c_g^{\text{tow}})\mathbb{P}[\tau^o_{fg}(t) > 0] \\
&= \tfrac{1}{2}\left(c_f^{\text{taxi}} - c_f^{\text{tow}} + c_g^{\text{taxi}} - c_g^{\text{tow}}\right) - \mathbb{P}[\tau^o_{fg}(t) > 0](c_g^{\text{taxi}} - c_g^{\text{tow}}) \qquad (4.7c)
\end{aligned}$$

- Case 3: f **arrival,** g **arrival:** Both f and g can either be towed by an ETV or taxi by itself when $\tau^o > 0$ (A11). We maximize the reduction in emission cost due to switching to electric towing from conventional taxi. As such, when there is overlap, we choose to tow the aircraft with the highest reduction in emission cost, i.e. the highest $c^{\text{taxi}} - c^{\text{tow}}$. Similar to the previous case, we have:

$$c_{fg}(\tau^o) = \tfrac{1}{2}\max_{h=f,g}\{c_h^{\text{taxi}} - c_h^{\text{tow}}\} + \tfrac{1}{2}\max_{h=f,g}\{c_h^{\text{tow}} - c_h^{\text{taxi}}\} \qquad \text{if} \qquad \tau^o > 0$$

such that we obtain:

$$\begin{aligned}
\mathbb{E}[c_{fg}(\tau^o_{fg}(t))] &= \mathbb{P}\left[\tau^o_{fg}(t) \leq 0\right] \mathbb{E}\left[c_{fg}(\tau^o_{fg}) | \tau^o_{fg}(t) \leq 0\right] \\
&\quad + \mathbb{P}\left[\tau^o_{fg}(t) > 0\right] \mathbb{E}\left[c_{fg}(\tau^o_{fg}) | \tau^o_{fg}(t) > 0\right] \\
&= \mathbb{P}\left[\tau^o_{fg}(t) \leq 0\right] \tfrac{1}{2}\left(c_f^{\text{taxi}} - c_f^{\text{tow}} + c_g^{\text{taxi}} - c_g^{\text{tow}}\right) \\
&\quad + \mathbb{P}\left[\tau^o_{fg}(t) > 0\right] \tfrac{1}{2}\left(\max_{h=f,g}\{c_h^{\text{taxi}} - c_h^{\text{tow}}\} + \max_{h=f,g}\{c_h^{\text{tow}} - c_h^{\text{taxi}}\}\right).
\end{aligned}$$

Now, we note that $c_f^{\text{taxi}} - c_f^{\text{tow}} + c_g^{\text{taxi}} - c_g^{\text{tow}} = \max_{h=f,g}\{c_h^{\text{taxi}} - c_h^{\text{tow}}\} + \min_{h=f,g}\{c_h^{\text{taxi}} - c_h^{\text{tow}}\}$, such that we obtain:

$$\begin{aligned}
\mathbb{E}[c_{fg}(\tau^o_{fg}(t))] &= (1 - \mathbb{P}[\tau^o_{fg}(t) > 0]) \tfrac{1}{2}\left(\max_{h=f,g}\{c_h^{\text{taxi}} - c_h^{\text{tow}}\} + \min_{h=f,g}\{c_h^{\text{taxi}} - c_h^{\text{tow}}\}\right) \\
&\quad + \mathbb{P}[\tau^o_{fg}(t) > 0] \tfrac{1}{2}\left(\max_{h=f,g}\{c_h^{\text{taxi}} - c_h^{\text{tow}}\} - \min_{h=f,g}\{c_h^{\text{taxi}} - c_h^{\text{tow}}\}\right) \\
&= \tfrac{1}{2}\left(c_f^{\text{taxi}} - c_f^{\text{tow}} + c_g^{\text{taxi}} - c_g^{\text{tow}}\right) - \mathbb{P}[\tau^o_{fg}(t) > 0] \min_{h=f,g}\left(c_h^{\text{taxi}} - c_h^{\text{tow}}\right) \\
& \qquad (4.7d)
\end{aligned}$$

- Case 4: f **arrival,** g **departure:** When there is an overlap, g must be towed (A12). If the overlap time is small enough that the costs of delaying g are less then the cost of letting f taxi by itself, we delay g and tow both f and g. In this case, we have:

$$c_{fg}(\tau^{\mathrm{o}}) = \tfrac{1}{2}\left(c_f^{\mathrm{taxi}} - c_f^{\mathrm{tow}} + c_g^{\mathrm{taxi}} - c_g^{\mathrm{tow}}\right) - \tau^{\mathrm{o}} c_g^{\mathrm{d}} \qquad \text{if} \qquad 0 \le c_g^{\mathrm{d}}\tau^{\mathrm{o}} \le c_f^{\mathrm{taxi}} - c_f^{\mathrm{tow}}.$$

If the overlap time is larger, when $c_g^{\mathrm{d}}\tau_{fg}^{\mathrm{o}} > c_f^{\mathrm{taxi}} - c_f^{\mathrm{tow}}$, we only tow g (without delay) and let f taxi by itself. In this case, we have:

$$c_{fg}(\tau^{\mathrm{o}}) = \tfrac{1}{2}(c_f^{\mathrm{tow}} - c_f^{\mathrm{taxi}}) + \tfrac{1}{2}(c_g^{\mathrm{taxi}} - c_g^{\mathrm{tow}}) \qquad \text{if} \qquad c_g^{\mathrm{d}}\tau^{\mathrm{o}} > c_f^{\mathrm{taxi}} - c_f^{\mathrm{tow}}.$$

We obtain the expected costs by conditioning for three cases: for $\tau_{fg}^{\mathrm{o}}(t) \le 0$, for $0 < \tau_{fg}^{\mathrm{o}} c_g^{\mathrm{d}} \le c_f^{\mathrm{taxi}} - c_f^{\mathrm{tow}}$, and for $c_g^{\mathrm{d}} \ge c_f^{\mathrm{taxi}} - c_f^{\mathrm{tow}}$. For these, we have:

$$\begin{aligned}
\mathbb{E}[c_{fg}(\tau_{fg}^{\mathrm{o}}) | \tau_{fg}^{\mathrm{o}}(t) \le 0] &= \tfrac{1}{2}\left(c_f^{\mathrm{taxi}} - c_f^{\mathrm{tow}} + c_g^{\mathrm{taxi}} - c_g^{\mathrm{tow}}\right) \\
\mathbb{E}[c_{fg}(\tau_{fg}^{\mathrm{o}}) | 0 < \tau_{fg}^{\mathrm{o}} c_g^{\mathrm{d}} \le c_f^{\mathrm{taxi}} - c_f^{\mathrm{tow}}] &= \tfrac{1}{2}\left(c_f^{\mathrm{taxi}} - c_f^{\mathrm{tow}} + c_g^{\mathrm{taxi}} - c_g^{\mathrm{tow}}\right) \\
&\quad - c_g^{\mathrm{d}} \mathbb{E}\left[\tau_{fg}^{\mathrm{o}} | 0 < \tau_{fg}^{\mathrm{o}} c_g^{\mathrm{d}} \le c_f^{\mathrm{taxi}} - c_f^{\mathrm{tow}}\right] \\
\mathbb{E}[c_{fg}(\tau_{fg}^{\mathrm{o}}) | \tau_{fg}^{\mathrm{o}} c_g^{\mathrm{d}} \ge c_f^{\mathrm{taxi}} - c_f^{\mathrm{tow}}] &= \tfrac{1}{2}(c_f^{\mathrm{tow}} - c_f^{\mathrm{taxi}}) + \tfrac{1}{2}(c_g^{\mathrm{taxi}} - c_g^{\mathrm{tow}})
\end{aligned}$$

We substitute these three to obtain the overall expected value:

$$\begin{aligned}
\mathbb{E}[c_{fg}(\tau_{fg}^{\mathrm{o}}(t))] = \mathbb{P}[\tau_{fg}^{\mathrm{o}}(t) \le 0] &\tfrac{1}{2}\left(c_f^{\mathrm{taxi}} - c_f^{\mathrm{tow}} + c_g^{\mathrm{taxi}} - c_g^{\mathrm{tow}}\right) \\
&+ \mathbb{P}[0 < \tau_{fg}^{\mathrm{o}} c_g^{\mathrm{d}} \le c_f^{\mathrm{taxi}} - c_f^{\mathrm{tow}}] \\
&\quad \left(\tfrac{1}{2}\left(c_f^{\mathrm{taxi}} - c_f^{\mathrm{tow}} + c_g^{\mathrm{taxi}} - c_g^{\mathrm{tow}}\right) - c_g^{\mathrm{d}} \mathbb{E}[\tau_{fg}^{\mathrm{o}} | 0 < \tau_{fg}^{\mathrm{o}} c_g^{\mathrm{d}} \le c_f^{\mathrm{taxi}} - c_f^{\mathrm{tow}}]\right) \\
&+ \mathbb{P}[\tau_{fg}^{\mathrm{o}} c_g^{\mathrm{d}} \ge c_f^{\mathrm{taxi}} - c_f^{\mathrm{tow}}] \left(\tfrac{1}{2}(c_f^{\mathrm{tow}} - c_f^{\mathrm{taxi}}) + \tfrac{1}{2}(c_g^{\mathrm{taxi}} - c_g^{\mathrm{tow}})\right),
\end{aligned}$$

such that after rearranging the terms, we obtain:

$$\begin{aligned}
\mathbb{E}[c_{fg}(\tau_{fg}^{\mathrm{o}}(t))] = \tfrac{1}{2}&\left(c_f^{\mathrm{taxi}} - c_f^{\mathrm{tow}} + c_g^{\mathrm{taxi}} - c_g^{\mathrm{tow}}\right) \\
&- \mathbb{E}\left[\tau_{fg}^{\mathrm{o}} | 0 < \tau_{fg}^{\mathrm{o}} c_g^{\mathrm{d}} \le c_f^{\mathrm{taxi}} - c_f^{\mathrm{tow}}\right] \mathbb{P}\left[0 < \tau_{fg}^{\mathrm{o}} c_g^{\mathrm{d}} \le c_f^{\mathrm{taxi}} - c_f^{\mathrm{tow}}\right] \\
&- (c_f^{\mathrm{taxi}} - c_f^{\mathrm{tow}}) \mathbb{P}\left[\tau_{fg}^{\mathrm{o}} c_g^{\mathrm{d}} \ge c_f^{\mathrm{taxi}} - c_f^{\mathrm{tow}}\right] \qquad (4.7e)
\end{aligned}$$

- Case 5: f **ETV,** g **arrival**: In the case that f is an ETV, the computation depends on its state. The value τ_{fg}^{o} is computed using a modified Equation 4.3:

$$\tau_{fg}^{\mathrm{o}}(t) = \tau_g^{\mathrm{p}}(t) - (\tau_f^{\mathrm{a}} + d^S(n_f^{\mathrm{a}}, n_g^{\mathrm{p}})/v_s).$$

In this case, the computations will be the same as in Case 1.

- Case 6: f **ETV,** g **departure:** The value of $\tau_{fg}^{\mathrm{o}}(t)$ is computed, and the case is reduced to case 2.

MILP model

We use the following MILP formulation, which aims to minimize the expected environmental and delay costs for the remainder of the day (after t):

$$\max \quad \sum_{g \in F'} \sum_{f \in F'_g \cup V_g} \mathbb{E}[c_{fg}(\tau^{o}_{fg}(t))] x_{fg} \tag{4.8a}$$

$$\text{s.t.} \quad 1 \geq \sum_{f \in F' : v \in V_f} x_{vf} \qquad \forall v \in V, \tag{4.8b}$$

$$1 \geq \sum_{g \in F'_f \cup V_f} x_{gf} = \sum_{g \in F' : f \in F'_g} x_{fg} \geq \mathbf{1}_{\{f \in F^{fix}\}} \qquad \forall f \in F' \setminus \{f^{end}\}, \tag{4.8c}$$

$$E_g \leq E_f + E(1 - x_{fg}) - x_{fg} E^X(f) + E^S(f,g) \qquad \forall g \in F', f \in (F'_g \cup V_g) \setminus (F'^c_g \cup V^c_g), \tag{4.8d}$$

$$E_g \leq E_f + E(1 - x_{fg}) - x_{fg} E^X(f) + E^S_c(f,g) - P^c \Delta t^c(f,g) \qquad \forall g \in F', f \in (F'_g \cup V_g) \cap (F'^c_g \cup V^c_g), \tag{4.8e}$$

$$\begin{aligned} E_g \leq\ & E_f - x_{fg}(E^X(f) + E^S_c(f,g)) \\ & + (1-\beta)(\alpha E - (E_f - x_{fg}(E^X(f) + E^S_c(f,q)))) \\ & + \beta P^c \Delta t^c(f,g) + E(1 - x_{fg}) \end{aligned} \qquad \forall g \in F', f \in F'_g \cup V_g \tag{4.8f}$$

$$x_{fg} \in \{0,1\} \qquad \forall g \in F', f \in F'_g \cup V_g \tag{4.8g}$$

$$E^X(f) + E^S_{c1}(f) \leq E_f \leq E - E^S_{c1}(f) \qquad \forall f \in F' \tag{4.8h}$$

Equation (4.8a) gives the objective function. Equations (4.8b) ensure that each vehicle is used at most once. Equations (4.8c) ensure that a flight is towed at most once, each flight from F^{fix} is towed, and that vehicle flow is conserved. By excluding f^{end}, it is ensured that all ETVs end the day at the depot with a full battery **(A5)**. Equations (4.8d) and (4.8e) connect the battery energy level between a flight or a towing vehicle and another flight. It considers both the case that there is no time to recharge the battery and that there is time to recharge it **(A4)**. Equations (4.8f) determine the battery energy level for subsequent flights if charging rate βP^c is used **(A3)**. Finally, the domain of each decision variable is specified in Equations (4.8g) and (4.8h). From the x variables in the solution, the list of to-be-towed flights F_v is obtained.

Solution example for a simple problem instance

In order to illustrate the model formulation, we discuss a small example. We consider a single ETV v, operating at an airport with a gate node g, runway r, and charging station c. We discuss the schedule of v between 6:00 and 9:00. We use $\Delta t^{reopt} = \Delta t^{fix} = 30$ minutes and $\Delta t^c_{\min} = 1$ hour.

We consider two aircraft $F = \{a, d\}$ where a is an arrival, and d a departure. Both take

20 minutes to tow, and use 10% of the battery energy. The evolution of the ELDT of a and the EOBT of d is shown in Table 4.2: a arrives earlier while d is slightly delayed.

The evolution of the schedule of v is given in Table 4.2 and Figure 4.7. At 6:40, v is charging, and has to charge until t_v = 7:20. Either aircraft can be towed by v, such that $F' = \{a, d\}$ and $V'_a = V'_d = \{v\}$, but they cannot be towed both by v, such that $F'_a = F'_d = \emptyset$. Aircraft a is assigned to v: $F_v = \{a\}$.

At 7:00 the ETV schedule is reoptimized. At this moment, a is scheduled to arrive earlier, whereas d is delayed, such that $F'_d = \{a\}$. Both a and d are assigned to v.

At 7:40, v starts towing a. From this moment, a is removed from F', F'_d and F_v. After this, v tows aircraft d, which is also removed from F' and F_v.

	Flight times		Optimization sets					ETV state				
t	ELDT $_a$	EOBT $_d$	F'	F'_a	F'_d	V'_a	V'_d	n_v	t_v	E_v/E	F_v	S_v
6:40	8:00	8:05	a,d	∅	∅	v	v	c	7:20	0.80	a	charging
7:00	7:50	8:10	a,d	∅	a	v	v	c	7:20	0.80	a,d	charging
7:20	7:45	8:10	a,d	∅	a	v	v	c	7:21	0.81	a,d	charging
7:40	7:40	8:10	d	∅	∅	∅	v	g	8:00	0.69	d	towing
8:00	7:40	8:10	d	∅	∅	∅	v	g	8:01	0.69	d	idle
8:20	7:40	8:10	∅	∅	∅	∅	∅	r	8:30	0.59	∅	towing

Table 4.2.: Evolution of the schedule of ETV v between 6:40 and 8:20. The ELDT and EOBT of aircraft a and d are shown, together with the optimization sets, as well as the state of v.

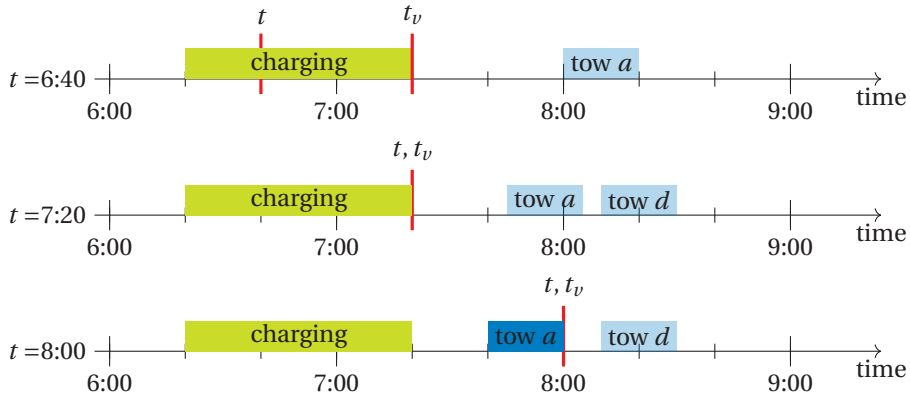

Figure 4.7.: Schedule of the ETV v at t = 6:40, 7:20, and 8:00.

4.5.2 Dynamic ETV planning - execution and conflict resolution

While the ETV planning model from Section 4.5.1 assigns the ETVs to aircraft, it does not describe how to execute the schedule when the true values of τ^{p} are revealed. This part of the framework is performed by Algorithm `ExecuteTows` (Alg. 3), which runs between global schedule reevaluations (Alg. 2). At each time t, the algorithm uses the latest available EOBTs and ELDTs to construct the most accurate pick-up time random variable $\tau^{\mathrm{p}}_f(t)$ to perform the schedule. As parameters, it requires a small time difference δt, and probability $\mathbb{P}_\theta$. It determines which flight to tow next and for how long to remain charging. In case the overlap time for two consecutively to-be-towed flights is positive, a scheduling conflict occurs, and the algorithm determines if a tow can be delayed or an aircraft is removed from the to-be-towed flights F_v.

Algorithm `ExecuteTows` is called every time an ETV v is idle or charging, and provides it with a next action to perform. There are four possible actions which can be taken: tow an aircraft, drive to a location, remain idle, or keep charging. As input, it considers the current state of v, $(n_v, t_v, E_v, F_v, S_v)$. As before (Section 4.5.1), it takes the action S'_v which yield the highest expected cost reduction, i.e. the one that minimize taxiing and delay cost. This action is provided to the ETV, together with the next state $(n'_v, t'_v, E'_v, F'_v, S'_v)$. A subroutine `NextFlight` 4 is used to determine the next to-be-towed flight.

4.6 Benchmark algorithms for stochastic towing vehicle planning

In order to assess the quality of the proposed planning model, the *Stochastic pick-up time ETV planning*, we consider two benchmarks. These provide an upper and a lower bound on the objective function. They use the same framework as in Section 4.5.1 and 4.5.2 but without using pick-up time random variables.

4.6.1 EOBT/ELDT Oracle ETV planning

The first benchmark assumes the AOBT and ALDT of all flights are known at the start of the day. With this information, there is no uncertainty in the problem and a planning can be made that uses the ETVs to maximum capacity. This provides an upper bound on the cost reduction the ETVs can provide.

4.6.2 Point estimate pick-up time ETV planning

Using the mean values of stochastic parameters is an often used approach for optimization problems under uncertainty [36]. For dynamic ETV scheduling, this translates to using the latest available EOBT and ELDT values as average point estimates for the pick-up time. As such, the pick-up time is not an evolving random variable, but an evolving deterministic variable.

Algorithm 3: `ExecuteTows` performs the ETV schedule

Data: ETV v at state t_v, n_v, E_v, F_v, and S_v; time difference δt, probability $\mathbb{P}_\theta$.
Result: Action S'_v and updated state t'_v, n'_v, q'_v and F'_v

1 Let δE be the amount by which the battery can be charged in δt time;
2 Let $F'_v = F_v \setminus \{f : f \in F_v \cap F^{arr} \wedge \tau^{\mathrm{p}}_f < t_v\}$;
3 **if** $F_v \neq \emptyset$ **then**
4 Get the next to-be-towed flight f using Algorithm 4 ;
5 Determine charging station $n^c = \arg\min_{n \in N^c}\{d^S(n_v, n) + d^S(n, n^{\mathrm{p}}_f)\}$;
6 Determine the required charge to tow f and reach a charging station E_{min};
7 Determine the available charging time t_c;
8 **if** $(\mathbb{E}[t_c] > \Delta t^c_{min}$ *and* $n_v \neq n^c)$ *or* $E_v < E_{min}$ **then**
9 S'_v= "drive"; $n'_v = n^c$; $E'_v = E_v - \mathscr{E}(0, v_s) \cdot d^S(n_v, n^c)$; $t'_v = t_v + \frac{d^S(n_v, n^c)}{v_s}$; $F'_v = F_v$;
10 **if** $(n_v = n^c$ *and* $E_v < E$ *and* $\mathbb{P}\left[t_v + \delta t + d^S(n_v, n^p_f)/v_s < \tau^p_f(t)\right] > \mathbb{P}_\theta$ $)$ *or* $E_v < E_{min}$ **then**
11 S'_v= "Charge"; $n'_v = n_v$; $E'_v = E_v + \delta E$; $t'_v = t_v + \delta t$;
12 **else**
13 **if** $n_v = n^p_f$ **then**
14 **if** t_v *is smaller than the actual pick-up time of* f **then**
15 S'_v= "remain idle"; $n'_v = n_v$; $E'_v = E_v$; $t'_v = t_v + \delta t$;
16 **else**
17 S'_v= "tow f"; $n'_v = \tau^{\mathrm{d}}_f$; $E'_v = E_v - E^X(f)$; $t'_v = t_v + (\tau^{\mathrm{d}}_f(t) - \tau^{\mathrm{p}}_f(t))$; $F'_v \leftarrow F'_v \setminus \{f\}$;
18 **end**
19 **else**
20 S'_v= "drive"; $n'_v = n^{\mathrm{p}}_f$; $E'_v = E_v - \mathscr{E}(0, v_s) d^S(n_v, n^{\mathrm{p}}_f)$; $t'_v = t_v + \frac{d^S(n_v, n^{\mathrm{p}}_f)}{v_s}$;
21 **end**
22 **end**
23 **else**
24 Let $\tau^{\mathrm{p}}_f(t) = t_e$, $m_f = 0$, $n^{\mathrm{p}}_f = n^{\mathrm{d}}_f = n^{dep}$ and continue on line 10;
25 **end**

4.7 Case study: managing a fleet of towing vehicles at Amsterdam Airport Schiphol

Airport taxi system and service roads

Figure 4.8 shows the layout of the airport, based on the Schiphol aerodrome charts [45]. The six runways and seven piers are represented by 19 nodes. These runway and gate nodes N^{rg} are shown as vertically hatched circles. We assume that five charging stations

Algorithm 4: Algorithm `NextFlight` for finding the next to-be-towed flight in the ETV planning.

Data: Current state $(n_v, t_v, E_v, F_v, S_v)$ of the ETV.
Result: Next to-be-towed flight h

if $|F_v| = 1$ **then**
  f is the only flight in F_v;
else
  Sort F_v by $\mathbb{E}[\tau^{\mathrm{p}}_f(t_v)] - d^S(n_v, n^{\mathrm{p}}_f)/v^s$;
  Let f be the first element of F_v;
  Set $h = f$;
  if $f \in F^{arr}$ **then**
    Sort the remaining flights of F_v by $\mathbb{E}[\tau^{\mathrm{p}}_f(t_v)] - d^S(n^{\mathrm{d}}_f, n^{\mathrm{p}}_g)/v^s$;
    Let g be the next flight with the lowest score ;
    if $g \in F^{arr}$ **then**
      if $c^{taxi}_f - c^{tow}_f + (c^{taxi}_g - c^{tow}_g)\mathbb{P}[\tau^o_{fg}(t_v) < 0] < c^{taxi}_g - c^{tow}_g$ **then**
        Set $h = g$;
    else
      if $\mathbb{E}[\tau^o_{fg}(t_v)]c^d_g > c^{taxi}_f - c^{tow}_f$ **then**
        set $h = g$;
    end
end

are available at the airport, $N^{CS} = \{C1, C2, C3, C4, C5\}$, displayed as horizontally hatched circles. The ETV depot is located at charging station $n^{dep} = C5$. The taxiway and service road networks connect these nodes. They are displayed as solid and dashed lines, respectively. Some taxiways may be traversed in one direction only, this is indicated with arrowheads.

ETV specifications

We consider an ETV suitable to tow narrow-body aircraft (a.o. the B737, A320, and E190). Table 4.3 shows the assumed ETV specifications. Actual data on ETV energy usage is not available. As such, we consider the following energy consumption model for an ETV:

$$\mathscr{E}(v, m) = \mu^g(v) \cdot (m + m_v)g \qquad \text{with} \qquad \mu^g(v) = \mu^0\left(1 + \tfrac{v}{v^0}\right) \tag{4.9}$$

where $\mathscr{E}$, the energy to tow over a unit distance, is a function of the velocity v, the mass of the ETV m_v and towed aircraft m (adapted from [46]). The rolling resistance coefficient μ^g is an increasing function of the velocity. Lastly, g denotes the gravitational acceleration. This model assumes a constant towing velocity, see **(A2)**, on a horizontal terrain, and only considers rolling resistance. For this resistance, it assumes that the wheels of the ETV and aircraft are of a similar size. While the model does not account for acceleration/braking or the effect of the weather conditions, it provides a sufficient

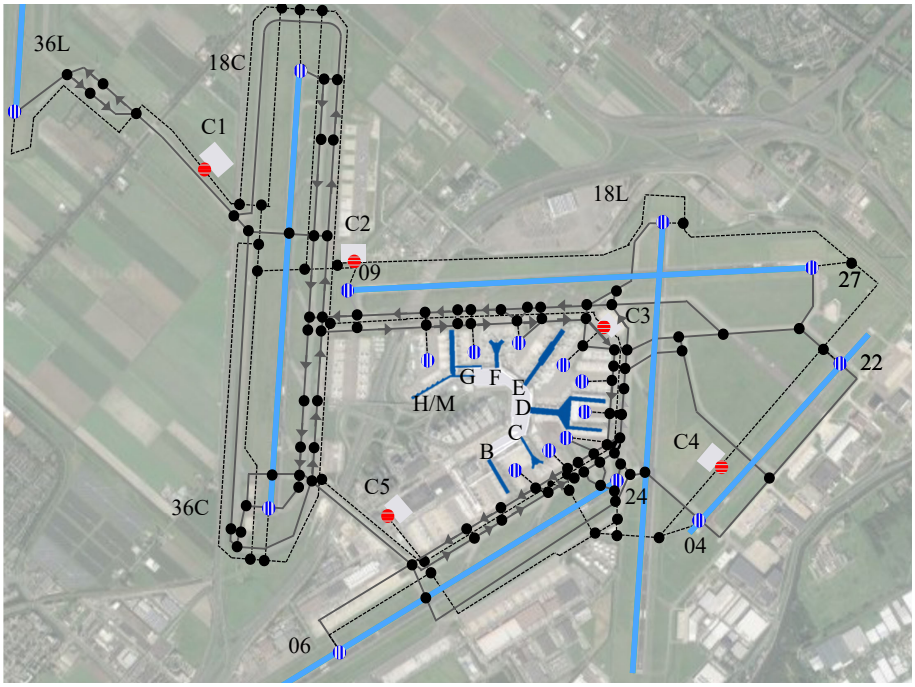

Figure 4.8.: Runways N^R and gate nodes N^G, together with taxiways (solid lines), service roads (dashed lines) and charging stations $(C1, ..., C5)$ at AAS. The map is based on the Schiphol aerodrome charts [45].

basis. Also, we note that the ETV planning framework can be considered regardless of the energy consumption model used.

Taxiing and towing costs

The taxiing and towing costs for a flight f are determined as follows:

$$c_f^{\text{taxi}} = c^{kero} \frac{d^X(n_f^{\text{p}}, n_f^{\text{d}})}{v_x} FF_f \cdot m_f \tag{4.10}$$

$$c_f^{\text{tow}} = c^{elec} E^X(f), \tag{4.11}$$

where c^{kero} is the cost of fuel consumption, FF_f the fuel flow of the aircraft type of f during taxiing, and c^{elec} the cost of electricity. The cost c^{kero} is the sum of the kerosene costs (€1.20 per liter [50]), and the emission costs (€90 per tonne CO_2 [51]). The fuel flow FF_f depends on the aircraft type and is taken from the ICAO *Engine Emissions Databank* [52]. The electricity cost c^{elec} is set at €0.25 per kWh [53]. The mass m_f is the MTOW or EOW of the aircraft for departures and arrivals, respectively.

The delay costs for a flight f depend on the aircraft type, and are assumed as per

Parameter	Explanation	Value	Ref
v^x [km/h]	towing speed	42.5	[8]
P^c [kW]	charging power	100	[30]
m [10^3kg]	ETV mass	15	[30]
E [kWh]	battery capacity	400	[30]
$\Delta t^c_{\min}[s]$	minimum charging time	3600	
$\Delta t^{\text{ec}}[s]$	engine cool-down time	180	[47]
$\Delta t^{\text{con}}[s]$	ETV connect-time	60	
$\Delta t^{\text{pb}}[s]$	push-back time	120	[48]
$\Delta t^{\text{rel}}[s]$	ETV disconnect time	60	[48]
α	charging curve factor	0.9	[43]
β	charging curve factor	0.1	[43]
μ^0	resistance factor	0.1	[46]
v^0 [km/h]	resistance base velocity	41	[46]
v_s [km/h]	service road velocity	30	[49]

Table 4.3.: ETV and towing process parameters.

European airline delay cost reference values [54], updated to account for inflation (20% since 2015).

Flight schedule

We consider the flight schedules of 15 days during the summer and fall of 2023, spaced at regular intervals, see Table 4.4. All days of operation start at 6 AM and end at 6 AM on the next day. The flight data has been acquired using the Schiphol Developer Portal [55], from where the EOBTs and ELDTs are retrieved every minute.

Obtaining the distributions of ΔOBT_δ and ΔLDT_δ

Using the flight data at Schiphol between July 1 and August 30 2023 (minus the days from Table 4.4), the distributions of the errors in the EOBT and ELDT have been determined. The random variables ΔOBT_δ and ΔLDT_δ are distributed accordingly. This is done as described in Section 4.3. Furthermore, in order to account for the different traffic levels during the day, ΔOBT_δ and ΔLDT_δ have been determined for every hour of the day separately. For each hour h, these are denoted by $\Delta\text{OBT}^h_\delta$ and $\Delta\text{LDT}^h_\delta$. To construct these, an arriving flight f at time t contributes $ALDT - ELDT_f(t)$ to the distribution of $\Delta\text{LDT}^h_\delta$, with $\delta = ELDT_f(t) - t$ and h. Conversely, to determine $\tau^{\text{p}}_f(t)$ (Equation 4.1), the random variable $\Delta\text{LDT}^h_\delta$ is used where h is the hour of $ELDT_f(t)$.

Experimental setup

The model from Section 4.5.1 has been implemented in the Gurobi Optimizer 10.0.2, on a pc with 17 AMD Ryzen 7-1700X processors. In order to accelerate the optimization,

Day	Flights	Taxi cost
Jul 13	1036	€ 606828
Jul 28	1045	€ 604120
Aug 3	1025	€ 588295
Aug 12	954	€ 558370
Aug 27	1021	€ 590674

Day	Flights	Taxi cost
Sep 2	928	€ 535086
Sep 11	1050	€ 603310
Sep 26	1029	€ 596247
Oct 3	1049	€ 602082
Oct 12	1069	€ 614734

Day	Flights	Taxi cost
Oct 27	1051	€ 602931
Nov 2	811	€ 463110
Nov 11	967	€ 550024
Nov 26	961	€ 547371
Dec 6	982	€ 571295

Table 4.4.: Flights (arrivals and departures of narrow-body aircraft) at Schiphol airport, for 15 distinct day from 2023, where *Taxi cost* gives $\sum_{f \in F} c_f^{\text{taxi}} - c_f^{\text{tow}}$ for each day.

the algorithm is hot-started with a greedy assignment. To obtain the final assignment, the model is optimized for a maximum of 5 minutes. Furthermore, a time interval of $\Delta t^{fix} = 45$ minutes is used (Assumption (A12)). Lastly, the probabilities $\mathbb{P}_\phi = 0.05$ (to define F'), $\mathbb{P}_\theta = 0.95$ (in Equation 4.5 and Algorithm 3), and $\delta = 1$ minute are used.

4.8 Case study: Numerical results

4.8.1 Sensitivity analysis of Δt^{reopt}

In order to find proper values for the schedule reevaluation time Δt^{reopt} (Algorithm 2), a sensitivity analysis has been performed. This is done using the flight data of July 13, 2023, and with a fleet of 5 ETVs (the same experiment as in Section 4.8.2).

Table 4.5 shows the results of the parameter tuning. For each value of Δt^{reopt}, the emission cost reduction $c^{\text{taxi}} - c^{\text{tow}}$, the delay cost incurred c^{d}, and total cost reduction $c^{\text{taxi}} - c^{\text{tow}} - c^{\text{d}}$ are given. Using lower values of Δt^{reopt} results in towing more aircraft, but also increases the delays caused by ETVs. Overall, the value of $\Delta t^{reopt} = 40$ minutes maximizes the total cost reduction, and is used in the remainder of this section.

4.8.2 Dispatching ETVs on the 13th of July 2023 at Schiphol

We illustrate our proposed ETV planning approach considering the flight schedule of July 13, 2023. We consider a fleet of 5 ETVs. On this day, 1036 narrow-body aircraft arrived and departed from Schiphol, with a total taxiing emission cost of €606828.

The results are given in Table 4.6. Using the *Stochastic pick-up time ETV planning*, 147 flights are towed, of which 72 arrivals and 75 departures, and a total cost reduction of

Δt^{reopt} [min]	15	20	25	30	35	40	45
Emission reduction [€]	79087	80151	80871	76771	76564	78335	75622
Delay [€]	10343	11465	10521	6441	7894	5540	5437
Cost reduction [€]	68744	66554	70350	70330	68652	75795	70185

Table 4.5.: Performance of the Stochastic pick-up time ETV planning algorithm (Section 4.5), using a 5 ETV fleet on July 13, 2023. Values of Δt^{reopt} between 15 and 45 minutes are tested. Let F^{tow} be the set of towed aircraft. *Emission reduction* gives $\sum_{f \in F^{tow}} c_f^{\text{taxi}} - c_f^{\text{tow}}$ (in €), *delay* the delay caused by towing operations ($\sum_f c_f^{\text{d}}$); *cost reduction* gives $\sum_{f \in F^{tow}} c_f^{\text{taxi}} - c_f^{\text{tow}} - c_f^{\text{d}}$.

4

€72795 is achieved. The total $c^{\text{taxi}} - c^{\text{tow}}$ of the towed flights is €78335, which is 12.9% of the total during this day. Because of towing, flights were delayed by a total of 60 minutes (on average 1 min/departure), resulting in a cost of €5540.

The *EOBT/ELDT Oracle ETV planning* (Section 4.6.1) achieves a cost reduction of **€106678** by towing 199 flights. The *Point estimate pick-up time ETV planning* (Section 4.6.2) achieves a cost reduction of **€58899**. Using this method, more flights are towed (182 against 134), but a similar total emission cost reduction $c^{\text{taxi}} - c^{\text{tow}}$ is achieved (€88215 against €78335). The major flaw of the *Point estimate* ETV planning method is the high delay costs it incurs, almost €30000 (or 319 minutes). Finally, Table 4.7 shows that a relative large share of the tows performed in this case were arriving flights (49% against 41% with perfect- and 29% with point estimate information). This is due to the smaller uncertainty in pick-up time of the arrival flights, see also Figure 4.1.

ETV planning method	Emission reduction [€]	[%]	Delay [€]	[min]	Cost reduction [€]	[%]
EOBT/ELDT Oracle (Section 4.6.1)	107387	18.2	708	38	**106678**	17.6
Stochastic pick-up time (Section 4.5)	78335	12.9	5540	60	**72795**	12.0
Point estimate pick-up time (Section 4.6.2)	88215	14.6	29315	319	**58899**	9.7

Table 4.6.: Performance of the three ETV planning algorithms (Section 4.5), using a 5 ETV fleet on July 13, 2023. Let F^{tow} be the set of towed aircraft. *Emission reduction* gives $\sum_{f \in F^{tow}} c_f^{\text{taxi}} - c_f^{\text{tow}}$ (in € and as percentage of total costs), *delay* the delay caused by towing operations (both in minutes and as $\sum_f c_f^{\text{d}}$); *cost reduction* gives $\sum_{f \in F^{tow}} c_f^{\text{taxi}} - c_f^{\text{tow}} - c_f^{\text{d}}$.

ETV planning method	All flights		Arrivals			
	# Tows	$c^{\text{taxi}} - c^{\text{tow}}$	# Tows		$c^{\text{taxi}} - c^{\text{tow}}$	
	[-]	[€]	[-]	[%]	[€]	[%]
EOBT/ELDT Oracle (Section 4.6.1)	199	110387	82	41.2	54949	49.8
Stochastic pick-up time (Section 4.5)	147	78335	72	49.0	42692	54.5
Point estimate pick-up time (Section 4.6.2)	172	88215	52	28.6	32683	37.3

Table 4.7.: Number of flights towed, using the three ETV planning algorithms presented in Section 4.5, using a 5 ETV fleet on July 13, 2023, with $c^{\text{taxi}} - c^{\text{d}}$ the total emission cost reduction.

The ETV schedules are shown in Figures 4.9, 4.10 and 4.11 for the *EOBT/ELDT Oracle* (4.9), *Point estimate pick-up time* (4.10a, 4.10b), and *Stochastic pick-up time* (4.11a, 4.11b) ETV planning. Towing an aircraft without delays is shown as solid blue bars, delayed towing as dotted red bars, charging as hatched green bars, and driving as light-grey bars. The current time t and the next optimization time $t + \Delta t^{reopt}$ are shown as vertical dashed lines. The schedule given by the *EOBT/ELDT Oracle ETV planning* does not change during the day, the schedules given by the *Stochastic pick-up time* and *Point estimate pick-up time ETV planning* algorithms are shown at two different times. The *Point estimate pick-up time ETV planning* leads to large delays, see Figure 4.10b and ETV 2 after 14:30. It also shows consecutively delayed tows: one flight is delayed, causing the next tow to be delayed as well. These are largely absent when stochastic pick-up times were accounted for (Figure 4.11a).

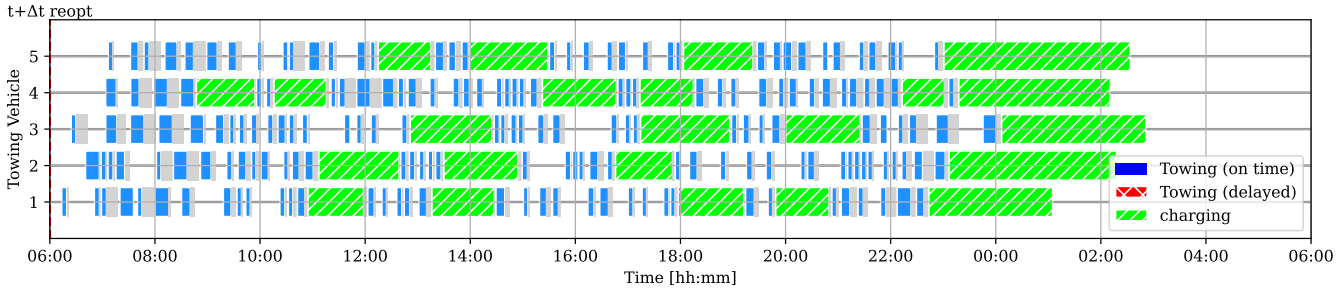

Figure 4.9.: ETV planning for July 13, 2023 for a fleet of 5 ETVs, using the *EOBT/ELDT Oracle ETV planning* algorithm from Section 4.5.

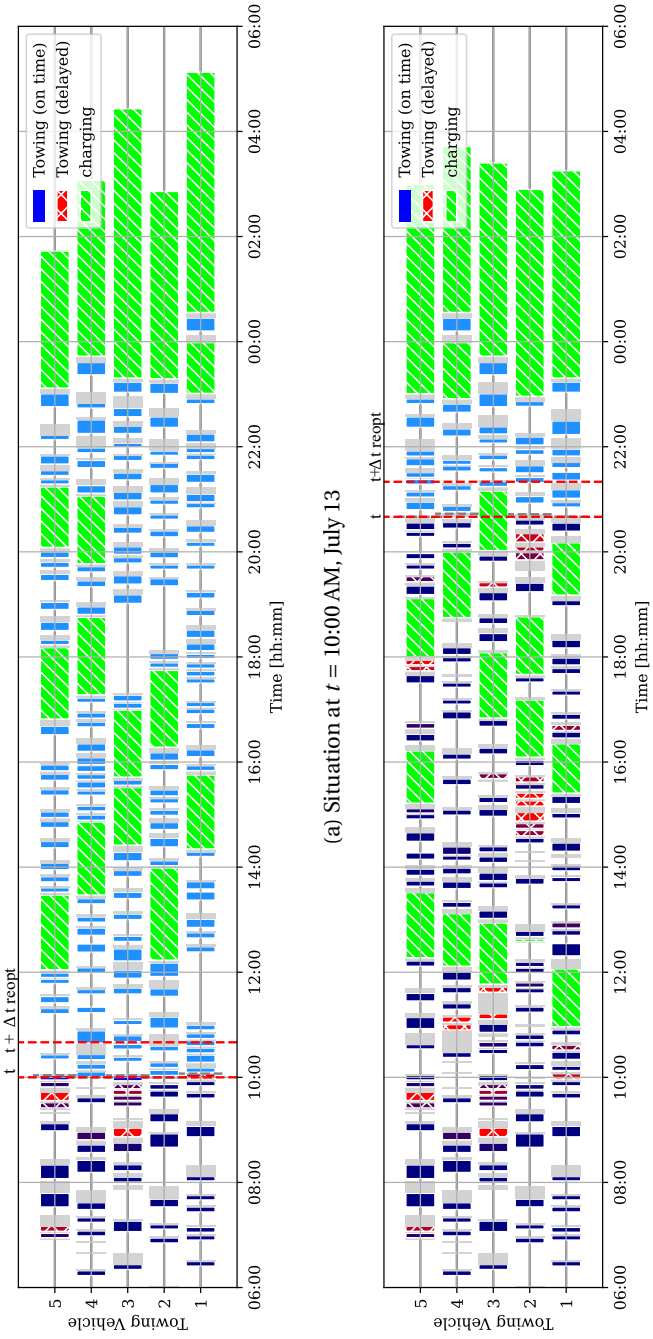

(a) Situation at t = 10:00 AM, July 13

(b) Situation at t = 8:40 PM, July 13

Figure 4.10.: ETV planning for July 13, 2023 for a fleet of 5 ETVs, using the *Point estimate pick-up time ETV planning* from Section 4.5.

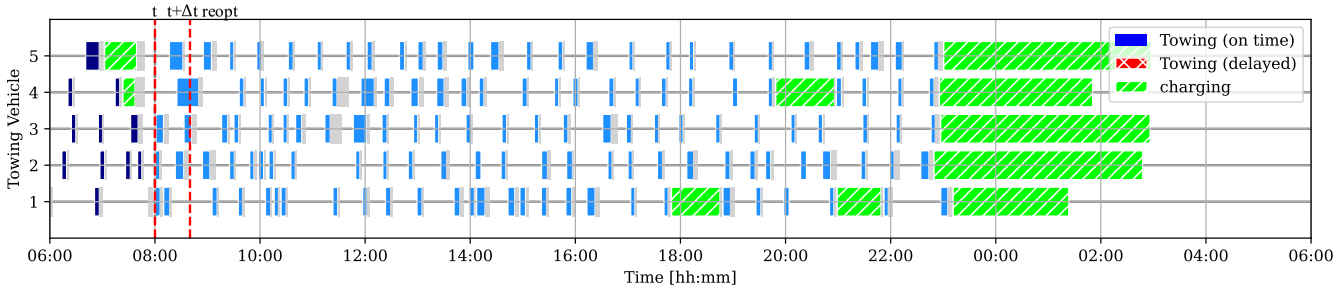

(a) Situation at t = 8 AM, July 13

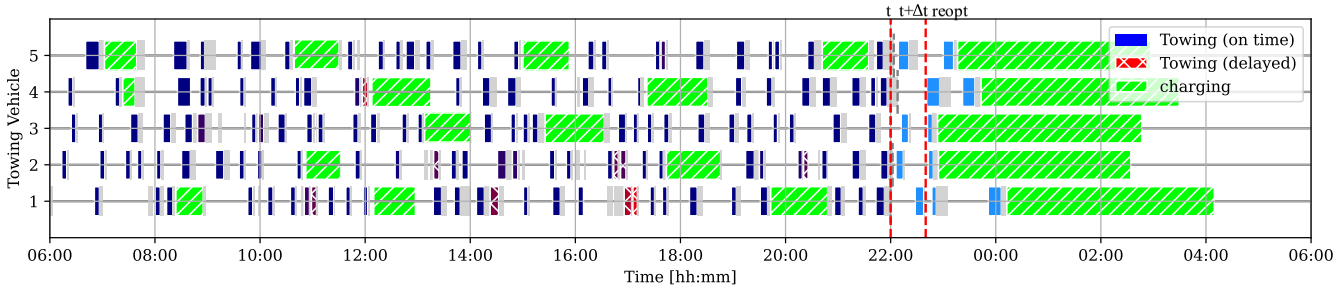

(b) Situation at t = 10 PM, July 13

Figure 4.11.: ETV planning for July 13, 2023 for a fleet of 5 ETVs, using the *Stochastic pick-up time ETV planning* algorithm from Section 4.5.

4.8.3 Dispatching ETVs at Schiphol considering 15 distinct days

To assess the general performance of the *Stochastic pick-up time ETV planning*, all three planning methods have been applied on 15 days of operations (see Table 4.4). For each day and each planning method, we consider ETV fleets from 0 up to 50 vehicles.

For each day of operations, fleet size, and planning method, we determined the taxi cost reductions $c^{\text{taxi}} - c^{\text{tow}}$ and the delay costs c^{d} of all towed flights. Figure 4.12 shows the median and 10-90 percentiles of these results for all methods per fleet size. It shows the emission cost reduction $c^{\text{taxi}} - c^{\text{tow}}$ (4.12a), delay cost c^{d} (4.12b), and total cost reduction $c^{\text{taxi}} - c^{\text{tow}} - c^{\text{d}}$ (4.12c). Additionally, in Figures 4.12a and 4.12c, the average maximum emission cost reduction of all flights are shown as a horizontal line.

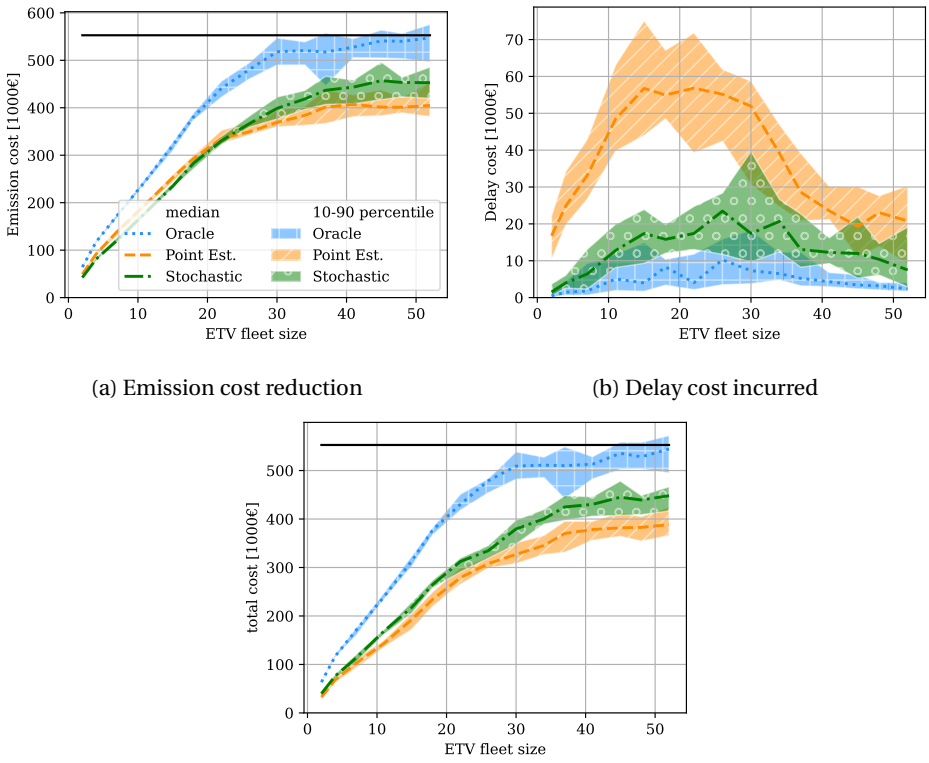

(a) Emission cost reduction

(b) Delay cost incurred

(c) Total cost reduction

Figure 4.12.: Cost reduction achieved by dispatching ETV fleets between 0 and 50 vehicles at *Schiphol* airport, for 15 days of operations (Table 4.4). The medians are shown as a line, the 10-90 percentiles as a shaded area.

Figure 4.12 shows a considerable difference in the performance of the planning algorithms for different ETV fleet sizes. The difference between the *Stochastic/Point-estimate*

pick-up time and the *EOBT/ELDT Oracle ETV planning* methods is largest during the scale-up of the ETV fleet: between 15 and 40 ETVs. At this stage there are not enough vehicles to tow a large fraction of the aircraft. In this case, the *Point estimate pick-up time* plan is able to tow more aircraft (4.12a), but incurs an especially large delay cost (4.12b). Both show an increasing delay cost up to 30 ETVs, after which it decreases to €10.000 for the *Stochastic pick-up time* and €20.000 for the *Point-estimate pick-up time ETV planning* (4.12b). Above 40 ETVs, the difference in cost reduction stagnates around €90.000 for the *Stochastic pick-up time ETV planning* method and €150.000 for the *Point estimate pick-up time ETV planning* method (4.12c). This is due to the loss of performance due to imperfect information.

Table 4.8 in detail the obtained results for fleets of 5, 20, and 40 ETVs. It shows the average results per ETV (i.e., cost reduction, delay, number of towing tasks per ETV), over all 15 days .

ETV planning method	Cost red. [€]	Delay [min]	Tows [#]	Arrivals [#]	Arrivals [%]	Departures [#]	Departures [%]
5 ETVs							
EOBT/ELDT Oracle	**24717**	8.3	44.9	18.0	40.1	26.9	59.9
Stochastic pick-up time	**17364**	12.4	27.8	13.6	48.9	14.2	51.1
Point estimate pick-up time	**15655**	47.2	35.8	13.0	36.2	22.8	63.8
20 ETVs							
EOBT/ELDT Oracle	**19955**	3.1	34.3	16.4	47.8	17.9	52.2
Stochastic pick-up time	**14760**	8.8	25.1	12.4	49.2	12.8	50.8
Point estimate pick-up time	**13144**	24.0	26.6	12.0	45.0	14.6	55.0
40 ETVs							
EOBT/ELDT Oracle	**13788**	1.6	23.9	11.2	46.7	12.7	53.3
Stochastic pick-up time	**11443**	3.7	20.3	9.8	48.4	10.5	51.6
Point estimate pick-up time	**9771**	7.4	18.4	8.9	48.4	9.5	51.6

Table 4.8.: Average performance *per ETV per day* of the three ETV planning methods, considering the flight schedules of the days in Table 4.4. ETV fleets of 5, 20, and 40 vehicles are shown. The *Cost red* is the total cost reduction $c^{\text{taxi}} - c^{\text{tow}} - c^{\text{d}}$ of all towed flights.

The *Stochastic pick-up time ETV planning* method leads to higher cost reductions than the *Point estimate pick-up time ETV planning*: €1600 per ETV per day, irrespective of the fleet size. Moreover, the gap between these two approaches and the *EOBT/ELDT Oracle ETV planning* decreases from over 29% to 15% for large fleet sizes. This is largely due to the reduction in delay costs. Also, the number of towed aircraft for the *Stochastic pick-up time ETV planning* decreases less then in the two other methods: from 38.1 to 15.1. This is due to the larger buffers used by this approach, see also Figure **??**. This approach also has a preference for towing arrivals for a small fleet of ETVs is considered (as seen in Section 4.8.2). This is no longer the case when we consider large fleets of ETVs.

Finally, when considering fleet sizes of 0-50 ETVs, the *Stochastic pick-up time ETV planning* method is able to achieve a cost reduction of **€12104** on average per ETV per day. This is 79.5% of the cost reduction achieved by the *EOBT/ELDT Oracle ETV planning* method, that achieved a reduction of **€15225**. This is a clear improvement over the *Point estimate pick-up time ETV planning* method, which achieves a cost reduction of **€10276** (67.5% of the *EOBT/ELDT Oracle*).

4.9 Conclusions

Our chapter proposes a stochastic and dynamic framework to dispatch a fleet of electric towing vehicles (ETVs) to tow aircraft by accounting for uncertain arrival and departure times of aircraft: the *Stochastic pick-up time ETV planning*. A planning is made indicating which aircraft is towed by which ETV and when the ETVs recharge their batteries. We create a schedule that maximizes fuel savings by replacing conventional taxiing with ETV towing. At the same time, we minimize the delay induced by the use of ETVs. This is done using a rolling horizon approach, where the stochastic arrival and departure times are updated periodically. From a methodological perspective, our approach extends the E-VRP-TW problem to instances with stochastic and dynamically evolving start times of time windows.

The *Stochastic pick-up time ETV planning* framework is illustrated for several days of operations from 2023 at Amsterdam Airport *Schiphol*. We consider a fleet of ETVs that tow narrow-body aircraft. We obtain schedules for ETV towing tasks and battery charging, which are updated periodically. Our approach is bench-marked against: (i) an approach that assumes a priori full knowledge of the actual arrival/departure times (*EOBT/ELDT Oracle ETV planning*), and (ii) an approach which assumes average point estimates of the arrival/departure times (*Point Estimate pick-up time ETV planning*). The results show that our proposed approach achieves an average taxiing cost reduction of €12104 per ETV per day (79.5% of the *EOBT/ELDT Oracle*), compared with €10276 cost reduction for the *Point Estimate pick-up time* planning (67.5% of the *EOBT/ELDT Oracle*, 84.9% of our proposed approach).

As future work, we aim to consider additional sources of disruption, such as decreased battery performance or changing runway configurations. Furthermore, the possibility of simultaneously minimizing taxiing/towing costs and ETV driving costs can be studied. To further improve the performance of the algorithm, hyper parameter tuning can be performed. Lastly, we plan to investigate effective policies for runway usage that boost environmental benefits.

references

[1] S. van Oosterom and M. Mitici. “An environmentally-aware dynamic planning of electric vehicles for aircraft towing considering stochastic aircraft arrival and departure times”. In: *Transportation Research Part C: Emerging Technologies* 169 (2024). DOI: 10.1016/j.trc.2024.104857.

[2] D. S. Lee, D. W. Fahey, A. Skowron, M. R. Allen, U. Burkhardt, Q. Chen, S. J. Doherty, S. Freeman, P. M. Forster, J. Fuglestvedt, A. Gettelman, R. R. De León, L. L. Lim, M. T. Lund, R. J. Millar, B. Owen, J. E. Penner, G. Pitari, M. J. Prather, R. Sausen, and L. J. Wilcox. “The contribution of global aviation to anthropogenic climate forcing for 2000 to 2018”. en. In: *Atmospheric Environment* 244 (Jan. 2021), p. 117834. ISSN: 1352-2310. DOI: 10.1016/j.atmosenv.2020.117834. URL: https://www.sciencedirect.com/science/article/pii/S1352231020305689 (visited on 10/26/2022).

[3] International Air Transport Association. *Global Outlook for Air Transport*. Tech. rep. Montreal: IATA, 2022. URL: https://www.iata.org/en/iata-repository/publications/economic-reports/global-outlook-for-air-transport---december-2022/ (visited on 05/01/2023).

[4] United Nations Framework Convention on Climate Change. *Paris Agreements*. Tech. rep. Paris: United Nations, 2015. URL: https://unfccc.int/sites/default/files/english_paris_agreement.pdf (visited on 06/23/2021).

[5] K. Ranasinghe, K. Guan, A. Gardi, and R. Sabatini. “Review of advanced low-emission technologies for sustainable aviation”. en. In: *Energy* 188 (Dec. 2019), p. 115945. ISSN: 0360-5442. DOI: 10.1016/j.energy.2019.115945. URL: https://www.sciencedirect.com/science/article/pii/S0360544219316299 (visited on 05/01/2023).

[6] E. Roosenbrand, J. Sun, and J. Hoekstra. “Contrail minimization through altitude diversions: A feasibility study leveraging global data”. In: *Transportation Research Interdisciplinary Perspectives* 22 (Nov. 2023), p. 100953. ISSN: 2590-1982. DOI: 10.1016/j.trip.2023.100953. URL: https://www.sciencedirect.com/science/article/pii/S2590198223002002 (visited on 01/31/2024).

[7] H. Khadilkar and H. Balakrishnan. “Estimation of aircraft taxi fuel burn using flight data recorder archives”. en. In: *Transportation Research Part D: Transport and Environment* 17.7 (Oct. 2012), pp. 532–537. ISSN: 13619209. DOI: 10.1016/j.trd.2012.06.005. (Visited on 11/15/2021).

[8] M. Lukic, P. Giangrande, A. Hebala, S. Nuzzo, and M. Galea. “Review, Challenges, and Future Developments of Electric Taxiing Systems”. In: *IEEE Transactions on Transportation Electrification* 5.4 (Dec. 2019). Conference Name: IEEE Transactions on Transportation Electrification, pp. 1441–1457. ISSN: 2332-7782. DOI: 10.1109/TTE.2019.2956862.

[9] T. Nikoleris, G. Gupta, and M. Kistler. “Detailed estimation of fuel consumption and emissions during aircraft taxi operations at Dallas/Fort Worth International Airport”. en. In: *Transportation Research Part D: Transport and Environment* 16.4 (June 2011), pp. 302–308. ISSN: 13619209. DOI: 10.1016/j.trd.2011.01.007. (Visited on 11/15/2021).

[10] M. Soltani, S. Ahmadi, A. Akgunduz, and N. Bhuiyan. “An eco-friendly aircraft taxiing approach with collision and conflict avoidance”. en. In: *Transportation Research Part C: Emerging Technologies* 121 (Dec. 2020), p. 102872. ISSN: 0968-090X. DOI: 10.1016/j.trc.2020.102872. (Visited on 12/13/2022).

[11] S. van Oosterom, M. Mitici, and J. Hoekstra. “Analyzing the impact of battery capacity and charging protocols on the dispatchment of electric towing vehicles at a large airport”. In: *AIAA AVIATION 2022 Forum*. AIAA AVIATION Forum. American Institute of Aeronautics and Astronautics, June 2022. DOI: 10.2514/6.2022-3920.

[12] EUROCONTROL. *Network Manager Annual Report 2022*. en. Tech. rep. Brussels: EUROCONTROL, Sept. 2023. URL: https://www.eurocontrol.int/publication/network-manager-annual-report-2022 (visited on 10/26/2023).

[13] EUROCONTROL. *Annual Network Operations Report 2022*. en. Tech. rep. Brussels: EUROCONTROL, May 2023. URL: https://www.eurocontrol.int/publication/annual-network-operations-report-2022 (visited on 10/26/2023).

[14] S. Chen, L. Wu, K. K. H. Ng, W. Liu, and K. Wang. “How airports enhance the environmental sustainability of operations: A critical review from the perspective of Operations Research”. In: *Transportation Research Part E: Logistics and Transportation Review* 183 (Mar. 2024), p. 103440. ISSN: 1366-5545. DOI: 10.1016/j.tre.2024.103440. URL: https://www.sciencedirect.com/science/article/pii/S1366554524000309 (visited on 03/08/2024).

[15] O. Bräysy and M. Gendreau. “Vehicle Routing Problem with Time Windows, Part I: Route Construction and Local Search Algorithms”. en. In: *Transportation Science* 39.1 (Feb. 2005), pp. 104–118. ISSN: 0041-1655, 1526-5447. DOI: 10.1287/trsc.1030.0056. (Visited on 01/27/2022).

[16] O. Bräysy and M. Gendreau. “Vehicle Routing Problem with Time Windows, Part II: Metaheuristics”. en. In: *Transportation Science* 39.1 (Feb. 2005), pp. 119–139. ISSN: 0041-1655, 1526-5447. DOI: 10.1287/trsc.1030.0057. (Visited on 01/27/2022).

[17] M. A. Figliozzi. “An iterative route construction and improvement algorithm for the vehicle routing problem with soft time windows”. en. In: *Transportation Research Part C: Emerging Technologies* 18.5 (Oct. 2010), pp. 668–679. ISSN: 0968090X. DOI: 10.1016/j.trc.2009.08.005. (Visited on 01/31/2022).

[18] M. W. P. Savelsbergh. “The Vehicle Routing Problem with Time Windows: Minimizing Route Duration”. en. In: *ORSA Journal on Computing* 4.2 (May 1992), pp. 146–154. ISSN: 0899-1499, 2326-3245. DOI: 10.1287/ijoc.4.2.146. (Visited on 01/31/2022).

[19] D. Taş. “Electric vehicle routing with flexible time windows: a column generation solution approach”. In: *Transportation Letters* 13.2 (Feb. 2021). Publisher: Taylor & Francis _eprint: https://doi.org/10.1080/19427867.2020.1711581, pp. 97–103. ISSN: 1942-7867. DOI: 10.1080/19427867.2020.1711581. URL: https://doi.org/10.1080/19427867.2020.1711581 (visited on 02/27/2023).

[20] R. Conrad and M. A. Figliozzi. “The Recharging Vehicle Routing Problem”. In: Institute of Industrial & System Engineers, 2011. URL: https://web.cecs.pdx.edu/~maf/Conference_Proceedings/2011_The_Recharging_Vehicle_Routing_Problem.pdf.

[21] S. Erdoğan and E. Miller-Hooks. “A Green Vehicle Routing Problem”. en. In: *Transportation Research Part E: Logistics and Transportation Review*. Select Papers from the 19th International Symposium on Transportation and Traffic Theory 48.1 (Jan. 2012), pp. 100–114. ISSN: 1366-5545. DOI: 10.1016/j.tre.2011.08.001. (Visited on 06/15/2021).

[22] A. Omidvar and R. Tavakkoli-Moghaddam. “Sustainable vehicle routing: Strategies for congestion management and refueling scheduling”. In: *2012 IEEE International Energy Conference and Exhibition (ENERGYCON)*. Florence, Italy: IEEE, Sept. 2012, pp. 1089–1094. ISBN: 978-1-4673-1454-1 978-1-4673-1453-4 978-1-4673-1452-7. DOI: 10.1109/EnergyCon.2012.6347732. (Visited on 01/27/2022).

[23] M. Schneider, A. Stenger, and D. Goeke. “The Electric Vehicle-Routing Problem with Time Windows and Recharging Stations”. In: *Transportation Science* 48.4 (Mar. 2014). Publisher: INFORMS, pp. 500–520. ISSN: 0041-1655. DOI: 10.1287/trsc.2013.0490. (Visited on 06/11/2021).

[24] G. Hiermann, J. Puchinger, S. Ropke, and R. F. Hartl. “The Electric Fleet Size and Mix Vehicle Routing Problem with Time Windows and Recharging Stations”. en. In: *European Journal of Operational Research* 252.3 (Aug. 2016), pp. 995–1018. ISSN: 0377-2217. DOI: 10.1016/j.ejor.2016.01.038. (Visited on 06/15/2021).

[25] G. Desaulniers, F. Errico, S. Irnich, and M. Schneider. “Exact Algorithms for Electric Vehicle-Routing Problems with Time Windows”. en. In: *Operations Research* 64.6 (Dec. 2016), pp. 1388–1405. ISSN: 0030-364X, 1526-5463. DOI: 10.1287/opre.2016.1535. (Visited on 01/27/2022).

[26] M. Keskin and B. Çatay. “Partial recharge strategies for the electric vehicle routing problem with time windows”. en. In: *Transportation Research Part C: Emerging Technologies* 65 (Apr. 2016), pp. 111–127. ISSN: 0968-090X. DOI: 10.1016/j.trc.2016.01.013. URL: https://www.sciencedirect.com/science/article/pii/S0968090X16000322 (visited on 02/03/2023).

[27] X. Zuo, Y. Xiao, M. You, I. Kaku, and Y. Xu. “A new formulation of the electric vehicle routing problem with time windows considering concave nonlinear charging function”. en. In: *Journal of Cleaner Production* 236 (Nov. 2019), p. 117687. ISSN: 0959-6526. DOI: 10.1016/j.jclepro.2019.117687. URL: https://www.sciencedirect.com/science/article/pii/S0959652619325375 (visited on 02/02/2023).

[28] E. Lam, G. Desaulniers, and P. J. Stuckey. “Branch-and-cut-and-price for the Electric Vehicle Routing Problem with Time Windows, Piecewise-Linear Recharging and Capacitated Recharging Stations”. en. In: *Computers & Operations Research* 145 (Sept. 2022), p. 105870. ISSN: 0305-0548. DOI: 10.1016/j.cor.2022.105870. URL: https://www.sciencedirect.com/science/article/pii/S0305054822001423 (visited on 02/02/2023).

[29] H. Diefenbach, S. Emde, and C. H. Glock. “Multi-depot electric vehicle scheduling in in-plant production logistics considering non-linear charging models”. en. In: *European Journal of Operational Research* 306.2 (Apr. 2023), pp. 828–848. ISSN: 0377-2217. DOI: 10.1016/j.ejor.2022.06.050. URL: https://www.sciencedirect.com/science/article/pii/S0377221722005252 (visited on 01/26/2023).

[30] E. v. Baaren and P. Roling. “Design of a zero emission aircraft towing system”. English. In: *AIAA AVIATION Forum, 17-21 June 2019, Dallas, Texas*. American Institute of Aeronautics and Astronautics Inc. (AIAA), 2019, AIAA. DOI: 10.2514/6.2019-2932. URL: https://research.tudelft.nl/en/publications/design-of-a-zero-emission-aircraft-towing-system (visited on 06/15/2021).

[31] S. van Oosterom, M. Mitici, and J. Hoekstra. “Dispatching a fleet of electric towing vehicles for aircraft taxiing with conflict avoidance and efficient battery charging”. en. In: *Transportation Research Part C: Emerging Technologies* 147 (Feb. 2023), p. 103995. ISSN: 0968-090X. DOI: 10.1016/j.trc.2022.103995.

[32] M. Zoutendijk and M. Mitici. “Fleet scheduling for electric towing of aircraft under limited airport energy capacity”. In: *Energy* 294 (May 2024), p. 130924. ISSN: 0360-5442. DOI: 10.1016/j.energy.2024.130924. URL: https://www.sciencedirect.com/science/article/pii/S0360544224006960 (visited on 03/08/2024).

[33] V. Pillac, M. Gendreau, C. Guéret, and A. L. Medaglia. “A review of dynamic vehicle routing problems”. In: *European Journal of Operational Research* 225.1 (Feb. 2013), pp. 1–11. ISSN: 0377-2217. DOI: 10.1016/j.ejor.2012.08.015. URL: https://www.sciencedirect.com/science/article/pii/S0377221712006388 (visited on 09/21/2023).

[34] S. Lorini, J.-Y. Potvin, and N. Zufferey. “Online vehicle routing and scheduling with dynamic travel times”. In: *Computers & Operations Research* 38.7 (July 2011), pp. 1086–1090. ISSN: 0305-0548. DOI: 10.1016/j.cor.2010.10.019. URL: https://www.sciencedirect.com/science/article/pii/S0305054810002480 (visited on 09/21/2023).

[35] D. Taş, N. Dellaert, T. van Woensel, and T. de Kok. “The time-dependent vehicle routing problem with soft time windows and stochastic travel times”. en. In: *Transportation Research Part C: Emerging Technologies* 48 (Nov. 2014), pp. 66–83. ISSN: 0968090X. DOI: 10.1016/j.trc.2014.08.007. (Visited on 01/31/2022).

[36] D. Bertsimas and M. Sim. “The Price of Robustness”. en. In: *Operations Research* (Feb. 2004). Publisher: INFORMS. DOI: 10.1287/opre.1030.0065. URL: https://pubsonline.informs.org/doi/abs/10.1287/opre.1030.0065 (visited on 09/28/2023).

[37] S. Pelletier, O. Jabali, and G. Laporte. “The electric vehicle routing problem with energy consumption uncertainty”. en. In: *Transportation Research Part B: Methodological* 126 (Aug. 2019), pp. 225–255. ISSN: 0191-2615. DOI: 10.1016/j.trb.2019.06.006. URL: https://www.sciencedirect.com/science/article/pii/S0191261519300153 (visited on 02/02/2023).

[38] L. Zhang, Z. Liu, L. Yu, K. Fang, B. Yao, and B. Yu. “Routing optimization of shared autonomous electric vehicles under uncertain travel time and uncertain service time”. In: *Transportation Research Part E: Logistics and Transportation Review* 157 (Jan. 2022), p. 102548. ISSN: 1366-5545. DOI: 10.1016/j.tre.2021.102548. URL: https://www.sciencedirect.com/science/article/pii/S1366554521003069 (visited on 09/27/2023).

[39] M. Keskin and B. Çatay. “A matheuristic method for the electric vehicle routing problem with time windows and fast chargers”. en. In: *Computers & Operations Research* 100 (Dec. 2018), pp. 172–188. ISSN: 0305-0548. DOI: 10.1016/j.cor.2018.06.019. URL: https://www.sciencedirect.com/science/article/pii/S0305054818301849 (visited on 02/02/2023).

[40] E. Messaoud. “A chance constrained programming model and an improved large neighborhood search algorithm for the electric vehicle routing problem with stochastic travel times”. en. In: *Evolutionary Intelligence* 16.1 (Feb. 2023), pp. 153–168. ISSN: 1864-5917. DOI: 10.1007/s12065-021-00648-0. URL: https://doi.org/10.1007/s12065-021-00648-0 (visited on 09/27/2023).

[41] A. Charnes and W. W. Cooper. “Chance-Constrained Programming”. In: *Management Science* 6.1 (Oct. 1959). Publisher: INFORMS, pp. 73–79. ISSN: 0025-1909. DOI: 10.1287/mnsc.6.1.73. URL: https://pubsonline.informs.org/doi/abs/10.1287/mnsc.6.1.73 (visited on 10/26/2023).

[42] M. Zoutendijk, S. van Oosterom, and M. Mitici. “Electric Taxiing with Disruption Management: Assignment of Electric Towing Vehicles to Aircraft”. In: San Diego: AIAA, June 2023.

[43] M. Mitici, M. Pereira, and F. Oliviero. “Electric flight scheduling with battery-charging and battery-swapping opportunities”. en. In: *EURO Journal on Transportation and Logistics* 11 (Jan. 2022), p. 100074. ISSN: 2192-4376. DOI: 10.1016/j.ejtl.2022.100074. (Visited on 10/25/2022).

[44] M. Zoutendijk and M. Mitici. “Fleet Scheduling for Electric Towing of Aircraft under Limited Airport Energy Capacity”. In: ().

[45] LVNL. *EHAM airport profile*. Jan. 2024. URL: https://eaip.lvnl.nl/web/2023-04-06-AIRAC/html/eAIP/EH-AD-2.EHAM-en-GB.html (visited on 01/11/2024).

[46] N. E. Daidzic. “Determination of taxiing resistances for transport category airplane tractive propulsion”. eng. In: *Advances in aircraft and spacecraft science* 4.6 (2017). Publisher: Techno-Press, pp. 651–677. ISSN: 2287-528X. DOI: 10.12989/aas.2017.4.6.651. URL: http://koreascience.or.kr/article/JAKO201732060819214.page (visited on 05/02/2023).

[47] N. M. Dzikus, R. Wollenheit, M. Schaefer, and V. Gollnick. “The Benefit of Innovative Taxi Concepts: The Impact of Airport Size, Fleet Mix and Traffic Growth”. en. In: *2013 Aviation Technology, Integration, and Operations Conference*. Los Angeles, CA: American Institute of Aeronautics and Astronautics, Aug. 2013. ISBN: 978-1-62410-225-7. DOI: 10.2514/6.2013-4212. (Visited on 11/01/2021).

[48] F. Dieke-Meier and H. Fricke. “Expectations from a steering control transfer to cockpit crews for aircraft pushback”. In: *Proceedings of the 2nd International Conference on Application and Theory of Automation in Command and Control Systems*. ATACCS ’12. Toulouse, FRA: IRIT Press, May 2012, pp. 62–70. ISBN: 978-2-917490-20-4. (Visited on 05/02/2023).

[49] Schiphol Health, Safety and Environment office. *Schiphol Regulations*. Tech. rep. Amsterdam, 2020. URL: https://www.schiphol.nl/en/download/1640595066/43q9kGoE92CccmEeC6awa4.pdf (visited on 05/02/2023).

[50] International Air Transport Association. *Jet Fuel Price Monitor*. en. URL: https://www.iata.org/en/publications/economics/fuel-monitor/ (visited on 12/21/2023).

[51] I. Tiseo. *Daily European Union Emission Trading System (EU-ETS) carbon pricing from 2022 to 2023*. en. URL: https://www.statista.com/statistics/1322214/carbon-prices-european-union-emission-trading-scheme/ (visited on 12/21/2023).

[52] ICAO. *ICAO Aircraft Engine Emissions Databank*. Tech. rep. July 2023. URL: https://www.easa.europa.eu/en/domains/environment/icao-aircraft-engine-emissions-databank.

[53] Statistics Netherlands. *Average energy prices for consumers*. en-GB. webpagina. Last Modified: 2023-12-12T06:30:00+01:00. Dec. 2023. URL: https://www.cbs.nl/en-gb/figures/detail/85592ENG?q=electricity%20price (visited on 12/21/2023).

[54] A. Cook and T. Graham. *European airline delay cost reference values*. en. Tech. rep. Eurocontrol, Dec. 2015. URL: https://www.eurocontrol.int/publication/european-airline-delay-cost-reference-values (visited on 05/18/2023).

[55] Schiphol. *Developer Center*. Dec. 2023. URL: https://www.schiphol.nl/en/developer-center/ (visited on 12/01/2023).

CHAPTER 5

Electric aircraft operations: scheduling and sizing the recharging infrastructure

In the previous chapters, we addressed how a full-electric fleet can be managed, now we focus on the required charging infrastructure. The energy transition is expected to result in a major increase in electricity demand. With limited energy production and transportation capacity available, using this infrastructure as efficient as possible is key.

In this chapter, therefore, we develop a model to size the required recharging infrastructure at an airport. We assume that the aircraft use swappable batteries. The charging infrastructure should be sufficient to service a fleet of electric aircraft, as not to cause disruptions to the flight schedule. It should also not be overly large, as this comes with extra investment costs. The model is formulated as a stochastic recourse model, where the amount of traffic during a day is uncertain. This model contains a subroutine which manages tactical scheduling of the charging infrastructure.

The model is applied to Norwegian Widerøe Airlines, with a network of 7 hub airports and 36 regional airports in Norway. We quantify the benefits of using our recourse model to optimize infrastructure, instead of optimizing for just one congested day (7% cost reduction) or one average day of operations (31% reduction).

Parts of this chapter have been published as:

S. van Oosterom and M. Mitici. "Optimizing the battery charging and swapping infrastructure for electric short-haul aircraft—The case of electric flight in Norway". English. In: *Transportation Research Part C: Emerging Technologies* 155 (2023). ISSN: 0968-090X. DOI: 10.1016/j.trc.2023.104313.

5.1 Introduction

To limit anthropogenic emissions, the aviation industry targets climate-neutrality by 2050 [2]. Opposed to the automotive sector, where electric vehicles are now fully rolled out across the globe by major manufacturers and hold a 10% share of total sales worldwide [3] with up to 80% in Norway [4], the low energy density of batteries has prevented a similar transition in the aviation sector. Emission reductions in aviation have for now been focused on e.g. improving operations by electric taxiing [5, 6] or electric urban air mobility [7, 8]. Nevertheless, battery technologies have greatly developed over the last ten years: gravimetric energy density has almost tripled [9], volumetric energy density has increased eightfold [10] and prices per kWh have decreased tenfold [11]. As such, battery technology is now at the level where it can be used for small electric aircraft [12–14].

Electric aircraft (e-AC) are becoming an alternative for high frequency commuter airlines operating short-haul flights in remote areas with low passenger volumes [15]. By using electric motors, which use less expensive energy and require less maintenance, these aircraft are cleaner and cheaper to operate than their kerosene-fueled equivalents. This would improve access to remote regions such as archipelagos, deltas and fjords, where the geography and low population density cannot justify an extensive road/train network.

From an operational point of view, however, replacing conventional aircraft with e-AC poses challenges. Batteries have to be recharged quickly in order to maintain short turnaround times. However, charging only during the turnaround of an aircraft results in a capricious energy demand with high peaks. To sustain this, an overly large and expensive charging infrastructure may be needed [16].

A way to circumvent these operational problems is to consider swapping batteries between flights. For this, we aim to determine the charging infrastructure (how many spare batteries are needed) and the charging schedule for these batteries. The objective of this chapter is to determine an optimal charging infrastructure while accounting for the variability of the operations over a large period of time. This is achieved by means of a recourse model that optimizes the infrastructure which considers an entire year of operations. This is in contrast to existing studies, which limit their optimization models to a single day of operations, such as a peak or average day of operations.

The recourse model has a hierarchical structure. It consists of one mixed-integer linear program as master problem and a second mixed-integer linear program as subroutine. The master problem determines an optimal total charging power and number of spare batteries at each airport (sizing the charging infrastructure). The objective is to minimize the infrastructure acquisition cost and the operational cost (cost of electricity and potential flight delays). To capture the seasonality of the air traffic, flight schedules from an entire year of operations are considered. In the subroutine, a schedule for battery swapping and charging is determined for one day of operations, given a charging infrastructure. We apply our model for Norwegian carrier Widerøe Airlines and its network of regional and hub airports . Widerøe, Scandinavia's largest regional airline, aims to introduce a fully electric aircraft to the

market by 2026 [13]. We consider an e-AC with the specifications of the already existing Eviation Alice aircraft. The results show that a total charging power of 4400 kW and 23 spare batteries are required, leading to a daily cost of €11600. We also quantify the benefit of optimizing the infrastructure over an entire year of operations, instead of optimizing for only a peak traffic day or a median traffic day.

The main contributions of this chapter are:

- We propose a recourse model that determines an optimal battery charging infrastructure for a network of airports, assuming a battery swap system. This recourse model is necessary to account for the variability of the flight schedule throughout the year when optimizing the charging infrastructure. This is in contrast to existing studies, which optimize the infrastructure considering a single (representative or peak) day of operations.
- Our proposed model minimizes the sum of the infrastructure acquisition costs (charging capacity and spare batteries), and the operational costs (electricity costs and flight delays due to battery charging).
- We illustrate our model for a network of 7 hub and 36 regional airports in Norway, using an existing flight schedule from a year of operations. We also consider an already existing configuration of an electric aircraft (Eviation Alice) designed for short-range flights.

The remainder of the chapter is structured as follows. In Section 5.2, we discuss literature on scheduling operations at- and sizing of- battery swapping stations, as well as e-AC charging infrastructure. In Section 5.3, we describe the problem of e-AC charging infrastructure management. In Section 5.4, the recourse model for e-AC charging infrastructure management is introduced. In Section 5.5, we illustrate the performance and results of our model in a case study for a regional carrier operating electric aircraft in Norway. In Section 5.6 we quantify the advantage gained by our recourse model which accounts for an entire year of operations, versus an optimization model which considers only a single day (peak-traffic or median-traffic day). Concluding remarks and future research directions are given in Section 5.7.

5.2 Prior work on battery swap systems

The concept of battery swaps systems (BSSs) as an alternative to plug-in charging has been proposed as a means of reducing recharge times, to protect the electricity grid against high and unpredictable demand, and to limit battery degradation [17, 18]. BSSs have mainly been studied in the context of electric cars, electrified public transport busses and delivery drones (see e.g. Schneider et al. [19], Ayad et al. [20], and Kwizera and Nurre [21]). Two research themes regarding BSSs are relevant for this study: the sizing of the BSS infrastructure, and the scheduling of charging of the batteries.

In the past years, several studies have addressed the operations' scheduling of BSSs, which considers determining when to recharge the batteries at the BSS to

ensure a sufficient stock. Worley and Klabjan [22] propose a model to optimize the charging schedule at a BSS for day-ahead planning, while considering a fixed and predetermined demand for full batteries. They formulate the problem as a mixed-integer linear program with the objective of maximizing the revenue by supplying full batteries to customers while minimizing the electricity costs. This model is expended by Nurre et al. [23], who add Vehicle-to-grid (V2G) charging as a possibility for increasing BSS revenue, and by Park et al. [24], who study the minimization of waiting time for charged batteries. All of these studies, however, assumed a known demand for batteries before optimization. Sarker et al. [17] were the first to recognize the uncertainty in the demand of a BSS, proposing a robust optimization approach to ensure a sufficient supply of fully charged batteries. However, this study was limited to using fixed charging times, as opposed to a state-of-charge dependent one. Additional studies have focused on minimizing battery degradation [21, 25, 26]. In this chapter, we assume that the flight schedule is known and consider deterministic planning like Worley and Klabjan [22] and Park et al. [24]. We expand upon the previous work done by considering partial charging, and our objective also considers the minimization of the waiting time for a full battery, apart from the electricity costs.

Inextricably linked with the optimization of the battery recharge schedule is the problem of recharge infrastructure sizing: determining how many batteries can be charged simultaneously and how many spare batteries to keep in stock at the station. Worley et al. [22] combine a day-ahead scheduling of a BSS with determining the required spare battery inventory. However, batteries cannot always be acquired a single day ahead, and are hence not a flexible asset. As such, there is a trade-off between making long-term investments in infrastructure (spare batteries and chargers), and short-term operational expenses related to the charging schedule (electricity costs, battery degradation, etc.). This is the reason why the two problems are not solved simultaneously in more recent studies. This two-phase approach to the problem was first proposed by Schneider et al. [19], who minimize the sum of the investment costs for batteries and chargers and the costs of operating the BSS (customers served against electricity cost). Customer arrival times are assumed to be exponentially distributed. Using a Monte-Carlo Dynamic Programming approach, a near-optimal policy for charge scheduling was developed. Sun et al. [27] consider a similar problem, but add a minimum level-of-service for the customers, while only considering fixed charging times. Later, Sun et al. [28] expand the problem to a three-phase approach where the number of required chargers and batteries is determines in two phases. Other studies focus on combining the sizing of BSSs with finding an optimal location (see Mak et al. [29] or Liu et al. [30]) or simultaneously routing the vehicles which use the BSS (see Ayad et al. [20]). For an extensive literature overview of optimization models for BSSs, we refer to Zhan et al. [31]. In this study, we consider a two-phase approach (sizing the charging capacity and spare batteries in the first phase, scheduling the recharging operations in the second), similar to Schneider et al. and Sun et al. [19, 27]. We extend these approaches in by considering a state-of-charge dependent time of charge for the batteries. We also allow for preemptive battery charging during the second phase.

There are a number of studies where optimization of battery charging operations is performed in the context of electric aircraft (e-AC). Justin et al. [32] consider the minimization of the required investment costs of the infrastructure (chargers and spare batteries) in order to support a BSS for small e-AC. In their analysis, flight schedules and battery recharge times are assumed to be known beforehand. They apply their models for Mukuele Airlines (Hawaii) and Cape Air (New England). Salucci et al. [33] perform a similar study, considering variable electricity prices throughout the day, but assume identical flight duration and battery recharge times (similar to Nurre et al. [23]). This work was further expanded by Trainelli et al. [34], who also considers the procurement and routing of a fleet of e-AC from a hub airport. They minimize the sum of the acquisition costs of the electric aircraft, charging points and spare batteries, and the electricity costs. A similar problem is studied by Mitici et al. [35], where a fixed electricity price is assumed. A hierarchical cost function is assumed to solve the problem more efficiently (first for aircraft fleet sizing and routing, then for charging infrastructure sizing and scheduling). Guo et al. [36] also consider the availability of electricity based on renewable energy sources. Finally, the sizing of aircraft charging infrastructure at the gates/apron has been studied by Doctor et al. [37].

None of these studies have separated the infrastructure sizing (number of aircraft, chargers, spare batteries) from the scheduling of operations. As such, these solutions are optimized for one day of operations, instead of for the (predicted) traffic throughout the entire year. A two-phase approach, such as in [19] or [27], which takes demand seasonality into account has been shown to outperform such a single-phase approach. We introduce a tactical-phase battery recharge scheduling model, an extension of the work of Justin et al. [32], But opposed to the previous literature on charging infrastructure for electric aircraft, we assume that the infrastructure size is predetermined and cannot be optimized simultaneously. For this, we introduce an infrastructure sizing model which accounts for demand variation throughout the year. This inclusion is the main contribution of our chapter.

5.3 Infrastructure sizing and scheduling for aircraft battery swap systems

Electric aircraft operations with battery swapping

We consider an airline operating a fleet of short-haul electric aircraft, each equipped with one battery. Let R and H denote the set of regional and hub airports, respectively, where these electric aircraft fly between. Aircraft can recharge their batteries at all airports during turnaround, but this is too short to fully recharge it. In order to quickly replenish the battery, the aircraft can swap it for a fully charged one during turnaround. We assume that only the hub airports have the infrastructure needed to swap the batteries of the electric aircraft. We also assume that a battery is swapped with a new, fully-charged battery every time an aircraft visits a hub airport.

Figure 5.1 shows an example of operations of one electric aircraft. At the start of the day, the aircraft flies from hub H1 to H2 via regional airports R1 and R2. At R2, the battery is partially recharged. This aircraft swaps its battery at H2. From H2, the aircraft flies to H3, where it swaps its battery again.

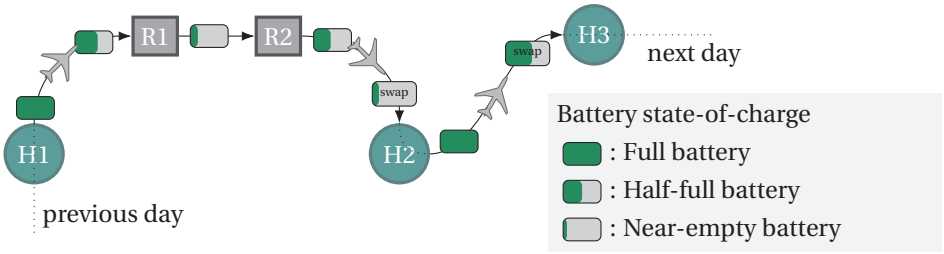

Figure 5.1.: Example of a day of operations for an electric aircraft.

5

Electric aircraft flight schedules

Let D denote a set of days of an entire year during which the airline operates. A flight schedule for day $d \in D$ consists of a list of arrival and departure times for an entire day of operations. Let T_d denote the time interval during one day when the aircraft fly to and from a set of airports (hubs and regional airports). Let F^{dh}_{arr} and F^{dh}_{dep} denote the set of flights operated by electric aircraft that arrive and depart at hub airport $h \in H$ on day $d \in D$, respectively. Let $\tau^{arr}_f \in T_d$ denote the arrival time of flight $f \in F^{dh}_{arr}$ and let $\tau^{dep}_f \in T_d$ denote the departure time of flight $f \in F^{dh}_{dep}$.

Battery swaps

We assume that each hub airport is equipped with one charging station. Upon arrival at a hub airport, the used battery of an electric aircraft is swapped with a new fully charged battery. Let B^{dh}_{arr} denote the set of batteries which arrive with flights F^{dh}_{arr}. For each flight $f \in F^{dh}_{arr}$, let $b_f \in B^{dh}_{arr}$ be the battery with which it arrives. Let τ^{tr} denote the time it takes to bring the used battery to the charging station. The same amount of time τ^{tr} is assumed to be required to bring a fully charged battery from the charging station to an aircraft. Thus $\tau^{s}_{b_f} = \tau^{arr}_f + \tau^{tr}$ is the time the battery $b_f \in B^{dh}_{arr}$ used for flight $f \in F^{dh}_{arr}$ arrives at the charging station. At the charging station, each battery charges at a constant rate P^c until it is fully charged. Let τ^c_b denote the required charging time of battery $b \in B^{dh}_{arr}$. Finally, in order to depart on time, a new battery for flight $f \in F^{dh}_{dep}$ needs to depart from the charging station to the gate at the latest time $\tau^e_f = \tau^{dep}_f - \tau^{tr}$.

Battery charging station

Let P_h denote the charging capacity at hub airport h, i.e., the total power with which batteries can be charged simultaneously at the airport. Let $P_h c^p \in \mathbb{R}_+$ denote the daily cost to provide this charging power at hub airport h. Let $n_h^s \in \mathbb{N}$ denote the number of spare batteries available at a hub airport h. Let $c^s \in \mathbb{R}_+$ be the daily cost of having one spare battery at a hub airport.

We assume that batteries can be charged preemptively. We also assume that the price of electricity varies throughout the day and is given by a function $c^e : T_d \to \mathbb{R}_+$ of time.

Figure 5.2 shows an example of a hub airport and its charging infrastructure, i.e., with charging power $P_h = 4P^c$ and $n_h^s = 12$ batteries available at this airport for swap, out of which 3 batteries are charging and 13 batteries are idle in the inventory, from which there are 4 which have to depart with an aircraft currently parked at the airport. Each aircraft needs to depart from the airport with a fully charged battery.

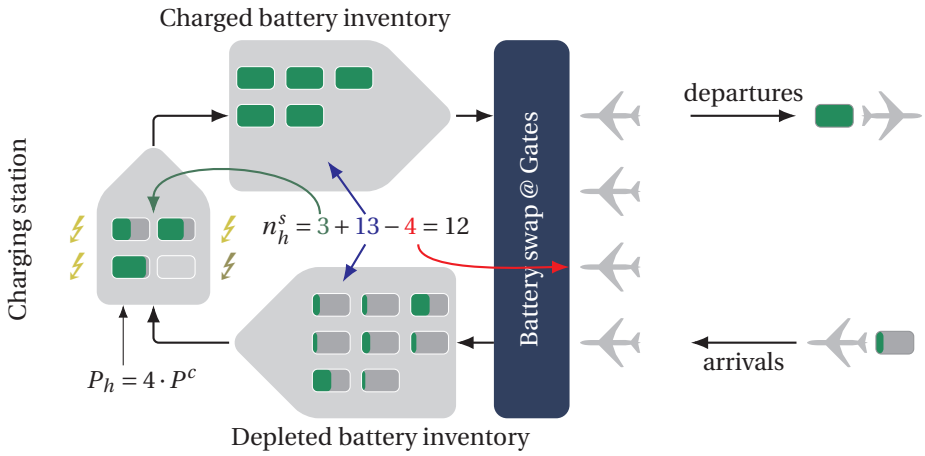

Figure 5.2.: Overview of the battery swapping and recharging process at an airport. The battery charging capacity at the airport is $P_h = 4P^c$ (at most four batteries can be charged at max power), and there at 12 spare batteries (three currently being charged, 13 waiting at the depot, minus four which should depart on the four parked aircraft).

5.3.1 Battery charging station sizing

Given a hub airport $h \in H$ and set of flight schedules during days D, the main objective of our study is to determine a suitable battery charging infrastructure size (P_h, n_h^s). This problem is solved once for each hub airport before the start of D, to allow time for charging station construction. The infrastructure is optimized to minimize the sum of the capital expenditures $(P_h c^p + n_h^s c^s)$ and average charging

schedule operating costs over D are as low as possible. The value of the latter for each $d \in D$ is given by the battery recharge schedule optimization (Subsection 5.3.2), which is used as a subroutine.

5.3.2 Swapped aircraft batteries recharge scheduling

Given a certain charging infrastructure size (charging capacity P_h and number of spare batteries n_h^s) and a flight schedule during day $d \in D$ at a hub $h \in H$, we aim to determine a charging schedule for batteries such that the charging schedule operating cost (electricity cost and flight delay cost) is minimized. For this, we need to determine which battery departs with which aircraft, and when to charge these batteries during the day. In the case that the infrastructure is not sufficiently large to ensure that flights depart on time, a penalty cost is incurred. This is a convex piecewise linear function of time, with breakpoints at T^{del}. Each time the flight delay is larger then some $\tau \in T^{del}$, a cost $c^{del}(\tau) \geq 0$ is incurred per unit of delay time. We assume that these delays are small and thus are assumed to be absorbed on route.

An overview of the model, with the interaction between the Battery charging station sizing problem and the Swapped aircraft batteries recharge scheduling problem, can be seen in Figure 5.3. The latter is used as a subroutine in order to evaluate the charging schedule operation cost for a given infrastructure size on a single day.

5.4 A recourse model infrastructure sizing and scheduling of swapped aircraft batteries

We propose a novel recourse model which manages the swapping and charging process for an airline operating a fleet of electric aircraft. This model is able to minimize the infrastructure and charging costs not just for a single day, but for an entire year of operations. consisting of the battery charging station sizing problem (long-term planning phase) and the swapped aircraft batteries recharge scheduling problem (medium-term planning phase). First, we propose a MILP which manages the charging schedule of the aircraft batteries, given a known flight schedule and charging infrastructure. This problem can be solved once a flight schedule is made known, weeks before the day of operations. Second, we propose a master-problem to determine the most cost-effective charging infrastructure over an entire year of operations. This uses the swapped aircraft batteries recharge scheduling model as a subroutine. This problem is solved years in advance of the day of operations.

An overview of all used notation can be found in Table 5.1.

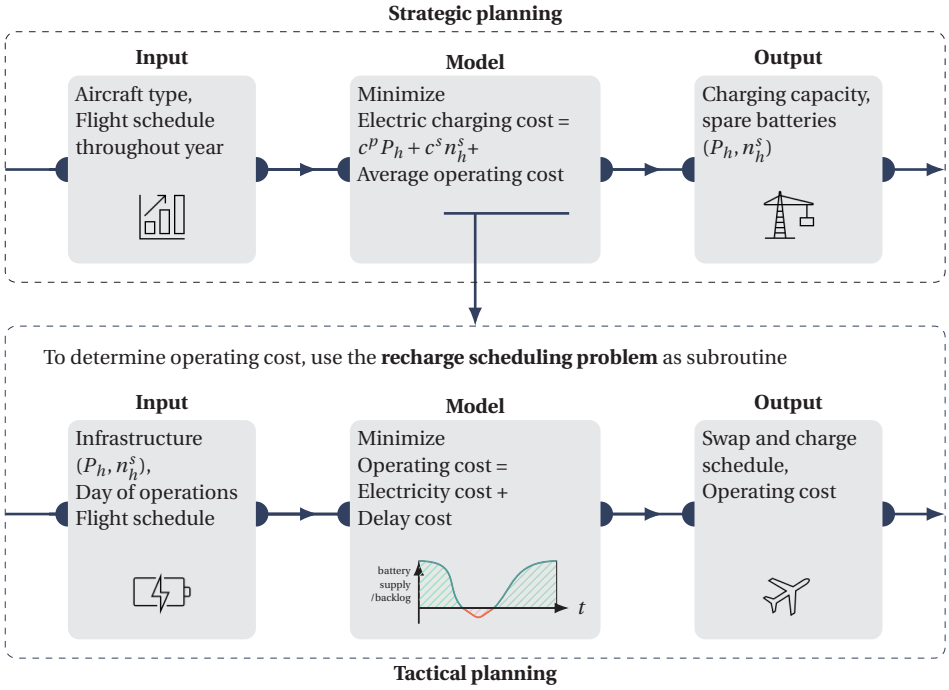

Figure 5.3.: Recourse model for sizing the charging infrastructure and recharge scheduling for e-AC battery swaps. Sizing the charging infrastructure is a strategic planning problem, whereas creating a recharge schedule is a tactical planning problem.

5.4.1 Tactical planning: Swapped aircraft batteries recharge scheduling problem

We first propose the swapped aircraft batteries recharging model, which considers a single day $d \in D$ and hub $h \in H$. The algorithm decides when each battery which arrives at the airport is charged, and to which outbound flight it is assigned. If, because of charging infrastructure limitations, batteries cannot be charged on time, outbound flights must wait until a fully charged battery is available. This formulation minimizes the sum of the cost for electricity used to charge the batteries and the cost of flight delays.

Let us first introduce the following notation for a hub $h \in H$. First, we discretize the day T_d in a set of intervals with length Δt. Let $T_d^{min} = \min(T_d)$ and $T_d^{max} = \max(T_d)$, the start and end of the day, respectively. As such we obtain $T_d^* = \{T_d^{min}, T_d^{min} + \Delta t, T_d^{min} + 2\Delta t, ..., T_d^{max}\}$. Second, we define the cumulative demand for charged batteries at time $t \in T_d^*$ as: $D_t^{dh} = |\{f \in F_{dep}^{dh} : \tau_f^e \leq t\}|$. This gives the total number of batteries which should have been charged by t in order to allow the flights to be performed on schedule. Third, a battery can only be charged once

Sets	
D	Days
H	Hub airports
R	Regional airports
F^{dh}_{arr}	Flights on day d arriving at hub h
F^{dh}_{dep}	Flights on day d departing from hub h
B^{dh}_{arr}	Batteries arriving with flights F^{dh}_{arr}
T_d	Time interval of day of operations d
T^*_d	Discretization of T_d
B^{dh}_t	Batteries from B^{dh}_{arr} arrived by t
Input Parameters	
τ^{arr}_a	Arrival time of flight f
τ^{dep}_a	Departure time of flight f
τ^{tr}	Transport time of batteries from aircraft to swapping stations
τ^s_b	Time battery $b \in B^{dh}_{arr}$ can start charging
τ^c_b	Recharge time of battery b
τ^e_f	Last time to charge a battery for departing flight f
P^c	Maximum battery charge rate
c^p	Charging capacity cost
c^s	Spare battery cost
c^e	Electricity cost
$c^{del}(\tau)$	Cost for flight delays greater than τ per unit of time
Δt	Discretization size of T^*_d
D^d_t	Cumulative demand for charged batteries by $t \in T^*_d$
n^o	Number of overnight stay batteries
Model variables	
$\tau^c_{bt} \in \mathbb{R}_+$	Charging time of battery b during $[t, t+\Delta t]$
$r_{bt} \in \{0,1\}$	Indicator: battery b fully charged by t
$S_t \in \mathbb{N}$	Cumulative supply of charged batteries by t
$P_h \in \mathbb{R}_+$	Charging capacity at hub h
$n^s_h \in \mathbb{N}$	Number of spare batteries at hub h
$\mathscr{C}_{dh} \in \mathbb{R}_+$	Cost of charging operations for day d at hub h
$\mathscr{C}_h \in \mathbb{R}_+$	Charging infrastructure cost at hub h

Table 5.1.: Overview of used nomenclature

it has arrived at the charging station, and for each time $t \in T^*_d$, the set of these batteries is given by $B^{dh}_t = \{b \in B^{dh}_{arr} : t \leq t^s_b\}$.

At the start of T_d, a number of aircraft may already be present at the airport, which stayed there overnight. The batteries with which these arrived are assumed to have been fully recharged by the start of T_d. Let n^o denote the number of these batteries.

Decision variables

We consider the decision variable τ^c_{bt}, which gives the amount of time the battery b is charged during the interval $[t, t+\Delta t]$, with $t \in T^*_d$ and $b \in B^{dh}_t$. Additionally, we use the binary variables r_{bt}, which indicate if a battery has been fully charged by $t \in T^*_d$, with $b \in B^{dh}_t$. Finally, the integer variable S_t gives the cumulative amount of fully charged batteries by $t \in T^*_d$.

Mixed-Integer Linear Problem Formulation

We consider the following MILP to manage the recharging schedule at hub h, given a charging infrastructure (P_h, n^s_h) and a flight schedule on day d, which minimizes the operational costs $\mathscr{C}_{dh}(P_h, n^s_h)$:

$$\mathscr{C}_{dh}(P_h, n_h^s) = \min_{p,r,S} \quad \sum_{t \in T_d^*} \left[\sum_{\tau \in T^{del}} \left(c^{del}(\tau) \max\{D_{t-\tau}^{fh} - S_t, 0\} \right) + c_t^e \sum_{b \in B_t^{dh}} \tau_{bt}^c P^c \right] \tag{5.1a}$$

$$\text{s.t.} \quad \sum_{t \in T_d^*} \tau_{bt}^c = \tau_b^c \qquad \forall b \in B_{arr}^{dh} \tag{5.1b}$$

$$\tau_{bt}^c \leq \Delta t \qquad \forall t \in T_d^*, b \in B_t^{dh} \tag{5.1c}$$

$$\sum_{b \in B_t^{dh}} \tau_{bt}^c P^c \leq \Delta t P_h \qquad \forall t \in T_d^* \tag{5.1d}$$

$$1 - r_{bt} \geq |T_d|^{-1} \left[\tau_b^c - \sum_{t' \leq t} \tau_{bt'}^c \right] \qquad \forall t \in T_d^*, b \in B_t^{dh} \tag{5.1e}$$

$$\sum_{b \in B_t^{dh}} r_{bt} + n_h^s + n^o = S_t \qquad \forall t \in T_d^* \tag{5.1f}$$

$$\tau_{bt}^c \geq 0, r_{bt} \in \{0,1\} \qquad \forall t \in T_d^*, b \in B_t^{dh} \tag{5.1g}$$

The operational costs (Equation (5.1a)) are given by the sum of the electricity costs, $c_t^e \sum_{b \in B_t^{dh}} \tau_{bt}^c P^c$, and the aircraft delays incurred, $\sum_{\tau \in T^{del}} \left(c^{del}(\tau) \max\{D_{t-\tau}^{fh} - S_t, 0\} \right)$, for each interval $[t, t + \Delta t]$ with $t \in T_d^*$. Constraints (5.1b) ensure that all batteries which arrive at the airport are charged by the end of the day, ensuring a supply of spare batteries on the next day. Constraints (5.1c) ensure that during each interval, batteries are not charged longer than the length of the interval, whereas Constraints (5.1d) ensure that the total charging capacity is not exceeded. Whether or not a battery is ready to be used on an outbound flight by t is determined in Constraints (5.1e), which force r_{bt} to be 0 as long as battery b is not fully charged. Finally, Constraints (5.1f) determine the cumulative supply of spare batteries.

5.4.2 Strategic planning: Battery charging station sizing problem

Second, we propose a recourse model which optimizes the charging infrastructure size, given the flight schedules which reflect the traffic demand variation during an entire year of operations D. This functions as the master problem of the recourse model, and is solved only once for the entire year. It determines the expected operational cost of a charging infrastructure by using the optimization model from Subsection 5.4.1 as a subroutine. These operational costs are added to the capital expenditures, i.e., the cost of acquiring and maintaining chargers and spare batteries to obtain the total costs, which we aim to minimize.

Decision variables

We consider the decision variables $P_h \in \mathbb{R}^+$ and $n_h^s \in \mathbb{N}$, the charging capacity and the number of spare batteries at hub airport h, respectively.

Recourse model formulation

We consider the following MILP to determine the suitable charging infrastructure size at a hub, given the distribution of flight schedules D, which minimizes the total cost $\mathscr{C}_h$:

$$\mathscr{C}_h = \min_{P_h, n_h^s} \quad c^p P_h + c^s n_h^s + \sum_{d \in D} \mathscr{C}_{dh}(P_h, n_h^s)/|D| \tag{5.2a}$$

$$P_h \geq 0 \tag{5.2b}$$

$$n_h^s \in \mathbb{N} \tag{5.2c}$$

In this formulation, $\mathscr{C}_h$ is the sum of the daily cost of the charging capacity, $c^p P_h$, the spare batteries $c^s n_h^s$, and the average operational costs $\sum_{d \in D} \mathscr{C}_{dh}(P_h, n_h^s)/|D|$, which is obtained from the tactical planning problem of Section 5.4.1 for each day $d \in D$.

Simulated Annealing Algorithm

The value of $\sum_{d \in D} \mathscr{C}_{dh}(P_h, n_h^s)$ cannot be evaluated trivially, hence regular MILP solution algorithms are unsuitable to solve this problem. As $\sum_{d \in D} \mathscr{C}_{dh}(P_h, n_h^s)$ is also non-convex in P_h and n_h^s, we use Simulated Annealing to find an approximate solution. The approach we use to optimize the airport charging infrastructure is given in Algorithm 5.

The algorithm first obtains an initial solution (lines 2 - 9). The expected operating costs for each solution are determined. After the initial solution is found, the algorithm iterates towards better solutions by selecting a solution in the neighbourhood of the current solution (line 11), evaluating the expected operating costs only for the current solution (line 12). The new solution is accepted if it is an improvement over the current one (line 14), or with a probability less than one if it is not (line 16, to avoid being stuck in local optima). This process continues until a stopping criterion is met.

5.5 Case study: optimizing the charging infrastructure for Widerøe Airlines (Norway)

In this section, we apply the model presented in Section 5.4 to the short-haul flight network of Norwegian Widerøe Airlines, using flight schedule based on the performed flights during October 2021 - October 2022.

We use the case of Widerøe Airlines because Norway has a strong position for early implementations of electric aircraft on commercial flights. Due to the challenging

Algorithm 5: Simulated Annealing algorithm to optimize airport battery charging infrastructure

Data: Hub h, Days with flights D, c^p, c^s, c^e, c^{del}, $(n^s_{min}, \Delta n^s, n^s_{max})$, $(P_{min}, \Delta P, P_{max})$, Λ_s, Λ_e, α
Result: Minimum cost charging capacity $\hat{P}$ and number of spare batteries $\hat{n^s}$

Initialize $\hat{P} = 0$, $\hat{n}^s = 0$, $\hat{\mathscr{C}} = \infty$ and $\Lambda = \Lambda_s$;
Let $n^{s*} = \{n^s_{min}, n^s_{min} + \Delta n^s, ..., n^s_{max}\}$;
Let $P^* = \{P_{min}, P_{min} + \Delta P, ..., P_{max}\}$;
for $(n^s, P) \in n^{s*} \times P^*$ **do**
    Determine $\mathscr{C}_h(P, n^s) = c^p P + c^s n^s + \sum_{d \in D} \mathscr{C}_{dh}(P, n^s)/|D|$;
    if $\mathscr{C}_h(P, n^s) \leq \hat{\mathscr{C}}_h$ **then**
        Set $\hat{P} \leftarrow P$, $\hat{n}^s \leftarrow n^s$ and $\hat{\mathscr{C}}_h \leftarrow \mathscr{C}_h(P, n^s)$;
    end
end
while $\Lambda \geq \Lambda_e$ **do**
    Select $\tilde{P} \in \hat{P} + [-\Delta P, \Delta P]$ and $\tilde{n}^s \in \hat{n}^s + [-\Delta n^s, \Delta n^s]$ randomly;
    Determine $\tilde{\mathscr{C}}_h(\tilde{P}, \tilde{n}^s) = c^p \tilde{P} + c^s \tilde{n}^s + \sum_{d \in D} \mathscr{C}_{dh}(\tilde{P}, \tilde{n}^s)/|D|$;
    if $\tilde{\mathscr{C}}_h(\tilde{P}, \tilde{n}^s) < \hat{\mathscr{C}}_h$ **then**
        Accept the new solution $(\tilde{P}, \tilde{n}^s)$;
    else
        Accept the new solution $(\tilde{P}, \tilde{n}^s)$ with probability $p = e^{-(\tilde{\mathscr{C}}_h(\tilde{P}, \tilde{n}^s) - \hat{\mathscr{C}}_h)/\Lambda}$;
    end
    if *We accept the new solution* **then**
        Set $\hat{P} \leftarrow \tilde{P}$, $\hat{n}^s \leftarrow \tilde{n}^s$, and $\hat{\mathscr{C}}_h \leftarrow \tilde{\mathscr{C}}_h(\tilde{P}, \tilde{n}^s)$;
    end
    Set $\Lambda \leftarrow \alpha \Lambda$;
end

terrain, air transport is often the only viable means of travel. This results in a market with a lot of low-passenger short-haul flights: around 77% of all domestic flights in the country are under 400 km [38]. In addition, Norway's electricity is for 98% produced with renewable resources [39] such that the electric aircraft can be operated sustainably.

The experiment was performed by implementing the algorithm with Gurobi Optimizer 9.1, on an Intel Core i7-10610U with 8 GB of RAM.

Short-haul network of Widerøe Airlines

Widerøe Airlines is the largest commuter operator in Scandinavia [38]. It operates a fleet of 23 De Havilland Canada Dash 8-100 aircraft (hereafter: Dash 8) for short-haul flights within and to Norway. These have a capacity of 40 passengers or a payload of 4500 kg. These aircraft account for the majority of Widerøe's fleet. We propose a scenario in which this fleet is replaced with electric aircraft, while keeping to the

existing flight schedule as much as possible. We have imported the flight data for the Dash 8 between 28 October 2021 and 27 October 2022, using data from Flightradar24 [40] for each aircraft of the Dash 8 fleet. We have used the actual time of departure, actual landing time, origin and departure of each flight. As such, cancelled flights have not been included in the data. The network spanned by these aircraft consists of 43 airports and 56000 flights; it is shown in Figure 5.4.

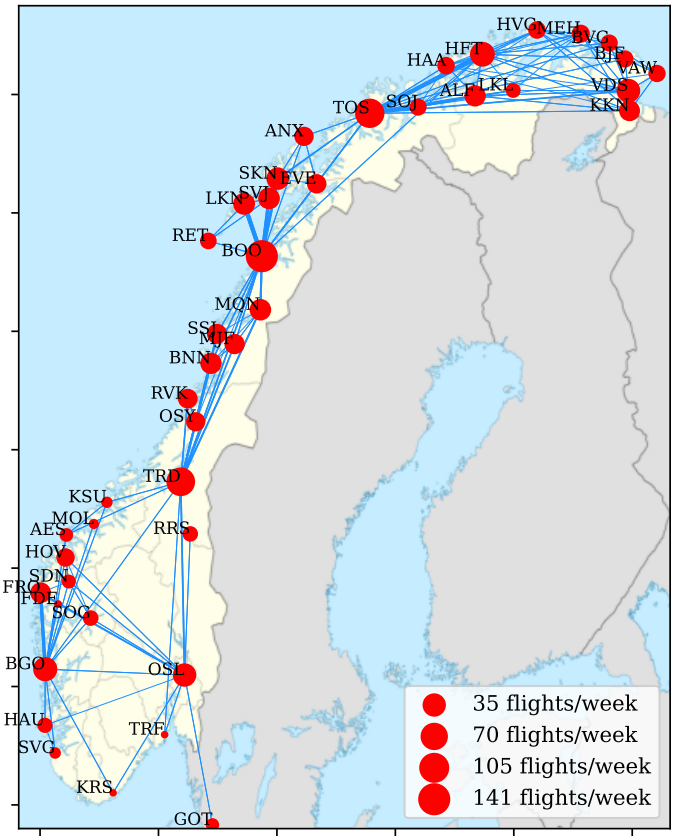

Figure 5.4.: Network of the Dash 8-100 of Widerøe airlines, flown between the 28th of October 2021 and the 27 of October 2022.

The used flight schedules in this case study are based on the analyzed historical flight data. We assume that all itineraries between hubs (possibly via regional airports) which were previously performed by the Dash 8 and are within range of the electric aircraft, are performed by the e-AC. The e-AC start each journey from a hub airport with a fully charged battery. If there are any stopovers at non-hub airports, it will recharge its battery during turnaround. This is done using the existing ground power infrastructure. Last, if there are two subsequent flights for an aircraft, from A to B and from B to C, and the first flight cannot be performed on time (due to

battery/charging limitations), then the aircraft directly flies from A to C. Flights A to B and B to C are not included in the schedule. We use these as our (365) flight schedules.

Assuming a range of 610 km (see the next subsection on the e-AC model) approximately 52000 of the 56000 flights which we have analyzed can be performed by the electric aircraft. A comparison of the number of flights visiting the 20 busiest airports can be seen in Figure 5.5. We propose to use the seven most visited airports in the network as hubs for the electric aircraft fleet, where batteries can be swapped. These airports are in the towns of Bodø (BOO, 15000 flights annually), Tromsø (TOS, 10000 flights), Trondheim (TRD, 10000 fligths), Oslo (OSL, 9000 flights), Bergen (BGO, 5000 flights), Hammerfest (HFT, 5000 flights) and Vadsø (VDS, 4000 flights). Table 5.2 shows the distribution of the number of daily flights on each of the selected hubs. Even though there is a significant variance in the number of daily flights, there is no seasonal difference for this fleet. This is because the Dash-8 100 aircraft are mainly used for commuting and to deliver cargo, and only to a lesser degree for tourism.

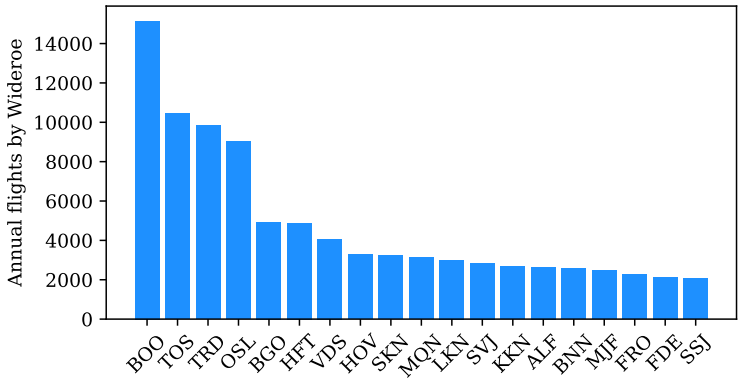

Figure 5.5.: Histogram of number of annual flights at the twenty most visited hubs of Widerøe. Flight data between October 28, 2021 and October 27, 2022 is used.

Specifications of the electric aircraft

We propose a scenario where the Dash-8 aircraft are replaced by an e-AC with the specifications of the Eviation Alice [41]. Currently in the certifying phase, the Alice is able to transport ten passengers or a payload of 1150 kg.

The Alice is currently able to fly a distance of 250 nm (approximately 480 km). Assuming a continuation of current battery development [11], this will increase to 610 km by 2025. It is equipped with a 820 kWh battery which requires slightly over 4 hours for a full recharge. We assume that the charging power available at hubs and regional airports is the same. The cruising speed of 260 kts is comparable to the 280 kts of the Dash 8-100, and as such we assume the flight duration is unchanged.

Hub airport		Daily flights			
IATA	City	average	median	std	peak
BGO	Bergen	9.4	10	4.2	22
BOO	Bodø	29.7	32	11.5	55
HFT	Hammerfest	12.8	13	6.7	27
OSL	Oslo	14.6	9	3.5	19
TOS	Tromsø	24.7	26	10.6	49
TRD	Trondheim	21.8	21	8.5	40
VDS	Vadsø	9.9	10	4.7	22
Network total		122.9	125	43.9	184

Table 5.2.: Daily flight statistics at the considered hubs of Widerøe. The average, median, standard deviation and maximum of the number of daily flights is given. Flight data between October 28, 2021 and October 27, 2022 is used.

We assume that 7% of the battery capacity is required for take-off [42]. All used characteristics of the aircraft can be found in Table 5.3. The electricity cost is derived from historical data [43], and a resolution of Δt = 15 minutes has been used.

Flight delay costs are derived from European industry data [44], which takes flight personnel, maintenance, fuel and passenger costs into account. We use the tactical costs of the ATR-43 as reference and scale them to account for the difference in size (10 passengers instead of 42) and inflation (20%). Using τ^{del} = {00:00, 00:45, 01:15}, we have found c^{del}(0:00) = €9.05, c^{del}(0:45) = €10.90, and c^{del}(1:15) = €10.95. The original data and this approximation are shown in Figure 5.6.

Because of this, the payload is about a quarter of the size of the payload of Dash 8. In this chapter we aim to maintain the original flight schedule without optimizing for the difference in the payload. This would required adding more flights to the schedule, and is addressed in Section 5.5.2.

5.5.1 Results - Optimizing the charging infrastructure for Widerøe Airlines

We apply the optimization framework from Section 5.4 to the flight network of Widerøe Airlines and the e-AC model to obtain the most cost-effective charging infrastructure at the 7 hub airports. We first discuss the results for the largest hub, Bodø, in detail. After this, we shall present the results for all hubs.

Bodø Lufthavn

Bodø Lufthavn is the most frequently visited airport in the network of Widerøe Airlines, and serves as a hub to connect the north of Norway with the south. The daily amount of traffic ranges up to 55 flights (on August 25, 2022) with a median of

Aircraft specifications		Economic assumptions	
Battery capacity	820 kWh [41]	Spare battery cost	80 €/day [32]
Range	610 km [45]	Charging capacity cost	0.4 €/kW/day [32]
Maximum power	2 × 700 kW [41]	Delay cost	9.05 - 29.90 €/min [44]
Maximum charging power	200 kW [42]	Peak electricity price	0.134 €/kWh [46]
Take-off and climbing energy	60 kWh [42]	Peak-hours	7 AM - 8 PM [43]
Battery transport time	30 min	off-peak electricity cost	0.067 €/kWh [43]
Final reserve	120 kWh [41]		

Table 5.3.: Eviation Alice performance and economic parameters.

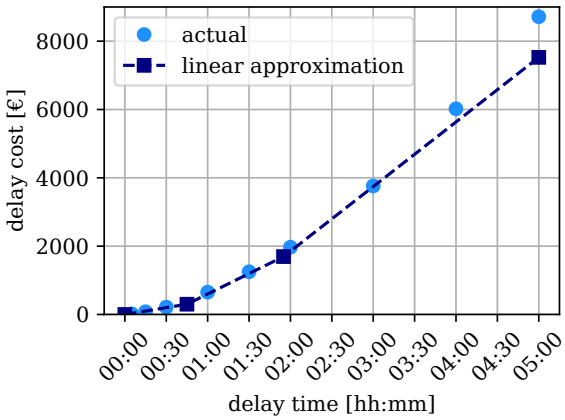

Figure 5.6.: Actual and piece-wise linear approximation of the flight delay costs. The actual costs are based on European reference values for the ATR-43 [44].

32 (on a.o. July 13, 2022) and an average of 29.7.

We have determined the most cost-effective charging infrastructure at Bodø Airport: $(P_h, n_s^h) = (900 \text{ kW}, 6)$. This requires an investment of $c^p P_h + c^s n_h^s$ =€1840 per day. Table 5.4 shows the optimal infrastructure size, operational characteristics, and costs on average over all days. In addition to the €1840 daily infrastructure investment, there are €1030 daily operational costs. These are mainly due to the electricity costs (8950 kWh consumption for €890) with average delays fairly minimal. On average over all days, the aircraft at Bodø are delayed for a total of 12 minutes, showing how much the optimal solution prefers to avoid disrupting the flight schedule.

			Size	Costs [€]
Infrastructure	Charging capacity P_h	[kW]	900	360
	Spare batteries n_h^s	[-]	6	1500
Operations	Energy consumption	[kWh]	8950	890
	Delays	[hh:mm]	00:12	140
	Total		-	2943

Table 5.4.: Infrastructure (charging capacity [P_h] and spare batteries [n_h^s]), average operational characteristics and costs (electricity and caused hours of delay) at Bodø Lufthavn.

Figure 5.7 shows the most efficient battery recharge schedule on the peak day (August 25, 2022), using the optimized infrastructure. Each bar in the figure represents a battery. The bar starts and ends when the battery arrives and departs from the charging station. The row in which a battery is placed is irrelevant: different batteries are placed on the same row in order to limit the number of rows in the figure. The color of the bar indicates the current state-of-charge. Additionally, the black arrows show the scheduled and actual departure times of the flights to which the batteries are assigned. At the start of the day, 11 batteries are available at the airport (six spare batteries and five batteries from flights which arrived on the previous day). As can be seen, batteries which are fuller when they arrive tend to be charged first, whereas the batteries which take longer to charge tend to spend more idle time at the airport. Also, three flight experience a delay, two of which are limited (15 minutes delay) and one is more severe (45 minutes). At the end of the day, 9 batteries (of which 6 are spares) remain at the airport. Given that these delays are in the order of a couple of minutes on the peak traffic day, we assume that these are absorbed en-route in the next leg.

The charging schedules on the peak traffic day (August 25, 2022) and a median traffic day (July 13, 2022) are further detailed in Figure 5.8. The spare battery stock (or backlog) is shown in the top row, and the electricity consumption and price are shown in the bottom row. On the median traffic day, there is almost always a fully charged spare battery in stock. Additionally, a large portion of the charging is done during the off-peak electricity pricing hours: only the bear minimum of charging is performed between 3 PM and 8 PM, after which it uses the full charging capacity. Contrasting this, the full charging capacity is almost constantly used on the peak day. As a result, battery backlog remains limited even though there is almost never a charged battery available during 10 AM and midnight. The longer delay from Figure 5.7 can be seen as battery backlog just before 12 PM. The fact that delays remain minimal even on the peak day shows the robustness of this infrastructure size.

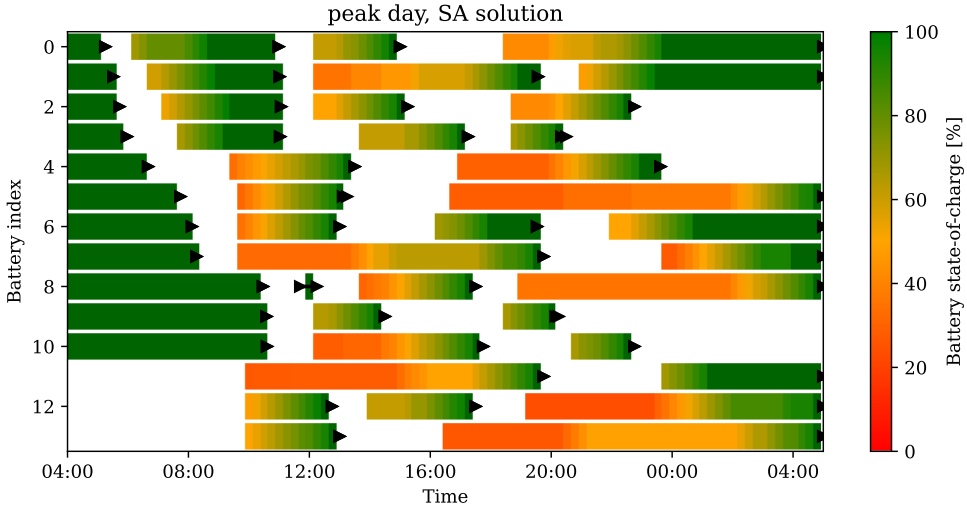

Figure 5.7.: Optimal recharging schedule of the swapped batteries at Bodø Lufthavn on the peak traffic day (August 25, 2022), using $P_h = 900$ kW and $n_h^s = 6$. Each bar represents a battery, which starts and ends when it arrives at and departs from the charging station, respectively. The color of the bar indicates the current battery state-of-charge. Each arrow shows the scheduled and actual departure time of the flights to which the batteries are assigned.

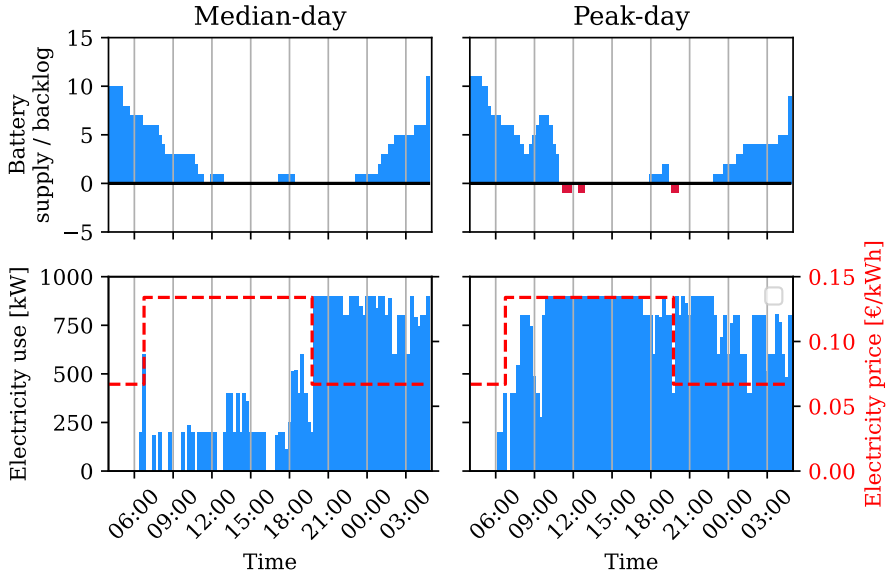

Figure 5.8.: Battery supply and backlog and electricity use and price throughout the median (July 13th, 2022) and peak (August 25th, 2022) days of operations at Bodø Lufthavn, using $P_h = 900$ kW and $n_h^s = 6$.

Charging infrastructure at Bergen, Bodø, Hammerfest, Oslo, Tromsø, Trondheim and Vadsø

Table 5.5 shows the optimized infrastructure, together with the average operations energy consumption, delays and costs for all seven hubs. The daily costs range from €970 at Hammerfest Lufthavn (HFT) up to €2890 at Bodø Lufthavn, accumulating to a network total of €11793 per day. It should be kept in mind that this does not account for the decrease in payload caused by using 10-seater aircraft instead of the 37-seater Dash-8. The table shows an approximate marginal cost of €100 per flight, which is independent of the difference in payload, of which the spare battery supply forms the biggest share. Furthermore, the delay costs are not proportional to the number of daily flights. For example, the average delay costs at Vadsø of €142 are larger than the costs at Bodø, of €140, which accommodates three times the number of flights.

	Hub airport		Infrastructure		Operations		Average Cost				
	Airport h	Flights	P_h	n_h^s	Energy	Delays	$c^p P_h$	$c^s n_h^s$	$\mathscr{C}_h^e$	$\mathscr{C}_h^{del}$	$\mathscr{C}_h$
	[-]	[-]	[kW]	[-]	[kWh]	[hh:mm]	[€]	[€]	[€]	[€]	[€]
BGO	Bergen	9.4	425	2	3553	00:13	170	500	300	123	1093
BOO	Bodø	29.7	900	6	8950	00:12	360	1500	890	140	2890
HFT	Hammerfest	12.8	413	2	2430	00:06	160	500	240	70	970
OSL	Oslo	14.6	612	3	4410	00:09	245	750	460	95	1550
TOS	Tromsø	24.7	812	4	6303	00:11	325	1000	642	120	2087
TRD	Trondheim	21.8	850	5	7330	00:09	340	1250	744	101	2478
VDS	Vadsø	9.9	400	2	255	00:14	160	500	260	142	1062
Network total		122.9	4412	25	33231	01:14	1600	6000	3392	801	11793

Table 5.5.: Infrastructure and expected operational cost for the considered hubs in the network. The first column lists the airport codes and average daily number of flights. Here, $\mathscr{C}_h^e$ and $\mathscr{C}_h^{del}$ give the average daily electricity and delay cost.

5.5.2 Sensitivity analysis: battery capacity and daily number of flights

We perform a sensitivity analysis to assess the impact of the technological and economical assumptions we have made on the results. This is done for the development of battery energy density and the daily number of flights. We evaluate the impact of these on the optimal infrastructure, as well as the computational requirements to solve the problems. We show the results for Bodø Airport.

Table 5.6 shows the impact of the aircraft battery performance. We assume that the energy density of the batteries increases by an annual rate of 8% [11], resulting in a 610km flight range. We compare this rate with a pessimistic scenario of 0% (range of 480 km) annual increase of the energy density, 4% (range of 540 km), 12% (range of 685 km) and 16% annual increase (range of 775 km). Table 5.6 shows the required infrastructure, investment, as well as the total optimization time and average optimization time per day subroutine.

The results show that above 540 km, range no longer is a limiting factor on the number of flights, stabilizing at around 29.6 - 29.8. Above this number, the energy requirements increase linearly, affecting the total costs. Only in the most pessimistic scenario (range of 480 km), the range does impede the flight schedule, reducing the number of daily flights by a quarter. In this case, the entire infrastructure is reduced in size and the costs decrease by a third. Finally, in all cases, the computational time is limited to under 30 minutes for the entire algorithm, and under half a second for each day of operations.

Battery development		**Infrastructure**		**Operations**		**Cost**	**Computational time**	
Range	# fl/day	P_h	n_h^s	Energy	Delays	$\mathscr{C}_h$	total	instance
km	-	kW	-	kWh	hh:mm	€	mm:ss	sec
480	22.3	755	5	6010	00:03	1862	21:05	0.403
540	29.6	865	7	8680	00:09	2796	24:24	0.451
610	29.7	900	6	8950	00:12	2890	26:00	0.459
685	29.8	1145	5	9270	00:10	3036	26:12	0.472
775	29.9	1345	5	9624	00:10	3566	26:29	0.480

Table 5.6.: Optimal charging infrastructure at Bodø Airport given various battery energy densities. Both the computational time of the infrastructure optimization and the average per daily recharge scheduling optimization are given. # fl/day gives the average number of flights per day. The green case represents the nominal case considered in Section 5.5.1.

Table 5.7 shows the impact of the number of electric flights performed on the infrastructure and costs. We assumed that the original schedule is adhered as much as possible, but this does decrease the total payload which can be carried to about 25% of the original schedule. We compare this with 50%, 75% and 100% by doubling, tripling, and quadrupling the number of times each flight is performed. Table 5.7

shows the average number of flights at Bodø, the infrastructure requirements and costs, and the optimization time.

The results show a sub-linear increase of the costs as a function of number of flights. The infrastructure does grow approximately linear with the number of flights, but the delays remain fairly limited. The computational time increased from 26 to 201 minutes for the infrastructure optimization and from 0.46 to 3.5 seconds for each recharge scheduling optimization.

Schedule	**Infrastructure**		**Operations**		**Cost**	**Optimization time**	
# fl/day	P_h	n_h^s	Energy	Delays	$\mathscr{C}_h$	total	per instance
-	kW	-	kWh	hh:mm	€	min	sec
30	900	6	8950	00:12	2890	26	0.459
60	1740	12	17900	00:15	5651	51	0.911
89	2410	17	26850	00:21	8075	108	1.90
119	3190	23	35800	00:27	10837	201	3.49

Table 5.7.: Optimal charging infrastructure at Bodø Airport given various average number of flights per day. Both the computational time of the infrastructure optimization and the average per daily recharge scheduling optimization are given. # fl/day gives the average number of flights per day. The green case represents the nominal case considered in Section 5.5.1.

5.6 Quantifying the benefit of recourse optimization over infrastructure optimization considering one day of traffic

5.6.1 Infrastructure optimization considering only a peak-day or a median-day of air traffic

In order to assess the performance of the recourse model proposed in Subsection 5.4.2, we consider two alternative battery charging infrastructure optimization approaches. These approaches optimize the infrastructure using only the flight schedule from a single day of operations. For this, we use either the peak traffic day (PD) or a median traffic day (MD), according to the total number of flights. Using a peak-day flight schedule corresponds to the desire to obtain an infrastructure which is able to cope with the most congested days, although this expensive infrastructure may be overly large during less busy days. Using a median day as reference leads to obtaining an infrastructure which performs well on most days of operations but may be insufficient during congested days.

The two alternative infrastructure optimization approaches use a version of the MILP from Subsection 5.4.1 modified in two respects. First, the charging capacity

P_h and the number of spare batteries n_h^s are model variables instead of input parameters. Second, their associated costs (c^p and c^s) are included in the objective function. As such, the following model is considered:

$$\mathscr{C}_{dh}^{SD} = \min_{P_h, n_h^s, \tau, r, S} \quad c^p P_h + c^s n_h^s + \sum_{t \in T_d^*} \left[\sum_{\tau \in \tau^{del}} \left(c^{del}(\tau) \max\{D_{t-\tau}^{fh} - S_t, 0\} \right) + c_t^e \sum_{b \in B_t^{dh}} \tau_{bt}^c P^c \right] \tag{5.3a}$$

$$\text{s.t.} \quad (5.1b) - (5.1g) \tag{5.3b}$$

$$P_h \geq 0, n_h^s \in \mathbb{N}$$

The objective function, Equation (5.1a), has been replaced by Equation (5.3a), and now computes the most cost-effective infrastructure for a single day d at hub h. The corresponding cost is denoted as $\mathscr{C}_{dh}^{SD}$. Constraints (5.1b) - (5.1g) are unaltered, and Constraint (5.3b) has been added to the model.

5.6.2 Results: quantifying the advantage of recourse infrastructure optimization for Widerøe Airlines at Bodø

We quantify the cost reduction gained by using the infrastructure optimized by the recourse MILP for Widerøe Airlines at Bodø Lufthavn. This original solution (see Subsection 5.5.1) takes the year-round flight schedule into account and is referred to as the $\mathscr{S}$(YR) solution hereafter. We compare it with optimized infrastructure for the peak- and median levels of traffic days of operations, using the algorithm from Section 5.6.1. For the peak- and median traffic days, we have used PD = August 25, 2022, with 55 flights, and MD = June 13, 2022, with 32 flights. The infrastructure solutions obtained with only these single days are referred to as the $\mathscr{S}$(PD) and $\mathscr{S}$(MD) solutions, respectively.

The three charging infrastructure solutions can be found in Table 5.8. For each solution $x \in \{\mathscr{S}(YR), \mathscr{S}(MD), \mathscr{S}(PD)\}$ the size of the different components is shown, together with the expected costs, similar to Table 5.5. The peak-traffic day optimized infrastructure consists of $(P_c^{\mathscr{S}(PD)}, n_h^{s,\mathscr{S}(PD)}) = (1130 \text{ kW}, 7)$, resulting in a daily infrastructure cost of €2180. It was computed in 12.7 seconds. The median-traffic day optimized infrastructure consists of $(P_c^{\mathscr{S}(MD)}, n_h^{s,\mathscr{S}(MD)}) = (800 \text{ kW}, 4)$ resulting in a daily infrastructure cost of €1320. This was computed in 5.7 seconds.

The total average daily costs of each solution x is given as:

$$\mathscr{C}^x = c^p P_h^x + c^s n_h^{s,x} + \sum_{d \in D} \mathscr{C}_{dh}(P_h^x, n_h^{s,x}) / |D| \tag{5.4}$$

For our analysis, $\mathscr{C}^{\mathscr{S}(YR)} = €2890$, compared to $\mathscr{C}^{\mathscr{S}} = €4730$ (+58%) for the $\mathscr{S}(MD)$ solution and $\mathscr{C}^{\mathscr{S}(PD)} = €3140$ (+6%) for the $\mathscr{S}(PD)$ solution. Table 5.8 shows a

breakdown of the costs, split up into charging capacity, spare battery, electricity and delay costs. Compared with the $\mathscr{S}(YR)$ solution, the $\mathscr{S}(PD)$ solution trades charging capacity for an extra battery and a significantly larger infrastructure investment, but reduces the expected delays and is able to profit from slightly lower electricity costs. On the other hand, the $\mathscr{S}(MD)$ solution consists of a relatively small charging capacity, but causes significant flight delays (on average a total of 2:36 hours daily).

		Infrastructure		**Operations**		
Solution x	Flights	P_h^x	$n_h^{s,x}$	Energy	Delays	
	[-]	[kW]	[-]	[kWh]	[hh:mm]	
$\mathscr{S}(YR)$	29.5*	900	6	8950	0:12	
$\mathscr{S}(PD)$	55	1130	7	8950	00:05	
$\mathscr{S}(MD)$	32	800	4	8950	02:36	

		Average Cost				
Solution x	Flights	$c^p P_h^x$	$c^s n_h^{s,x}$	$\mathscr{C}^{e,x}$	$\mathscr{C}^{del,x}$	$\mathscr{C}^x$
		[€]	[€]	[€]	[€]	[€]
$\mathscr{S}(YR)$	29.5*	360	1500	890	140	2890
$\mathscr{S}(PD)$	55	430	1750	870	80	3140
$\mathscr{S}(MD)$	32	320	1000	950	1925	4195

Table 5.8.: Infrastructure and average electricity consumption and flight delays at Bodø Lufthavn, with their associated daily costs ($c^p P_h^x$, $c^s n_h^{s,x}$, $\mathscr{C}^{e,x}$, and $\mathscr{C}^{del,x}$, respectively) for three infrastructures x. We consider the recourse optimisation model (YR) vs. the optimisation model for only one peak-traffic day SD(PD) and only one median-traffic day SD(MD). The PD is August 25th, 2022. The MD is July 13th, 2022. For (*) there are on average 29.7 flights/day considering the entire year of operations.

Last, Figure 5.9 shows the cost of the three infrastructure solutions depending on the number of flights on the days of operation. Each point represents one of the 356 days of operations, which are sorted by number of flights. Generally speaking, the daily costs increase with the number of flights. Additionally, the $\mathscr{S}(MD)$ and $\mathscr{S}(YR)$ infrastructures are stressed more for a large number of flights then the $\mathscr{S}(PD)$ infrastructure.

Note that for a small number of flights, not the $\mathscr{S}(MD)$ but the $\mathscr{S}(YR)$ solution has the lowest total costs, aided by the flexibility of a larger charging capacity. For busier days, the $\mathscr{S}(PD)$ solution starts to outperform the other two, with the costs of the $\mathscr{S}(YR)$ and $\mathscr{S}(MD)$ solutions increasing to €5000 and €24000 (not on chart), respectively.

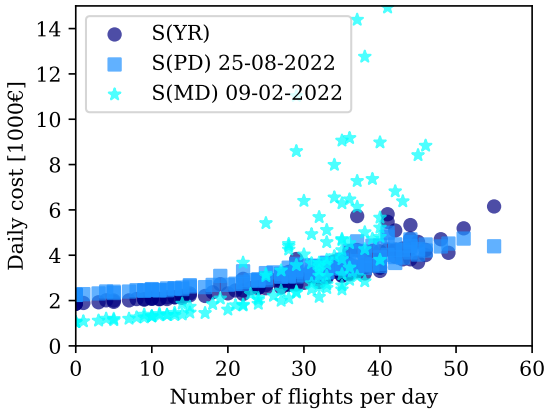

Figure 5.9.: Daily infrastructure costs $\mathscr{C}_{dh}(P_h^x, n_h^{s,x})$ when considering $(P_h^{\mathscr{S}(YR)}, n_h^{s,\mathscr{S}(YR)}) = (900\text{kW}, 6)$, $(P_h^{\mathscr{S}(PD)}, n_h^{s,\mathscr{S}(PD)}) = (1130\text{kW}, 7)$, and $(P_h^{\mathscr{S}(MD)}, n_h^{s,\mathscr{S}(MD)}) = (800\text{kW}, 4)$, during the period 28th October 2021 - 27th October 2022. Each point represents a single day of operations.

5.7 Conclusions

This chapter proposes a two-phase recourse model optimization framework for battery swap and recharge operations for an airline operating a fleet of short-haul electric aircraft. This framework integrates the scheduling of swapped battery recharges with the sizing of the recharge infrastructure, without merging them completely to account for the fact that the infrastructure size cannot be altered daily. The objective for the former is to minimize the charging station operational costs, comprised of the electricity and the caused delay cost. For the latter, the objective is to minimize the sum of the infrastructure acquisition cost and the average operational cost throughout the year. The scheduling problem, posed as a mixed-integer linear program, is used as a subroutine for the infrastructure sizing problem, which is solved using a simulated annealing algorithm.

Our optimization framework is applied in a case study for Norway's Widerøe Airlines, where the airline's fleet of DHC Dash 8-100 aircraft is replaced with a fleet of electric aircraft based on Eviation Alice's specifications. We use flight data from 28 October 2021 and 27 October 2022 and keep to the original schedule as much as possible. It is assumed that the aircraft will be able to swap their batteries at the seven most visited airports in the network, such that approximately 52000 out of the 56000 analysed flights can be performed. The results show that a combined power supply consists of 4412 kW and that 25 spare batteries are required, such that the daily cost of this charging infrastructure is €11793. However, this analysis does not account for the decrease in payload which results from replacing the 40-seats Dash-8 with the 10-seats Alice. The actual infrastructure cost are bounded from above by multiplying the found values by a factor of 4.

We also propose two baseline infrastructure sizing solutions, which minimize the charging infrastructure size given only one day of operations: the peak- or median-traffic day. Overall, these approaches achieve an optimality gap of 8% and 45%, respectively. Infrastructure optimized for the peak day tends to be oversized on average, resulting in high capital expenditures but relatively low operational costs. Infrastructure optimized for the median day, on the other hand, is used well on average days but results in major flight delay on peak load days.

As future work, the model can be extended for an airline operating different e-AC models with different specifications and charging needs. Second, when applied to an airline with seasonality in the flight schedule, the option of a seasonally varying spare battery stock can be studied. Third, the impact of uncertainty during the operational phase (as in Chapter 4 can be studied. Considering this planning phase can help to create a more realistic assessment of the performance of the charging infrastructure. Finally, the placement of the battery swapping locations can be studied. Such a model would identify the most suitable airports to place the battery swapping stations, rather than assume that all hub airports are used.

references

[1] S. van Oosterom and M. Mitici. “Optimizing the battery charging and swapping infrastructure for electric short-haul aircraft—The case of electric flight in Norway”. English. In: *Transportation Research Part C: Emerging Technologies* 155 (2023). ISSN: 0968-090X. DOI: 10.1016/j.trc.2023.104313.

[2] UNFCCC. *International Aviation Climate Ambition Coalition - COP26 Declaration*. https://ukcop26.org/cop-26-declaration-international-aviation-climate-ambition-coalition/. Nov. 2021. (Visited on 01/12/2022).

[3] L. Paoli, A. Dasgupta, and S. McBain. *International Energy Agency: Electric Vehicles*. Tech. rep. International Energy Agency, Sept. 2022. URL: https://www.iea.org/reports/electric-vehicles.

[4] V. Klesty. “Electric cars hit 65% of Norway sales as Tesla grabs overall pole”. In: *Reuters* (Jan. 2022). URL: https://www.reuters.com/business/autos-transportation/electric-cars-take-two-thirds-norway-car-market-led-by-tesla-2022-01-03/ (visited on 10/26/2022).

[5] M. Soltani, S. Ahmadi, A. Akgunduz, and N. Bhuiyan. “An eco-friendly aircraft taxiing approach with collision and conflict avoidance”. en. In: *Transportation Research Part C: Emerging Technologies* 121 (Dec. 2020), p. 102872. ISSN: 0968-090X. DOI: 10.1016/j.trc.2020.102872. (Visited on 12/13/2022).

[6] R. Guo, Y. Zhang, and Q. Wang. “Comparison of emerging ground propulsion systems for electrified aircraft taxi operations”. In: *Transportation Research Part C: Emerging Technologies* 44 (2014), pp. 98–109. ISSN: 0968-090X. DOI: https://doi.org/10.1016/j.trc.2014.03.006.

[7] L. A. Garrow, B. J. German, and C. E. Leonard. “Urban air mobility: A comprehensive review and comparative analysis with autonomous and electric ground transportation for informing future research”. en. In: *Transportation Research Part C: Emerging Technologies* 132 (Nov. 2021), p. 103377. ISSN: 0968-090X. DOI: 10.1016/j.trc.2021.103377. (Visited on 12/13/2022).

[8] Q. Shao, M. Shao, and Y. Lu. “Terminal area control rules and eVTOL adaptive scheduling model for multi-vertiport system in urban air Mobility”. en. In: *Transportation Research Part C: Emerging Technologies* 132 (Nov. 2021), p. 103385. ISSN: 0968-090X. DOI: 10.1016/j.trc.2021.103385. (Visited on 12/13/2022).

[9] M.-S. Balogun, H. Yang, Y. Luo, W. Qiu, Y. Huang, Z.-Q. Liu, and Y. Tong. "Achieving high gravimetric energy density for flexible lithium-ion batteries facilitated by core–double-shell electrodes". en. In: *Energy & Environmental Science* 11.7 (July 2018). Publisher: The Royal Society of Chemistry, pp. 1859–1869. ISSN: 1754-5706. DOI: 10.1039/C8EE00522B. (Visited on 10/26/2022).

[10] N. Muralidharan, E. C. Self, M. Dixit, Z. Du, R. Essehli, R. Amin, J. Nanda, and I. Belharouak. "Next-Generation Cobalt-Free Cathodes – A Prospective Solution to the Battery Industry's Cobalt Problem". en. In: *Advanced Energy Materials* 12.9 (2022). _eprint: https://onlinelibrary.wiley.com/doi/pdf/10.1002/aenm.202103050, p. 2103050. ISSN: 1614-6840. DOI: 10.1002/aenm.202103050. (Visited on 10/26/2022).

[11] M. Ziegler and J. Trancik. "Re-examining rates of lithium-ion battery technology improvement and cost decline". en. In: *Energy & Environmental Science* 14.4 (2021). Publisher: Royal Society of Chemistry, pp. 1635–1651. DOI: 10.1039/D0EE02681F. (Visited on 10/26/2022).

[12] F. Holland. "DHL Express buys electric cargo planes for U.S. package delivery from start-up Eviation". In: *CNBC News* (Aug. 2021). URL: https://www.cnbc.com/2021/08/03/dhl-express-buys-eviation-electric-planes-for-us-package-delivery.html (visited on 10/26/2022).

[13] L. E. Taraldsen. "Norway's Wideroe to Fly First Zero-Emission Passenger Plane". In: *Bloomberg* (Nov. 2021). URL: https://www.bloomberg.com/news/articles/2021-11-10/norway-s-wideroe-plans-first-zero-emission-plane-in-five-years (visited on 10/26/2022).

[14] N. Taylor-Marriott. "American Cape Air Orders 75 Electric Airplanes From Eviation". In: *Simple Flying* (Apr. 2022). URL: https://simpleflying.com/eviation-announces-75-plane-order-from-cape-air-for-electric-plane/ (visited on 10/26/2022).

[15] C. Y. Justin, A. P. Payan, and D. N. Mavris. "Integrated fleet assignment and scheduling for environmentally friendly electrified regional air mobility". en. In: *Transportation Research Part C: Emerging Technologies* 138 (May 2022), p. 103567. ISSN: 0968-090X. DOI: 10.1016/j.trc.2022.103567. (Visited on 10/26/2022).

[16] A. P. Brdnik, R. Kamnik, S. Bozicnik, and M. Marksel. "Ground infrastructure investments for operation of hybrid-electric aircraft". en. In: *IOP Conference Series: Materials Science and Engineering* 1226.1 (Feb. 2022). Publisher: IOP Publishing, p. 012073. ISSN: 1757-899X. DOI: 10.1088/1757-899X/1226/1/012073. (Visited on 10/26/2022).

[17] M. R. Sarker, H. Pandžić, and M. A. Ortega-Vazquez. "Optimal Operation and Services Scheduling for an Electric Vehicle Battery Swapping Station". In: *IEEE Transactions on Power Systems* 30.2 (Mar. 2015). Conference Name: IEEE Transactions on Power Systems, pp. 901–910. ISSN: 1558-0679. DOI: 10.1109/TPWRS.2014.2331560.

[18] U. Sultana, A. B. Khairuddin, B. Sultana, N. Rasheed, S. H. Qazi, and N. R. Malik. "Placement and sizing of multiple distributed generation and battery swapping stations using grasshopper optimizer algorithm". en. In: *Energy* 165 (Dec. 2018), pp. 408–421. ISSN: 0360-5442. DOI: 10.1016/j.energy.2018.09.083. (Visited on 10/23/2022).

[19] F. Schneider, U. W. Thonemann, and D. Klabjan. "Optimization of Battery Charging and Purchasing at Electric Vehicle Battery Swap Stations". In: *Transportation Science* 52.5 (Oct. 2018). Publisher: INFORMS, pp. 1211–1234. ISSN: 0041-1655. DOI: 10.1287/trsc.2017.0781. (Visited on 10/25/2022).

[20] A. Ayad, N. A. El-Taweel, and H. E. Z. Farag. “Optimal Design of Battery Swapping-Based Electrified Public Bus Transit Systems”. In: *IEEE Transactions on Transportation Electrification* 7.4 (Dec. 2021). Conference Name: IEEE Transactions on Transportation Electrification, pp. 2390–2401. ISSN: 2332-7782. DOI: 10.1109/TTE.2021.3083106.

[21] O. Kwizera and S. G. Nurre. “Using drones for delivery: A two-level integrated inventory problem with battery degradation and swap stations”. undefined. In: *Proceedings of the Industrial and Systems Engineering Research Conferences* (2018), pp. 1–6.

[22] O. Worley and D. Klabjan. “Optimization of battery charging and purchasing at electric vehicle battery swap stations”. In: *2011 IEEE Vehicle Power and Propulsion Conference*. ISSN: 1938-8756. Sept. 2011, pp. 1–4. DOI: 10.1109/VPPC.2011.6043182.

[23] S. G. Nurre, R. Bent, F. Pan, and T. C. Sharkey. “Managing operations of plug-in hybrid electric vehicle (PHEV) exchange stations for use with a smart grid”. en. In: *Energy Policy* 67 (Apr. 2014), pp. 364–377. ISSN: 0301-4215. DOI: 10.1016/j.enpol.2013.11.052. (Visited on 10/23/2022).

[24] S. Park, L. Zhang, and S. Chakraborty. “Battery assignment and scheduling for drone delivery businesses”. In: *2017 IEEE/ACM International Symposium on Low Power Electronics and Design (ISLPED)*. July 2017, pp. 1–6. DOI: 10.1109/ISLPED.2017.8009165.

[25] H. Wu, G. K.-H. Pang, K. L. Choy, and H. Y. Lam. “A charging-scheme decision model for electric vehicle battery swapping station using varied population evolutionary algorithms”. en. In: *Applied Soft Computing* 61 (Dec. 2017), pp. 905–920. ISSN: 1568-4946. DOI: 10.1016/j.asoc.2017.09.008. (Visited on 10/24/2022).

[26] A. Asadi and S. Nurre Pinkley. “A stochastic scheduling, allocation, and inventory replenishment problem for battery swap stations”. en. In: *Transportation Research Part E: Logistics and Transportation Review* 146 (Feb. 2021), p. 102212. ISSN: 1366-5545. DOI: 10.1016/j.tre.2020.102212. (Visited on 10/23/2022).

[27] B. Sun, X. Tan, and D. H. K. Tsang. “Optimal Charging Operation of Battery Swapping and Charging Stations With QoS Guarantee”. In: *IEEE Transactions on Smart Grid* 9.5 (Sept. 2018). Conference Name: IEEE Transactions on Smart Grid, pp. 4689–4701. ISSN: 1949-3061. DOI: 10.1109/TSG.2017.2666815.

[28] B. Sun, X. Sun, D. H. K. Tsang, and W. Whitt. “Optimal battery purchasing and charging strategy at electric vehicle battery swap stations”. en. In: *European Journal of Operational Research* 279.2 (Dec. 2019), pp. 524–539. ISSN: 0377-2217. DOI: 10.1016/j.ejor.2019.06.019. (Visited on 10/21/2022).

[29] H.-Y. Mak, Y. Rong, and Z.-J. M. Shen. “Infrastructure Planning for Electric Vehicles with Battery Swapping”. In: *Management Science* 59.7 (July 2013). Publisher: INFORMS, pp. 1557–1575. ISSN: 0025-1909. DOI: 10.1287/mnsc.1120.1672. (Visited on 10/23/2022).

[30] W. Liu, S. Niu, H. Xu, and X. Li. “A New Method to Plan the Capacity and Location of Battery Swapping Station for Electric Vehicle Considering Demand Side Management”. en. In: *Sustainability* 8.6 (June 2016). Number: 6 Publisher: Multidisciplinary Digital Publishing Institute, p. 557. ISSN: 2071-1050. DOI: 10.3390/su8060557. (Visited on 10/23/2022).

[31] W. Zhan, Z. Wang, L. Zhang, P. Liu, D. Cui, and D. G. Dorrell. “A review of siting, sizing, optimal scheduling, and cost-benefit analysis for battery swapping stations”. en. In: *Energy* 258 (Nov. 2022), p. 124723. ISSN: 0360-5442. DOI: 10.1016/j.energy.2022.124723. (Visited on 10/21/2022).

[32] C. Y. Justin, A. P. Payan, S. I. Briceno, B. J. German, and D. N. Mavris. “Power optimized battery swap and recharge strategies for electric aircraft operations”. en. In: *Transportation Research Part C: Emerging Technologies* 115 (June 2020), p. 102605. ISSN: 0968-090X. DOI: 10.1016/j.trc.2020.02.027. (Visited on 06/16/2021).

[33] F. Salucci, L. Trainelli, R. Faranda, and M. Longo. “An optimization Model for Airport Infrastructures in Support to Electric Aircraft”. In: *2019 IEEE Milan PowerTech*. June 2019, pp. 1–5. DOI: 10.1109/PTC.2019.8810713.

[34] L. Trainelli, F. Salucci, C. E. D. Riboldi, A. Rolando, and F. Bigoni. “Optimal Sizing and Operation of Airport Infrastructures in Support of Electric-Powered Aviation”. en. In: *Aerospace* 8.2 (Feb. 2021), p. 40. ISSN: 2226-4310. DOI: 10.3390/aerospace8020040. (Visited on 05/04/2022).

[35] M. Mitici, M. Pereira, and F. Oliviero. “Electric flight scheduling with battery-charging and battery-swapping opportunities”. en. In: *EURO Journal on Transportation and Logistics* 11 (Jan. 2022), p. 100074. ISSN: 2192-4376. DOI: 10.1016/j.ejtl.2022.100074. (Visited on 10/25/2022).

[36] Z. Guo, X. Zhang, N. Balta-Ozkan, and P. Luk. “Aviation to Grid: Airport Charging Infrastructure for Electric Aircraft”. en. In: Volume 10: Sustainable Energy Solutions for Changing the World: Part II, Dec. 2020. DOI: 10.46855/energy-proceedings-7180. (Visited on 10/25/2022).

[37] F. Doctor, T. Budd, P. D. Williams, M. Prescott, and R. Iqbal. “Modelling the effect of electric aircraft on airport operations and infrastructure”. en. In: *Technological Forecasting and Social Change* 177 (Apr. 2022), p. 121553. ISSN: 00401625. DOI: 10.1016/j.techfore.2022.121553. (Visited on 05/03/2022).

[38] T. Bærheim, J. J. Lamb, J. K. Nøland, and O. S. Burheim. “Potential and Limitations of Battery-Powered All-Electric Regional Flights–A Norwegian Case Study”. In: *IEEE Transactions on Transportation Electrification* (2022). Conference Name: IEEE Transactions on Transportation Electrification, pp. 1–1. ISSN: 2332-7782. DOI: 10.1109/TTE.2022.3200089.

[39] Olje- og energidepartementet. *Renewable energy production in Norway*. en-GB. Redaksjonellartikkel. Publisher: regjeringen.no. May 2016. URL: https://www.regjeringen.no/en/topics/energy/renewable-energy/renewable-energy-production-in-norway/id2343462/ (visited on 12/22/2022).

[40] Flightradar24. *Wideroe routes and destinations*. en. Nov. 2022. URL: https://www.flightradar24.com/data/airlines/wf-wif/routes (visited on 11/22/2022).

[41] Eviation. *Alice*. en-US. July 2022. URL: https://www.eviation.com/aircraft/ (visited on 11/22/2022).

[42] M. Hepperle. “Electric Flight - Potential and Limitations”. en. In: Lisbon, Portugal, Oct. 2012. URL: https://elib.dlr.de/78726/1/MP-AVT-209-09.pdf (visited on 10/27/2022).

[43] Nordpool Group. *Hourly electricity prices*. Dec. 2022. URL: https://www.nordpoolgroup.com/en/Market-data1/Dayahead/Area-Prices/ALL1/Hourly/ (visited on 12/22/2022).

[44] A. Cook and T. Graham. *European airline delay cost reference values*. en. Tech. rep. Eurocontrol, Dec. 2015. URL: https://www.eurocontrol.int/publication/european-airline-delay-cost-reference-values (visited on 05/18/2023).

[45] B. A. Adu-Gyamfi and C. Good. "Electric aviation: A review of concepts and enabling technologies". en. In: *Transportation Engineering* 9 (Sept. 2022), p. 100134. ISSN: 2666-691X. DOI: 10.1016/j.treng.2022.100134. (Visited on 11/22/2022).

[46] S. sentralbyrå. *Electricity prices*. en. Nov. 2022. URL: https://www.ssb.no/en/energi-og-industri/energi/statistikk/elektrisitetspriser (visited on 11/22/2022).

CHAPTER 6

eVTOL battery management: integrating maintenance planning into flight operations

After routing and charging operations, the following two chapters discuss how battery maintenance can be integrated into operations. The batteries used for the aviation applications we consider are going to be put under significant stress, causing faster degradation. The safe use of these batteries is a boundary condition. Predictive maintenance planning, based on prognostics and health management, provides an interesting approach to address this.

In this chapter, therefore, we develop a prognostic model to predict the remaining useful life (RUL) of batteries, and use this for maintenance planning. We consider a probabilistic model, which outputs a probability density for the RUL, as opposed to a single point estimate. These prognostics are integrated into the predictive maintenance planning problem, formulated as a integer linear program, which aims to minimize the maintenance costs.

The model is implemented to plan maintenance for a fleet of electric vertical take-off and landing aircraft (eVTOL) batteries. We show that using probabilistic prognostics leads to 30% less break-downs then when RUL point estimates are considered. This framework is used as a benchmark to test against an integrated predictive maintenance planning model, presented in the next chapter.

Parts of this chapter have been published as:

M. Mitici and S. van Oosterom. "Adaptive predictive maintenance for the batteries of electric Vertical Take-off and Landing (eVTOL) aircraft using Remaining Useful Life prognostics". In: *Proceedings of the 34th European Safety and Reliability Conference.* Stavanger, Norway, June 2025

6.1 Introduction

Urban areas are expected to be confronted with increasing traffic congestion in the near future. At the same time, sustainability targets related to carbon emission reduction are becoming a priority. Electrical Vertical Take-off and Landing (eVTOL) aircraft are seen as a promising emerging technology for transportation in urban areas as it enhances intercity connectivity and acts as an eco-friendly complement to ground transportation [2, 3]. Existing eVTOL designs achieve flight ranges of 50-100km, at an average speed of 200km/hr, having a payload of up to 500-800kg. These characteristics make eVTOLs suitable for city commuting, urban air taxing or emergency medical services [4]. For safe and reliable eVTOL operations, however, the management of the eVTOL batteries is crucial. This includes a continuous health monitoring of the batteries, periodic assessments of the state of health of the batteries and estimates of degradation trends, as well as effective strategies for battery replacement [5].

Current eVTOL designs assume Lithium-ion batteries due to their high energy density, low self-discharge rates and feasible costs. The battery management for this battery chemistry has been studied extensively for ground vehicles. Particular attention has been given to the estimation of the State-of-Health (SOH) and the Remaining Useful Life (RUL) of the Lithium-ion batteries using either model-based , data-driven approaches, physics-based or hybrid approaches [6]. In comparison with Lithium-ion batteries for ground vehicles, however, the battery management of eVTOLs poses additional challenges: the take-off and landing of eVTOLs are safety-critical flight phases when the discharge rates of the batteries are higher than during the cruise phase. In the long-run, this is expected to have a direct impact on the overall health condition of the batteries. In this chapter we focus on data-driven RUL prognostics for eVTOL Lithium-ion batteries, where we distinguish between battery measurements taken during the take-off, cruise and landing phases of the eVTOL flight. Moreover, we further employ the obtained RUL prognostics to specify reliable and cost-efficient battery replacement strategies that are continuously adapted as more measurements become available and the prognostics are updated.

Several data-driven approaches for RUL prognostics of Lithium-ion batteries have been proposed in the last years [7–9]. In [10] the authors estimate the RUL using a long-short term memory recurrent neural network with particle filtering, achieving less than 10% error under different training phases. In [11] a hybrid convolutional neural network is combined with a long short-term memory and a deep neural network to predict the RUL of Lithium-ion batteries. The superior performance of this approach, relative to several other data-driven methods, is proven for the datasets provided by NASA and NASA and Center for Advanced Life Cycle Engineering (CALCE). In [12] a long short-term memory recurrent neural network is proposed to estimate the RUL of the batteries. The estimation errors achieved are below 0.13% in the last phase of the battery lifetime (last 10 cycles).

The studies above envision that the batteries are subject to moderate discharge rates, as in the case of electric ground vehicles. However, for eVTOLs, the take-off and landing phases of the flight are performed at higher C-rate than during the cruise phase. In this chapter we consider the [13] dataset of eVTOL batteries. This dataset includes distinct

eVTOL mission profiles and battery measurements specified for the take-off, cruise, and landing phase of the flights. Few studies have developed SOH and/or RUL estimates for eVTOL batteries using this dataset. In [14] a k-nearest neighbours approach is shown to achieve a high accuracy for SOH estimation of the batteries. However, the authors considers only the measurements recorded during the cruise phase of the flight, which is a strong limitation of the approach given that the take-off and landing are safety-critical phases of the eVTOL operations, with a direct impact on the health of the batteries. In [15], an Extreme Gradient Boosting model is shown to achieve the highest accuracy for RUL estimation of eVTOL batteries, when compared with other methods such as Support Vector regression, Random Forrest regression, Gaussian Process regression, and Multi-layer Perception. Here, the authors specify features for every phase of the flight (take-off, landing, and cruise). These existing studies, however, develop point estimates of the RUL. In contrast, in this chapter we estimate the distribution of the RUL (probabilistic RUL prognostics). Thus, we quantify the uncertainty associated with the RUL estimates.

In this chapter we propose an adaptive predictive maintenance planning of eVTOL batteries, where data-driven RUL prognostics are integrated in an optimisation model for battery replacement. First, probabilistic RUL prognostics for eVTOL batteries are developed using a Mixture Density Network, i.e. we estimate the distribution of the RUL. These prognostics are further integrated into a reliable and cost-efficient maintenance planning model for a fleet of eVTOLs. We propose an integer linear programming model for the replacement of batteries at fleet level, taking into account the RUL prognostics of the batteries, the eVTOL flight missions, and the availability of a common eVTOL hub to perform battery replacements. The aim of the planning is to limit the risk of the batteries being in use beyond them reaching their End-of-Life (EOL), while maximizing the number of flight missions performed with each battery (or, equivalently, minimizing the wasted battery life). The obtained planning of battery replacements is adapted over time, as more measurements become available and the RUL prognostics are themselves updated. When considering eVTOL operations for a period of 10 years, the results show that planning battery replacements using probabilistic RUL prognostics, rather than using point estimates of the RUL, results in up to 30% less unscheduled battery replacements due to batteries reaching their EOL unexpectedly. The results also show that, although the probabilistic RUL prognostics are imperfect, planning battery replacements based on these prognostics results in less than 1 yearly unscheduled battery replacements in comparison to an Oracle planning approach where the actual EOL of the batteries is known in advance.

6.2 Problem description: health monitoring for battery maintenance operations

We consider a fleet V of eVTOL aircraft. Each eVTOL performs round trips to and from a hub. Each eVTOL performs n trips per day. The batteries are continuously monitored during operations. For each eVTOL $v \in V$, sensor measurements $\mathbf{x}_t^v \in \mathbb{R}^M$, $t \geq 0$, are recorded every time unit during operations, with M the total number of parameters recorded. During operations, the battery is constantly degrading until it reaches its End-

of-Life (EOL).

Based on the measurements recorded up to time t for the battery of eVTOL v, a probabilistic RUL prognostics (the distribution of the RUL) for the battery is obtained at time t .

eVTOL batteries are replaced at a hub. If a battery is replaced before its EOL is reached, a cost $c_{replace}$ is incurred. Battery replacement takes an entire day (during which the eVTOL cannot fly). At the start of a current day, battery replacements can be planned for the next days. Per day, at most h eVTOL batteries can be replaced at the eVTOL hub. If an eVTOL reaches its EOL unexpectedly, then an unscheduled replacement is performed immediately at a cost $c_{unscheduled} >> c_{replace}$.

We are interested in identifying reliable and cost-efficient times of replacements for the batteries of the fleet of eVTOLs taking into account the probabilistic RUL prognostics, as well as the flight schedule of the eVTOLs and the capacity of the eVTOL hub.

6.3 Electric aircraft battery data description

We consider the condition-monitoring dataset for Sony-Murata 18650 VTC-6 cell Lithium-ion batteries [13]. These batteries are used to perform a sequence of flight missions for electric take-off and landing (eVTOL) aircraft. These cells are considered for EVTOLs as they can sustain a high power demand while providing a cell specific energy of 230Wh/kg [13].

A flight mission consists of a series of phases: a Constant Current (CC) battery Charging phase, a Constant Voltage (CV) battery Charging phase, a Rest period, a Take-off segment at a given power, a Cruise segment at a given duration and power, a Landing segment at a given power. Each battery performs the sequence of missions according to a mission profile, which specifies the Cruise duration (sec), Power during take-off, cruise and landing (W), CC and CV rates, the cell surface temperature, and the total number of missions, see Table 6.1. In total, dataset [13] considers a total of 22 mission profiles, see Table 6.1. Of these, there are three baseline mission profiles (MP1, MP13 and MP20). The remaining 19 mission profiles are derived from these baseline profiles by altering various mission characteristics.

Sensor measurements: during each flight mission, the following measurements are recorded: time (sec), cell terminal voltage (V), cell current (mA), energy supplied to the cell during charge (Wh), charge supplied to the cell during charge (mAh), energy extracted from the cell during discharge (Wh), charge extracted from the battery cell during discharge (mAh), cell surface temperature ($^{\circ}C$), and cycle number (-).

Capacity tests: After every 50th flight mission, the battery charge capacity is measured. This is done by discharging it at a rate C/5 until the voltage drops below 2.5V and SOC=0%. This is followed by a period of rest during which the battery's temperature drops below 30 $^{\circ}C$. Following this cooling phase, the battery is fully charged at a charging rate of 1 C-rate and a constant voltage of 4.2V. This is followed by the battery performing the next mission, referred to as the "capacity test", see Table 6.1. The very first mission is a capacity test.

End-of-Life: We say that a battery reaches EOL as soon as its capacity reaches 85% of the initially measured battery capacity. This is measured during the capacity tests.

	Cruise duration	Power Take-off	Power Cruise	Power Landing	CC	CV	Temperature	VAH	#Missions	#Cap. tests
MP1	**800s**	**54W**	**16W**	**54W**	**1C**	**4.2V**	**25°C**	**VAH01**	**847**	**17**
MP2	125% of 800s	54W	16W	54W	1C	4.2V	25°C	VAH02	625	13
MP3	800s	90% of 54W	90% of 16W	90% of 54W	1C	4.2V	25 °C	VAH05	1615	29
MP4	800s	54W	16W	54W	50% of 1C	4.2V	25°C	VAH06	9290	20
MP5	800s	54W	16W	54W	1C	95.24% of 4.2V	25°C	VAH07	339	6
MP6	800s	54W	16W	54W	1C	4.2V	80% of 25°C	VAH09	8527	27
MP7	800s	54W	16W	54W	1C	4.2V	120% of 25°C	VAH10	1431	28
MP8	800s	80% of 54W	80% of 16W	80% of 54W	1C	4.2V	25 °C	VAH11	2249	45
MP9	50% of 800s	54W	16W	54W	1C	4.2V	25°C	VAH12	2349	46
MP10	75% 800s	54W	16W	54W	1C	4.2V	25°C	VAH13	1042	20
MP11	125% of 800s	54W	16W	54W	1C	4.2V	25°C	VAH15	554	11
MP12	800s	54W	16W	54W	150% of 1C	4.2V	25°C	VAH16	559	11
MP13	**800s**	**54W**	**16W**	**54W**	**1C**	**4.2V**	**25°C**	**VAH17**	**1002**	**20**
MP14	800s	54W	16W	54W	150% of 1C	4.2V	25°C	VAH20	611	12
MP15	125% of 800s	54W	16W	54W	1C	4.2V	25°C	VAH22	579	11
MP16	800s	54W	16W	54W	1C	97.62% of 4.2V	25°C	VAH23	697	14
MP17	800s	54W	16W	54W	50% of 1C	4.2V	25°C	VAH24	801	16
MP18	800s	54W	16W	54W	1C	4.2V	80% of 25°C	VAH25	554	11
MP19	75% of 800s	54W	16W	54W	1C	4.2V	25°C	VAH26	1164	23
MP20	**800s**	**54W**	**16W**	**54W**	**1C**	**4.2V**	**25°C**	**VAH27**	**587**	**12**
MP21	800s	90% of 54W	90% of 16W	90% of 54W	1C	4.2V	25°C	VAH28	1182	23
MP22	800s	54W	16W	54W	1C	4.2V	140% of 25°C	VAH30	919	18

Table 6.1.: Mission profile characteristics, based on [13].

Existing studies define the EOL of batteries as the first moment the capacity of the battery is below a threshold of $T = 80\%$ of the nominal battery capacity. To the best of our knowledge, thresholds for the EOL of eVTOL batteries have not been formally established. In preliminary studies on eVTOL batteries such as [5, 15, 16] a conservative EOL threshold of 85% of a nominal battery capacity has been considered. In line with these studies, we consider a conservative EOL threshold of $T = 85\%$.

Data processing of mission profiles: Dataset [13] reports tester malfunction for VAH09. As such, we will not consider VAH09 (MP06) for our analysis.

6.4 Battery health feature engineering

Based on the sensor measurements (see Section 6.3), we consider a total of 32 features [15] that are related to the charging, discharging, and temperature of the battery. Let $F = \{MP1, ...MP22\}$ denote the set of mission profiles. Let M_b denote the set of missions performed under mission profile $f \in F$. We consider the following features for each mission $1 \leq m \leq M_b$ and profile $f \in F$.

Charging-related features: the duration of each charging segment (CC, CV, Rest), denoted by $\Delta^{(charge,segment,f,m)}$; the amount of charge supplied to the battery $Qcrg^{f,m}$; the last measured battery capacity $C^{measure,b,m}$. Figure 6.1 shows $Qcrg$ for MP1.

Discharge-related features:

For each mission segment (take-off, cruise, landing), let $\Delta^{(discharge,segment,f,m)}$ denote the duration of each discharging segment, the maximum, minimum, mean, and the variance of the voltage, which we denote by $V_{max}^{(segment,f,m)}$, $V_{min}^{(segment,f,m)}$, $V_{mean}^{(segment,f,m)}$,

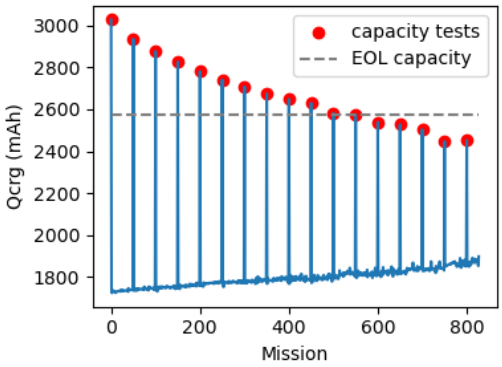

Figure 6.1.: $Qcrg$ for MP1. The values measured at the capacity tests are shown as dots.

$V_{var}^{(segment,f,m)}$; the maximum, mean, and variance of the extracted charge, which we denote by $Qdis_{max}^{(segment,f,m)}$, $Qdis_{mean}^{(segment,f,m)}$, $Qdis_{var}^{(segment,f,m)}$, respectively.

Temperature-related features: the maximum temperature during each discharging segment, denoted by $T_{max}^{(segment,b,m)}$.

6

Feature selection

We select the 16 most important features for RUL prognostics based on their Shapley values [17]. The relative importance of each feature is given in Table 6.2. The top 50% of the features with the highest importance, $V_{min}^{take-off}$ through $Qdis_{max}^{take-off}$, have been selected for RUL prognostics development. These values are referred to as $\mathbf{x}_m^f \in \mathbb{R}^{16}$. These values are normalized using a z-score normalization [18]:

$$\hat{\mathbf{x}}_m^b = \frac{\mathbf{x}_m^f - \mu}{\sigma}, \tag{6.1}$$

where μ and σ refer to the mean and standard deviation of the dataset.

6.5 Probabilistic battery useful life prognostics using Mixture Density Networks

In this section we propose a Mixed Density Network (MDN) [19, 20] to estimate the distribution of the RUL of the eVTOL batteries.

Figure 6.2 illustrates the architecture of the MDN considered, with an input layer, L dense hidden layers, and the output layer. The network has parameters θ. The input vector of normalized features from the current and previous missions before each capacity test m, $m-50$, ...$m-50N$ (see Section 6.4) $\hat{\mathbf{x}}$ is mapped to a three-fold output: the means $\mu_j(\hat{\mathbf{x}},\theta)$, the standard deviations $\sigma_j(\hat{\mathbf{x}},\theta)$, and a mixture coefficient $\alpha_j(\hat{\mathbf{x}},\theta)$. With

Feature	Importance	Feature	Importance
$V_{min}^{take-off}$	**95.4**	$Qdis_{max}^{cruise}$	45.9
$V_{mean}^{take-off}$	**94.7**	T_{max}^{cruise}	45.4
$C^{measure}$	**93.4**	$T_{max}^{landing}$	41.1
$V_{var}^{take-off}$	**92.4**	$T_{max}^{take-off}$	38.8
V_{max}^{cruise}	**87.8**	Δ^{rest}	36.5
$Qcrg$	**87.1**	$V_{max}^{landing}$	35.5
Δ^{CV}	**86.5**	$\Delta^{take-off}$	23.4
V_{min}^{cruise}	**78.8**	Δ^{cruise}	19.7
V_{mean}^{cruise}	**63.8**	$\Delta^{landing}$	19.4
$V_{var}^{landing}$	**59.3**	Δ^{CC}	12.9
$V_{mean}^{landing}$	**57.4**	$Qdis_{var}^{cruise}$	3.5
$V_{max}^{take-off}$	**57.2**	$Qdis_{max}^{landing}$	2.4
$V_{min}^{landing}$	**51.6**	$Qdis_{mean}^{cruise}$	2.3
$Qdis_{var}^{take-off}$	**47.7**	V_{var}^{cruise}	2.2
$Qdis_{mean}^{take-off}$	**46.5**	$Qdis_{var}^{landing}$	1.4
$Qdis_{max}^{take-off}$	**45.9**	$Qdis_{mean}^{landing}$	1.2

Table 6.2.: SHAP values (importance) for the 32 considered features; top 50% of the features are selected for RUL prognostics (in **bold**).

this, the probability density of the RUL is estimated as a mixture of J normal distributions as follows:

$$p(\text{RUL}|\hat{\mathbf{x}},\theta) = \sum_{j=1}^{J} \alpha_j(\hat{\mathbf{x}},\theta)\phi\left(\text{RUL}|\mu_j(\hat{\mathbf{x}},\theta),\sigma_j(\hat{\mathbf{x}},\theta)\right),$$

where ϕ denotes the pdf of the normal distribution, given mean μ and standard deviation σ. Instead of using a least-square loss, the loss function of the MDN is given by the negative log-likelihood:

$$L(\hat{\mathbf{x}},\text{RUL},\theta) = -\sum_{j=1}^{J} \log p(\text{RUL}|\hat{\mathbf{x}},\theta).$$

6.5.1 Results - probabilistic RUL prognostics

We illustrate the RUL estimation methodology for the eVTOL batteries. We employ a 6-fold cross validation to train and test the MDN. For each fold, several eVTOLs are randomly selected for testing. The test data of each fold contains one randomly selected baseline mission profile (out of a total of three baseline mission profiles of VAH01, VAH17, and VAH27) and 5 additional mission profiles. Each fold contains a total of approximately 6.000 missions.

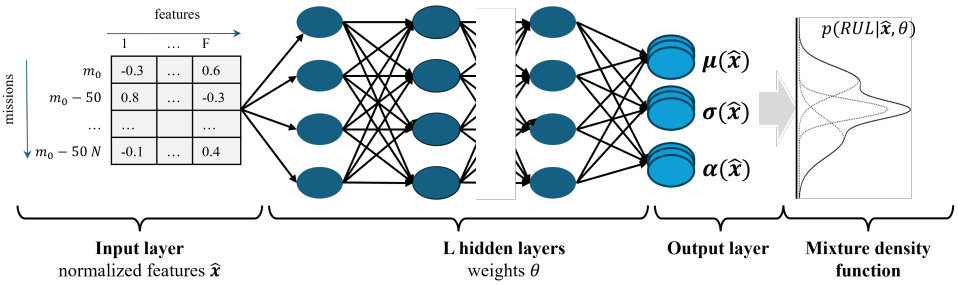

Figure 6.2.: Architecture of the MDN neural network used to generate probabilistic RUL prognostics.

Following hyper-parameter tuning, we consider $L = 6$ dense hidden layers. The layers have 24, 122, 116, 116, 90, and 38 units, respectively. The first five layers use the ReLu activation function, and the last one a tanh activation function. The output of the MDN consists of a mixture of $J = 3$ normal distributions. The MDN is optimised using the RMSprop [21] algorithm with a learning rate of 0.01.

Table 6.3 gives the performance of the MDN for each eVTOL in the test set of each fold: the Mean Absolute Error (MAE), the Root Mean Square Error (RMSE), and the Continuous Ranking Probability Score (CRPS). The results show that the typical MAE is around 30 missions. Additionally, in nearly all folds, our approach leads to a low CRPS score, indicating a sharp estimate of the distribution of the RUL.

Figure 6.3 shows three examples of the estimated distribution of the RUL: VAH20 for fold 1, VAH13 for fold 2, and VAH22 for fold 3. The figure shows the actual RUL (dashed line), as well as the expected predicted RUL (the mean of the estimated distribution of the RUL) and the 5-95 percentile of the estimated RUL distribution every 10th mission. For VAH13 and VAH22, the distribution of the RUL is centered around the actual RUL. For VAH13, the variance of the estimated RUL distribution decreases as the battery reaches its EOL. For VAH20, despite having a high CRPS score, the estimate distribution of the RUL is increasingly sharp as the battery reaches its EOL.

6.6 Adaptive maintenance planning of eVTOLs using RUL prognostics

In Section 6.5 we obtained estimates of the distribution of the RUL of eVTOL batteries after every mission. We assume that each eVTOL perfoms n missions per day (Section 6.2). For maintenance planning of the batteries of the fleet V of eVTOLs, we consider the estimated RUL distribution $RUL^v_{d_0}$, $v \in V$, at the start of each day d_0.

To ensure safe eVTOL operations, we define the following target day d^*_v to reliably replace the battery of eVTOL $v \in V$:

$$d^*_v = d_0 + \max\{d : \mathbb{P}[RUL^v_{d_0} \leq d] \leq P^*, d \in \mathbb{N}\}, \tag{6.2}$$

with $d_0 + d$ a battery replacement day, $d > 0$, and P^* a reliability threshold. Here, we

Fold 1				**Fold 2**			
VAH#	MAE	RMSE	CRPS	VAH#	MAE	RMSE	CRPS
VAH01	63.69	68.15	47.29	VAH01	56.1	62.42	43.2
VAH02	35.41	37.37	24.92	VAH05	29.4	37.0	19.65
VAH13	17.06	20.81	13.02	VAH06	61.21	64.88	47.26
VAH20	56.06	59.04	42.51	VAH13	32.78	36.06	22.36
VAH28	22.01	25.47	18.12	VAH15	22.54	24.2	14.79
VAH30	17.5	21.47	12.1	VAH16	20.32	22.34	14.41
ALL	35.29	38.72	26.33	**ALL**	37.06	41.15	26.94
Fold 3				**Fold 4**			
VAH#	MAE	RMSE	CRPS	VAH#	MAE	RMSE	CRPS
VAH10	10.4	12.33	7.18	VAH02	20.21	27.1	18.22
VAH11	66.9	75.07	53.55	VAH06	29.36	33.22	19.54
VAH17	34.45	38.83	24.11	VAH17	23.04	27.71	15.99
VAH22	9.62	13.74	8.33	VAH20	57.5	59.24	42.48
VAH23	98.7	125.89	72.87	VAH26	21.85	27.41	17.86
VAH25	51.79	74.78	37.48	VAH30	7.59	9.46	7.85
ALL	45.31	56.77	33.92	**ALL**	26.59	30.69	20.32
Fold 5				**Fold 6**			
VAH#	MAE	RMSE	CRPS	VAH#	MAE	RMSE	CRPS
VAH05	23.88	28.56	16.24	VAH10	5.59	7.35	6.41
VAH12	52.09	59.95	39.32	VAH12	61.23	66.06	48.09
VAH15	11.31	13.89	8.25	VAH22	11.77	14.98	8.44
VAH16	17.53	21.85	13.57	VAH24	20.93	25.28	14.27
VAH24	11.84	16.03	9.8	VAH25	39.64	50.91	28.39
VAH27	26.8	34.61	21.95	VAH27	36.84	40.62	24.11
ALL	23.91	29.15	18.19	**ALL**	29.33	34.2	21.62

Table 6.3.: Probabilistic RUL prognostics performance: MAE, RMSE, CRPS (flight missions).

ensure that the probability of the battery reaching its EOL before maintenance day d_0+d is at most P^*.

The eVTOL battery replacements are ideally planned as late as possible to minimize battery waste, while satisfying the reliability criteria in eq. 6.2, i.e., while limiting the probability that the battery is still in use after it reaches its EOL.

We consider a rolling horizon planning approach. At current day d_0 we consider planning a battery replacement withing a window $D_{d_0} = [d_0+1, d_0+k]$ based on the prognostics available at d_0. We next slide to a new day $d_0+l, l \geq 1$, when we update the

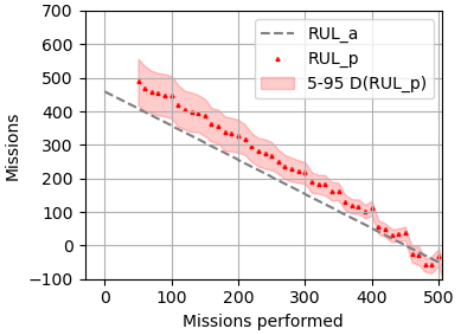

(a) VAH20, fold 1

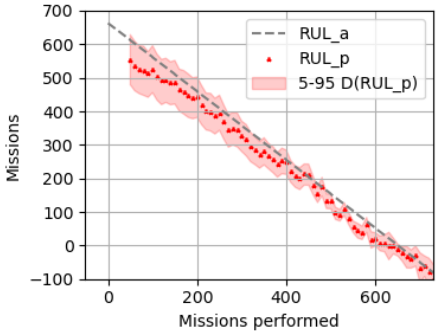

(b) VAH13, fold 2

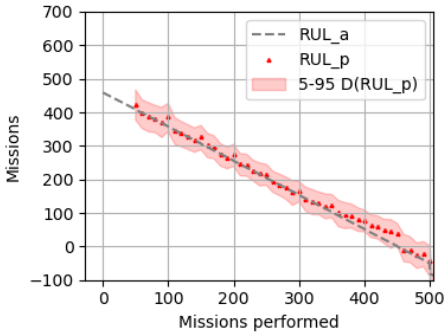

(c) VAH22, fold 3

Figure 6.3.: The actual RUL RUL_a, the expected predicted RUL RUL_p and the 5-95 percentile of the estimate distribution of the RUL for VAH20, VAH13, VAH22.

prognostics with newly available measurements, and consider a new planning window $D_{d_0+l} := [d_0+1+l, d_0+l+k]$.

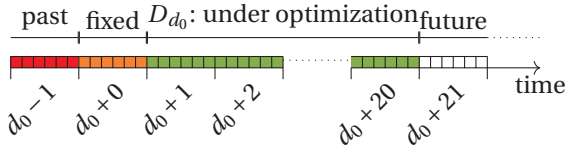

Figure 6.4.: Illustration of the maintenance planning time window at current day d_0, with $k = 20$, such that $D_{d_0} = [d_0+1, d_0+20]$.

At day d_0 we decide whether to plan a battery replacement at some day d in the planning window D_{d_0}, or to postpone the decision for the next planning window D_{d_0+l}. In case eVTOL $v \in V$ is scheduled for battery replacement before d_v^*, a penalty c_{early} is incurred for every wasted day of the battery life. In case eVTOL $v \in V$ is scheduled for

battery replacement after d_v^*, then a penalty c_{late} is incurred for every day the battery is used after the target d_v^*. We consider a cost c_{vd} of planning a battery removal at day $d \in D_{d_0}$, where:

$$c_{vd} = c_{early}(d_v^* - d)^+ + c_{late}(d - d_v^*)^+. \tag{6.3}$$

We define $c_{early} = c_{replace}/L$, where L is a nominal average battery life of the eVTOLs. We define $c_{late} = (c_{unscheduled} - c_{replace})/L$. In case the battery replacement of eVTOL $v \in V$ is postponed for the next planning window, then a cost $c_v^{postpone}$ is incurred for every day the target replacement day d_v^* is exceeded, where:

$$c_v^{postpone} = c_{late}(d_0 + k + l - d_v^*)^+. \tag{6.4}$$

We consider the following integer linear program to plan battery replacements on day d_0.

Decision variables:

$$y_{vd} = \begin{cases} 1, & \text{battery of } v \in V \text{ is planned} \\ & \text{for replacement on } d \in D_{d_0}, \\ 0, & \text{otherwise,} \end{cases} \tag{6.5}$$

$$z_v = \begin{cases} 1, & \text{replacement for battery of} \\ & v \in V \text{ is not planned in } D_{d_0} \\ 0, & \text{otherwise.} \end{cases} \tag{6.6}$$

Objective function: The aim is to minimize the total costs of battery maintenance:

$$\min_{y,z} \sum_{1 \le v \le |V|} \left(\sum_{d \in D_{d_0}} c_{vd} y_{vd} \right) + c_v^{postpone} z_v \tag{6.7}$$

Constraints:

We consider the following constraints:

$$\sum_{d \in D_{d_0}} y_{vd} + z_v = 1 \qquad \forall v \in V, \tag{6.8}$$

$$\sum_{v \in V} y_{vd} \le h \qquad \forall d \in D_{d_0}. \tag{6.9}$$

Constraint (6.8) ensures that at day d_0 a battery replacement is planned for each eVTOL, or that the battery replacement is postponed. Constraint (6.9) ensures that the daily battery replacement capacity H of the eVTOL hub is not exceeded.

6.6.1 Results

We consider $|V| = 50$ eVTOLs. Each eVTOL performs $n = 10$ flight missions (to and from the eVTOL hub) per day. For maintenance planning, 50 eVTOL batteries are randomly sampled from the test sets of all the six folds (see Section 6.5). At $d_0 = 1$, the ages of

the eVTOLs batteries are initialised as a random value between 0 and their actual EOL. We consider $P^* = 0.1$, $k = 10, h = 1$, $l = 1, c_{replace} = 100, c_{unscheduled} = 1000$, and $L = 50$. A simulation of 10 years of eVTOL operations has been performed. As soon as one eVTOL battery is replaced or reaches its EOL (unscheduled battery replacement), this battery is replaced with a randomly selected battery from the test sets of all six folds (see Section 6.5). The age of this new battery is then initiated at 0 missions.

Following a simulation of 10 years, 1.786 batteries were used. Of these 1.786 batteries, **1.704** were replaced before their EOL, and **82** batteries needed unscheduled replacement since they reached their EOL unexpectedly. Our approach results in a total yearly cost of **25.240** units. Figure 6.5 shows a histogram of the wasted life of the batteries (in days), i.e., the number of days the batteries were not used because they were preventively replaced and thus did not reach their EOL. Using our approach, the batteries were used for up to 88,1% of their actual lifetime.

Figure 6.6 shows two distinct planning moments for the eVTOL batteries. At $d_0 = 105$, we consider a planning window of $D_{105} = [106, 125], l = 1, k = 20$ when the batteries of eVTOLs $0, 1, 4, 6, 7, 8, 11, 13, 16, 18, 22$ are planned to be replaced within the next days [106,125]. EVTOL 11 is planned for battery replacement the next day (this replacement can no longer be changed since no further planning re-optimisation can be done). EVTOL 16 is having the battery replaced on day 116, which is just before this battery reaches its EOL on day 117. As of now, the battery of EVTOL 18 will fail at day 122 before its planned replacement. However, this planning may be re-optimized in the next days since the next re-planning moment $d_0 + l = 106 < 122$.

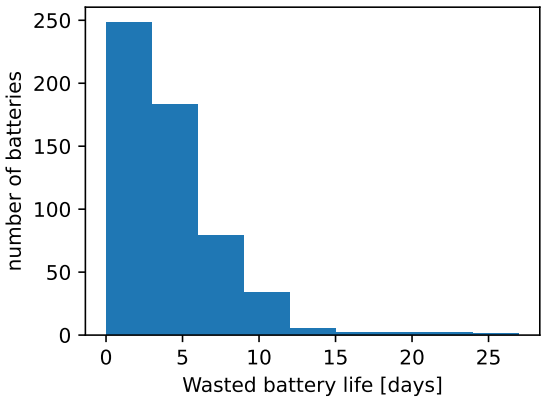

Figure 6.5.: Histogram of the wasted battery life - based on the simulation of 10 year of eVTOL operations.

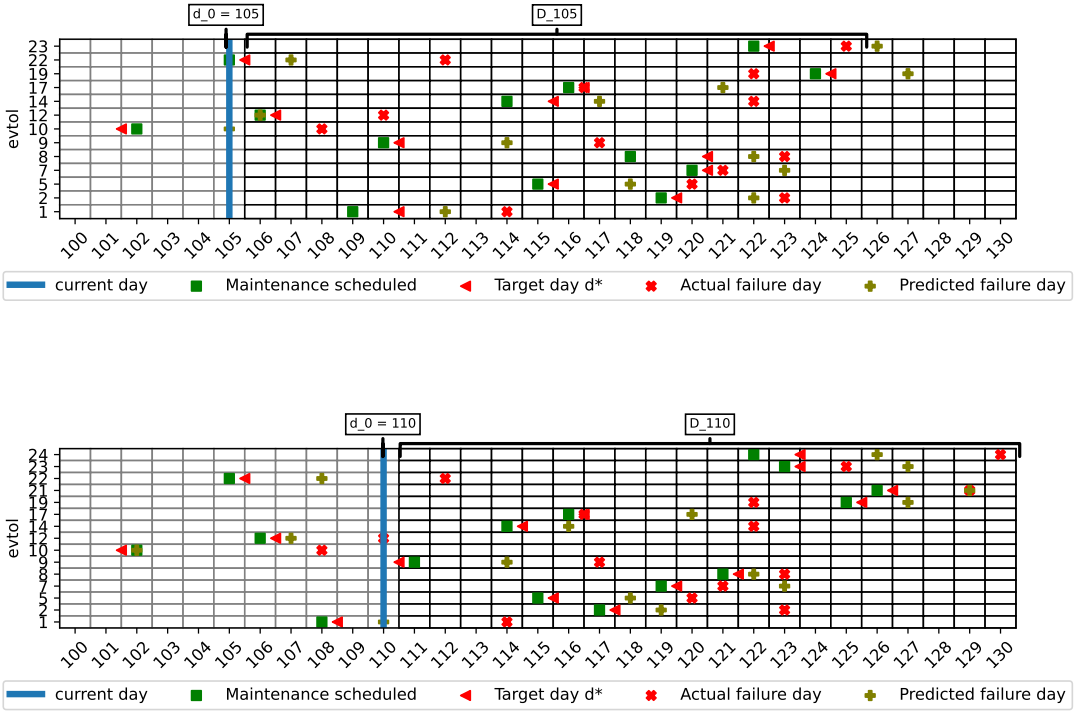

Figure 6.6.: Maintenance planning for the 50 eVTOLs selected in the period 100th day - 130th day. The figure shows only the eVTOLs that are subject to maintenance planning. Two distinct planning moments are shown at $d_0 = 105$ with planning time window $D_{d_0} = [105+1, 105+20]$ and $l = 1, k = 20$, and at $d_0 = 110$ with planning time window $D_{d_0} = [110+1, 110+20]$ and $l = 1, k = 20$.

6.6.2 Performance evaluation against maintenance planning benchmarks

We compare our approach with two benchmarks: *Oracle planning* and *RUL point-estimate planning* algorithms. Both use the same framework as our proposed maintenance planning approach. The *Oracle planning* assumes that the actual RUL of the batteries is known in advance. As such, $d^* = EOL$ of the batteries. The *RUL point-estimate planning* uses the mean of the estimated RUL distribution (point estimate, instead of the distribution) such that $d^* = d_0 + \mathbb{E}[RUL^v_{d_0}]$.

Figures 6.7 and 6.8 show the total yearly amount of batteries replaced for the three considered planning approaches. As expected, the Oracle leads to **0** unscheduled battery replacements. The *RUL point-estimate planning* leads to the highest number of unscheduled battery replacements (**436** unscheduled battery replacements in 10 years of eVTOL operations) and the highest total costs among all three approaches. This shows the relevance of considering the estimation of the distribution of the RUL when planning maintenance (leading to 82 unscheduled replacements), instead of using RUL point estimates.

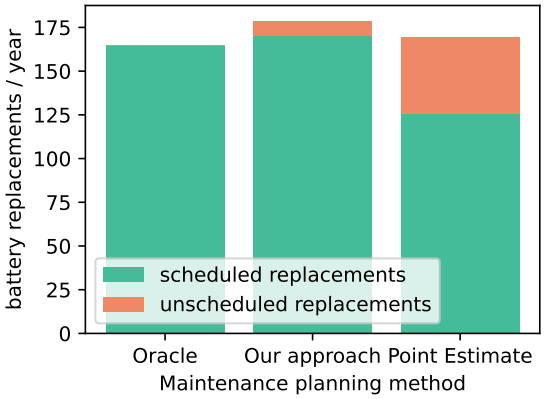

Figure 6.7.: Average number of batteries used per year, given the *Oracle, the RUL point estimate (RUL point)* and *Our (RUL distribution)* planning.

6.7 Conclusion

This chapter proposed a data-driven predictive maintenance planning model for Lithium-ion batteries of electric Take-Off and Landing (eVTOL) aircraft. Sensor measurements are continuously recorded on the condition of the batteries. Based on these measurements, we employ Mixed Density Networks to estimate the distribution of the RUL of the batteries, i.e., we obtain probabilistic RUL prognostics. These prognostics are further integrated into an adaptive maintenance planning model that specifies optimal replacement times. The planning model is adapted periodically, as more measurements

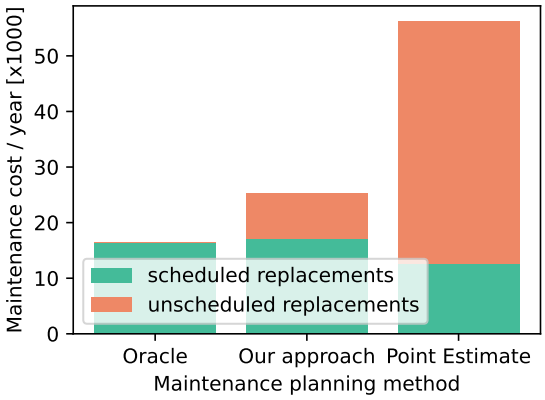

Figure 6.8.: Average maintenance costs per year, given the *Oracle*, *the RUL point estimate (RUL point)*, and *Our (RUL distribution)* planning.

become available. The aim is to limit the risk of using the eVTOL beyond them reaching their End-of-Life (EOL), while minimizing overall costs.

The results show that probabilistic RUL prognostics benefit the planning of the eVTOL maintenance. Firstly, despite the prognostics being imperfect, we show that the number of unscheduled battery replacements due to batteries reaching their EOL unexpectedly is low (1-2 unscheduled yearly replacements), when compared with an Oracle planning which has perfect knowledge of the actual EOL of the batteries. Secondly, we show that it is beneficial to estimate the distribution of the RUL (probabilistic RUL prognostics) instead of average values (point estimates) of the RUL when planning maintenance. The results show that up to 30% less yearly unscheduled battery replacements are achieved when considering probabilistic RUL prognostics for maintenance planning, rather than RUL point estimates.

Overall, our approach outlines an end-to-end framework for data-driven predictive maintenance of Lithium-ion batteries with reliability and cost-related objectives.

references

[1] M. Mitici and S. van Oosterom. “Adaptive predictive maintenance for the batteries of electric Vertical Take-off and Landing (eVTOL) aircraft using Remaining Useful Life prognostics”. In: *Proceedings of the 34th European Safety and Reliability Conference*. Stavanger, Norway, June 2025.

[2] H. Wei, B. Lou, Z. Zhang, B. Liang, F.-Y. Wang, and C. Lv. “Autonomous navigation for eVTOL: Review and future perspectives”. In: *IEEE Transactions on Intelligent Vehicles* (2024).

[3] S. Xiang, A. Xie, M. Ye, X. Yan, X. Han, H. Niu, Q. Li, and H. Huang. “Autonomous eVTOL: A summary of researches and challenges”. In: *Green Energy and Intelligent Transportation* (2023), p. 100140.

[4] N. Polaczyk, E. Trombino, P. Wei, and M. Mitici. “A review of current technology and research in urban on-demand air mobility applications”. In: *8th Biennial Autonomous VTOL technical meeting and 6th Annual electric VTOL Symposium*. Vertical Flight Soc. Mea, Arizona. 2019, pp. 333–343.

[5] M. Mitici, L. Jenneskens, Z. Zeng, and D. Coit. “Predictive Maintenance Planning For Batteries Of Electric Take-Off And Landing (eVTOL) Aircraft Using State-of-Health Prognostics”. In: *the 34th European Safety and Reliability Conference*. 2024, p. 117.

[6] H. Tian, P. Qin, K. Li, and Z. Zhao. “A review of the state of health for lithium-ion batteries: Research status and suggestions”. In: *Journal of Cleaner Production* 261 (2020), p. 120813.

[7] Y. Toughzaoui, S. B. Toosi, H. Chaoui, H. Louahlia, R. Petrone, S. Le Masson, and H. Gualous. “State of health estimation and remaining useful life assessment of lithium-ion batteries: A comparative study”. In: *Journal of Energy Storage* 51 (2022), p. 104520.

[8] M.-F. Ge, Y. Liu, X. Jiang, and J. Liu. “A review on state of health estimations and remaining useful life prognostics of lithium-ion batteries”. In: *Measurement* 174 (2021), p. 109057.

[9] Y. Li, K. Liu, A. M. Foley, A. Zülke, M. Berecibar, E. Nanini-Maury, J. Van Mierlo, and H. E. Hoster. “Data-driven health estimation and lifetime prediction of lithium-ion batteries: A review”. In: *Renewable and sustainable energy reviews* 113 (2019), p. 109254.

[10] R. Xie, R. Ma, S. Pu, L. Xu, D. Zhao, and Y. Huangfu. “Prognostic for fuel cell based on particle filter and recurrent neural network fusion structure”. In: *Energy and AI* 2 (2020), p. 100017.

[11] B. Zraibi, C. Okar, H. Chaoui, and M. Mansouri. “Remaining useful life assessment for lithium-ion batteries using CNN-LSTM-DNN hybrid method”. In: *IEEE Transactions on Vehicular Technology* 70.5 (2021), pp. 4252–4261.

[12] Z. Du, L. Zuo, J. Li, Y. Liu, and H. T. Shen. “Data-driven estimation of remaining useful lifetime and state of charge for lithium-ion battery”. In: *IEEE Transactions on Transportation Electrification* 8.1 (2021), pp. 356–367.

[13] A. Bills, S. Sripad, L. Fredericks, M. Guttenberg, D. Charles, E. Frank, and V. Viswanathan. “A battery dataset for electric vertical takeoff and landing aircraft”. In: *Scientific Data* 10.1 (2023), p. 344.

[14] L. Granado, M. Ben-Marzouk, E. S. Saenz, Y. Boukal, and S. Jugé. “Machine learning predictions of lithium-ion battery state-of-health for eVTOL applications”. In: *Journal of Power Sources* 548 (2022), p. 232051.

[15] M. Mitici, B. Hennink, M. Pavel, and J. Dong. “Prognostics for Lithium-ion batteries for electric Vertical Take-off and Landing aircraft using data-driven machine learning”. In: *Energy and AI* 12 (2023), p. 100233.

[16] J. Alba-Maestre, K. Prud’homme van Reine, T. Sinnige, and S. G. Castro. “Preliminary propulsion and power system design of a tandem-wing long-range eVTOL aircraft”. In: *Applied Sciences* 11.23 (2021), p. 11083.

[17] M. Scott, L. Su-In, *et al.* “A unified approach to interpreting model predictions”. In: *Advances in neural information processing systems* 30 (2017), pp. 4765–4774.

[18] J. Urbano, H. Lima, and A. Hanjalic. “A New Perspective on Score Standardization”. In: *Proceedings of the 42nd International ACM SIGIR Conference on Research and Development in Information Retrieval*. SIGIR’19. New York, NY, USA: Association for Computing Machinery, July 2019, pp. 1061–1064. ISBN: 978-1-4503-6172-9. DOI: 10.1145/3331184.3331315. (Visited on 09/25/2024).

[19] C. M. Bishop. “Mixture density networks”. In: (1994).

[20] C. Gu, Y. Zhao, and C. Zhang. “Learning to predict diverse human motions from a single image via mixture density networks”. In: *Knowledge-Based Systems* 253 (2022), p. 109549.

[21] M. Riedmiller and H. Braun. “A direct adaptive method for faster backpropagation learning: the RPROP algorithm”. In: *IEEE International Conference on Neural Networks*. Mar. 1993, 586–591 vol.1. DOI: 10.1109/ICNN.1993.298623. URL: https://ieeexplore.ieee.org/document/298623 (visited on 09/25/2024).

CHAPTER 7

eVTOL battery management: integrating operations with end-to-end maintenance planning

Predictive maintenance planning is usually considered in a two-stage approach, sequentially addressing (1) remaining useful life (RUL) estimation and (2) using these to perform maintenance planning. However, the objective of in the first stage, approaching the actual RUL as best as possible, does not guarantee that the total maintenance costs are also minimized. A maintenance planning model with this objective has not yet been studied.

In this chapter, we therefore develop a planning model which combines the two stages: the end-to-end maintenance planning model. A machine learning algorithm is trained to estimate the maintenance cost coefficients. The planning problem is taken into account during training, such that the algorithm is optimized to minimize the decision regret: the difference between the actual and optimal maintenance costs.

The model is implemented for battery maintenance for a fleet of electric vertical take-off and landing aircraft (EVTOL). We show that, when compared with the framework developed in the previous chapter, the number of breakdowns is reduced by 21%, and the maintenance costs by 9%. Compared with this algorithm, the decision regret is reduced from 49% to 36%.

Parts of this chapter are submitted as:

S. van Oosterom and M. Mitici. "End-to-end predict-then-optimize for maintenance planning of Lithium-Ion batteries". In: *Submitted to Transportation Research Part C: Emerging Technologies* (2025).

7.1 Introduction

Modern assets are continuously monitored by an increasing number of sensors that generate large amounts of data. Think of monitoring emerging technologies like, for example, wind turbines, high-speed railway systems and trains, or aircraft [2, 3]. Such data is used to foresee faults and failures, or to obtain Remaining Useful Life (RUL) prognostics. This information enables the optimization of maintenance planning of assets [4–7]. This is often referred to as predictive maintenance planning.

Recent studies on predictive maintenance propose two-stage approaches where the RUL prognostics and maintenance planning are decoupled [8–15]. In the first stage, condition monitoring measurements are used to estimate the Remaining Useful Life (RUL) of each individual asset using, for example, supervised machine learning [14]. The RUL prognostics are typically estimated as a point values, for example for turbofan engines using a convolution neural network [14, 16]. More recent studies have also focussed on developing probabilistic estimates of the RUL, by e.g. [5]. In the second stage, these RUL prognostics are integrated into maintenance planning for a set of assets, with limited maintenance capacity. This is implemented as e.g., a threshold-based approach [12], an integer linear program [14], a Markov Decision Process [17], a Model Predictive Control [18], or a Reward-Renewal process [19]. The advantage of such a two-stage approach is that is allows for a modular combination of data-driven, asset-specific RUL prognostics and advanced maintenance planning models.

In the first stage of such approaches, the focus is on obtaining RUL prognostics with a high accuracy such that the difference between the actual RUL and the estimated RUL is minimal. However, in the second (planning) stage, an improvement in the accuracy of RUL estimates does not guarantee an improvement in the maintenance planning decisions and the associated costs. The performance gap in terms of these costs is measured by the *decision regret*: the difference between the true cost obtained with an optimal decision based on perfect RUL prognostics (Oracle) and the true cost obtained with decisions based on the data-driven generated RUL estimates. The reason behind this gap is the fact that the RUL prognostics, even when their accuracy is high, are trained obtained with machine learning models that are oblivious of the objectives of the maintenance planning models. Overcoming this problem requires feedback from the maintenance planning model (second stage) towards the RUL regressor (first stage).

For general optimization problems with uncertain variables, end-to-end frameworks have been recently introduced to account for the shortcomings of two-stage planning approaches [20–22]. This class of problems is referred to as Predict-Then-Optimize (PTO) problems. In end-to-end optimization, similar to the two-stage approaches, a machine learning regressor is trained to estimate the model parameters from measured data. In such end-to-end approaches, however, the regressor is trained with knowledge of the optimization problem itself. This is performed by integrating the decision regret in the training of the regressor. Several end-to-end algorithms have been developed for this, such as the *Smart Predict-then-Optimize* (SPO+) loss [23–25], the *differentiable black-box solver* [26], and the *differentiable perturbed*

optimizer (DPO) [27]. For an overview of end-to-end optimization frameworks, see Tang and Khalil [28].

In this chapter, we propose an end-to-end framework for data-driven, dynamic predictive maintenance planning of a set of assets. Our approach uses health-monitoring measurements to estimate maintenance planning costs, while incorporating the decision regret into a loss function which expands the existing SPO+ loss. This approach is distinct from existing studies on predictive maintenance that use a two-stage approach where data is used in the first stage to estimate the best possible RUL estimates, while these estimates are further used for maintenance planning in a second stage, as performed in Chapter 6 [5, 14, 16]. In this chapter, instead, *decision regret-minimizing prognostics are made*. Compared to standard end-to-end optimization frameworks, our approach differs in two ways. Firstly, we consider the case when the sensor measurements are uncorrelated across assets. This is a relevant consideration in practice, where assets (in our case, batteries) are use independently of each other. This consideration is leveraged by designing and training the machine learning algorithm to generate maintenance costs for each asset separately. This approach, however, is different from conventional end-to-end frameworks, where all unknown parameters are estimated by a single machine learning model, allowing faster training. Secondly, we assume that the maintenance planning decisions can be re-evaluated over time. This is leveraged by formulating the problem as a rolling horizon model, instead of the conventional single stage decision problem used for end-to-end optimization frameworks. Lastly, for every stage in the rolling horizon, we formulate the maintenance planning problem as an Integer Linear Program (ILP). Compared to a fully machine learning approach to optimize maintenance planning, such as reinforcement learning [29], the use of an ILP provides transparency to the overall planning approach. To the best of our knowledge, this is an innovative approach for maintenance planning problems specifically designed for predictive maintenance.

We illustrate our approach for a fleet of electric Vertical Takeoff and Landing (eVTOL) aircraft equipped with Li-ion batteries. We apply our end-to-end framework for predictive maintenance planning of these eVTOL batteries. We compare our approach with conventional two-stage maintenance planning approaches, which make use of RUL prognostics. The results show that our end-to-end framework leads to a 21% reduction in the total number of unforeseen battery failures when compared to the (best-case) two-stage maintenance planning framework. In this context, we also show that our approach reduces the decision regret (of maintenance costs) by 30%.

The main contributions of this chapter are:

- We develop an end-to-end, dynamic framework for predictive maintenance of a set of assets, where the health condition measurements of the assets are directly informing the maintenance scheduling model. This is in contrast with the majority of studies on predictive maintenance that use a two-stage approach where in the first stage data-driven RUL estimates are obtained, which are informing the maintenance scheduling model in a second, independent stage [12, 14, 30].

- We show that predictive maintenance planning for a set of assets can be formulated as a general end-to-end optimization problem [28]. Distinct from general end-to-end optimization problems, we *decompose* the end-to-end optimization problem into identical maintenance planning problems for each individual asset. This is enabled by the fact that the sensor measurements are uncorrelated across assets.

- We apply our framework to plan maintenance for Li-ion batteries of a fleet of eVTOL aircraft. We show that this method increases the reliability of the maintenance schedules while reducing costs compared to a two-stage predictive maintenance approach.

The remainder of this chapter is structured as follows. In Section 7.2, the maintenance planning problem for a set of assets is introduced. In Section 7.3 we discuss the predictive maintenance planning model formulation. We discuss the conventional two-stage predictive maintenance planning models, based on estimates of the Remaining Useful Life of the assets. After this, we introduce our proposed end-to-end predictive maintenance planning framework. In Section 7.4, we apply our framework for the case of maintenance planning of Li-ion batteries of a fleet of eVTOL aircraft. The results of this case study are presented in Section 7.5. Conclusions are given in Section 7.6.

7.2 Predictive maintenance planning for a set of assets

We consider a set $\mathscr{A}$ of assets and a maintenance planning horizon of days $\mathscr{D}$. The state-of-health of each asset degrades over time until an asset failure (the end-of-life is reached). When this occurs, the asset is immediately maintained to a good-as-new condition and a large penalty $c_{\text{unscheduled}}$ is incurred.

Each asset is continuously monitored by sensors: let $\mathbf{x}_a \in \mathbb{R}^n$ denote the measurements of asset $a \in \mathscr{A}$ at the start of day $d \in \mathscr{D}$, where n denotes the number of sensor measurement features. These measurements provide information on the health condition of the assets.

To avoid failures, this data may be leveraged to preemptively maintain assets. The costs of preventive maintenance is $c_{\text{replace}} \ll c_{\text{unscheduled}}$. At most H assets can be replaced per day. For both working and failed assets, maintenance takes an entire day.

At the start of the current day $d_0 \in \mathscr{D}$, maintenance is planned for days $d_0+1, d_0+2, \ldots$. Maintenance that needs to be performed exactly on the current day d_0 is fixed. Next, we shift to the new current day d_0+1 and the maintenance planning horizon $d_0+2, d_0+3, \ldots$.

We are interested in determining which assets should be scheduled for replacement by leveraging the measurements $(\mathbf{x}_a)_{a\in\mathscr{A}}$. We aim to determine an optimal replacement day for each assets such that (1) failures are avoided due to

high failure costs, while (2) assets are used as long as possible, or equivalently the wasted life of the assets is minimized.

7.3 Predictive maintenance planning model formulation

In this section we introduce four modeling paradigms for the dynamic predictive maintenance planning problem from Section 7.2. Firstly, we consider the maintenance planning model for the idealized case in which the *actual* RUL of each asset is known in advance (an oracle perspective). We next consider the same planning problem, but for the case when the RUL is not known in advance (the realistic perspective). For this, we propose three algorithms where: (i) only a *point estimate* of the actual RUL of the assets is obtained at various moments in time based on the sensor measurements of these assets; these estimates then become the input of a maintenance planning model (Section 7.3.2), (ii) the *distribution* of the actual RUL of the assets is obtained at various moments in time; these estimated distributions then become the input of a maintenance planning model (Section 7.3.2), and (iii) the sensor measurements are directly used to estimate the cost coefficients of the same maintenance planning model (Section 7.3.3) without the intermediate step of estimating the RUL of the assets.

Algorithm 6 shows the rolling horizon predictive maintenance framework. We consider planning maintenance of a set $\mathscr{A}$ of assets. At the start of the current day $d_0 \in \mathscr{D}$, the (unknown) Remaining Useful Life (RUL), i.e., the days until the end-of-life, of asset a is denoted by r_a. The assets which failed on $d_0 - 1$ and the assets which are scheduled for maintenance on d_0 are denoted by $\mathscr{A}^f$ and $\mathscr{A}^s$, respectively. At the start of the current day d_0 we plan replacements of the assets $a \in \mathscr{A}' = \mathscr{A} \setminus (\mathscr{A}^f \cup \mathscr{A}^s)$ within a time window $\mathscr{D}_{d_0} = \{d_0 + 1, ..., d_0 + k\}$, $k \geq 1$. The replacements planned exactly on d_0 are fixed. After planning and performing maintenance, we shift to the next day $d_0 + 1$, the next planning window $\mathscr{D}_{d_0+1} := \{d_0 + 2, ..., d_0 + k + 1\}$, and re-compute the maintenance schedule, see also Figure 7.1.

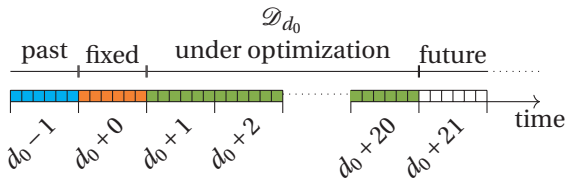

Figure 7.1.: Illustration of the maintenance planning time window at current day d_0, with $k = 20$, $\mathscr{D}_{d_0} = \{d_0 + 1, d_0 + 2, ...d_0 + 20\}$.

For maintenance planning, we consider a linear programming formulation. At d_0,

the decision variables considered are:

$$y_{ad} = \begin{cases} 1, & \text{if maintenance for asset } a \text{ is scheduled on day } d_0 + d, \\ 0, & \text{otherwise,} \end{cases} \tag{7.1a}$$

$$y_a^{\text{postpone}} = \begin{cases} 1, & \text{if maintenance for asset } a \text{ is not scheduled in } \mathscr{D}_{d_0}, \\ 0, & \text{otherwise,} \end{cases} \tag{7.1b}$$

with $d \in \{1, ..., k\}$. For any asset $a \in \mathscr{A}'$, let $\mathbf{y}_a = (y_{a1}, ..., y_{ak}, y_a^{\text{postpone}})^T$. Let $\mathbf{y} = (\mathbf{y}_a)_{a \in \mathscr{A}'}$ denote the vector of all decision variables.

Algorithm 6: Rolling horizon predictive maintenance planning for a set of assets.

Data: Set of assets $\mathscr{A}$, days of operations $\mathscr{D}$, hangar capacity H, maintenance costs $c_{\text{unscheduled}}$ and c_{replace}.
Result: Maintenance schedule at total cost C

Initialize $C = 0$;
Initialize scheduled maintenance days for assets for $a \in \mathscr{A}$: $d_a \leftarrow$ `None` ;
for *days* $d_0 \in \mathscr{D}$ **do**
  Obtain the condition measurements $\mathbf{x}_a$ from the assets $a \in \mathscr{A}$;
  Obtain the failed assets $\mathscr{A}^f \subset \mathscr{A}$, and the to-be-maintained assets $\mathscr{A}^s = \{a \in \mathscr{A} : d_a = d_0\}$;
  Set $\mathscr{A}' = \mathscr{A} \setminus (\mathscr{A}^f \cup \mathscr{A}^s)$;
  Plan maintenance for assets $\mathscr{A}'$, obtain the decision variables y and y^{postpone} (Section 7.3.1, 7.3.2, 7.3.3) ;
  for *asset* $a \in \mathscr{A}'$ **do**
    Set $d_a \leftarrow d_0 + d$ if $y_{ad} = 1$ or $d_a \leftarrow$`None` if $y_a^{postpone} = 1$;
  end
  Use assets $\mathscr{A}'$ for operations;
  Perform maintenance on assets $\mathscr{A}^f \cup \mathscr{A}^s$;
  Set $C \leftarrow C + c_{\text{unscheduled}}|\mathscr{A}^f| + c_{\text{replace}}|\mathscr{A}^s|$;
end

7.3.1 Oracle maintenance planning

We first consider the situation in which the *actual* RUL of the assets is known in advance. As before, let r_a denote the actual RUL of asset $a \in \mathscr{A}'$ at d_0. We aim to determine an optimal maintenance schedule for all assets $a \in \mathscr{A}'$. Clearly, the optimal moment to replace asset a is at $d_0 + r_a$. The cost to maintain an asset $a \in \mathscr{A}'$ in d days such that $d + d_0 \in \mathscr{D}_{d_0}$, given RUL r_a is:

$$c(d, r_a) = \frac{c_{\text{replace}}}{L}(r_a - d)^+ + \frac{c_{\text{unscheduled}} - c_{\text{replace}}}{L}(r_a - d)^-, \tag{7.2}$$

where c_{replace} and $c_{\text{unscheduled}}$ are the costs of a planned replacement, and of an unscheduled replacement due to a failure, respectively (see Section 7.2). Also, L denotes a nominal useful life of the assets. In case the replacement is postponed to the next planning window, the following cost c^{postpone} is incurred:

$$c^{\text{postpone}}(r_a) = \frac{c_{\text{unscheduled}} - c_{\text{replace}}}{L}(r_a - k - 1)^{-}. \tag{7.3}$$

For any asset $a \in \mathscr{A}'$, let:

$$\mathbf{c}_a = \mathbf{h}(r_a) := (c(r_a, 1), ..., c(r_a, k), c^{\text{postpone}}(r_a))^T \in \mathbb{R}^{k+1}, \tag{7.4}$$

Let $\mathbf{c} = (\mathbf{c}_a)_{a \in \mathscr{A}'}$ denote the vector of all maintenance costs.

We consider the following optimization model to plan maintenance for the set $\mathscr{A}$ of assets:

$$\min_{y} \quad \mathbf{c}^T \mathbf{y}, \tag{7.5a}$$

$$\text{s.t.} \quad \mathbb{1}^T \mathbf{y}_a = 1 \qquad \forall a \in \mathscr{A}', \tag{7.5b}$$

$$\sum_{a \in \mathscr{A}} y_{ad} \leq H \qquad \forall d \in \{1, ..., k\}, \tag{7.5c}$$

$$\mathbf{y}_a \in \{0,1\}^{k+1} \qquad \forall a \in \mathscr{A}'. \tag{7.5d}$$

Here, equation (7.5a) gives the cost of the planned maintenance. Constraints (7.5b) ensures that for each asset, maintenance is planned or postponed, where $\mathbb{1}$ denotes the all-ones vector. Constraints (7.5c) ensure that the hangar capacity is not exceeded. Last, constraints (7.5d) ensure that the variables take binary values.

7.3.2 Two-stage algorithms for the predictive maintenance problem

The RUL r_a of an asset $a \in \mathscr{A}$ is in fact not known in advance. By extension, the cost vector $\mathbf{c}_a$ is also unknown. What is often available are sensor measurements $\mathbf{x}_a$ continuously recorded for an asset a. As such, predictive maintenance planning is a Predict-Then-Optimize (PTO) problem [28]. Many studies leverage this data $\mathbf{x}_a$, using for example machine learning regressors $g(\mathbf{x}_a, \theta)$ to estimate the RUL of asset $a \in \mathscr{A}'$. Subsequently, the estimated RUL is considered in maintenance planning models to generate maintenance cost estimates $\hat{\mathbf{c}}$ [14]. We note that this approach is a *two-stage* PTO approach in the sense that the training of the machine learning regressors for RUL estimation, and the generation of the RUL estimates is performed independent of the maintenance planning models and without knowledge of c_{replace}, $c_{\text{unscheduled}}$, and the average asset lifetime at the moment of RUL generation.

In the following, we distinguish between i) a two-stage maintenance planning where g generates a point estimate of the RUL (2S-P algorithm, Section 7.3.2), and ii) a two-stage maintenance planning where g generates a distribution of the RUL (2S-D algorithm, Section 7.3.2). All algorithms are summarized in Table 7.1.

	Oracle	Two-stage planning 2S-P	Two-stage planning 2S-D	E2E-M planning
Data-driven estimated variable	n.a.	RUL point estimate $\hat{r}_a$	RUL distribution estimate $\hat{p}_a$	Maintenance cost coefficients $\hat{\mathbf{c}}_a$
RUL estimate	actual RUL r_a	$\hat{r}_a = g_{2SP}(\mathbf{x}_a, \theta_{2SP})$ (first stage)	$\hat{p}_a = g_{2SD}(\mathbf{x}_a, \theta_{2SD})$ (first stage)	none
Maintenance costs estimate	$\mathbf{c}_a = \mathbf{h}(r_a)$	$\hat{\mathbf{c}}_a = \mathbf{h}(\hat{r}_a)$ (second stage)	$\hat{\mathbf{c}}_a = \mathbf{h}_{2SD}(\hat{p}_a)$ (second stage)	$\hat{\mathbf{c}}_a = f(\mathbf{x}_a, \theta_{E2E})$

Table 7.1.: The Oracle, the two-stage maintenance planning with RUL Point estimates $\hat{r}_a$ (2S-P, Sec. 7.3.2), the 2Stage maintenance planning with RUL Distribution estimates $\hat{p}_a$ (2S-D, Sec. 7.3.2), and the End-to-end Maintenance (E2E-M, Sec. 7.3.3) planning for asset a in a rolling horizon framework. Here, $\mathbf{x}_a$ is the sensor data of asset a, g, and f are machine learning regressors with parameters θ, and h are cost functions.

Two Stage predictive maintenance planning with RUL **Point** estimates (2S-P)

Conventionally, a two-stage approach for the predictive maintenance problem uses RUL point estimates (a 2S-P approach) [6]. Figure 7.2 shows such an 2S-P approach.

Stage 1:
A machine learning regressor g_{2SP} with parameters θ_{2SP} generates point estimates of the RUL of an asset $a \in \mathscr{A}'$: $\hat{r}_a = g_{2SP}(\mathbf{x}_a, \theta_{2SP})$, where $\mathbf{x}_a$ are sensor measurements. It estimates the RUL by minimizing a loss function $\mathscr{L}_{2SP}$, given by the 2-norm:

$$\mathscr{L}_{2SP}(r, \hat{r}) = \|r - \hat{r}\|_2. \tag{7.6}$$

We note that the training g is performed independently from the subsequent maintenance planning problem. The model g is both trained and tested in this phase.

Stage 2:
After g_{2SP} is trained, it is deployed for maintenance (Algorithm 6, line 7). First, the regressor g_{2SP} generates RUL point estimates $\hat{r}_a$ for asset $a \in \mathscr{A}'$ based on the current asset measurements $\mathbf{x}_a$. These RUL estimates are now integrated in the maintenance planning model, by applying $\mathbf{h}(\cdot)$ to the RUL estimates (see also Eq. (7.4) in the Oracle planning model where the actual RUL r_a is assumed known):

$$\hat{\mathbf{c}}_a = \mathbf{h}(\hat{r}_a). \tag{7.7}$$

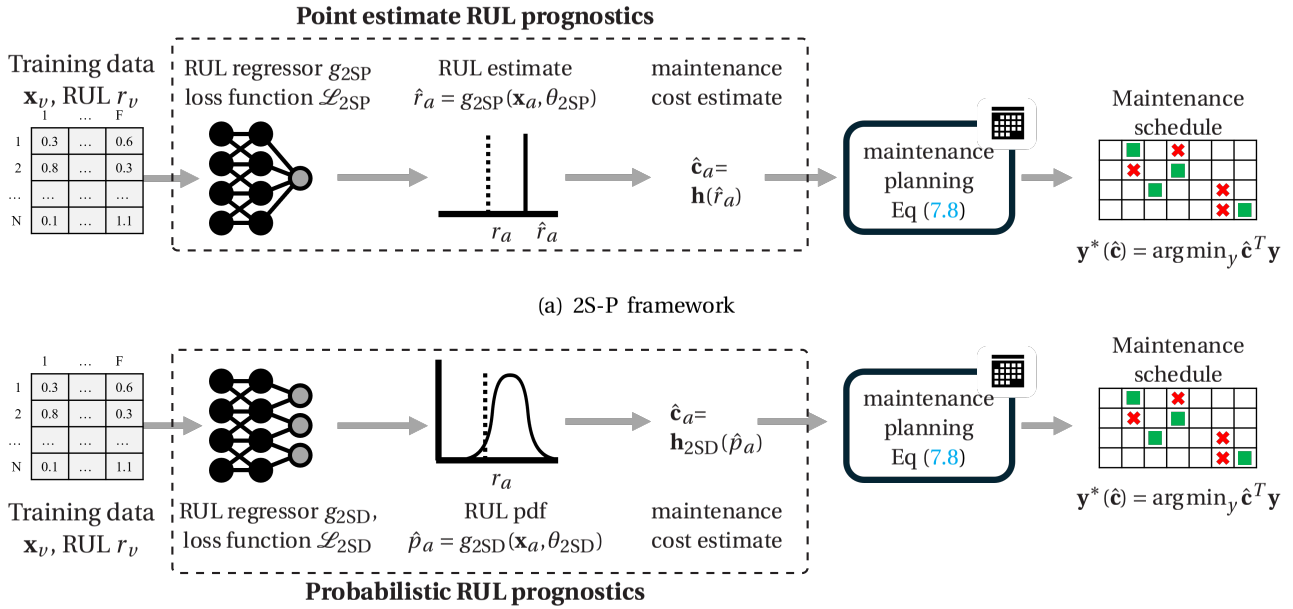

Figure 7.2.: Two-stage approach for predictive maintenance planning problem, using RUL point estimates (2S-P) or probabilistic estimates (2S-D). A machine learning (ML) regressor is trained on a dataset $\mathscr{D}$ of sensor measurements to predict the RUL by minimizing a loss function $\mathscr{L}_{2SP}$ or $\mathscr{L}_{2SD}$. After training, the RUL estimates are used to specify a maintenance cost function $h(\hat{\mathbf{c}}_a)$ to be minimized.

The combined cost estimates for all assets are denoted by $\hat{\mathbf{c}} := (\hat{\mathbf{c}}_a)_{a \in \mathscr{A}'}$. We now consider the maintenance problem $\min_y \hat{\mathbf{c}}^T \mathbf{y}$ subject to the constraints (7.5b)-(7.5d). Let $\mathbf{y}^*(\hat{\mathbf{c}})$ denote the optimal maintenance decisions for this problem:

$$\mathbf{y}^*(\hat{\mathbf{c}}) = (\mathbf{y}_a^*(\hat{\mathbf{c}}))_{a \in \mathscr{A}'} := \arg\min_{\mathbf{y}} \hat{\mathbf{c}}^T \mathbf{y} \quad \text{s.t.} \quad (7.5b) - (7.5d). \tag{7.8}$$

With these maintenance decisions $\mathbf{y}^*(\hat{\mathbf{c}})$, maintenance is planned in the next step of Algorithm 6.

Two Stage predictive maintenance planning with RUL Distribution estimates (2S-D)

More recent studies have explored the possibility of using probabilistic RUL prognostics for maintenance planning, i.e., the distribution of the RUL is estimated in the first phase [11]. This approach is also shown in Figure 7.2.

Stage 1:
Instead of generating RUL point estimates, a machine learning regressor g_{2SD} is trained to generate a probability density of the RUL of an asset $a \in \mathscr{A}'$. This model has parameters θ_{2SD}, and the estimated RUL probability density is denoted by $\hat{p}_a = g_{2SD}(\mathbf{x}_a, \theta_{2SD})$ for an asset a. The model is trained to minimize a loss function $\mathscr{L}_{2SD}$. This loss function depends on the used model, an example of $\mathscr{L}_{2SD}$ being the negative log-loss function [31].

Stage 2:
In the second stage, after training the model, g_{2SD} is applied in maintenance planning (Algorithm 6, line 7). The regressor generates for an asset $a \in \mathscr{A}'$ the pdf of its RUL $\hat{p}_a$ for the current measurements $\mathbf{x}_a$. Using $\hat{p}_a$, the expected maintenance costs $\hat{\mathbf{c}}_a$ are computed. To perform maintenance on day $d_0 + d$, the associated cost estimate is given by:

$$\hat{c}_{\text{dist}}(d, \hat{p}_a) = \sum_{r \geq 0} c(d, r) \hat{p}_a(r), \tag{7.9}$$

where $c(d,r)$ is given in Equation (7.2), r denotes the RUL, and $\hat{p}_a(r)$ is the probability that the RUL of asset a is r days. The expected costs of postponing maintenance are given by:

$$\hat{c}_{\text{dist}}^{\text{postpone}}(\hat{p}_a) = \sum_{r=0}^{k} c^{\text{postpone}}(r) \hat{p}_a(r), \tag{7.10}$$

where $c^{\text{postpone}}(r)$ is given in Equation (7.3). The estimated maintenance costs $\hat{\mathbf{c}}_a$ are given by:

$$\hat{\mathbf{c}}_a = \mathbf{h}_{2SD}(\hat{p}_a) := (\hat{c}_{\text{dist}}(1, \hat{p}_a), \hat{c}_{\text{dist}}(2, \hat{p}_a), \ldots, \hat{c}_{\text{dist}}(k, \hat{p}_a), \hat{c}_{\text{dist}}^{\text{postpone}}(\hat{p}_a))^T. \tag{7.11}$$

Using these cost $\hat{\mathbf{c}}_a$, the maintenance planning problem in (7.8) is considered and maintenance decisions $\mathbf{y}^*(\hat{\mathbf{c}})$ are obtained. With these maintenance decisions $\mathbf{y}^*(\hat{\mathbf{c}})$, maintenance is planned in the next step of Algorithm 6.

7.3.3 End-to-end predictive maintenance planning (E2E-M)

The merits of the two-stage approaches for maintenance planning in Sections 7.3.2 and 7.3.2 have been discussed in detail in several studies such as Consilvio et al. [14] and Lee et al. [30]. However, these two-stage approaches provide not guarantee that the estimates $\hat{\mathbf{c}}$ are as close to $\mathbf{c}$ as possible, or that the actual maintenance cost is minimized. Specifically, these approaches do not optimize for the decision regret, i.e., the cost gap between the true optimal solution and the one acquired using $\hat{\mathbf{c}}$, which is defined as:

$$\mathscr{L}_{\text{regret}}(\hat{\mathbf{c}}, \mathbf{c}) = \sum_{a \in \mathscr{A}} \mathbf{c}_a^T \mathbf{y}_a^*(\hat{\mathbf{c}}) - \mathbf{c}_a^T \mathbf{y}_a^*(\mathbf{c}), \tag{7.12}$$

with

$$\mathbf{y}^*(\hat{\mathbf{c}}) = (\mathbf{y}_a^*(\hat{\mathbf{c}}))_{a \in \mathscr{A}'} := \arg\min_{\mathbf{y}} \{\hat{\mathbf{c}}^T \mathbf{y} \quad \text{s.t.} \quad (7.5b) - (7.5d)\},$$
$$\mathbf{y}^*(\mathbf{c}) = (\mathbf{y}_a^*(\mathbf{c}))_{a \in \mathscr{A}'} := \arg\min_{\mathbf{y}} \{\mathbf{c}^T \mathbf{y} \quad \text{s.t.} \quad (7.5b) - (7.5d)\}.$$

To address this, we propose a novel, end-to-end PTO algorithm to address the rolling horizon predictive maintenance problem by directly minimizing the actual maintenance costs based on the sensor measurements, without the need to generate RUL estimates. As opposed to the two-stage approaches 2S-P and 2S-D, the machine learning regressor in this framework is trained to minimize the decision regret $\mathscr{L}_{\text{regret}}(\hat{\mathbf{c}}, \mathbf{c})$.

Figure 7.3 shows the proposed end-to-end framework. We note that during training, the machine learning regressor $f(\mathbf{x}_a, \theta_{\text{E2E}})$ generates estimates $\hat{\mathbf{c}}_a$. Using these estimates, the model receives feedback on the decision regret from the maintenance planning problem. Based on the feedback on the regret, the parameters θ_{E2E} of the regressor f are updated. We note that this feedback loop is not present for the 2-stage approaches, where after the RUL is estimated in the first stage, there is no further feedback between the first stage and the second, planning stage.

Training the maintenance cost regressor

A machine learning regressor f with parameters θ_{E2E} is trained to generate estimates for the maintenance costs for a single asset a: $\hat{\mathbf{c}}_a = f(\mathbf{x}_a, \theta_{\text{E2E}})$. We consider the following maintenance problem for a single asset:

$$\mathbf{y}_a^{*,\text{single}}(\mathbf{c}_a) = \arg\min_{y_a} \mathbf{c}_a^T \mathbf{y}_a \qquad \text{s.t.} \quad \mathbf{y}_a \in B_{k+1} := \{\mathbf{y}_a : \mathbb{1}^T \mathbf{y}_a = 1, \quad \mathbf{y}_a \in \{0,1\}^{k+1}\}. \tag{7.13}$$

We note that eq. (7.5c) in the maintenance model is not mentioned here since we consider a single asset.

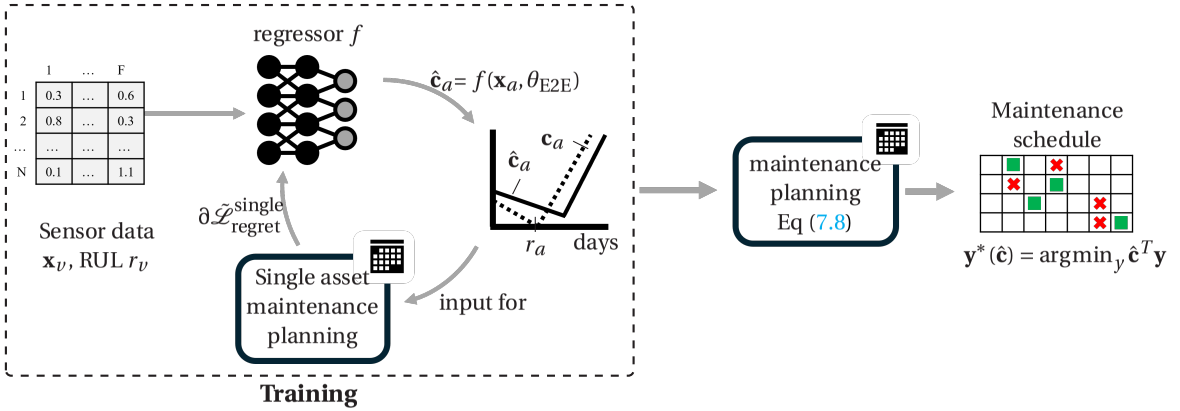

Figure 7.3.: *End-to-end maintenance* framework for the predictive maintenance planning problem. A machine learning regressor f is trained on sensor data, with regret of the maintenance planning problem in a feedback loop. f generates maintenance cost estimates, using the loss function $\tilde{\mathscr{L}}^{\text{single}}_{\text{regret}}$, a proxy for $\mathscr{L}_{\text{regret}}$. After training, the cost estimates are used to plan maintenance.

To train f, information of the decision regret of this problem is received in a feedback loop, with the regret for a single asset being defined as:

$$\mathscr{L}^{\text{single}}_{\text{regret}}(\hat{\mathbf{c}}_a, \mathbf{c}_a) = \mathbf{c}_a^T \mathbf{y}_a^{*,single}(\hat{\mathbf{c}}_a) - \mathbf{c}_a^T \mathbf{y}_a^{*,single}(\mathbf{c}_a), \tag{7.14}$$

where $\mathbf{y}_a^{*,single}(\hat{\mathbf{c}}_a)$ and $\mathbf{y}_a^{s*}(\mathbf{c}_a)$ denote the optimal decisions for (7.13) for the estimated and true costs, respectively.

The model f is trained by applying the gradient descent algorithm to $\mathscr{L}^{single}_{\text{regret}}$, see Algorithm 7. However, $\mathscr{L}^{single}_{\text{regret}}$ is not differentiable. To use the gradient descent algorithm, $\mathscr{L}^{single}_{\text{regret}}$ is substituted by an approximation $\tilde{\mathscr{L}}^{single}_{\text{regret}}(\hat{\mathbf{c}}_a, \mathbf{c}_a)$ introduced in Elmachtoub et al. [23]:

$$\begin{aligned}\mathscr{L}^{single}_{\text{regret}}(\hat{\mathbf{c}}_a, \mathbf{c}_a) \approx \tilde{\mathscr{L}}^{single}_{\text{regret}}(\hat{\mathbf{c}}_a, \mathbf{c}_a) &:= -\min_{\mathbf{y}_a \in B_{k+1}} \{(2\hat{\mathbf{c}}_a - \mathbf{c}_a)^T \mathbf{y}_a\} + 2\hat{\mathbf{c}}_a^T \operatorname*{arg\,min}_{\mathbf{y}_a \in B_{k+1}} \{\mathbf{c}_a^T \mathbf{y}_a\} - \min_{\mathbf{y}_a \in B_{k+1}} \{\mathbf{c}_a^T \mathbf{y}_a\}, \\ &= -\min\{2\hat{\mathbf{c}}_a - \mathbf{c}_a\} + 2\hat{\mathbf{c}}_a^T \operatorname*{arg\,min}_{\mathbf{y}_a \in B_{k+1}} \{\mathbf{c}_a^T \mathbf{y}_a\} - \min\{\mathbf{c}_a\},\end{aligned} \tag{7.15}$$

which is differentiable w.r.t. $\hat{\mathbf{c}}_a$, convex and has the following subgradient:

$$2 \operatorname*{arg\,min}_{\mathbf{y}_a \in B_{k+1}} \{\mathbf{c}_a^T \mathbf{y}_a\} - 2 \operatorname*{arg\,min}_{\mathbf{y}_a \in B_{k+1}} \{(2\hat{\mathbf{c}}_a - \mathbf{c}_a)^T \mathbf{y}_a\} \in \frac{\partial \tilde{\mathscr{L}}^{\text{single}}_{\text{regret}}(\hat{\mathbf{c}}_a, \mathbf{c}_a)}{\partial \hat{\mathbf{c}}_a}, \tag{7.16}$$

which can easily be evaluated. This subgradient is substituted in:

$$\frac{\partial \mathscr{L}^{\text{single}}_{\text{regret}}(\hat{\mathbf{c}}_a)}{\partial \theta_{\text{E2E}}} \approx \frac{\partial \tilde{\mathscr{L}}^{\text{single}}_{\text{regret}}(\hat{\mathbf{c}}_a)}{\partial \hat{\mathbf{c}}_a} \frac{\partial \hat{\mathbf{c}}_a}{\partial \theta_{\text{E2E}}},$$

such that the gradient descent algorithm (Algorithm 7) can be used.

Maintenance scheduling

Once regressor f is trained, is is deployed for maintenance planning (Algorithm 6, line 7). The estimated costs $\hat{\mathbf{c}}_a$ are computed for each asset from the measurements $\mathbf{x}_a$. The combined estimates are denoted by $\hat{\mathbf{c}} := (\hat{\mathbf{c}}_a)_{a \in \mathscr{A}'}$. Using these cost estimates, the maintenance planning problem Eq. (7.8) is solved and maintenance decisions $\mathbf{y}^*(\hat{\mathbf{c}})$ are obtained. With these maintenance decisions $\mathbf{y}^*(\hat{\mathbf{c}})$, maintenance is planned in the next step of Algorithm 6.

7.4 Case study: predictive maintenance planning for eVTOL Lithium-ion batteries

In this section, we will apply our end-to-end predictive maintenance planning framework to a fleet of electric Vertical Take-Off and Landing (eVTOL) aircraft.

eVTOLs are short-range electric aircraft which fulfill a need for greener and quieter flights and address increasing concerns about urban traffic congestion. These aircraft

Algorithm 7: Batch gradient descent algorithm for training the machine learning regressor used in the E2E Maintenance framework.

Data: Machine learning algorithm f, batched dataset of RUL-labeled sensor data $(\mathbf{x}_a, r_a)$, number of iterations i, learning rate α
Result: Trained f

```
Initialize parameters θ_E2E;
for iterations i do
    for batch of data {(x_a, r_a)} do
        Sample data (x_a, r_a) from the batch;
        Compute the cost coefficients c_a = (c(r_a,1),...,c(r_a,k),c^postpone(r_a))^T (Eq. (7.2) and (7.3));
        Predict the cost coefficients ĉ_a = f(x_a, θ_E2E);
        Determine y*_a(c_a) and y*_a(ĉ_a);
        Compute ∂L̃^single_regret/∂θ_E2E using Eq. (7.16);
        Let θ_E2E ← θ_E2E − α∂L̃^single_regret/∂θ_E2E;
    end
end
```

are designed to carry a payload up to 800 kg over a distance of up to 100 km. Currently, several legacy manufacturers as well as start-ups are developing eVTOLs [32]. Envisioned applications are (among others) on-demand urban passenger transportation and emergency response services [33–35].

Battery health management is one of the most important obstacles for eVTOL operations [36]. Currently, Lithium-ion batteries are the most frequently considered batteries for eVTOLs, due to their relatively good performance and affordability. However, due to the high performance requirements for eVTOL operations, these batteries are prone to quick degradation, which may lead to safety concerns. As such, monitoring the health of the battery in combination with predictive maintenance scheduling, as we propose, is crucial.

7.4.1 Dataset on condition monitoring of Li-ion batteries of eVTOLs

We consider the condition dataset for the Sony-Murata 18650 VTC-6 Li-Ion batteries [37]. These batteries are cycled through an eVTOL mission simulation in the A^3 Vahana eVTOL, designed by Acubed/Airbus. Each mission consists of a charging phase and a flight phase. The charging phase consists of: constant current charging (CC), constant voltage charging (CV) and a rest period. The flight phase consists of: the takeoff, cruise and landing phase.

A total of 22 batteries are considered. Each battery is cycled though missions with different parameters, referred to as the mission profile (MP) or Vahana (VAH). The parameters of these profiles can be seen in Table 7.2. Three of these batteries are

performed according to the baseline mission profile (MP1, MP13, and MP14). The other mission profiles are variations on these.

	Cruise time	Power Take-off	Power Cruise	Power Landing	CC	CV	Temp.	Vahana	#Missions	#Capacity tests
MP1	**800s**	**54W**	**16W**	**54W**	**1C**	**4.2V**	**25°C**	**VAH01**	**847**	**17**
MP2	**1000s**	54W	16W	54W	1C	4.2V	25°C	VAH02	625	13
MP3	800s	**48.6W**	**14.4W**	**48.6W**	1C	4.2V	25 °C	VAH05	1615	29
MP4	800s	54W	16W	54W	**0.5C**	4.2V	25°C	VAH06	9290	20
MP5	800s	54W	16W	54W	1C	**4V**	25°C	VAH07	339	6
MP6	800s	54W	16W	54W	1C	4.2V	**20°C**	VAH09	8527	27
MP7	800s	54W	16W	54W	1C	4.2V	**30°C**	VAH10	1431	28
MP8	800s	**43.2W**	**12.8W**	**43.2W**	1C	4.2V	25 °C	VAH11	2249	45
MP9	**400s**	54W	16W	54W	1C	4.2V	25°C	VAH12	2349	46
MP10	**600s**	54W	16W	54W	1C	4.2V	25°C	VAH13	1042	20
MP11	**1000s**	54W	16W	54W	1C	4.2V	25°C	VAH15	554	11
MP12	800s	54W	16W	54W	**1.5C**	4.2V	25°C	VAH16	559	11
MP13	**800s**	**54W**	**16W**	**54W**	**1C**	**4.2V**	**25°C**	**VAH17**	**1002**	**20**
MP14	800s	54W	16W	54W	**1.5C**	4.2V	25°C	VAH20	611	12
MP15	**1000s**	54W	16W	54W	1C	4.2V	25°C	VAH22	579	11
MP16	800s	54W	16W	54W	1C	**4V**	25°C	VAH23	697	14
MP17	800s	54W	16W	54W	**0.5C**	4.2V	25°C	VAH24	801	16
MP18	800s	54W	16W	54W	1C	4.2V	**20**°C	VAH25	554	11
MP19	**600s**	54W	16W	54W	1C	4.2V	25°C	VAH26	1164	23
MP20	**800s**	**54W**	**16W**	**54W**	**1C**	**4.2V**	**25°C**	**VAH27**	**587**	**12**
MP21	800s	**48.6W**	**14.4**	**48.6W**	1C	4.2V	25°C	VAH28	1182	23
MP22	800s	54W	16W	54W	1C	4.2V	**35°C**	VAH30	919	18

Table 7.2.: Mission profile characteristics of the Sony-Murata 18650 Li-ion batteries used for Vahana operations simulation [37].

Sensor measurements

During the missions, the battery is monitored with a number of sensors. Every 10 seconds, the following are recorded: the cell voltage, the current, the energy and charge supplied during the charging phase, the energy and charge supplied by the battery during the flight phase, and the surface temperature.

Over time, the charge capacity of the batteries decrease. However, the true capacity cannot be measured without fully discharging the battery. In order to do this, a capacity test is performed every 50 missions. During this test, the battery is discharged until the voltage drops below 2.5V. This is followed by a cooldown period. After this, the battery is recharged until it is at full capacity.

The eVTOL batteries can only be used if its charge capacity is high enough. We say that the battery reaches its end-of-life (EOL) once its capacity is 85% of the original capacity.

Figure 7.4 shows an example of how the battery capacity decreases with each mission (on MP1/VAH01). The total capacity drops from 300 mAh on the first capacity test/mission to 2450 mAh on the 17th capacity test (800th mission). The battery EOL is reached at the 12th capacity test (750th mission).

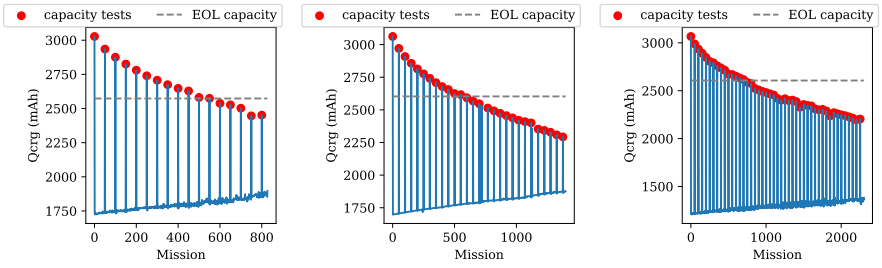

(a) VAH01 (b) VAH10 (c) VAH12

Figure 7.4.: Battery capacity for batteries VAH01, VAH10, and VAH12. The values measured at the capacity tests are shown as dots. Batteries VAH01, VAH10, and VAH12 have a useful life of 600, 600, and 750 cycles, respectively.

7

Feature engineering

The sensor measurements have been processed into 32 features. Let $\mathcal{F} = \{MP1, MP2, ..., MP22\}$ denote the set of mission profiles. For each mission profile $f \in \mathcal{F}$, let M_f denote the number of missions performed by f. For each $f \in \mathcal{F}$ and mission number $1 \leq m \leq M_f$, we consider the following features:

Charging phase features. We store the amount of charge supplied $Qcrg^{f,m}$, the duration of each charging segment (CC, CV, Rest) $\Delta t^{segment,f,m}$, and the last measured charge capacity $Qlast^{f,m}$.

Flight phase features. For each mission segment during flight (take-off, cruise, and landing), we store the duration $\Delta t^{segment,f,m}$. Additionally, we store the maximum, minimum, mean, and variance of the battery voltage in each phase, denoted by $V_{max}^{segment,f,m}$, $V_{min}^{segment,f,m}$, $V_{mean}^{segment,f,m}$, and $V_{var}^{segment,f,m}$, respectively. Additionally, we store the maximum, minimum, and variance of the extracted charge during each segment, denoted by $Qdis_{max}^{segment,f,m}$, $Qdis_{min}^{segment,f,m}$ and $Qdis_{var}^{segment,f,m}$, respectively. Last, for each segment, we record the maximum cell temperature $T_{max}^{segment,f,m}$.

Feature selection

From the generated features, we select the most important half to generate prognostics for maintenance planning. This is done based on the Shapley values [38], which are given in Table 7.3. The features $V_{min}^{take-off}$ through $Qdis_{max}^{take-off}$ are selected.

Last, these features are subjected to normalization. This is done with z-score normalization, which scales the data to a mean of 0 and a variance of 1 [39]. In order to capture the degradation of the batteries, the features from the current mission, as well as 50 missions (1 capacity test) back are used. This is the data that shall be used in order to perform predictive maintenance for the eVTOL batteries.

Feature	Shapley	Feature	Shapley
$V_{min}^{take-off}$	**95.4**	$Qdis_{max}^{cruise}$	45.9
$V_{mean}^{take-off}$	**94.7**	T_{max}^{cruise}	45.4
$Qlast$	**93.4**	$T_{max}^{landing}$	41.1
$V_{var}^{take-off}$	**92.4**	$T_{max}^{take-off}$	38.8
V_{max}^{cruise}	**87.8**	Δ^{rest}	36.5
$Qcrg$	**87.1**	$V_{max}^{landing}$	35.5
Δ^{CV}	**86.5**	$\Delta^{take-off}$	23.4
V_{min}^{cruise}	**78.8**	Δ^{cruise}	19.7
V_{mean}^{cruise}	**63.8**	$\Delta^{landing}$	19.4
$V_{var}^{landing}$	**59.3**	Δ^{CC}	12.9
$V_{mean}^{landing}$	**57.4**	$Qdis_{var}^{cruise}$	3.5
$V_{max}^{take-off}$	**57.2**	$Qdis_{max}^{landing}$	2.4
$V_{min}^{landing}$	**51.6**	$Qdis_{mean}^{cruise}$	2.3
$Qdis_{var}^{take-off}$	**47.7**	V_{var}^{cruise}	2.2
$Qdis_{mean}^{take-off}$	**46.5**	$Qdis_{var}^{landing}$	1.4
$Qdis_{max}^{take-off}$	**45.9**	$Qdis_{mean}^{landing}$	1.2

Table 7.3.: SHAP values (importance) for the 32 considered features; top 50% of the features are selected for maintenance planning prognostics (in **bold**).

7.4.2 Predictive maintenance planning for a fleet of eVTOLs

In this section, we illustrate the predictive maintenance planning for eVTOL batteries using (i) machine learning to predict point estimates of the battery RUL, and integrate this in a integer linear program to plan maintenance (2S-P), (ii) machine learning to predict the distribution of the battery RUL, and integrate this in a integer linear program to plan maintenance (2S-D), and (iii) machine learning to directly estimate the maintenance cost coefficients of an integer linear program that plans maintenance (E2E-M).

Parameters of the eVTOL fleet operations and maintenance

We consider maintenance planning for a fleet of eVTOLs $\mathscr{A}$. Each eVTOL is equipped with one of the batteries from Section 7.4.1. The fleet consists of 25 eVTOLs. Each eVTOL performs 10 trips per day, five round trips to and from the hub, such that a capacity test is performed every five days.

Each eVTOL battery is monitored by a number of sensors, from which 16 features are deduced, as described in Section 7.4.1. Based on this battery health data, maintenance may be planned. Replacing a battery costs $c_{\text{replace}} = 100$. To perform scheduled battery maintenance, $H = 1$ hangar is available. When a breakdown occurs, at the EOL, the eVTOL battery is immediately replaced at a cost of $c_{\text{unscheduled}} = 1000$. As described in Section 7.2, maintenance takes one day and may be planned one day in advance. We use a rolling horizon of $k = 10$ days to plan maintenance. A total planning horizon of $\mathscr{D} = 10$ years is considered.

A six-fold cross validation is used to train and test the regressors. For each fold, six eVTOLs are randomly used for testing, while ensuring that one baseline mission profile (VAH01, VAH17 or VAH27) is used. The eVTOLs used for testing can be seen in The other eVTOLs are used for training. The testing eVTOLs for each fold are given in Table 7.4.

Fold	Testing baseline battery	Testing other batteries
1	VAH01	VAH02, VAH13, VAH20, VAH28, VAH30
2	VAH01	VAH05, VAH06, VAH13, VAH15, VAH16
3	VAH17	VAH19, VAH11, VAH22, VAH23, VAH25
4	VAH17	VAH02, VAH06, VAH20, VAH26, VAH30
5	VAH27	VAH05, VAH12, VAH15, VAH16, VAH24
6	VAH27	VAH10, VAH12, VAH22, VAH24, VAH25

Table 7.4.: eVTOL batteries in the test set of each fold.

Two stage predictive maintenance planning with RUL point estimates (2S-P)

For the 2S-P algorithm, as in Section 7.3.2, we use a Long Short-Term Memory (LSTM) regressor $g_{\text{2SP}}(\cdot, \theta_{\text{2SP}})$ to generate RUL point estimates of the eVTOL batteries. As before, θ_{2SP} denotes the parameters of the LSTM.

The LSTM is a recurrent neural network (RNN), capable of learning long-term dependencies [40]. The LSTM solves the vanishing and exploding gradient problems by adding a memory cell and gate mechanism. A generic architecture of the LSTM and the architecture of a LSTM unit can be found in Yu et al. [41].

Figure 7.5 shows the architecture of our LSTM network. The input of the network consists of the normalized battery sensor measurements from the current mission m and fifty missions $m-50$ (one capacity test) ago. This data (see Section 7.4.1) is fed through L layers of 2 LSTM units. To avoid overfitting, a Monte Carlo dropout layer

is added after every LSTM layer except the last. After this, a fully connected layer is applied, which outputs the RUL point estimates of the batteries. The loss function of the network minimizes the deviation from the true RUL (Eq. (7.6)).

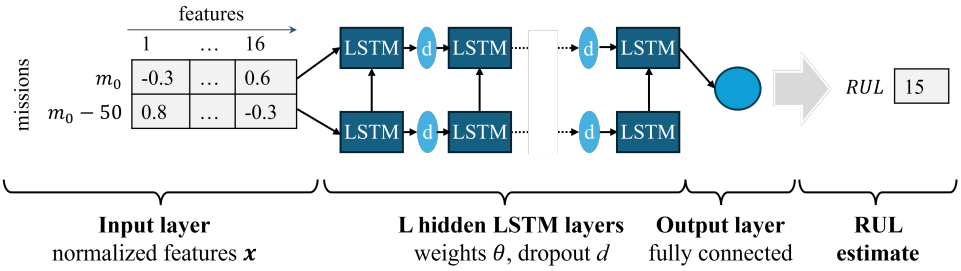

Figure 7.5.: LSTM architecture for the RUL regressor used in the two-stage predict-then-optimize algorithm for predictive maintenance planning. It is used i) without random dropout during testing, to obtain RUL point prognostics g_{2SP}, and ii) with random dropout during testing, to obtain probabilistic RUL prognostics g_{2SD}.

Two stage predictive maintenance planning with RUL distribution estimates (2S-D)

To obtain RUL distribution estimates for the 2S-D algorithm, as in Section 7.3.2, we use two regressors: a LSTM with Monte Carlo dropout in the testing phase [42], and a Mixture Density Network (MDN) [31].

LSTM with Monte Carlo dropout in the testing phase:
The LSTM network from Section 7.4.2 with Monte Carlo dropout in the testing phase is used to estimate the distribution of the RUL of the batteries (probabilistic RUl prognostics).

Mixture Density Network:
Mixture Density Networks (MDNs) are feed forward neural networks that generate the distributions of non-Gaussian unknowns [31]. The MDN estimates the RUL distribution as a linear combination of several Gaussian distributions. We have trained an MDN to obtain probabilistic RUL prognostics, as shown in Figure 7.6. Specifically, the sensor measurements $\mathbf{x}_a$ are fed through L fully connected hidden layers. After this, it is fed through an MDN output layer to J normal distributions, consisting of a three-fold output. These are the means $\mu_j(\mathbf{x}_a, \theta_{2SD})$, the standard deviations $\sigma_j(\mathbf{x}_a, \theta_{2SD})$ and the mixture coefficients $\alpha_j(\mathbf{x}_a, \theta_{2SD})$, with $j = 1, \ldots J$. The probability density of the output (RUL) is given by:

$$\hat{p}_a(r_a|\mathbf{x}_a, \theta_{2SD}) = \sum_{j=1}^{J} \alpha_j(\mathbf{x}_a, \theta_{2SD}) \phi(r_a|\mu_j(\mathbf{x}_a, \theta_{2SD}), \sigma_j(\mathbf{x}_a, \theta_{2SD})), \tag{7.17}$$

where ϕ denotes the pdf of a normal distribution. The network is trained on the loss function:

$$\mathscr{L}_{MDN}(r_v, \mathbf{x}_v) = -\log \hat{p}_a(r_v|\mathbf{x}_v, \theta_{2SD}), \tag{7.18}$$

which is the negative log-likelihood of r_v given the probability density function $\hat{p}_a$.

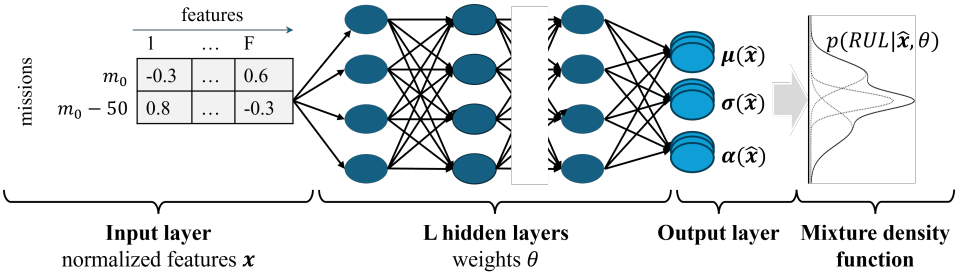

Figure 7.6.: MDN architecture for the RUL regressor used in the two-stage predict-then-optimize algorithm for predictive maintenance planning with probabilistic RUL prognostics, g_{2SD}.

End-to-end predictive maintenance planning (E2E-M)

For the E2E-M algorithm, see Section 7.3.3, we directly obtain estimates of the maintenance costs in the planning model using an LSTM regressor. This LSTM $f(\cdot, \theta_{E2E})$ has parameters θ_{E2E}, see also Figure 7.5. The architecture is similar to the network used for the 2S-P algorithm, but has a different output layer, i.e. the cost coefficients of the maintenance planning ILP model.

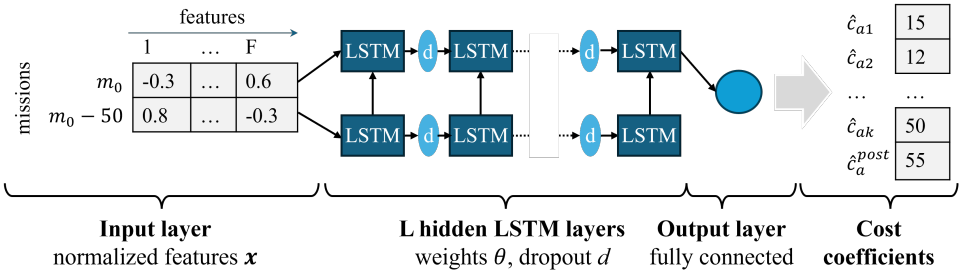

Figure 7.7.: LSTM architecture used for the *end-to-end maintenance* framework.

7.4.3 Hyperparameter tuning

A hyperparameter tuning has been performed on each algorithm from Section 7.4.2. A grid-based search was used to perform this.

For the LSTM used to obtain point estimate and probabilistic RUL prognostics (Section 7.4.2, 7.4.2), the following parameters are used. We consider $L = 4$ hidden LSTM layers. The layers have 176, 126, 116, and 110 units, respectively. During training and testing, a dropout rate of 0.5 is applied after the second layer. The LSTM is optimized using the RMSprop algorithm [43] with a learning rate of 0.01.

For the MDN used to obtain probabilistic RUL prognostics (Section 7.4.2), the following parameters are used. We consider $L = 6$ dense hidden layers. The layers have 24, 122, 116, 116, 90, and 38 units, respectively. The first five layers use the ReLu activation function, and the last one a tanh activation function. The output of the MDN consists of a mixture of $J = 3$ normal distributions. The MDN is optimized using the RMSprop [43] algorithm with a learning rate of 0.01.

For the LSTM used to obtain maintenance cost estimates (Section 7.4.2), the following parameters are used. We consider $L = 5$ hidden layers. The size of the output of each hidden layer, including the last, is 64 units. To avoid overfitting, a dropout rate of 0.2 is used during the testing phase. The LSTM is optimized using the Adam algorithm [43] with a learning rate of 0.005.

7.5 Results

7.5.1 Comparing end-to-end (E2E-M) and two-stage (2S-P, 2S-D) maintenance planning algorithms

Each algorithm (Oracle planning, two-stage with RUL point (2S-P) and distribution (2S-D) estimates, and end-to-end maintenance (E2E-M)) has applied to 100 simulations for eVTOL fleet maintenance planning for a planning period of $\mathscr{D} = 10$ years. Table 7.5 shows the average results of each algorithm over all 100 runs. It shows the number of batteries replaced as well, the lifetime of the batteries once they were replaced, and the accompanying costs. The used batteries and costs have been split into scheduled and unscheduled maintenance.

Table 7.5 shows that the Oracle planning algorithm requires (on average) 1664.4 batteries during the 10 years of operations. Of these, only a small number is not replaced before breakdown (4.5), leading to a total maintenance cost of 170490. It shows that form the other PTO methods, the End-to-End Maintenance algorithm leads to the fewest breakdowns (63.1) and the lowest regret: 36%. The two stage method with RUL distribution prognostics leads, with both the MDN and LSTM, to a larger number of breakdowns, with a corresponding regret of 49% and 62%, respectively. The two stage method with RUL point estimates uses the lowest amount of batteries (with a 94.8% utilization) but incurs a large number of breakdowns.

To explain the results, we use the preferred maintenance day. The preferred maintenance day for an eVTOL, d^* is defined as the day with the lowest maintenance costs:

$$d^* = \begin{cases} \arg\min_d \hat{\mathbf{c}}_{ad}, & \text{if } \min_d \hat{\mathbf{c}}_{ad} \leq \hat{\mathbf{c}}_a^{\text{postpone}} \\ \text{post} & \text{else,} \end{cases} \tag{7.19}$$

such that $d^* \in \{1, ..., k-1, \text{post}\}$, where 'post' corresponds to recommending postponing

Method		Maintained batteries (#)					
	Regressor	on time	broken down	total	Battery life used	costs	regret
Oracle	-	1659.9	4.5	1664.4	97.9%	170490.0	0%
2S-P	LSTM	1125.2	594.6	1719.8	94.8%	707120.0	315%
2S-D	LSTM	1692.9	107.7	1800.6	88.9%	276990.0	62%
2S-D	MDN	1740.1	79.2	1819.3	90.2%	253210.0	49%
E2E-M	LSTM	1692.4	63.1	1755.5	91.0%	268340.0	36%

Table 7.5.: Maintenance performance indicators for the planning algorithms and regressors. The number of maintained batteries (on-time, broken down, and total) are given, together with the average used lifetime of the batteries, the maintenance costs, and the maintenance cost regret w.r.t. the Oracle.

maintenance. For the 2S method with point distributions d^* is given by the RUL estimate.

Figure 7.8 shows the preferred maintenance days for three PTO algorithms: 2S with LSTM point estimates (7.8a), 2S with MDN distribution estimates (7.8b), and E2E with LSTM estimates (7.8c). Each figure shows the target maintenance days as a function of the RUL. The target maintenance days are shown for all eVTOLs of all six folds. For each RUL between 0 and 20, the average target maintenance day is given, as well as the 25 and 75 percentile values. The dashed line indicates the actual RUL value.

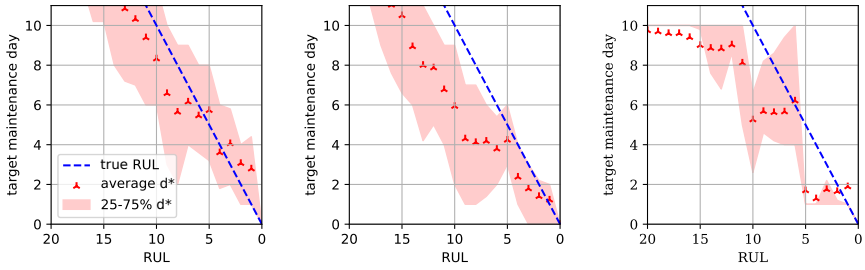

(a) Two-stage RUL point estimates algorithm with LSTM regressor.

(b) Two-stage RUL distribution algorithm with MDN regressor.

(c) End-to-End Maintenance algorithm with LSTM regressor.

Figure 7.8.: Maintenance target days d^* for different RUL values over all battery types (Table 7.6). The average target day (triangles), as well as the 25th and 75th percentile (shaded area) are given. The true target day, or the actual RUL, is given by a dashed line.

For the End-to-End Maintenance algorithm (Figure 7.8c), the figure shows how conservative the target maintenance days are. The 75-percentile value is almost never larger than the actual RUL (shown as a dashed line). Furthermore, the effect of the capacity tests can be seen, with large changes around RUL values 5, 10, and 15. At a RUL of 5 days, the target maintenance day is 1 (recommending immediate replacement of the batteries) for all eVTOLs.

Figures 7.8a and 7.8b show the target maintenance days for the 2S methods. It can be seen that the former gives target days closest to the actual RUL, but does quite often overestimate the RUL. On the other hand, the target days of the latter are still close to the actual RUL, but almost they are almost always smaller than the RUL. When compared to the End-to-End Maintenance method with LSTM, there is a notable difference in the last five days before EOL, as the End-to-End Maintenance algorithm almost always recommends immediate maintenance, whereas the two stage algorithm proposes to wait another day.

Overall, we observe that the target days of the 2S-P algorithm are very aggressive, risking a large number of failures. We also observe that when the actual RUL is low (smaller than 5), the target days recommended by the E2E-M algorithm are more conservative then for the other algorithms. This reduces the time the batteries are used, but also reduces the risk of a battery failure.

These target days are translated into the utilization of the batteries, which is shown in Figure 7.9. The figure shows a histogram of the RUL of the batteries at the moment they were maintained (and restored to as-good-as-new condition). It can be seen that the RUL of the batteries is larger for the End-to-End Maintenance method, which are sometimes replaced 10 days in advance. For the two stage method with RUL point estimates, there is a large number of batteries with either 1 or 0 days of RUL left.

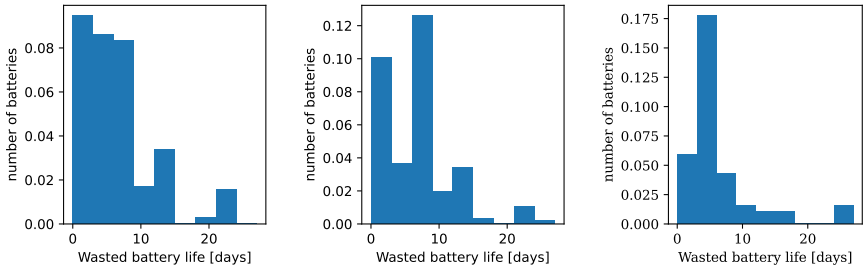

(a) 2S-P algorithm with LSTM regressor.

(b) 2S-D algorithm with MDN regressor.

(c) E2E-M algorithm with LSTM regressor.

Figure 7.9.: Histogram of the RUL (in days) of the maintained batteries at the moment of their maintenance.

7.5.2 Results for the End-to-End Maintenance (E2E-M) planning algorithm

For the remainder of the section, we shall discuss the results of our variant of the End-to-End Maintenance algorithm.

Table 7.6 gives the performance of the LSTM for each fold. It gives the average Root Mean Square Error (RMSE) of the maintenance costs as well as the regret for single eVTOL maintenance planning. The results show that the typical regret is around 40%.

Fold#	RMSE [-]	$\mathscr{L}_{\text{regret}}$ [%]
1	9.92	34.6
2	13.78	29.3
3	5.96	55.6
4	10.29	45.3
5	6.45	51.1
6	3.9	37.5
ALL	8.38	42.2

Table 7.6.: Performance of the End-to-End Maintenance algorithm. For each fold, the average RMSE of the cost estimates and the decision regret (Equation 7.12) are given.

7

E2E-M maintenance cost estimates

Using the trained LSTM networks, the maintenance costs of each eVTOL for each RUL have been estimated. These estimates are discussed in this section.

Figure 7.10 shows three examples of the estimated maintenance costs: VAH01 in fold 1 (7.10a), VAH10 for fold 3 (7.10b), and VAH12 for fold 6 (7.10c). The figure shows a heatmap of the maintenance costs $\hat{\mathbf{c}}_{ad}$ and $\hat{\mathbf{c}}_{a}^{\text{postpone}}$ for each value of the actual RUL (horizontal, from 40 to 0) and maintenance options (vertical): repairing in $d = 1$ up to $d = 9$ days, and postponing maintenance. The costs are normalized for each RUL, with dark colours corresponding to low costs, and light colours to high costs.

In Figure 7.10, the target day is shown as a white dot. This target maintenance day is defined, as in Figure 7.8, as the day with the lowest estimated costs given the current RUL.

The cost estimates for VAH1 and VAH12 are more conservative then those for VAH10: the target maintenance day starts converging to 1 around a RUL of 16 days (160 cycles). Furthermore, for VAH01, the target maintenance day is already imminent, 8 days before the end-of-life. Last, one can notice the effects of the capacity tests every 5 days on the estimated costs for VAH01 and VAH12, where distinct differences are visible around 15, 10, and 5 days of RUL. This can be

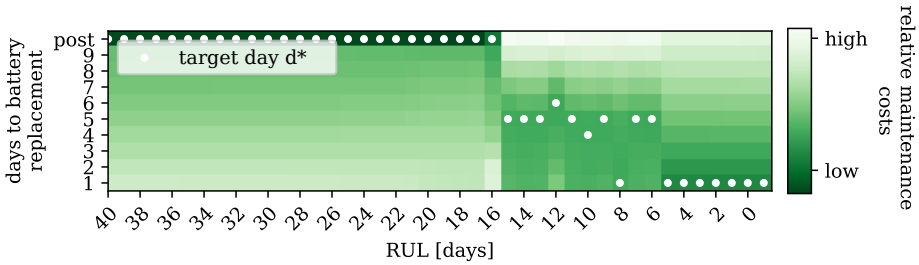

(a) VAH01, fold 1

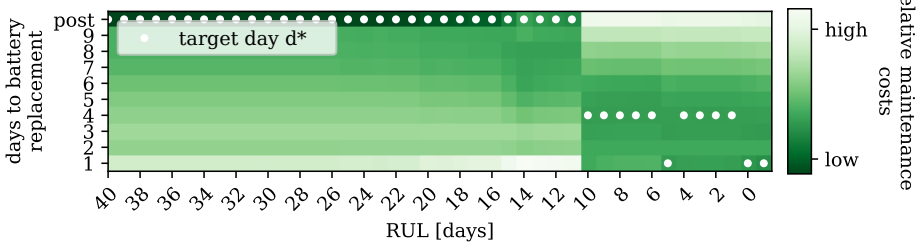

(b) VAH10, fold 3

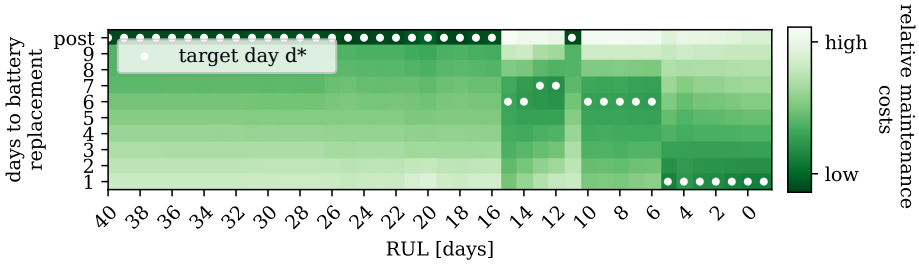

(c) VAH12, fold 6

Figure 7.10.: Heatmap of the maintenance cost estimates obtained by the End-to-End Maintenance algorithm (E2E-M) with the LSTM network (Section 7.4.2) for three batteries. The estimates are shown from a RUL of 40 days (400 cycles) to the EOL. The vertical axis gives the maintenance options: repairing in $d = 1$ up to $d = 9$ days, and postponing maintenance. The estimates shown are normalized for each RUL value.

explained by the fact that at every capacity test, a new capacity measurement (from which the RUL is derived) is performed, which the LSTM takes into account when estimating the maintenance costs.

End-to-End Maintenance example maintenance schedule

Last, we show an illustrative example where the estimated maintenance costs are integrated into maintenance planning. Figure 7.11 shows how a maintenance schedule evolves over five days. Figures 7.11a, 7.11b, and 7.11c show the schedules at days 45, 48, 49, and 50, respectively. From day 45, battery maintenance is planned for eVTOLs 2, 6, 8, 10, 14, and 15, shown as rows in each figure. For each eVTOL with planned maintenance, we show the EOL (red cross), target maintenance (yellow arrow) and scheduled maintenance (green square) days. In case maintenance is planned before the EOL, a green solid line is shown. In case it is planned after the EOL, a red dashed line is shown.

Using the rolling horizon approach, the maintenance decisions of the previous days are performed on the next day. At the start of day 46, maintenance is planned for eVTOL 14 on day 47. This is performed on day 47 while the other maintenance decisions are reevaluated.

At the start of day 51 a conflict arises. For eVTOLs 2 and 8, the battery maintenance is scheduled close to the actual EOL and target days, with eVTOL2 planned for maintenance on the EOL day. The schedule for eVTOL 6 is interesting, as the target day for this eVTOL follows the EOL closely on all days except day 49. On this day, immediate maintenance is recommended and performed. Because the hanger capacity is limited, this poses a problem for eVTOLs 2, 4 and 8, which all need to be maintained around the same time. Maintenance for eVTOLs 2 and 8 are scheduled after their target days (52). Additionally, eVTOL 10 reaches its EOL before maintenance is planned, and is repaired immediately.

7.6 Conclusions

This chapter proposes an end-to-end, dynamic framework for the maintenance planning problem for a set of assets. Sensor continuously monitor the state of health of the assets. Based on these sensor measurements, maintenance for each asset is planned, with the objective of planning maintenance as close near the end-of-life of the asset as possible. For this, a limited maintenance capacity is available. In case the asset fails unexpectedly, a large penalty is incurred. Using an End-to-End Maintenance framework, we train a machine learning regressor to generate estimates for the costs of maintaining the assets. Compared to existing studies on end-to-end approaches for general predict-then-optimize problems, we leverage the fact that the health measurements of different assets are uncorrelated. By assuming this, we are able to estimate the maintenance costs for each asset separately, allowing for faster and more effective training. Secondly, we incorporate the dynamic aspect of the maintenance planning problem by developing a rolling horizon algorithm. Also, compared with the majority of studies on predictive maintenance, which make use of two-stage approaches, our approach proposed a way of planning maintenance by including feedback from the maintenance planning problem while training the maintenance cost estimation regressor.

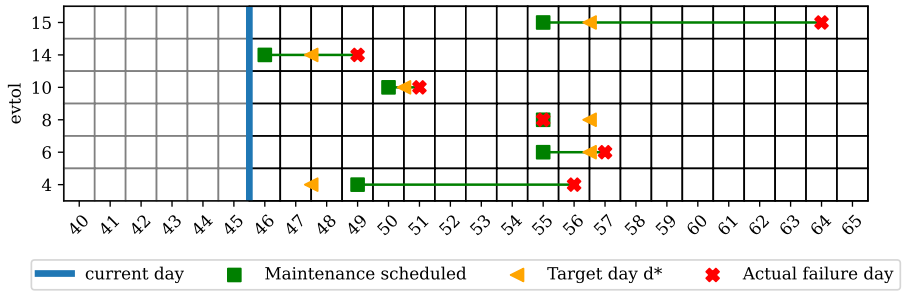

(a) current day 46

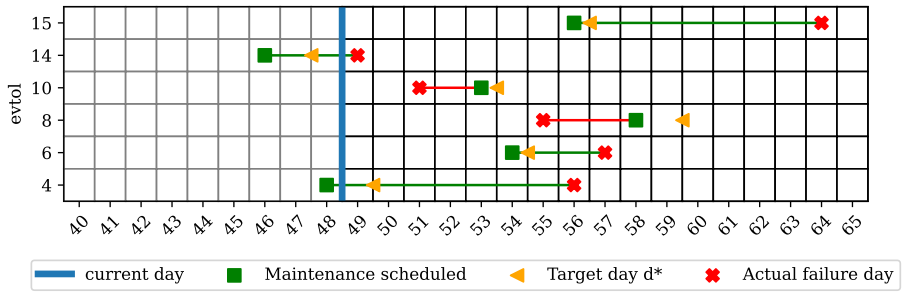

(b) current day 49

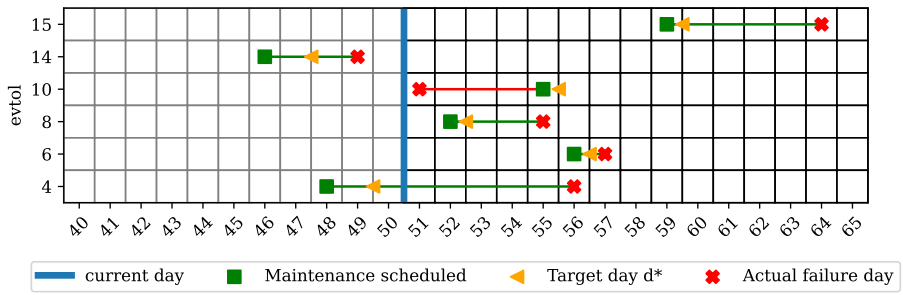

(c) current day 51

Figure 7.11.: Illustration of the evolution of the maintenance schedule, generated with the End-to-End Maintenance algorithm (E2E-M), for three days (46, 49, and 51). Days 40 through 65 and eVTOLs which have an EOL within this window are shown. For each eVTOL, the EOL is shown as a (red) cross, together with the current target day as a (yellow) triangle. The current scheduled maintenance day is shown as a (green) square, connected to the EOL day.

The proposed framework is applied in a case study for a fleet of 25 electric vertical take-off and landing (eVTOL) aircraft. These perform round trips to and from a hub airport. Each eVTOL is equipped with a battery which degrades across time. A dataset of sensor measurements related to the temperature, voltage, and the current of the batteries is used to inform the maintenance planning of the batteries and associated costs [37]. The proposed End-to-End Maintenance framework is implemented with a Long-Short Term Memory (LSTM) regressor. When compared with the optimal maintenance decisions available at an Oracle, 36% extra maintenance costs are incurred, with only 6 battery failures per year (3.6%). This is a significant improvement when compared to a conventional two-stage maintenance planning model. In this case, 49% extra maintenance costs are incurred, with 8 battery failures per year.

Overall, this study lays the groundwork for data-driven, end-to-end, dynamic predictive maintenance for a set of assets. As future work, we plan to extend our proposed end-to-end framework for the case of more complex maintenance planning cases, with increasing more dependencies between the maintenance needs of the assets and the operational practices specified for these assets.

references

[1] S. van Oosterom and M. Mitici. “End-to-end predict-then-optimize for maintenance planning of Lithium-Ion batteries”. In: *Submitted to Transportation Research Part C: Emerging Technologies* (2025).

[2] V. Badea, Z. Alin, and R. Boncea. “Big Data in the Aerospace Industry”. In: *Informatica Economica* 22 (Mar. 2018), pp. 17–24. DOI: 10.12948/issn14531305/22.1.2018.02.

[3] J. Tautz-Weinert and S. J. Watson. “Using SCADA data for wind turbine condition monitoring – a review”. en. In: *IET Renewable Power Generation* 11.4 (2017). _eprint: https://ietresearch.onlinelibrary.wiley.com/doi/pdf/10.1049/iet-rpg.2016.0248, pp. 382–394. ISSN: 1752-1424. DOI: 10.1049/iet-rpg.2016.0248. (Visited on 02/03/2025).

[4] L. Ren, L. Zhao, S. Hong, S. Zhao, H. Wang, and L. Zhang. “Remaining Useful Life Prediction for Lithium-Ion Battery: A Deep Learning Approach”. In: *IEEE Access* 6 (2018). Conference Name: IEEE Access, pp. 50587–50598. ISSN: 2169-3536. DOI: 10.1109/ACCESS.2018.2858856. URL: https://ieeexplore.ieee.org/document/8418374 (visited on 12/08/2024).

[5] L. Biggio, A. Wieland, M. A. Chao, I. Kastanis, and O. Fink. “Uncertainty-Aware Prognosis via Deep Gaussian Process”. In: *IEEE Access* 9 (2021). Conference Name: IEEE Access, pp. 123517–123527. ISSN: 2169-3536. DOI: 10.1109/ACCESS.2021.3110049. URL: https://ieeexplore.ieee.org/document/9530487 (visited on 12/08/2024).

[6] I. de Pater, A. Reijns, and M. Mitici. “Alarm-based predictive maintenance scheduling for aircraft engines with imperfect Remaining Useful Life prognostics”. In: *Reliability Engineering & System Safety* 221 (May 2022), p. 108341. ISSN: 0951-8320. DOI: 10.1016/j.ress.2022.108341. (Visited on 08/27/2024).

[7] A. Jamshidi, S. Hajizadeh, Z. Su, M. Naeimi, A. Núñez, R. Dollevoet, B. De Schutter, and Z. Li. “A decision support approach for condition-based maintenance of rails based on big data analysis”. In: *Transportation Research Part C: Emerging Technologies* 95 (Oct. 2018), pp. 185–206. ISSN: 0968-090X. DOI: 10.1016/j.trc.2018.07.007. (Visited on 12/08/2024).

[8] Q. Deng, B. F. Santos, and R. Curran. “A practical dynamic programming based methodology for aircraft maintenance check scheduling optimization”. In: *European Journal of Operational Research* 281.2 (Mar. 2020), pp. 256–273. ISSN: 0377-2217. DOI: 10.1016/j.ejor.2019.08.025. (Visited on 12/08/2024).

[9] P. J. van Kessel, F. C. Freeman, and B. F. Santos. “Airline maintenance task rescheduling in a disruptive environment”. In: *European Journal of Operational Research* 308.2 (July 2023), pp. 605–621. ISSN: 0377-2217. DOI: 10.1016/j.ejor.2022.11.017. (Visited on 12/08/2024).

[10] X. Liu, Q. Sun, Z.-S. Ye, and M. Yildirim. “Optimal multi-type inspection policy for systems with imperfect online monitoring”. In: *Reliability Engineering & System Safety* 207 (Mar. 2021), p. 107335. ISSN: 0951-8320. DOI: 10.1016/j.ress.2020.107335. (Visited on 12/08/2024).

[11] J. Lee and M. Mitici. “Deep reinforcement learning for predictive aircraft maintenance using probabilistic Remaining-Useful-Life prognostics”. In: *Reliability Engineering & System Safety* 230 (Feb. 2023), p. 108908. ISSN: 0951-8320. DOI: 10.1016/j.ress.2022.108908. (Visited on 12/08/2024).

[12] C. Chen, G. Zhu, J. Shi, N. Lu, and B. Jiang. “Dynamic Predictive Maintenance Scheduling Using Deep Learning Ensemble for System Health Prognostics”. In: *IEEE Sensors Journal* PP (Oct. 2021), pp. 1–1. DOI: 10.1109/JSEN.2021.3119553.

[13] K. T. P. Nguyen and K. Medjaher. “A new dynamic predictive maintenance framework using deep learning for failure prognostics”. In: *Reliability Engineering & System Safety* 188 (Aug. 2019), pp. 251–262. ISSN: 0951-8320. DOI: 10.1016/j.ress.2019.03.018. URL: https://www.sciencedirect.com/science/article/pii/S0951832018311050 (visited on 12/08/2024).

[14] A. Consilvio, A. D. Febbraro, and N. Sacco. “A Rolling-Horizon Approach for Predictive Maintenance Planning to Reduce the Risk of Rail Service Disruptions”. In: *IEEE Transactions on Reliability* 70.3 (Sept. 2021). Conference Name: IEEE Transactions on Reliability, pp. 875–886. ISSN: 1558-1721. DOI: 10.1109/TR.2020.3007504. (Visited on 11/28/2024).

[15] Z. Allah Bukhsh, A. Saeed, I. Stipanovic, and A. G. Doree. “Predictive maintenance using tree-based classification techniques: A case of railway switches”. In: *Transportation Research Part C: Emerging Technologies* 101 (Apr. 2019), pp. 35–54. ISSN: 0968-090X. DOI: 10.1016/j.trc.2019.02.001. (Visited on 12/08/2024).

[16] I. d. Pater and M. Mitici. “Novel Metrics to Evaluate Probabilistic Remaining Useful Life Prognostics with Applications to Turbofan Engines”. en. In: *PHM Society European Conference* 7.1 (June 2022). Number: 1, pp. 96–109. ISSN: 2325-016X. DOI: 10.36001/phme.2022.v7i1.3320. (Visited on 05/17/2024).

[17] P. C. Lopes Gerum, A. Altay, and M. Baykal-Gürsoy. “Data-driven predictive maintenance scheduling policies for railways”. In: *Transportation Research Part C: Emerging Technologies* 107 (Oct. 2019), pp. 137–154. ISSN: 0968-090X. DOI: 10.1016/j.trc.2019.07.020. (Visited on 12/08/2024).

[18] Z. Su, A. Jamshidi, A. Núñez, S. Baldi, and B. De Schutter. “Integrated condition-based track maintenance planning and crew scheduling of railway networks”. In: *Transportation Research Part C: Emerging Technologies* 105 (Aug. 2019), pp. 359–384. ISSN: 0968-090X. DOI: 10.1016/j.trc.2019.05.045. (Visited on 12/08/2024).

[19] M. Mitici, I. de Pater, A. Barros, and Z. Zeng. “Dynamic predictive maintenance for multiple components using data-driven probabilistic RUL prognostics: The case of turbofan engines”. In: *Reliability Engineering & System Safety* 234 (June 2023), p. 109199. ISSN: 0951-8320. DOI: 10.1016/j.ress.2023.109199. (Visited on 04/04/2024).

[20] T. Vanderschueren, T. Verdonck, B. Baesens, and W. Verbeke. “Predict-then-optimize or predict-and-optimize? An empirical evaluation of cost-sensitive learning strategies”. In: *Information Sciences* 594 (May 2022), pp. 400–415. ISSN: 0020-0255. DOI: 10.1016/j.ins.2022.02.021. URL: https://www.sciencedirect.com/science/article/pii/S0020025522001542 (visited on 12/08/2024).

[21] J. Kotary, V. D. Vito, J. Christopher, P. V. Hentenryck, and F. Fioretto. *Predict-Then-Optimize by Proxy: Learning Joint Models of Prediction and Optimization*. arXiv:2311.13087 [cs]. Nov. 2023. DOI: 10.48550/arXiv.2311.13087. URL: http://arxiv.org/abs/2311.13087 (visited on 12/08/2024).

[22] J. Zhang, E. Shan, L. Wu, J. Yin, L. Yang, and Z. Gao. “An End-to-End Predict-Then-Optimize Clustering Method for Stochastic Assignment Problems”. In: *IEEE Transactions on Intelligent Transportation Systems* 25.9 (Sept. 2024). Conference Name: IEEE Transactions on Intelligent Transportation Systems, pp. 12605–12620. ISSN: 1558-0016. DOI: 10.1109/TITS.2024.3385029. (Visited on 12/08/2024).

[23] A. N. Elmachtoub and P. Grigas. *Smart "Predict, then Optimize"*. arXiv:1710.08005 [cs, math, stat]. Nov. 2020. DOI: 10.48550/arXiv.1710.08005. (Visited on 03/15/2024).

[24] J. Mandi, E. Demirovi, P. Stuckey, and T. Guns. “Smart Predict-and-Optimize for Hard Combinatorial Optimization Problems”. In: *Proceedings of the AAAI Conference on Artificial Intelligence* 34 (Apr. 2020), pp. 1603–1610. DOI: 10.1609/aaai.v34i02.5521.

[25] X. Chang, J. Wu, H. Sun, and X. Yan. “A Smart Predict-then-Optimize method for dynamic green bike relocation in the free-floating system”. In: *Transportation Research Part C: Emerging Technologies* 153 (Aug. 2023), p. 104220. ISSN: 0968-090X. DOI: 10.1016/j.trc.2023.104220. (Visited on 12/08/2024).

[26] M. Vlastelica, A. Paulus, V. Musil, G. Martius, and M. Rolínek. *Differentiation of Blackbox Combinatorial Solvers*. arXiv:1912.02175 [cs]. Feb. 2020. DOI: 10.48550/arXiv.1912.02175. URL: http://arxiv.org/abs/1912.02175 (visited on 12/08/2024).

[27] Q. Berthet, M. Blondel, O. Teboul, M. Cuturi, J.-P. Vert, and F. Bach. “Learning with Differentiable Pertubed Optimizers”. In: *Advances in Neural Information Processing Systems*. Vol. 33. Curran Associates, Inc., 2020, pp. 9508–9519. URL: https://papers.nips.cc/paper/2020/hash/6bb56208f672af0dd65451f869fedfd9-Abstract.html (visited on 12/08/2024).

[28] B. Tang and E. B. Khalil. “PyEPO: a PyTorch-based end-to-end predict-then-optimize library for linear and integer programming”. en. In: *Mathematical Programming Computation* (July 2024). ISSN: 1867-2957. DOI: 10.1007/s12532-024-00255-x. (Visited on 08/29/2024).

[29] C. P. Andriotis and K. G. Papakonstantinou. “Managing engineering systems with large state and action spaces through deep reinforcement learning”. In: *Reliability Engineering & System Safety* 191 (Nov. 2019), p. 106483. ISSN: 0951-8320. DOI: 10.1016/j.ress.2019.04.036. (Visited on 02/05/2025).

[30] J. Lee and M. Mitici. “An integrated assessment of safety and efficiency of aircraft maintenance strategies using agent-based modelling and stochastic Petri nets”. In: *Reliability Engineering & System Safety* 202 (Oct. 2020), p. 107052. ISSN: 0951-8320. DOI: 10.1016/j.ress.2020.107052. (Visited on 12/08/2024).

[31] C. M. Bishop. *Mixture density networks*. en-GB. Monograph. Num Pages: 438543 Place: Birmingham Publisher: Aston University. Birmingham, UK: Aston University, 1994. (Visited on 01/24/2025).

[32] L. Granado, M. Ben-Marzouk, E. Solano Saenz, Y. Boukal, and S. Jugé. "Machine learning predictions of lithium-ion battery state-of-health for eVTOL applications". In: *Journal of Power Sources* 548 (Nov. 2022), p. 232051. ISSN: 0378-7753. DOI: 10.1016/j.jpowsour.2022.232051. (Visited on 04/03/2024).

[33] T. Hagspihl, R. Kolisch, and S. Schiffels. "Planning an airport shuttle network with air taxis using choice-based optimization". en. In: *OR Spectrum* (Jan. 2025). Company: Springer Distributor: Springer Institution: Springer Label: Springer Publisher: Springer Berlin Heidelberg, pp. 1–35. ISSN: 1436-6304. DOI: 10.1007/s00291-024-00801-y. (Visited on 02/03/2025).

[34] L. A. Garrow, B. J. German, and C. E. Leonard. "Urban air mobility: A comprehensive review and comparative analysis with autonomous and electric ground transportation for informing future research". en. In: *Transportation Research Part C: Emerging Technologies* 132 (Nov. 2021), p. 103377. ISSN: 0968-090X. DOI: 10.1016/j.trc.2021.103377. (Visited on 12/13/2022).

[35] M. Waltz, O. Okhrin, and M. Schultz. "Self-organized free-flight arrival for urban air mobility". In: *Transportation Research Part C: Emerging Technologies* 167 (Oct. 2024), p. 104806. ISSN: 0968-090X. DOI: 10.1016/j.trc.2024.104806. (Visited on 02/14/2025).

[36] M. Mitici, B. Hennink, M. Pavel, and J. Dong. "Prognostics for Lithium-ion batteries for electric Vertical Take-off and Landing aircraft using data-driven machine learning". In: *Energy and AI* 12 (Apr. 2023), p. 100233. ISSN: 2666-5468. DOI: 10.1016/j.egyai.2023.100233. (Visited on 02/28/2024).

[37] A. Bills, S. Sripad, L. Fredericks, M. Guttenberg, D. Charles, E. Frank, and V. Viswanathan. "A battery dataset for electric vertical takeoff and landing aircraft". en. In: *Scientific Data* 10.1 (June 2023). Publisher: Nature Publishing Group, p. 344. ISSN: 2052-4463. DOI: 10.1038/s41597-023-02180-5. (Visited on 01/24/2025).

[38] S. Lundberg and S.-I. Lee. *A Unified Approach to Interpreting Model Predictions*. arXiv:1705.07874 [cs]. Nov. 2017. DOI: 10.48550/arXiv.1705.07874. (Visited on 02/06/2025).

[39] J. Urbano, H. Lima, and A. Hanjalic. "A New Perspective on Score Standardization". In: *Proceedings of the 42nd International ACM SIGIR Conference on Research and Development in Information Retrieval*. SIGIR'19. New York, NY, USA: Association for Computing Machinery, July 2019, pp. 1061–1064. ISBN: 978-1-4503-6172-9. DOI: 10.1145/3331184.3331315. (Visited on 09/25/2024).

[40] D. E. Rumelhart, G. E. Hinton, and R. J. Williams. "Learning representations by back-propagating errors". en. In: *Nature* 323.6088 (Oct. 1986). Publisher: Nature Publishing Group, pp. 533–536. ISSN: 1476-4687. DOI: 10.1038/323533a0. (Visited on 01/24/2025).

[41] Y. Yu, X. Si, C. Hu, and J. Zhang. "A Review of Recurrent Neural Networks: LSTM Cells and Network Architectures". In: *Neural Computation* 31.7 (July 2019), pp. 1235–1270. ISSN: 0899-7667. DOI: 10.1162/neco_a_01199. (Visited on 01/24/2025).

[42] M. Wei, H. Gu, M. Ye, Q. Wang, X. Xu, and C. Wu. “Remaining useful life prediction of lithium-ion batteries based on Monte Carlo Dropout and gated recurrent unit”. In: *Energy Reports* 7 (Nov. 2021), pp. 2862–2871. ISSN: 2352-4847. DOI: 10.1016/j.egyr.2021.05.019. (Visited on 01/24/2025).

[43] S. Ruder. *An overview of gradient descent optimization algorithms*. arXiv:1609.04747 [cs]. June 2017. DOI: 10.48550/arXiv.1609.04747. (Visited on 02/06/2025).

CHAPTER 8

Conclusion

A look into the future:

> The year is 2050. Europe has created an ecosystem for the pan-European aviation companies to thrive. It is because of this that Europe has become the global leader in the field of sustainable aviation, enabled by improvement in aircraft designs, alternative fuels, air traffic management systems, and purposeful economic measures. Among others, towing of aircraft by electric vehicles has reduced energy use for flights, and has created cleaner and safer working conditions at airports. Electric aircraft now operate in the Nordic regions and on archipelagos to ensure fast and emission-free transport. Where passenger volumes are too small, eVTOLs provide an on-demand taxi service to remote locations. All of these wouldn't have been possible without safe and efficient operations optimization. But it all starts with simple beginnings...

In the hope of getting somewhere close to a future with sustainable aviation, this thesis presents three frameworks to optimize operations for electric aviation technologies. The first framework describes how electric assets can be implemented in operations while accounting for the recharge times (Chapters 2 through 4). The second framework describes how to approach limitations in the recharging technology, which provides a cost-benefit analysis of the charging infrastructure of capital investment against operating costs (Chapter 5). The last framework describes how battery maintenance can be introduced into operations through a data-driven predictive maintenance approach (Chapters 6 and 7). Together, these frameworks provide insight into the implementation of these technologies into the aviation sector.

8.1 Reflections on the research objectives

Considering the new technologies and the challenges identified in the introduction, the objective of the research in this dissertation is *The design of data-driven models to perform operations planning of the technologies from 1.3, integrated into current operations,*

for optimal efficiency. The relates sub-objectives focus on the deployment of the technologies, the required charging infrastructure, and the battery maintenance planning. The key findings related to these are presented in Sections 8.1.1, 8.1.1 and 8.1.3, respectively.

8.1.1 Asset routing and assignment

Answer to Research Objective 1.1

To design a charging policy for electric towing vehicles, in order to tow as many aircraft as possible.

We have developed the **preemptive charging policy** with minimum charging time for electric towing vehicles (Chapter 2). This policy is used in the design of the more holistic ETV scheduling framework.

Why this method?

The charging policies introduced in literature, the night-charging and constant-time policies, were found to provide little schedule flexibility, resulting in a lower ETV efficiency and higher peak loads on the electricity grid. Using the preemptive charging policy, ETVs can be recharged during off-peak hours, and used during peaks with little requirements. By introducing a minimum charging time is beneficial because (i) it lowers the number of charging cycles, reducing battery degradation, (ii) lowers the number of airport surface movements, and (iii) reduces schedule volatility.

Case study and numerical results

These policies are applied in a case study at Amsterdam Schiphol airport. We found that under a nominal battery size, using our preemptive policy results in requiring 29 ETVs to tow all flights. This is significantly less than when a constant-time policy (40 ETVs, +37%) or night-charging policy (60, +207%) is used.

Answer to Research Objective 1.2

To design a centralized on-line routing algorithm for electric towing vehicles, which minimizes the total towing time, for a given airport and flight schedule.

We have developed two routing algorithms: a **greedy heuristic** algorithm, and a **MILP-based optimization** algorithm (Chapter 3). The greedy heuristic is used in the larger ETV scheduling framework.

Why this method?

The discrete structure of the airport surface roads significantly reduces routing options, enabling a (partially) discrete optimization approach. The MILP-based routing algorithm is able to address a large number of conflicts simultaneously, avoiding naive

decisions with negative consequences at a later moment. This ensures optimized routing decisions. The greedy algorithm, on the other hand, has lighter computational requirements. This enables real-time re-evaluation of routes, which allows it to be used during the operational planning phase.

Case study and numerical results

These models are applied in a case study at Amsterdam Schiphol airport. The average additional taxiing time of the flights is 10.2 seconds for the MILP-based algorithm, and 13.4 seconds for the greedy algorithm. Both gaps w.r.t. the optimal time are relatively small. Additionally, the computational performance of the greedy algorithm is significantly better: 19 seconds against 8158 seconds are required to plan operations for a day of operations.

Future work

This algorithm assumes simplified vehicle dynamics. This is addressed in more detail in Section 8.2.3. Additionally, these algorithms can be leveraged to create appropriate dynamic buffer times for the ETV-to-aircraft problem. Using dynamic buffers will increase the robustness of the ETV schedule.

Answer to Research Objective 1.3

To design an online aircraft-to-ETV assignment model that maximizes the environmental benefit of an ETV fleet of a given size, for a given flight schedule.

A **rolling horizon MILP-based optimization** algorithm has been developed, which takes battery performance limitations into account (Chapters 3 and 4). The method is able to process flight schedule disturbances. It is used to minimize taxiing emissions and additional delays as much as possible.

Why this method?

Using a MILP to reevaluate the ETV schedule combines a number of advantages. First, it ensures a balanced recharging schedule, such that the ETV availability during peak hours is maximized. Second, it is the first algorithm which is able to not only react to operational disturbances, but that *anticipates* these. Third, because of the modular nature, it is able to accommodate other operational disturbances (such as taxiing and charging time uncertainties), and allows for advanced delay prognostics as an input. Last, it is able to provide insight into why different flights are towed subsequently. Using a global re-evaluation of the schedule is computationally expensive, but can be performed within an appropriate time window.

Case study and numerical results

The algorithm is applied to a case study at Amsterdam Schiphol airport. It reaches 79.5% of the highest possible performance, which is obtained when full knowledge of the flight delays is known in advance. Furthermore, it performs 18% better than an algorithm which only is able to react to disruptions (See figure 8.1 for an example schedule). Performing a cost-benefit analysis of the number of ETVs provides fleet sizing decision

support.

Future work

Currently, this algorithm can be expanded in several ways. Most notably, it aims to minimize the overall taxiing pollution and fuel burn, without fairly distributing the benefits over all airlines and airport areas. Furthermore, it assumes that the schedule suggested by the algorithm is executed immediately and without alterations. These limitations are discussed further in Section 8.2.2.

To sum up, we present our first conclusion:

C1 The ability to anticipate flight delays has a large influence on the efficiency with which an ETV fleet can be used.

Modern systems allow for real-time access to the latest flight information. In a rolling horizon predict-then-optimize framework, this information can be leveraged for ETV assignment. Having information on the distribution of the arrival and departure times of flights enables a robust and dynamic assignment. We have demonstrated that using relatively simple historical data to perform this significantly increases the impact of an ETV fleet w.r.t. using the latest point estimates.

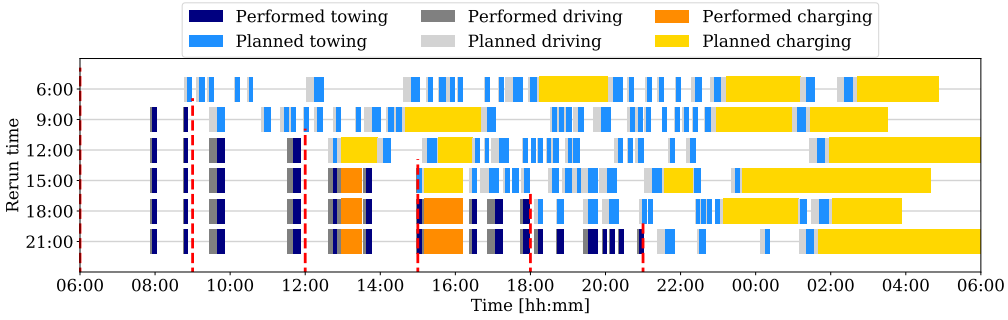

Figure 8.1.: Evolving ETV schedule, presented in Chapter 3 (Figure 3.18).

8.1.2 Charging infrastructure management

Answer to Research Objective 2.1

To design a model to optimize the battery swapping and charging process for a given infrastructure, airport, and day of operations.

A **MILP-based optimization** algorithm has been designed to manage charging operations during the tactical phase. The results show the benefits of a swapping system: a more evenly spread demand for electricity across the day, without long turnarounds.

Why this method?

By using a MILP formulation, we are able to penalize both peak-hour electricity use and delays due to insufficient charging infrastructure. By setting appropriate cost coefficients, the minimization of the latter is prioritized. Additionally, this algorithm guarantees optimality of the solution within a short optimization time. As such, it is suitable to be used as a subroutine in the charging infrastructure sizing problem of Objective 2.2.

Answer to Research Objective 2.2

To design a model to determine the optimal swapping and charging infrastructure size for a given airport.

A **two-stage recourse model** has been developed to size the charging infrastructure of a battery swapping system (Chapter 5). This is solved with a **simulated annealing** algorithm.

Why this method?

The charging infrastructure optimization algorithms introduced in literature were found to ignore the multi-staged nature of this problem, i.e. the distinction between strategic and tactical phase decisions was not considered. Our recourse algorithm does take this into account, and enables a balance between the capital expenditures, made for infrastructure acquisition, with operational expenditures, used for electricity and delays. Furthermore, the simulated annealing algorithm offers a light-weight optimization approach, allowing a large number of scenarios to be studied.

Case study and numerical results

Our algorithm is applied to study the electrification of a domestic aviation network in Norway. Figure 8.2 shows an example of a charging schedule. It is bench-marked it against an algorithm that optimizes the infrastructure for given operational parameters, corresponding to either the peak-day or an average day, as seen in literature. When compared with these algorithms, we have shown that the recourse algorithm reduces the overall costs of the infrastructure by 31% and 7%, respectively.

Future work

The model assumptions can be relaxed in several of ways. Though the costs of causing a delay significantly outweigh the costs of using off-peak electricity, delays can occur in the solution. However, the algorithm does not account for the propagation of these delays through the network. Such a model would be required to address the charging operations at all airports simultaneously. This limitation is addressed in the recommendations of Section 8.4.

Summarizing, we present our second conclusion:

C2 Considering the demand variation can be leveraged to support ETV and charging infrastructure sizing decisions.

Under limited information on future demand, it is often not possible to determine an optimal infrastructure size. We have demonstrated that considering a variation in demand provides significant benefits. For ETVs, we have considered different days of operations with different fleet sizes. With this, we have quantified the expected value and variance in the environmental benefits of using the ETVs. For electric aircraft charging, we have considered different days of operations with a varying charging infrastructure. We have shown that utilizing the optimal infrastructure for a peak day leads to under-utilization. (Shown in Chapters 4 and 5.)

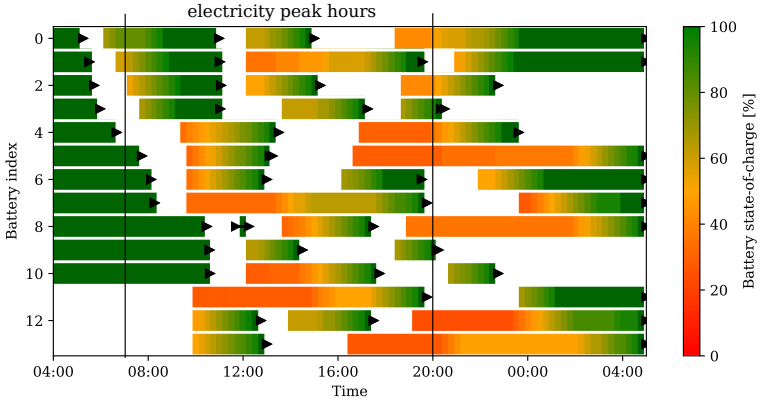

Figure 8.2.: Battery charging schedule of swapped batteries at BodøLufthavn, presented in Chapter 5 (Figure 5.7).

8

8.1.3 Battery maintenance planning

Answer to Research Objective 3.1

To develop a prognostics and health management model for batteries used for electric aircraft.

A **mixture density network** (MDN) and **Long short-term memory network** (LSTM) have been developed to generate probabilistic remaining useful life prognostics (Chapters 6 and 7).

Why this method?

When developing health estimators to incorporate into maintenance planning of critical components, a quantification of the prognostics uncertainty is essential. The MDN regressor is designed with this regard. For the LSTM network, this is achieved using random dropout during the testing phase. Additionally, the battery degradation is a temporal process, which is naturally accommodated by an LSTM.

Case study and numerical results

Both regressors are applied in a case study on a dataset of batteries which are cycled through various eVTOL mission simulations. For most batteries, a Continuous Ranked Probability Score of 24.5 is obtained. Figure 8.3 shows an example of these prognostics. We have shown that using probabilistic prognostics reduces the risk of RUL overestimation.

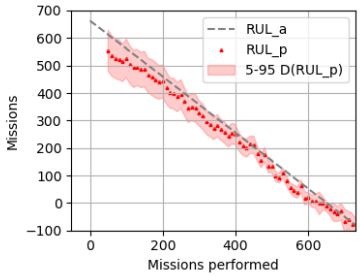

Figure 8.3.: Probabilistic RUL prognostics for an eVTOL battery, presented in Chapter 6 (Figure 6.3).

Answer to Research Objective 3.2

To develop a planning model which uses these prognostics to perform maintenance planning for a fleet of vehicles operating from a central hub airport.

Two predictive maintenance scheduling model has been developed, using a **two-stage** algorithm with probabilistic RUL prognostics, and an **end-to-end** algorithm using maintenance cost estimates (Chapter 7).

8

Why this method?

Maintenance of safety-critical systems requires regular health-monitoring. Predictive maintenance integrates this data into the planning process. This allows for dynamic decision making with insight into the process. Using probabilistic prognostics or end-to-end optimization also ensures that the maintenance decisions are conservative enough, avoiding battery failures. Moreover, the end-to-end method takes the structure of the maintenance planning problem into account while training the regressor, enabling an integrated, instead of post-hoc, approach.

Case study and numerical results

The algorithms are applied in a study on a dataset of batteries which are used various eVTOL mission simulations. The end-to-end optimization method outperforms the two-stage method: the additional maintenance costs are 49% and 36%, respectively, with 0.32 and 0.25 battery failures per eVTOL per year. This shows the potential of using an end-to-end maintenance planning model.

Future work

This method can be adapted to account for operations in which multiple hubs, where the vehicles are parked, are used. Additionally, it can be placed into a larger scheduling framework. This will be addressed in Section 8.2.1.

As such, we present our third conclusion:

C3 Integrating the maintenance scheduling problem into the training of a battery maintenance cost estimation algorithm reduces breakdowns and maintenance costs when compared to a sequential approach.

Introducing full-electric assets into aviation operations raise new questions on battery maintenance operations. Battery monitoring sensors have opened the possibility of applying the predictive maintenance framework in operations. In this dissertation, we have developed an end-to-end predictive maintenance algorithm. When compared to the two-stage approach, we have demonstrated that this algorithm results in a lower number of failures, while simultaneously increasing the average lifetime an asset is used. (As shown in Chapters 6 and 7).

8.2 Reflections on the research limitations

As introduced in Section 1.6, several boundaries to the research scope have been defined. Additionally, the methods which have been employed to address the research objectives have their own limitations. In this section, we provide an overview of the boundaries of the research, as well as their implications.

8.2.1 Airport and airline planning phases

Different airport and airline planning decisions are made at different frequencies and time horizons in mind. Recognizing this distinction, as well as the interaction between these different phases is an essential aspect of this thesis. This interaction can come in many forms. For example, whenever an eVTOL needs to go under maintenance, they are not available for a certain amount of time (as we have seen in Chapters 6 and 7). As such, in order to fulfil all duties, additional eVTOLs are required.

We have studied the interaction between strategic (long-term), tactic (medium term) and operational (short term) decisions. For ETVs, we considered the interaction between all phases in Chapter 4, for charging infrastructure, the interaction between the strategic and tactic phases in Chapter 5, and for battery maintenance, the interaction between the tactic and operational planning phases in Chapter 7. However, even with expanding the latter two problems to all planning phases, this covers a limited part of the problem. For a holistic approach, an integrated approach is required, as used by airlines and airports in practice (see Figure 8.4). In this approach, decisions on different domains (maintenance, asset and personnel scheduling, and revenue streams) are integrated, and performed in a full rolling horizon approach. A full operations management framework for the

ETVs/eACs/eVTOLs needs to expand in this direction, while using the output of this dissertation as a basis.

If the problems expand and intertwine, the developed models might no longer suffice. For these operations, one possible avenue to explore are simplified or machine learning algorithms.

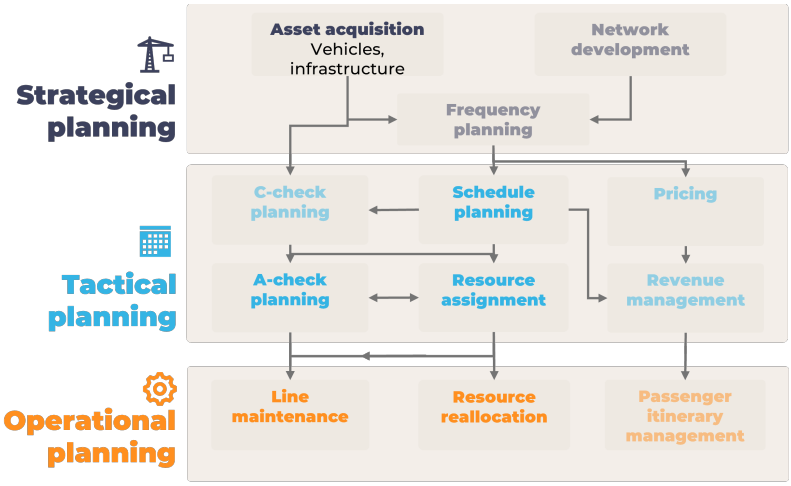

Figure 8.4.: Airline and airport planning framework (adapted from Belobaba et al. [1]). Dark-gray cells are covered in this dissertation.

8.2.2 Human agents

Human safety, preference, and agency requirements are an integral part of operations research during all planning phases. This is manifested in a variety of ways. Most notably, there are scheduling problems which revolve around humans, like assignments of personnel to vehicles [1] or taxi assignment [2]. But even in problems which do not revolve around humans, human requirements are often modelled in there. For example, bus routes are planned in a way that allows enough rest time for the chauffeur, ensuring workable and safe conditions. Last, human autonomy is often included in operations research problems, by e.g. using a framework which allows a planner or chauffeur to deviate from the output recommended by the algorithm. All these factors ensure that operations research can be applied.

The focus throughout all chapters of this thesis has been to design algorithms which yield a high utilization/efficiency of the technologies. As such, human requirements and human agency are not fully modelled and implemented. As for the first, the human requirements, the drawback of ignoring this is limited. Some of the safety and preference requirements have been modelled, and we assume others can be added without fundamentally changing the structure and performance of the models. In the chapters,

we have indicated where this is the case. As for the second, regarding human agency, this is not studied in this thesis. As such, throughout the chapters, it is assumed that the schedules generated by the algorithms are always implemented, and that they are flawlessly performed. By adding additional constraints to the model, this feature can be implemented.

8.2.3 Vehicle performance, dynamics and environmental modelling

Modelling the energy requirements, dynamics, and environmental impact of the technologies we have discussed is a challenge by itself. As this dissertation considers maximizing the impact of the mentioned technologies, some working assumptions and baseline models of these processes are required. They are required as input for the algorithms which we create in order to achieve this.

These models are far from a perfect approximation of these processed, but the operations research algorithms we have developed stand on their own merit. In chapter 3 for example, the taxiing time of ETVs was modelled without considering the requirement to slow down for turns. However, it is not a part of this dissertation to develop detailed models of the vehicle dynamics and their environmental impact. Neither is this required to achieve the research objectives. Only a significant change in the parameter values, e.g. the introduction of a battery with very short charging times, will change the structure of the problem, and the models required to address it.

8.2.4 Fairness modelling

When addressing the research objective, the models which we have developed often consider the minimization of a value aggregated over a number of different tasks. We considered, e.g., the minimization of the total delay over all flights in Chapter 5, or the maximization of towed aircraft in Chapter 4. This is a limited utilitarian view of addressing these problems.

This approach is problematic for two reasons. First, and less important, the benefits and costs for one task may not be measured appropriately in this thesis This can be overcome by changing the cost parameters of the algorithms. Second, more important, a more egalitarian distribution of all costs and/or benefits may be more appropriate, especially in situations with multiple stakeholders. This was e.g. done when minimizing the maximum additional towing time in Chapter 3. By changing the objective function from an aggregate to a min-max function, we deem this limitation to be surmountable.

8.3 Scientific contributions

In this section, the concrete contributions to literature are enumerated. We distinguish between methodological and applied contributions.

Methodological contributions

MC1 A routing algorithm for electric towing vehicles at a large airport.

This dissertation is the first study to develop a routing model and algorithm suitable for electric towing vehicle operations. The model accounts for the ability of ETVs to traverse the airport at a varying velocity, avoiding the need for stop-and-go situations at taxiway intersections. A heuristic algorithm was also developed, allowing for real-time re-evaluations of the schedule. The corresponding development contributed to the following journal publication:

S. van Oosterom, M. Mitici, and J. Hoekstra. "Dispatching a fleet of electric towing vehicles for aircraft taxiing with conflict avoidance and efficient battery charging". en. In: *Transportation Research Part C: Emerging Technologies* 147 (Feb. 2023), p. 103995. ISSN: 0968-090X. DOI: 10.1016/j.trc.2022.103995

MC2 Integrated three-phase electric vehicle routing problem with stochastic pick-up times in a dynamic setting.

This dissertation studied the ETV-to-aircraft assignment problem, formulated as an E-VRP-TW model, and developed suitable algorithms. This model is the first of it's kind that anticipates uncertainty in pick-up times and incorporates this in a rolling horizon framework. It is also general enough to incorporate other disruptions. We have also demonstrated how the model can be embedded in a larger framework to study the required vehicle fleet size. The corresponding contribution led to the following journal publication:

S. van Oosterom and M. Mitici. "An environmentally-aware dynamic planning of electric vehicles for aircraft towing considering stochastic aircraft arrival and departure times". In: *Transportation Research Part C: Emerging Technologies* 169 (2024). DOI: 10.1016/j.trc.2024.104857

MC3 A battery swap scheduling and infrastructure sizing model.

This dissertation developed operations optimization models and algorithms for the understudied concept of battery swap systems for aircraft. The impact of the size of the charging capacity on operations during the tactical stage is taken into account, resulting in a balanced infrastructure. This is the first model for this problem to distinguish between the strategical and tactical planning stage decisions. The corresponding contribution led to the following journal publication:

S. van Oosterom and M. Mitici. "Optimizing the battery charging and swapping infrastructure for electric short-haul aircraft—The case of electric flight in Norway". English. In: *Transportation Research Part C: Emerging Technologies* 155 (2023). ISSN: 0968-090X. DOI: 10.1016/j.trc.2023.104313

MC4 An end-to-end predict-then-optimize algorithm for predictive maintenance for a set of assets.

This dissertation studies the integration of battery maintenance scheduling into operations. It introduced the first algorithm that incorporates the maintenance

scheduling problem into the estimation of the state-of-health prognostics. This development improves the robustness of the resulting maintenance schedule while reducing maintenance costs. The corresponding contribution was submitted as the following publication under review:

S. van Oosterom and M. Mitici. "End-to-end predict-then-optimize for maintenance planning of Lithium-Ion batteries". In: *Submitted to Transportation Research Part C: Emerging Technologies* (2025)

Applied contributions

AC1 Quantification of the investment required for an ETV fleet at *Amsterdam Airport Schiphol*.

This research the first to quantify the required ETV fleet size with an efficient dispatchment algorithm that accounts for operational disruptions. This analysis is performed using the algorithms developed in Chapters 2 through 4. The results show the importance of taking operational disruptions into account, as well as the importance of anticipating (instead of only reacting) to these.

AC2 An overview of the required infrastructure for the domestic Norwegian aviation network.

We performed the first study on the required infrastructure investments for an aircraft battery swapping system for the Norwegian domestic network. This is done using the model developed in Chapter 5. The results show that significant investments are required along the Trondheim-Bodø-Tromsøaxis, with minor investments in the north and south of Norway.

AC3 Integration of data-driven health prognostics of the eVTOL batteries into maintenance planning.

We have applied the predictive maintenance planning framework, and our end-to-end optimization algorithm, to the dataset of Sony-Murata 18650 batteries cycled through eVTOL operation simulations. With 25 eVTOLs operating 5 round trips from a hub per day, we have demonstrated that the gathered sensor data can be integrated into a predictive maintenance framework.

8.4 Recommendations for future research

A number of open challenges still exist that complicate the introduction of electric aviation operations research models and algorithms into common practice. Based on the work performed in this dissertation, some recommendations are presented in this section.

R1 Development and implementation of a concept of operations for ETVs and electric aircraft.

The development and implementation of the three technologies which have been discussed is still in the early stages. A diesel-hybrid ETV is in operations in one

airport with tests underway at others, the first full electric aircraft of 10 passengers is yet to be certified, and eVTOLs which exists are only used for demonstrators. Without having a commercially endorsed and tested mode of operations for these technologies, the operations optimization models and algorithms rely on guesswork. As is, these models can only be validated to a small degree. Therefore, a standardized and accepted mode of operations is required to develop these models and the accompanying algorithms.

R2 Development of models and algorithms for situations in which electric technologies coexist with other technologies.

An underlying aspect of each model considered in this thesis was an operation of only the electric assets. These models are used to set a destination for the future of aviation. However, these technologies will not be the only ones used. First, during the transition towards sustainable aviation, the current technologies will be phased out, but will still be operating (e.g. ETVs will work side-by-side of push-back trucks). Additionally, besides electric assets, hydrogen and SAF applications will also be used. Models can be developed for operations with a mix of these three technologies.

R3 Combining the routing, charging, and maintenance planning problems into an overarching framework.

In this thesis, we have considered the problems of routing, assignment, charging, and maintenance separately. The next step in creating a framework to manage electric assets in aviation is the combination of these problems into a larger framework. This framework would be analogous to the one presented in Figure 8.4 (for airlines). Using such a framework, a realistic estimate for the strategic decisions can be made, which forms the first step towards full implementation of these technologies.

R4 The development of intuitive optimization algorithms.

Current research focuses on optimizing the performance of the assets. However, when integrating these technologies into practice, these need to be integrated into a system of interconnected problems (explained above). In this case, the current algorithms may not be able to provide the required computational performance. Additionally, it is not always possible to reason why the algorithms reach certain decisions. To address these issues, simpler heuristic algorithms should be developed, which provide insight in the decision making process.

R5 The inclusion of fairness metrics in the scheduling frameworks and algorithms.

As noted in Section 8.2.4, the developed algorithms use a simplified aggregated utilitarian objective. However, in practice, they may not suffice. Future research can explore the validation of the current objectives in each problem. Where required, the objective coefficients can be updated to include additional effects. If needed, the aggregated-form objectives can be replaced by a min-max objective. Algorithms should be developed to accompany these new models.

Bibliography

[1] P. Belobaba, A. R. Odoni, and C. Barnhart. *The Global Airline Industry*. 1st ed. Hoboken: John Wiley & Sons, Ltd, 2009.

[2] A. Glaschenko, A. Ivaschenko, G. Rzevski, and P. Skobelev. "Multi-Agent Real Time Scheduling System for Taxi Companies". en. In: Budapest, Hungary, 2009. URL: https://aamas.csc.liv.ac.uk/Proceedings/aamas2009/pdf/03_Industrial_Track/13_70_it.pdf.

[3] S. van Oosterom, M. Mitici, and J. Hoekstra. "Dispatching a fleet of electric towing vehicles for aircraft taxiing with conflict avoidance and efficient battery charging". en. In: *Transportation Research Part C: Emerging Technologies* 147 (Feb. 2023), p. 103995. ISSN: 0968-090X. DOI: 10.1016/j.trc.2022.103995.

[4] S. van Oosterom and M. Mitici. "An environmentally-aware dynamic planning of electric vehicles for aircraft towing considering stochastic aircraft arrival and departure times". In: *Transportation Research Part C: Emerging Technologies* 169 (2024). DOI: 10.1016/j.trc.2024.104857.

[5] S. van Oosterom and M. Mitici. "Optimizing the battery charging and swapping infrastructure for electric short-haul aircraft—The case of electric flight in Norway". English. In: *Transportation Research Part C: Emerging Technologies* 155 (2023). ISSN: 0968-090X. DOI: 10.1016/j.trc.2023.104313.

[6] S. van Oosterom and M. Mitici. "End-to-end predict-then-optimize for maintenance planning of Lithium-Ion batteries". In: *Submitted to Transportation Research Part C: Emerging Technologies* (2025).

[7] P. van Oosterom, S. van Oosterom, H. Liu, R. Thompson, M. Meijers, and E. Verbree. "Organizing and visualizing point clouds with continuous levels of detail". In: *ISPRS Journal of Photogrammetry and Remote Sensing* 194 (Dec. 2022), pp. 119–131. ISSN: 0924-2716. DOI: 10.1016/j.isprsjprs.2022.10.004. (Visited on 12/13/2024).

[8] M. Mitici and S. van Oosterom. "Adaptive predictive maintenance for the batteries of electric Vertical Take-off and Landing (eVTOL) aircraft using Remaining Useful Life prognostics". In: *Proceedings of the 34th European Safety and Reliability Conference*. Stavanger, Norway, June 2025.

[9] M. Zoutendijk, S. van Oosterom, and M. Mitici. "Electric Taxiing with Disruption Management: Assignment of Electric Towing Vehicles to Aircraft". In: San Diego: AIAA, June 2023.

[10] M. Cousy, V. Peyruqueou, C. Pierre, P. Cyrille, D.-B. Vo, J. Garcia, M. Mihaela, S. van Oosterom, A. Sharpanskykh, M. v. D. Burg, P. Roling, E. Spiller, S. Gottofredi, and P. Lanzi. "AEON: Toward a concept of operation and tools for supporting engine-off navigation for ground operations". en. In: Oct. 2022. URL: https://enac.hal.science/hal-03859908 (visited on 02/20/2024).

[11] S. van Oosterom, M. Mitici, and J. Hoekstra. "Analyzing the impact of battery capacity and charging protocols on the dispatchment of electric towing vehicles at a large airport". In: *AIAA AVIATION 2022 Forum*. AIAA AVIATION Forum. American Institute of Aeronautics and Astronautics, June 2022. DOI: 10.2514/6.2022-3920.

APPENDIX A

Overview of notation

A.1 Overview of notation used in Chapter 3

We provide an overview of the notation used in the problem description and model formulation from chapter 3.

Sets		
General		
N_R	-	Runway entrance and exit nodes
N_G	-	Gates
N_X	-	Taxiway junctions
N_S	-	Service road junctions
E_X	-	Roads in the taxiway system
E_S	-	Roads in the service road system
E_X^G (E_X^R)	-	Roads connecting the taxiway to the gates (runways)
E_S^G (E_S^R)	-	Roads connecting the service roads to the gates (runways)
N_{CS}	-	ETV charging stations
A	-	To-be-towed aircraft
W	-	Aircraft weight classes
$A^w \subset A$	-	To-be-towed aircraft of weight class w
$A^{arr,w}$ ($A^{dep,w}$)	-	Arriving (departing) aircraft of weight class w
MILP Phase 1		
N_a	-	junctions in the taxiway crossed by aircraft a
A_n	-	Aircraft which cross junction $n \in N_X$
A_n^{con}	-	Possible separation infringement aircraft pair
A_{nm}^{ot}	-	Possible overtake aircraft pair at junction n
A_{nm}^{ho}	-	Possible head-on collision aircraft pair at taxiway nm

Continued on next page

A

Table A.1 – continued from previous page

MILP Phase 2		
E_a	-	Taxiway roads traversed by aircraft a
A_a^{in}	-	Aircraft towable before towing aircraft a
A_a^{out}	-	Aircraft towable after towing aircraft a
Parameters		
General		
$d_X(e)$ ($d_S(e)$)	m	Length of taxiway (service road) e
n^{dep}	-	ETV depot location
$n^s(a)$ ($n^e(a)$)	-	Pick-up (drop-off) location for aircraft a
$t^s(a)$	s	Pick-up time for aircraft a
$m(a)$	kg	Mass of aircraft a
t^{EWU} (t^{ECD})	s	Engine warm-up (cool-down) time
t^{Con} (t^{DCon})	s	ETV connecting (de-connecting) time
t^{PB}	s	Push-back time
m_w	kg	Mass of ETV of weight class w
v_s	m/s	Velocity of ETVs on the service roads
$v^w_{min}(e)$ ($v^w_{max}(e)$)	m/s	minimum (maximum) velocity of ETV from class w on road e
a^{max}	m/s^2	maximum acceleration/deceleration rate of a towed aircraft
P_w	kW	Energy consumption rate of ETV from class w
P^c_w	kW	Charging rate of ETV from class w
α	-	Fast-charging threshold
β	-	Slow-charging to fast-charging rate ratio
Q_w		Battery capacity of ETV from class w
t^c_{min}	s	Minimum ETV charging time
MILP Phase 1		
$t^w_{min}(e)$ ($t^w_{max}(e)$)	s	minimum (maximum) traversing time of an aircraft of weight class w on taxiway e
$t^{end}_{max}(a)$	s	Latest arrival time of aircraft a at its drop-off point
MILP Phase 2		
t^a_e	s	travelling time of aircraft a on taxiway e
$t^{end}(a)$	s	drop-off time of the ETV of aircraft a
$q^X(a)$	kWh	energy consumed by an ETV towing aircraft a
$q^S_f(a)$	kWh	energy consumed by an ETV driving from the depot to pick-up point of aircraft a
$q^S_l(a)$	kWh	energy consumed by an ETV driving from the drop-off point of aircraft a to the depot
$q^S(a,b)$	kWh	energy consumed by an ETV driving from the drop-off point of a to the pick-up point of b

Continued on next page

Table A.1 – continued from previous page

$q_C^S(a,b)$	kWh	energy consumed by an ETV driving from the drop-off point of a to the pick-up point of b via the charging station
$q_C^S(a)$	kWh	energy consumed by an ETV driving to the pick-up point of a from the closest charging station
$t^C(a,b)$	s	time available for charging an ETV between towing a and b
Variables		
MILP Phase 1		
t_n^a	s	arrival time of aircraft a at junction n
Δt_n^a	s	time aircraft a takes to d_{sep} clear of junction n
z_n^{ab}	-	binary, true if aircraft a passes junction n before b
MILP Phase 2		
x_{ab}	-	Binary, true if aircraft a is towed directly before b by the same ETV
x_a^f	-	Binary, true if aircraft a is the first towed by an ETV on this day
x_a^l	-	Binary, true if aircraft b is the last towed by an ETV on this day
q_a	kWh	State of charge of the ETV which tows aircraft a at the start of towing

Table A.1.: Overview of notation used in the problem description and formulation.

A.2 Overview of notation used in Chapter 4

An overview of the used nomenclature from Chapter 4 can be found in Table **??**.

Sets		
T	-	Day of operations
V	-	ETV fleet
N	-	Nodes in the airport road network
N^{rg}	-	Runway/gate nodes in N
N^c	-	charging station nodes in N
A	-	Arcs in the airport road network
A^X	-	Taxiway roads in A
A^S	-	Service roads in A
F	-	Arriving and departing flights
F^{arr}	-	Arriving flights
F^{dep}	-	Departing flights

Continued on next page

A

Table A.2 – continued from previous page

F'	-	Flights which can still be towed after the current time
F'_f	-	Flights which can be towed by the same ETV before towing f
V_f	-	ETVs which can tow flight f given their current state
F'^c_f	-	Flights which can be towed before f by the same ETV, with time to recharge between the tows
Parameters		
ETV parameters		
E	kWh	ETV battery energy capacity
$\mathscr{E}$	kWh/m	ETV energy usage per unit distance
P^c	kW	recharge power
α, β	-	bilinear charging cure coefficients
v^x	m/s	towing velocity
v^s	m/s	driving velocity
Δt^{ec}	s	engine cool-down time
Δt^{con}	s	ETV connect time
Δt^{rel}	s	ETV release time
Δt^{pb}	s	aircraft push-back time
$\mu^g(v)$	m/s	rolling resistance coefficient at velocity v
μ^0, v^0	m/s	rolling resistance coefficients
Airport parameters		
n^{dep}	-	ETV depot node
d^X	m	taxiway distance
d^S	m	service road distance
Aircraft parameters		
n^{p}_f	-	pick-up location of aircraft f
n^{d}_f	-	drop-off location of f
m_f	kg	mass of f
FF_f	kg/s	fuel flow of f while towing
$ALDT_f$	s	actual landing time of f
$ELDT_f(t)$	s	estimated landing time of f at time t
ΔLDT_δ	s	random variable of $ALDT - ELDT$ at δ time before the $ELDT$
$AOBT_f$	s	actual off-block time of f
$EOBT_f(t)$	s	estimated off-block time of f at t
ΔOBT_δ	s	random variable of $AOBT - EOBT$ at δ time before the $EOBT$
$\tau^{\text{p}}_f(t)$	s	desired pick-up time random variable of f at time t
$\tau^{\text{d}}_f(t)$	s	desired drop-off time random variable of f at time t

Continued on next page

Table A.2 – continued from previous page

$\tau^{o}_{fg}(t)$	s	overlap time random variable at time t if f and g are consecutively towed by the same ETV
ETV planning parameters		
$\Delta t^{c}(f,g)$	s	recharge time between towing aircraft f and g
Δt^{fix}	s	schedule fix time for departing aircraft
Δt^{reopt}	s	time between ETV planning reevaluations
$\Delta t^{c}_{\min}$	s	minimum allowed recharge time
n^{a}_{v}	-	First available location of ETV v
E_{v}	kWh	battery energy of v at first available moment
$\tau^{a}_{v}(t)$	s	First available moment of ETV v at current time t
f_{end}	-	artificial flight
F^{fix}	-	departing flights which have to be assigned to an ETV
$E^{X}(f)$	kWh	energy required to tow f
$E^{S}(f,g)$	kWh	energy required to drive from the drop-off of f to the pick-up of g
$E^{S}_{c}(f,g)$	kWh	energy required to drive from the drop-off of f to the pick-up of g via a charging station
$E^{S}_{c1}(f)$	kWh	energy required to drive from the drop-off point of f to the furthest charging station
δt	s	ETV planning reevaluation time
Cost parameters		
c^{taxi}_{f}	€	cost of letting aircraft f taxi
c^{tow}_{f}	€	cost of towing f
c^{d}_{f}	€/s	cost of delaying f for a unit time
$c_{fg}(t)$	€	cost reduction of towing f directly before g, given an overlap time t
c^{kero}	€/L	kerosene cost
c^{elec}	€/kWh	electricity cost
Model variables		
x_{fg}	-	binary, true if aircraft f is towed directly before g by the same ETV
E_{f}	kWh	ETV battery charge directly after towing f

Table A.2.: Overview of nomenclature used in Chapter 4.

Curriculum Vitæ

Simon Johannes Maria van Oosterom was born on August 9th, 1998 in Amersfoort, The Netherlands. He started a Bachelor of Mathematics and Physics in 2016 at the Delft University of Technology. He completed the double degree by conducting research on exoplanet surface mapping. He represented the study association for physics (VvTP) as an ambassador during the study trip to Brazil. In 2019, he decided that he was not made to study physics (too many experiments with wires) and started the master *Industrial and Applied Mathematics* at the TU Delft. During this time, he specialized in combinatorics, discrete mathematics, mathematical optimization and operations research. This time was made more interesting by a certain pandemic. In 2020 and 2021, he conducted his MsC thesis “Investment Optimized Airport Infrastructure for Battery and Hydrogen Canister Swaps" at the *Royal Netherlands Aerospace Centre NLR* and graduated Cum Laude.

Inspired by the aviation applications of operations research, Simon started his PhD at the Faculty of Aerospace Engineering (TU Delft). This project was supervised by Prof. dr. ir. Jacco Hoekstra and Dr. Mihaela Mitici, who had also guided him during the master thesis. His research was funded by the European Union’s SESAR JU project AEON (Advanced Engine-Off Navigation). The work focussed on developing operations research models and algorithms for electric aviation. His work has been awarded an Anna Valicek award for best student paper in aviation operations research. Alongside his research, he assisted in several courses and supervised a bachelor’s *Design Synthesis Engineering* project.

In addition to his research, Simon is engaged in several political and societal organizations. After he picked up windsurfing in 2019, this hobby has gotten progressively out of hand. He is an active member of the Delft student windsurfing club, organizing events and developing creative content. From time to time he wakes up in cold sweat thinking of the ‘scientific’ articles he wrote for the members magazine. He is also an active member of the CDJA and CDA where he has supervised campaigns, pushes for more philosophical background for its members, and supports the Delft city council delegation, which in practice tend to boil down to running from one task to the next while making it sound like you did your homework.

List of Publications

Journal papers:

5. S. van Oosterom and M. Mitici. “End-to-end predict-then-optimize for maintenance planning of Lithium-Ion batteries”. In: *Submitted to Transportation Research Part C: Emerging Technologies* (2025)

4. S. van Oosterom and M. Mitici. “An environmentally-aware dynamic planning of electric vehicles for aircraft towing considering stochastic aircraft arrival and departure times”. In: *Transportation Research Part C: Emerging Technologies* 169 (2024). DOI: 10.1016/j.trc.2024.104857

3. S. van Oosterom and M. Mitici. “Optimizing the battery charging and swapping infrastructure for electric short-haul aircraft—The case of electric flight in Norway”. English. In: *Transportation Research Part C: Emerging Technologies* 155 (2023). ISSN: 0968-090X. DOI: 10.1016/j.trc.2023.104313

2. S. van Oosterom, M. Mitici, and J. Hoekstra. “Dispatching a fleet of electric towing vehicles for aircraft taxiing with conflict avoidance and efficient battery charging”. en. In: *Transportation Research Part C: Emerging Technologies* 147 (Feb. 2023), p. 103995. ISSN: 0968-090X. DOI: 10.1016/j.trc.2022.103995

1. P. van Oosterom, S. van Oosterom, H. Liu, R. Thompson, M. Meijers, and E. Verbree. “Organizing and visualizing point clouds with continuous levels of detail”. In: *ISPRS Journal of Photogrammetry and Remote Sensing* 194 (Dec. 2022), pp. 119–131. ISSN: 0924-2716. DOI: 10.1016/j.isprsjprs.2022.10.004. (Visited on 12/13/2024)

Conference papers:

4. M. Mitici and S. van Oosterom. “Adaptive predictive maintenance for the batteries of electric Vertical Take-off and Landing (eVTOL) aircraft using Remaining Useful Life prognostics”. In: *Proceedings of the 34th European Safety and Reliability Conference*. Stavanger, Norway, June 2025

3. M. Zoutendijk, S. van Oosterom, and M. Mitici. “Electric Taxiing with Disruption Management: Assignment of Electric Towing Vehicles to Aircraft”. In: San Diego: AIAA, June 2023

2. M. Cousy, V. Peyruqueou, C. Pierre, P. Cyrille, D.-B. Vo, J. Garcia, M. Mihaela, S. van Oosterom, A. Sharpanskykh, M. v. D. Burg, P. Roling, E. Spiller, S. Gottofredi, and P. Lanzi. “AEON: Toward a concept of operation and tools for supporting engine-off navigation for ground operations”. en. In: Oct. 2022. URL: https://enac.hal.science/hal-03859908 (visited on 02/20/2024)

1. S. van Oosterom, M. Mitici, and J. Hoekstra. “Analyzing the impact of battery capacity and charging protocols on the dispatchment of electric towing vehicles at a large airport”. In: *AIAA AVIATION 2022 Forum*. AIAA AVIATION Forum. American Institute of Aeronautics and Astronautics, June 2022. DOI: 10.2514/6.2022-3920

Awards:

1. Anna Valicek Award, *Annual student paper compitition from the Airline Group of the International Federation of Operations Research Societies (AGIFORS), 2022. For the paper ““Dispatching a fleet of electric towing vehicles for aircraft taxiing with conflict avoidance and efficient battery charging".*

Within the next decades, aviation will need to be converted into a sustainable industry. In this light, electric aviation poses an interesting group of opportunities, deployable in different settings.

These vehicles are faced with range and charging limitations, an underdeveloped charging infrastructure, and extra battery maintenance requirements. For these reasons, they will impact aviation operations, and operations planning. To accommodate these technologies, new planning models and algorithms are required.

In this dissertation, we shall develop operations research models and algorithms specially designed for electric aviation. We pay special attention to the interaction between the different planning stages and use a variety of methods.

TU Delft